



HAL
open science

Probabilistic single fibre characterisation to improve stochastic strength modelling of unidirectional composites

Faisal Islam

► **To cite this version:**

Faisal Islam. Probabilistic single fibre characterisation to improve stochastic strength modelling of unidirectional composites. Mechanics [physics]. Université Paris sciences et lettres, 2020. English. NNT : 2020UPSLM066 . tel-03272250

HAL Id: tel-03272250

<https://pastel.hal.science/tel-03272250>

Submitted on 28 Jun 2021

HAL is a multi-disciplinary open access archive for the deposit and dissemination of scientific research documents, whether they are published or not. The documents may come from teaching and research institutions in France or abroad, or from public or private research centers.

L'archive ouverte pluridisciplinaire **HAL**, est destinée au dépôt et à la diffusion de documents scientifiques de niveau recherche, publiés ou non, émanant des établissements d'enseignement et de recherche français ou étrangers, des laboratoires publics ou privés.

THÈSE DE DOCTORAT
DE L'UNIVERSITÉ PSL

Préparée à MINES ParisTech

EN: Probabilistic single fibre characterisation to improve stochastic strength modelling of unidirectional composites

FR: Caractérisation probabiliste monofilamentaire pour améliorer la modélisation stochastique de la résistance des composites unidirectionnelles

Soutenue par

Faisal ISLAM

Le 3 juin 2020

École doctorale n°621

**Ingénierie des Systèmes,
Matériaux, Mécanique,
Energétique**

Spécialité

Mécanique

Composition of the jury :

Peter DAVIES Ingénieur de Recherche, IFREMER	<i>Rapporteur</i>
Vincent PLACET Ingénieur de Recherche, Université de Franche-Comté	<i>Rapporteur</i>
Véronique MICHAUD Associate Professor, EPFL	<i>Examineur</i>
James THOMASON Professor, University of Strathclyde	<i>Examineur</i>
Nicolas SAINTIER Professor des Universités, ENSAM I2M	<i>Président</i>
Sébastien JOANNÈS Chargé de Recherche, Mines ParisTech	<i>Examineur</i>
Lucien LAIARINANDRASANA Directeur de recherche, MINES ParisTech	<i>Directeur de thèse</i>

Acknowledgements

I would like to express my sincere gratitude to my supervisors Dr. Sébastien Joannès and Prof. Lucien Laiarinandrasana for their support, guidance and numerous interesting discussions throughout this PhD project. I am also very grateful to Dr. Anthony Bunsell and Dr. Alain Thionnet for sharing their knowledge and scientific advice and for the many insightful suggestions during my interactions with them.

I would like to acknowledge the funding from the European Union's Horizon 2020 research and innovation programme under the Marie Skłodowska-Curie grant agreement No. 722626 (FibreMod, www.fibremodproject.eu) for supporting my research and the several professional trainings received during my PhD. which provided me with incomparable opportunities for career development in an international environment ranging across different continents.

A particular thanks to the technical staff of the Materials Centre of Ecole des Mines de Paris: especially Julie and Jean-Christophe who have greatly contributed with their expertise to the success of a major part of the work produced in this PhD, embarking with enthusiasm and success on technical challenges never faced before. Thanks to Zak for all his help with administrative tasks.

I would like to thank my closest collaborators from Dia-Stron Ltd.: Dr. Steve Bucknell and Yann Leray; from Weizmann Institute of Science: Prof. Daniel Wagner and Carol Rodricks; and from Chomarar Ltd.: Dr. Vicky Singery and Dr. Ashok Rajpurohit for the fruitful research and collaborations we had during the years of my PhD. Additionally, a very important thanks goes to all the FiBreMoD project partners and PhD students for the challenging discussions and professional growth opportunities that the several consortium meetings and project events have provided. The FiBreMoD early stage researchers deserve a special mention for their support and the collective effort we put into reaching the milestones of the project.

I would like to thank all the members of the Materials Centre and the many other colleagues and friends that I have met and collaborated with at Ecole des Mines of Paris. Thanks for having a very productive environment for research and for always being so helpful and friendly. I would also like to thank all members of the examination committee for their feedback during the interim presentations and their corrections of this manuscript.

I would like to thank my friends, and colleagues Jan Rojek, Martinus and Ashok Rajpurohit who shared with me, day-by-day, pains and glories of this PhD and of these three years in France. A special thanks goes to my old friends from India: Atul, Aaquib, Nadeem

and Shaheer with whom I kept good friendships despite the distance and the different professional paths undertaken over the years.

Again, I will forever be thankful to Sébastien for all his help in many different academic and non-academic ways. His help in all practical aspects is deeply appreciated. He has been my role model as a scientist, mentor, and supervisor.

Finally, the most profound thanks goes to my family, who gave me a very strong professional and life ethic which I am extremely proud of.

Contents

Acknowledgements	1
List of publications	13
Preamble	15
Background and Motivation	15
Aim	15
Thesis as part of the FiBreMoD project	16
1 Introduction	17
1.1 Structural applications of fibre reinforced composites	17
1.2 Predictive models for fibre composites	18
1.2.1 Issues with model predictions	18
1.3 Constituent properties: Input data for models	19
1.3.1 Fibre strength	20
1.3.2 Matrix and interfacial properties	22
1.4 Main objectives of the thesis	23
1.5 Thesis outline	24
Chapter summary in French	26
2 Fibre strength and Weibull distribution: state-of-the-art	29
2.1 Introduction	29
2.1.1 Fibres used in composite materials	30
2.2 Fibre strength	31
2.2.1 Weakest link model for fibre strength	31
2.2.2 Representation of fibre strength with Weibull distribution	32
2.2.3 Physical interpretation of Weibull distribution parameters	33
2.3 Fibre strength characterisation	33
2.3.1 Fibre bundle test	35
2.3.2 Fragmentation test	36
2.3.3 Loop test	37
2.3.4 Single fibre test	38
2.3.5 Estimation of Weibull parameters from fibre strength data set	40
2.4 Issues in determining fibre strength	41
2.5 Issues with the standard Weibull distribution	42
2.5.1 Extrapolation of distribution parameters	42
2.5.2 Discrepancy between experimental results and Weibull model	42

2.5.3	Uncertainty in results	43
2.6	Conclusions	44
	Chapter summary in French	46
3	Critical parameters in fibre strength measurement: identification and evaluation	47
3.1	Introduction	49
3.2	Critical parameters in fibre strength measurement	50
3.2.1	Sources of uncertainty	50
3.2.2	Fibre tensile strength : Theoretical formulation	50
3.2.3	Measurement uncertainty	54
3.2.4	Experimentation	55
3.2.5	Evaluation of measurement uncertainty in input quantities	56
3.2.6	Propagation of uncertainty to fibre tensile strength	58
3.3	Sensitivity analysis	61
3.3.1	Sensitivity analysis for fibre tensile strength	62
3.3.2	Estimation of sensitivity for tensile strength at other gauge lengths	63
3.4	Conclusions	64
	Chapter summary in French	67
4	Uncertainty in fibre strength distribution	69
4.1	Introduction	71
4.1.1	Causes of uncertainty in Weibull parameters	71
4.2	Uncertainty due to measurement	72
4.2.1	Fibre strength distribution	73
4.2.2	Estimation of measurement uncertainty on Weibull parameters	74
4.3	Uncertainty due to sampling randomness	76
4.3.1	Confidence Interval	77
4.3.2	Calculation of confidence interval for Weibull parameters	77
4.3.3	Confidence Region	81
4.3.4	Effect of sample size	82
4.4	Conclusions	83
	Chapter summary in French	85
5	Variability in predictions of composite strength models due to uncertain input properties	87
5.1	Introduction	89
5.2	Mines ParisTech model	89
5.2.1	Mechanism of longitudinal tensile failure of unidirectional composites	90
5.2.2	Microscopic scale: Fibre failure model and the RVE	90
5.2.3	Macroscopic analysis: Simplified FE^2 model	91
5.3	Methods	91
5.3.1	Steps in simulation	91
5.3.2	Simulation framework	93
5.3.3	Input fibre strength: Hypothetical properties with uncertainties	94
5.3.4	Loading conditions	95
5.4	Results and discussions	97

5.4.1	Monotonic loading	97
5.4.2	Sustained loading	100
5.5	Conclusions	102
	Chapter summary in French	104
6	Experimental and statistical investigation of fibre properties	107
6.1	Introduction	109
6.2	Material and methods	110
6.2.1	Material	110
6.2.2	Methods	110
6.2.3	Advantages of using the semi-automated testing method	114
6.3	Experimentation	116
6.3.1	Fibre dimensional measurement	116
6.3.2	Fibre tensile strength measurement	118
6.4	Results and discussions	118
6.4.1	Fibre dimensional analysis	118
6.4.2	Measurement of Poisson's ratio	121
6.4.3	Tensile strength	124
6.4.4	Strength distribution	127
6.4.5	Effect of sample size on the confidence interval	131
6.5	Conclusions	132
6.5.1	Scope for improvement in the fibre testing system	135
	Chapter summary in French	136
7	Weibull analysis based on Bayesian approach	137
7.1	Introduction	139
7.2	Cause of misfit: Fibre preselection effect	140
7.2.1	Fibre preselection effect	140
7.2.2	Simulated experiment for demonstrating fibre preselection effect	140
7.2.3	Need for improvements in analysis	143
7.3	Truncated Weibull analysis based on Bayesian approach	143
7.3.1	Existence of truncation in fibre strength data	143
7.3.2	Theoretical formulation	144
7.4	Experiments, Results and Discussions	147
7.4.1	Experimentation	147
7.4.2	Fibre strength results	147
7.4.3	Standard Weibull analysis	147
7.4.4	Truncated Weibull analysis	150
7.5	Conclusions	153
	Chapter summary in French	154
8	Conclusions and perspectives	155
8.1	Conclusions	155
8.2	Perspectives	157
8.2.1	Limitations of extrapolating fibre strength	157
8.2.2	Modification of Weibull distributions	158
8.3	Scope for future work	159

Chapter summary in French	162
A Weakest link model and Weibull distribution	175
B Microscale matrix properties	177
B.1 Introduction	177
B.2 Microscale matrix properties: state of the art	178
B.3 Materials and methods	180
B.3.1 Materials	180
B.3.2 Specimen preparation	180
B.3.3 Microscopy	180

List of Figures

1.1	Some structural applications of fibre reinforced composite materials.	18
1.2	Weibull parameter values for T700 carbon fibres reported in literature	22
2.1	Rovings of different fibre types used in composite materials.	31
2.2	Schematic representation of a chain consisting of N links.	32
2.3	Effects of the shape, scale and location parameters on Weibull distribution. . . .	34
2.4	Schematic view of the initial part of the load-strain curve for a bundle test . . .	35
2.5	Schematic of a specimen for a single fibre fragmentation test	36
2.6	Schematic of a single fibre loop test.	38
2.7	Schematic of a single fibre mounted on a card frame	39
3.1	(a) Schematic diagram of a single fibre mounted on a card frame, (b) Major issues with sample preparation leading to inaccurate measurement of gauge length, (c) Angular misalignment in the fibre specimen	51
3.2	Schematic diagram showing the effect of fibre misalignment on the effective load on the fibre.	52
3.3	The actual card frame used for preparing the fibre specimens.	55
3.4	Failure stress vs failure strain scatterplot for all fibre tensile tests	61
3.5	Sensitivity indices of different input quantities in tensile strength measurement of fibres at different gauge lengths	65
4.1	Estimated Weibull plot for experimentally determined fibre strength	73
4.2	Weibull distributions simulated by varying fibre strength data points within the uncertainty region	75
4.3	Simulated Weibull distributions based on sampling and measurement uncertainty.	79
4.4	Simulated fibre strength data sets.	80
4.5	Scatter between the shape and scale parameters of the simulated Weibull distributions.	80
5.1	Representative Volume Element at the microscopic scale with the fibres distributed in a regular square array.	91
5.2	RVEs of the material damage state resulting from sequential fibre breaks and corresponding i-plets.	92
5.3	Flowchart of the simplified FE^2 multiscale fibre break model.	92

5.4	(a) Specimen of dimensions 64 mm × 4 mm × 1 mm. (b) A C3D8 linear 3-D brick element consisting of 8 RVEs. (c) An RVE with 32 fibres	94
5.5	Characteristic curves for the monotonic loading condition	96
5.6	Characteristic curves for the sustained loading condition	97
5.7	Simulated composite behaviour for different input fibre strength distributions with varying scale parameters.	98
5.8	Simulated composite behaviour for different input fibre strength distributions with varying shape parameters.	99
5.9	Simulated composite behaviour for different input fibre strength distributions with varying scale parameters, under the sustained loading condition.	100
5.10	Simulated composite behaviour for different input fibre strength distributions with varying shape parameters, under the sustained loading condition.	102
6.1	(a) Dia-Stron Fibre Dimensional Analysis System (FDAS770, Isometric view). (b) Working of the FDAS770 (top view). (c) Zoomed-in image of the translation stage.	111
6.2	(a) Plastic tabs used for mounting one end of a fibre. (b) Well defined gauge length with proper alignment.	112
6.3	A 20 sample cassette loaded with fibre specimens ready to be tested.	113
6.4	(a) ALS Vacuum suction for specimen pick up (b) transfer of specimen to testing site.	113
6.5	(a) Testing site: Combination of the LEX/LDS system. (b) Testing setup installed with the LEX/LDS system.	114
6.6	Schematic diagram of unwrapping a fibre surface on a 2-D plane to show the different locations at which dimensional measurements were recorded.	117
6.7	Histograms showing the variations in measured fibre diameters for all fibres of the different gauge lengths: (a) $L_0=30$ mm, (b) $L_0=20$ mm, (c) $L_0=4$ mm	119
6.8	Variation in apparent fibre diameter along the axial length for different angular positions: (a) for Fibre 1. (b) for Fibre 2	120
6.9	Variation in measured fibre diameter along the angular direction, for a fixed plane (apparent cross-section), for: (a) fibre 1 (b) fibre 2. Unit: micrometres.	121
6.10	Schematic of the change in axial and lateral dimensions of the fibre on elongation.	122
6.11	Reduction in measured fibre diameter with elongation.	123
6.12	Boxplots for fibre strengths for the three gauge lengths with mean and median values	124
6.13	Fibre strength plotted against failure stress for all fibres, along with corresponding histograms, for tensile tests done at gauge lengths of 30 mm. The straight line represents the mean Young's modulus.	126
6.14	Fibre strength plotted against failure stress for all fibres, along with corresponding histograms, for tensile tests done at gauge lengths of 20 mm. The straight line represents the mean Young's modulus	126
6.15	Fibre strength plotted against failure stress for all fibres, along with corresponding histograms, for tensile tests done at gauge lengths of 4 mm. The straight line represents the mean Young's modulus	127

6.16	Fibre strength plotted against fibre diameter for all fibres, for tensile tests done at all the different gauge lengths	128
6.17	Best fit Weibull plots for the 2-parameter distribution for all three gauge lengths, along with experimental data points	129
6.18	Best fit Weibull plots for the 3-parameter distribution for all three gauge lengths	131
6.19	Simulated fibre strength data sets.	133
7.1	Distribution used for determining the break limit for individual fibre strength values. It is a folded normal distribution with a mean of 2 GPa and a standard deviation of 0.5 GPa.	142
7.2	Weibull plot showing simulated fibre strength data for a Weibull distribution with $\sigma_0=4.5$ GPa and $m = 4.0$, along with the fibre strength data set after simulating the fibre preselection effect.	142
7.3	Relationship between location parameter (σ_u) and truncation limit (σ_r) for different cases. (a) Case 1: $\sigma_u = 0$ (b) Case 2: $0 < \sigma_u < \sigma_r$ (c) Case 3: $\sigma_u = \sigma_r$	144
7.4	Histogram of the experimentally generated fibre strength data.	148
7.5	Best representative standard 2 and 3-parameter Weibull distributions along with experimental fibre strength data.	149
7.6	Truncated and predicted Weibull distributions for the three cases.	151
8.1	Comparison of the scale parameters obtained from extrapolation with that obtained from experimental results.	158
A.1	Schematic representation of a chain consisting of N links.	175
B.1	(a) Fibre manufacturing process used by Hobbiebrunken et al. (b) Fibre manufacturing process used by Misumi et al.	179
B.2	Cross-section of a carbon fibre reinforced composite material. The epoxy phase can be seen to have non-regular shapes.	180
B.3	Schematic of the cross section of the group of wires. The epoxy settled in the cavities near the point of contact of consecutive wires resulting in epoxy fibres.	181
B.4	An epoxy fibre. The fibre is twisted along the length due to the twists given to the teflon wires for consolidation.	181
B.5	Microscopic image of the cross-section of the wires with epoxy settled in the cavities between the wires.	181
B.6	Microscopic image of the cross section of a prepared epoxy fibre.	182

List of Tables

1.1	Weibull distribution parameters for T700 carbon fibres reported in literature. The scale parameter (σ_0) normalized for $L_0 = 30$ mm. ‘SFT’ stands for single fibre tests, ‘Fragm.’ stands for fibre fragmentation tests, and ‘Bundle’ stands for fibre bundle tests.	21
3.1	Best estimate values of all quantities for one single fibre tensile test	56
3.2	Measurement uncertainty values of all input quantities for the given fibre tensile test example, along with expanded uncertainty for a confidence level of 95% and 99%.	58
3.3	Sensitivity coefficient values of all quantities	60
3.4	Best estimates and measurement uncertainty of fibre strength for 30 tensile tests	61
3.5	Sensitivity measures of each input quantity for the given single fibre tensile test example	62
3.6	Average sensitivity measures for each input quantity for the set of 30 single fibre tensile test	63
3.7	Sensitivity indices of different input quantities in tensile strength measurement of fibres at different gauge lengths	64
4.1	Weibull parameters for experimentally determined fibre strengths	73
4.2	Weibull parameters for virtual fibre strength data sets	75
4.3	Amplification of measurement uncertainties of the Weibull Scale parameter (σ_0) upon extrapolation to shorter gauge lengths.	76
4.4	Weibull parameters and associated 95% confidence interval for overall uncertainty due to measurement and sampling.	79
4.5	Amplification of uncertainties (due to sampling randomness) of the Weibull Scale parameter (σ_0) upon extrapolation to shorter gauge lengths.	81
4.6	Best estimated values for selective B-strengths along with the 95% confidence intervals for overall uncertainty due to measurement and sampling	83
4.7	Effect of sample size on estimated 95% confidence interval of Weibull scale parameter σ_0 (B63.2 strength)	83
5.1	Elastic properties of an undamaged UD ply for 64% fibre volume fraction.	94
5.2	Different levels of the shape and scale parameters of the input fibre strength distribution	95

5.3	Simulated failure stress values of the composite for input fibre strength distributions having different scale parameters and same shape parameter . . .	98
5.4	Simulated failure stress values of the composite for input fibre strength distributions having different shape parameters and same scale parameter . . .	99
5.5	Simulated lifetime of the composite structure for input fibre strength distributions having different scale parameters and same shape parameter . . .	101
5.6	Simulated lifetime of the composite structure for input fibre strength distributions having different shape parameters and same scale parameter . . .	101
6.1	Fibre properties supplied by the manufacturer	110
6.2	Comparison of semi-automated and standard manual single fibre testing methods	116
6.3	Total number of fibre strength results determined for each gauge length . .	118
6.4	Mean, median and mode values of fibre diameters for the different gauge lengths	119
6.5	Mean, standard deviation and coefficient of variation (CoV) of the average Young's modulus for tests done at the three gauge lengths	125
6.6	Maximum likelihood parameters for the 2-parameter Weibull distribution .	129
6.7	Maximum likelihood parameters for the 3-parameter Weibull distribution .	130
6.8	Effect of sample size on the confidence interval of the median strength of the simulated fibre strength data sets.	134
7.1	Truth table demonstrating the survival and failure of fibres to simulate the preselection effect. X represents a rejected point while O represents a selected point.	141
7.2	Relationship between location parameter (σ_u) and truncation limit (σ_r) for different values of ω	145
7.3	Single fibre tensile strength data set for a gauge length of 30 mm.	147
7.4	Parameters for standard Weibull distributions.	148
7.5	Parameters for truncated Weibull distributions for different cases.	150
7.6	Parameters for predicted Weibull distributions for the 3 cases.	152
8.1	Weibull distribution parameters for different gauge lengths	157

List of publications

Parts of the work presented in this thesis have been disseminated through a number of written publications and oral communications. These are listed below, as of January 2020.

Peer-reviewed journal publications

- F. Islam, S. Joannès, S. Bucknell, Y. Leray, A. Bunsell, L. Laiarinandrasana, “Investigation of tensile strength and dimensional variation of T700 carbon fibres using an improved experimental setup”, *Journal of Reinforced Plastics and Composites*, 2020, 39 (3-4), 144-162.
- F. Islam, S. Joannès, L. Laiarinandrasana, “Evaluation of critical parameters in tensile strength measurement of single fibres”, *Journal of Composites Science*. 2019, 3, 69.
- S. Joannès, F. Islam, L. Laiarinandrasana, “Uncertainty in fibre strength characterisation due to uncertainty in measurement and sampling randomness”, *Applied Composite Materials*, 2020, 27, 165-184.
- F. Islam, S. Joannès, L. Laiarinandrasana, A. Bunsell, “Weibull analysis based on Bayesian approach to model the strength behaviour of brittle fibres”, (*Under Review*)

Refereed conference publications

- F. Islam, S. Joannès, L. Laiarinandrasana, “Propagation of uncertainty from constituents to structural assessments in composite strength modelling”, in *23rd International Conference on Composites Structures (ICCS 23)*, September 1-4, 2020, Porto, Portugal
- F. Islam, S. Joannès, L. Laiarinandrasana, “Adaptation of Weibull analysis to represent strength behaviour of brittle fibres”, in *International Conference on Composite Materials (ICCM-22)*, August 11-16, 2019, Melbourne, Australia
- A. Rajpurohit, F. Islam, S. Joannès, S. Bucknell, V. Singery, L. Laiarinandrasana, “Characterization and statistical analysis of fibre strength at various processing stages”, in *International Conference on Composite Materials (ICCM-22)*, August 11-16, 2019, Melbourne, Australia
- F. Islam, S. Joannès, S. Bucknell, Y. Leray, A. Bunsell, L. Laiarinandrasana, “Towards accurate and efficient single fibre characterization to better assess failure

strength distribution”, in *European Conference on Composite Materials (ECCM-18)*, June 24-28, 2018, Athens, Greece

- F. Islam, S. Joannès, S. Bucknell, Y. Leray, A. Bunsell, L. Laiarinandrasana, “Improvements in determination of carbon fibre strength distribution using automation and statistical data analysis”, in *Fiber Society’s Spring 2018 Conference*, June 12-14, 2018, Tokyo, Japan

Conference abstracts

- M.P. Widjaja, F. Islam, S. Joannès, A. Bunsell, G. Mair, “The effect of input properties on the predicted failure of a type IV composite pressure vessel using a multiscale model”, in *FiBreMoD Conference*, December 11-12 2019, Leuven, Belgium
- R. J. Lunn, F. Islam, Y. Leray, S. Joannès, S. Bucknell and D.M. Stringer, “Further Insights into the Fatigue of Hair Fibres through Statistical Analysis and Relevance to Hair Care Applications”, in *HairS’19 Symposium*, September 11-13, 2019, Schluchsee, Germany
- F. Islam, S. Joannès, L. Laiarinandrasana, “Effect of uncertainty in characterization on the variability of fibre strength distributions”, in *International Conference on Recent Advancements in Composite Materials*, February 25-28, 2019, IIT-BHU, Varanasi, India

The research leading to these results was done within the framework of the FiBreMoD project and received funding from the European Union’s Horizon 2020 research and innovation programme under the Marie Skłodowska-Curie grant agreement No 722626.

Preamble

Background and Motivation

Fibre reinforced composite materials are used in load-bearing structural applications for the aerospace, automotive, transportation and energy industry. For such high performance and critical applications, there are risks of serious complications on failure. Material rupture or structural failure can result in catastrophic consequences. These applications therefore necessitate reliable structural health monitoring techniques for evaluating the damage tolerance and useful lifetime of the structures. These assessments can be assisted by computational strength and damage models, which should ideally be able to predict failure and useful life of these critical composite structures accurately.

Many complex computational models have been developed to simulate the failure processes in fibre reinforced composites which lead to the ultimate failure of structures. These models are used for predicting the failure strength and for the lifetime analysis of composite structures. Since the properties of composite materials are governed by the properties of their constituents and their interactions, the reliability of the model predictions is strongly dependent on the accuracy of the constituent properties used as input. Uncertainty in fibre or matrix properties may result in variability in the predicted strength and lifetime of composite structures. The reliability of model predictions thus depends upon a strong understanding of the constituent properties and any uncertainties associated with it. Any uncertainties in input data raises doubts on the strength and lifetime predicted by the models and restricts their reliability. Due to a lack of reliable structural assessment models, composite structures are still overdesigned to ensure safety, which negates the potential weight-saving benefits that can be achieved with fully optimized structures.

Aims

The overall aim of this thesis is to develop a better understanding of the constituent properties of fibre reinforced composites, i.e. the properties of fibres and matrix, and to improve their characterisation process. More accurate constituent properties will empower composite strength models to make reliable predictions for the behaviour and lifetime of composite structures.

FiBreMoD project

FiBreMoD is a Marie Skłodowska-Curie Innovative Training Network (ITN) project which brings together universities, research centres and companies from different countries worldwide. The project aims to train 13 Early-Stage Researchers (ESRs) to become multi-talented and interdisciplinary researchers that will be highly coveted in the field of composites. The different academic and industrial partners in FiBreMoD include:

- Katholieke Universiteit Leuven (KUL), Leuven, Belgium
- Imperial College of Science and Technology, London, United-Kingdom
- University of Southampton, Southampton, United-Kingdom
- Ecole des Mines de Paris (Mines ParisTech), Evry, France
- Weizmann Institute of Science, Rehovot, Israel
- Bundesanstalt für Materialforschung und -prüfung (BAM), Berlin, Germany
- Toyota Motor Europe (TME), Brussels, Belgium
- Siemens Industry Software NV, Leuven, Belgium
- Chomarat Textiles Industries, Le Cheylard, France
- Dia-Stron Ltd., Andover, United-Kingdom

Thesis as part of the FiBreMoD project

Limiting the climate change induced temperature increase to less than 2°C will require strong reductions in greenhouse gas emissions. Lightweight materials and fibre-reinforced composites in particular, are a key enabling technology to achieve this goal. Current composite applications are however strongly overdesigned due to a lack of reliable design tools and predictive models for their mechanical properties. The objectives of the FiBreMoD project is to develop and apply models to improve the design of composite structures made with continuous fibre materials. The final application is the design of high pressure vessels and automotive parts.

Obtaining reliable input data is crucial for any model. There are significant concerns in the way the input data for fibre break models for unidirectional composites are typically obtained. This thesis aims at achieving a breakthrough in the reliability of methods for generating input data for the models. The goal is to enable composite failure models to make blind predictions. Parts of the work described in this thesis were conducted during research visits to Dia-Stron Ltd., Weizmann Institute of Science and Chomarat Textiles Industries.

Chapter 1

Introduction

Contents

1.1	Structural applications of fibre reinforced composites	17
1.2	Predictive models for fibre composites	18
1.2.1	Issues with model predictions	18
1.3	Constituent properties: Input data for models	19
1.3.1	Fibre strength	20
1.3.2	Matrix and interfacial properties	22
1.4	Main objectives of the thesis	23
1.5	Thesis outline	24
	Chapter summary in French	26

1.1 Structural applications of fibre reinforced composites

Fibre reinforced composite materials have very strong structural capabilities, especially when both mechanical performance and light weight are desired. They have benefits over other structural materials such that for a given density, they possess higher stiffness and strength. These materials also offer better impact and corrosion resistance, and possess excellent weathering stability. These properties make them an ideal material to be used for structural applications. They are thus widely used in critical load-bearing structures for the aerospace, automotive, transportation and wind energy industry [1, 2], some of which are shown in Figure 1.1. Just the pressure vessels and structural components for the aerospace industry represent together about 40% by volume of the total composite market [3].

In the transportation industry, composite pressure vessels are used for the storage and transportation of high pressure liquids and gases. Compressing hydrogen and natural gas and storing it within a pressure vessel is an efficient storage method in terms of energy density. In commercial aircrafts, the use of composite materials has seen a sharp increase since the 1990s. In the last two civilian aircrafts produced, composite materials make up half of the weight of the structure, with 53% of Airbus A350 XWB (2014) and 46% of



Figure 1.1: Some structural applications of fibre reinforced composite materials [4, 5, 6, 7].

Airbus A220 (2016) been made up of composite materials [8]. In the automotive industry, composites have mainly been used in expensive cars that are produced in limited volume such as Lamborghini’s Aventador and Tesla’s Roadster. However, the use of composites in high volume automotive production is gradually increasing with the BMW i3 being one of the first high volume cars made of composite materials. In the wind energy industry, composite materials are used typically in blades and nacelles of wind turbines. Renewable energy is the fastest growing energy source (7.6% p.a.). It is eventually expected to displace coal to become the single largest source of global power generation by 2040 [9, 10] and the use of structural composites is expected to continue its steep rise.

Key aspects of designing composite structures

In-service safety and reliable lifetime assessments are key challenges for high performance load-bearing applications and require great care to be taken during their design. The design of composite material structures can be assisted by computational models for predicting their mechanical properties at both component and structural level. Critical structures such as composite pressure vessels which are used for the storage of hydrogen or other gases at high pressures require very accurate computational models, so that the predictions can be used with confidence in industrial applications [11].

1.2 Predictive models for fibre composites

The strength and damage behaviour of composite materials is inherently complex and thus predicting the mechanical behaviour of composite structures remains highly challenging. Many ongoing studies of different composite material research groups are focussed on developing computational composite strength and damage models to predict the mechanical behaviour of composite materials and structures leading to their lifetime assessment. Some of these models are mentioned here: (i) a multiscale finite-element simulation method [12, 13] from Mines ParisTech, (ii) an analytical hierarchical scaling law for composite fibre bundles from Imperial College London [14], and (iii) direct numerical simulations of composite fibre bundles from KU Leuven [15]. These models were also compared in a recently conducted benchmarking exercise [16]. Detailed reviews of these and other models are available in literature [14, 17].

1.2.1 Issues with model predictions

To assess the predictions made by composite strength and damage models, worldwide failure and benchmarking exercises have been conducted [16, 18]. The predictions made

by the different models were found to spread over a large range, thus suggesting the reason for the lack of confidence of industry in such models. These discrepancies were found to occur for many aspects of damage and failure, such as ultimate strength, failure strain, and clustering of fibre-breaks. Moreover, there were differences between the mechanical behaviour predicted by the models and that observed experimentally. The large spread in modelling predictions and deviation from experimental results can be linked to two main reasons:

- An incomplete understanding of the complex interaction between the fibres and matrix in fibre reinforced composites which governs their failure mechanism.
- Lack of reliable constituent properties which are used as input for the models.

There are several previous and ongoing studies for obtaining a better understanding of the failure mechanisms in fibre reinforced composites to improve the state-of-the-art models. However, obtaining representative constituent properties to be used as input for these models has received less attention. There are significant experimental and theoretical challenges in obtaining reliable input data, some of which are explained in the next sub-sections. There are also inherent variabilities in the properties of the constituents that lead to variability in the strength of the composite materials. There is a need for the models to also address this variability to improve the reliability of the mechanical behaviour predicted by the models.

Due to the lack of reliable predictive models, composite components are still overdesigned which leads to larger and heavier parts along with sub-optimal structural performance.

1.3 Constituent properties: Input data for models

The mechanical behaviour of fibre reinforced composites is governed by the properties of its constituents, i.e. fibres and matrix, and on the interaction between them. In light of this understanding, longitudinal tensile strength models thus require information about two key concepts: (i) the fibre strength distribution (ii) stress concentration around broken fibres. The stress concentration depends upon the properties of the matrix material and of the fibre-matrix interface. The properties of the fibres, matrix and the interface are together used as input in these models for evaluating the damage and failure behaviour of the composite structures [19].

In order to have a precise and complete understanding of the behaviour of composite materials and structures, it is very important to determine the accurate characteristics of the constituents. The reliability of model predictions depends on the accuracy of the input data used, mainly of the properties of fibres, since they are the principal load bearing constituents of fibre reinforced composites subjected to longitudinal loads [20, 21].

A small change in input data can cause a significant variation in model predictions such as in the failure strength or in the time to failure of a composite structure and therefore any error in input constituent properties would lead to inaccurate model predictions. This behaviour has been highlighted in one of the previous works, where the predicted time to failure for composite structures has been shown to be strongly sensitive to the input data used [22]. For example, the predicted time to failure for a composite specimen studied

increased by a factor of ten on decreasing the standard deviation of input fibre strength distribution to a third of its initial value. It is therefore crucial for the success of composite strength models that the fibre, matrix and interfacial properties used as model input are determined with the best possible accuracy and any associated uncertainty is quantified appropriately.

The major input properties which are used by the models and the issues in accurately determining them are discussed in the next subsections.

1.3.1 Fibre strength

There is a large variation in the strength of fibres and therefore their strength cannot be represented by a single average value. Fibre strength is typically represented by using statistical distribution functions, of which the Weibull distribution is the most popular. Weibull proposed a distribution that addresses the variation in strength of brittle fibres and could be used to represent their strength behaviour [23]. Many studies have proposed modifications to this distribution for representing fibre strength but the standard 2-parameter Weibull probability distribution function given by Equation 1.1 has been the most widely used representation. In this equation, it is assumed that the section of the fibre remains constant along its length, the scope for which will be discussed in the forthcoming chapters.

$$P_R(\sigma) = 1 - \exp \left[- \left(\frac{L}{L_0} \right) \left(\frac{\sigma}{\sigma_0} \right)^m \right] \quad (1.1)$$

where, $P_R(\sigma)$ is the probability of fibre failure for an applied stress level σ , L being the characteristic gauge length, L_0 the reference gauge length, σ_0 the scale parameter, m the shape parameter or Weibull modulus. The scale parameter, σ_0 , represents the strength at which 63.2% of the fibres within a population would fail. The shape parameter, m , represents the scatter in strength around the mean value. Fibre strengths are typically reported in terms of the Weibull shape and scale parameters. These parameters are also fed into the composite strength models, and are one of the most important input properties.

Issues with fibre strength data

On analysing the fibre strength properties available in literature, it has been observed that there are differences in results reported by different authors, even for the same type of fibres. For T700 carbon fibres, which are very popular in fibre reinforced composites for structural applications, the Weibull distribution parameters (m and σ_0) for the tensile strength reported by different studies are compiled in Table 1.1. The scale parameter σ_0 , depends on the gauge length used, so all reported scale parameter values have also been normalised for a gauge length of $L_0 = 30$ mm using the widely used Weibull scaling equation given by Equation 1.2, which is derived from Equation 1.1. $\sigma_{0,1}$ and $\sigma_{0,2}$ are scale parameter values determined for fibre gauge lengths of $L_{0,1}$ and $L_{0,2}$, respectively and m is the shape parameter of the obtained distribution. The normalised scale parameter values are also given in Table 1.1. The extrapolation technique using the Weibull scaling equation however must be used with caution and various scientific papers address this complex topic [24, 25, 26]. The implication of using such an extrapolation function for

estimating the strength of fibres will be discussed in later chapters.

$$\sigma_{0,2} = \sigma_{0,1} \left(\frac{L_{0,1}}{L_{0,2}} \right)^{1/m} \quad (1.2)$$

Table 1.1: Weibull distribution parameters for T700 carbon fibres reported in literature. The scale parameter (σ_0) normalized for $L_0 = 30$ mm. ‘SFT’ stands for single fibre tests, ‘Fragm.’ stands for fibre fragmentation tests, and ‘Bundle’ stands for fibre bundle tests.

S.N.	Type of fibre	Testing method	Gauge length (mm)	Sample size, N	Shape, m	Scale, σ_0 (GPa)	Scale, σ_0 (Norm.) (GPa)	Author
1	T700	SFT	20	30	5.6	5.4	5.02	Feih [27]
2	T700	SFT	20	30	5.39	-	-	Hao [28]
3	T700	SFT	10	20	3.5	7.7	5.63	Deng [29]
			20	20	5	6.2	5.72	
			30	20	4	6.2	6.20	
			40	20	3.7	6	6.49	
50	20	4	5.8	6.59				
4	T700	SFT	20	10	4.68	3.63	2.87	Lutz [30]
5	T700	SFT	10	20	12.01	3.92	3.58	Na [31]
6	T700	Fragm.	30	6	4.8	8.5	8.50	Deng [29]
7	T700	Fragm.	20	-	5.6	5.47	-	Matveev [32]
8	T700	Bundle	20	15	17.53	1.98	1.93	Ting [33]
9	T700	Bundle	8	-	12.06	4.41	3.95	Zhou [34]

Figure 1.2(a) shows the scatter in the shape parameter values for different gauge lengths as reported by different authors, while Figure 1.2(b) shows the scale parameter values, normalised for a gauge length of 30 mm. Since different studies have used different methodologies for determining the fibre strength distribution, results obtained from the different processes are represented by different geometric shapes in the plot. Values determined by using the single fibre testing (SFT) methodology are depicted with a circle and the size of the circles are in proportion to the sample size that was used to determine these results, as also given in Table 1.1. Values determined by using the fragmentation and bundle testing methodologies are depicted by diamond and square shaped markers, respectively. The shape parameter is observed to vary between 3.5-17.5 which is a huge variation. The normalised scale parameter values are also observed to have a big variation and lie between 1.9-8.5 GPa.

The possible reasons for the differences in results need to be discussed in order to have a better understanding of the reliability that could be associated with each result available in literature. Authors usually do not comment on the uncertainty that can be associated with their obtained parameter values, or possible sources of errors which can affect the accuracy of the determined results. Although it has only been mentioned by a few studies

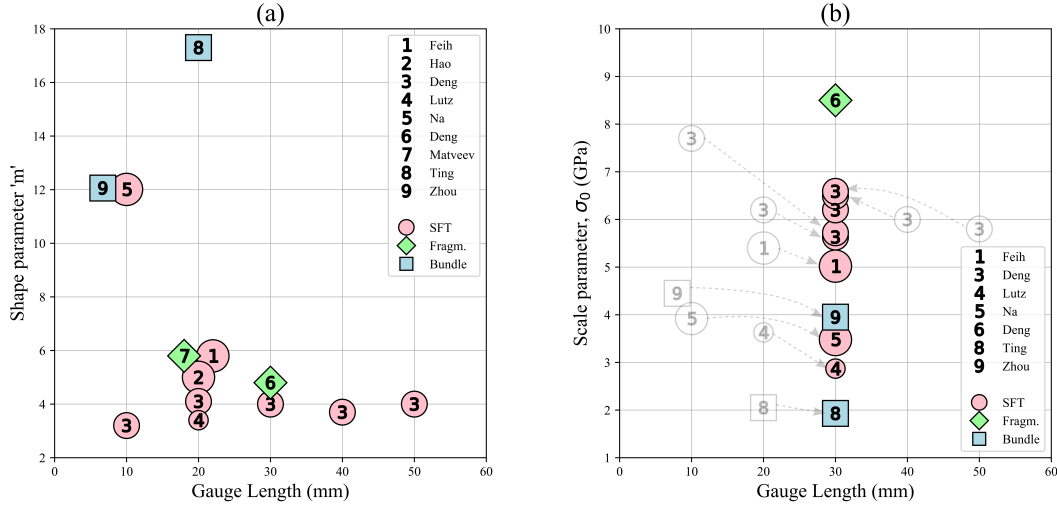


Figure 1.2: Weibull parameter values for T700 carbon fibres reported in literature for: a) Shape parameter b) Scale parameter. Circular, diamond and square-shaped markers represent results from the single fibre tests (SFT), fibre fragmentation tests and fibre bundle tests, respectively. The scale parameter values have been normalised for a gauge length of 30 mm using the Weibull scaling equation (Equation 1.2). The values originally reported are also shown.

that there is possibility of uncertainty in results [35], the exact causes of uncertainties and their effects on fibre strength results have not been investigated in detail.

1.3.2 Matrix and interfacial properties

After fibre strength, the second key aspect for any strength model is the stress redistribution around fibre breaks under longitudinal loading. When a fibre breaks, the surrounding matrix is subjected to a multi-axial stress state. This leads to an increase in the stress of the surrounding fibres, which is often described in terms of stress concentration factors (SCFs). The magnitude of stress concentrations is governed by the matrix and interfacial properties.

Matrix properties such as stiffness and strength contribute to the longitudinal tensile strength of composites. Whether the matrix has a perfectly elastic, perfectly plastic, visco-elastic or visco-plastic nature can cause further complexities in the model.

During fibre breaks, large interfacial stress components can arise at the fibre-matrix interface which can cause the matrix to debond. The debonding depends mainly on interfacial shear strength, the strain energy release rate, the fibre-matrix friction and the matrix yield strength. Significant obstacles still remain in accurately determining these necessary input data.

Issues with matrix and interfacial property data

Most matrix systems have complex behaviour, i.e. they are not linearly elastic, but visco-elastic materials. Most models however have simplified this behaviour by treating the matrix as perfectly elastic or perfectly plastic. Moreover, matrix properties which determine the fibre-matrix debonding are often very challenging to be measured. Many strength models in the literature even ignore debonding altogether.

More importantly, the matrix properties used as input data for strength models are always measured on macroscale specimens. However, some studies have suggested that it is very likely that the macroscale matrix behaviour is different from that at the microscale. This can result in significant differences between the model predictions and the mechanical behaviour of an actual composite material. A new method for characterizing the microscale properties of the matrix will be introduced in this thesis.

1.4 Main objectives of the thesis

It is evident that accurate input constituent properties are important for the success of composite strength models in determining reliable results. However, it has been shown that there is discrepancy in available constituent properties, mainly in the fibre strength distribution; and even for the same type of fibre, different studies have reported different results [26]. This makes the selection of input data for composite models ambiguous and also raises doubts on the reliability of the model predictions.

The main objective of this thesis is to develop a better understanding of the constituent properties of fibre reinforced composites. The discrepancy or variation in reported constituent properties could be due to a combination of many factors, as characterizing the properties of the constituents can be challenging. Some factors that can result in inaccurate characterisation are: measurement uncertainty, experimental errors, non-representativeness of the chosen sample set for data generation and analysis, the data-reduction technique used, etc. The effects of these factors need to be investigated to obtain a better understanding of the uncertainty associated with the constituent properties, and to find the causes behind these uncertainties.

Since fibres are the principal load bearing constituents of unidirectional composites, most of the research described in this thesis deals with fibres, in order to understand and improve their characterisation process, by identifying and discriminating between different causes of uncertainties. The knowledge of the causes behind uncertainties can enable appropriate measures to be taken in order improve the characterisation of constituent properties by appropriately tackling the underlying causes.

To achieve the mentioned objectives, the following research will be described in this thesis:

- Investigation of the variation in tensile strength and morphology of structural fibres
- Identification and evaluation of critical parameters which contribute to errors in fibre strength measurement
- Statistical quantification of uncertainty in fibre strength distribution parameters and identification of different causes for these uncertainties

- Simulating the effect of uncertainty in input properties on the variability of composite model predictions
- Formulation of an improved data reduction technique to model the statistical variation in strength of brittle fibres

1.5 Thesis outline

With an objective of understanding and improving the fibre strength characterisation process, Chapter 2 discusses the state-of-the-art. It includes analysis of major issues and challenges associated with different characterisation techniques, and with the Weibull distribution which is used to represent fibre strength behaviour.

In Chapter 3, different possible sources of errors due to experimental limitations in the single fibre testing process have been identified. Their effect on fibre tensile strength has been analytically modelled. This model is then used to evaluate the uncertainty in experimentally determined fibre strength at different gauge lengths.

Chapter 4 uses uncertainty in fibre strength calculated in Chapter 3 to determine its effects on the fibre strength distribution using a statistical Monte-Carlo method. These results are also analysed to elucidate the effect of sampling on the results.

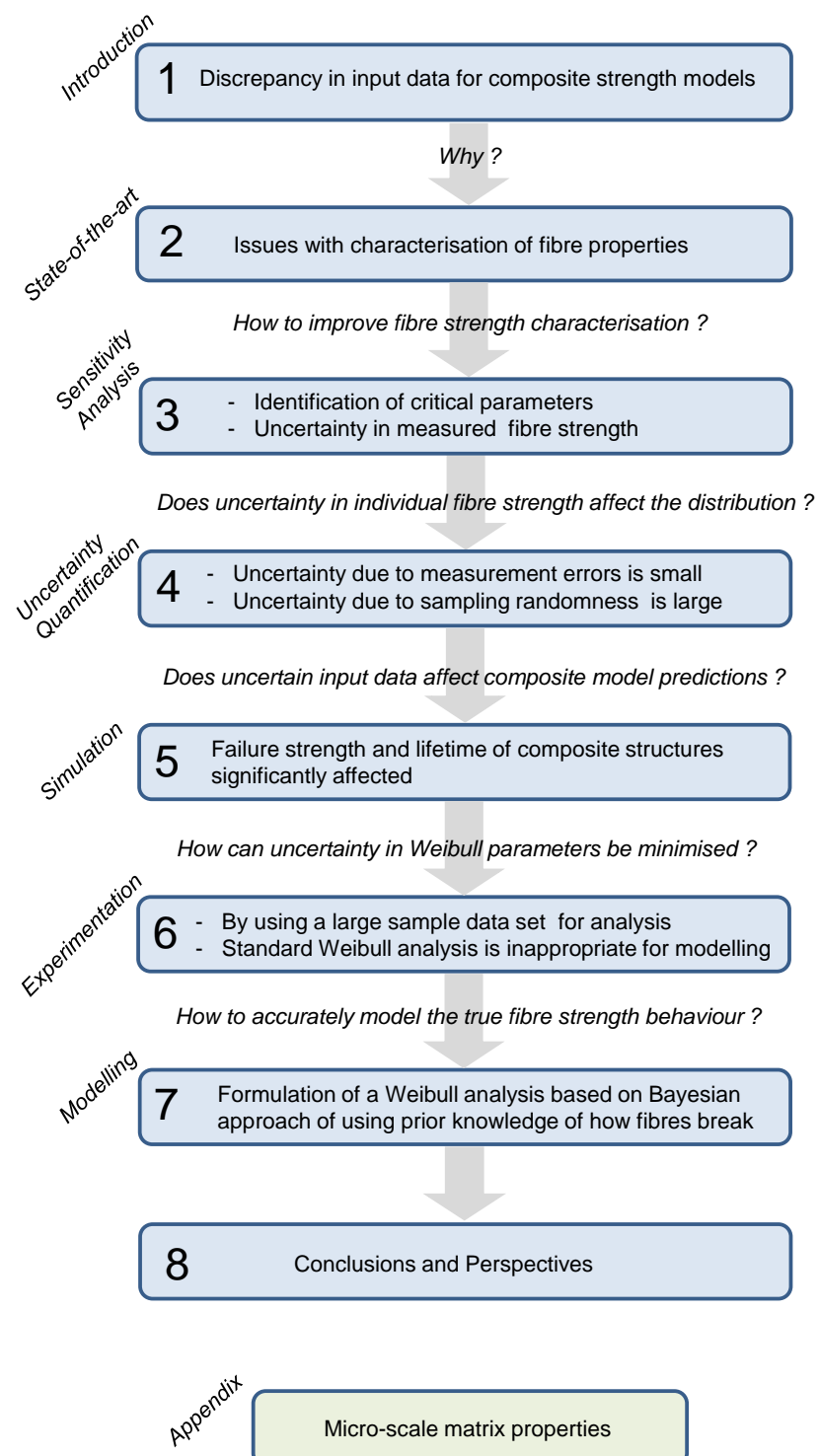
The understanding of uncertainty in fibre strength distributions gained from Chapters 3 and 4 is then used to find its effect on the structural behaviour predictions of composite strength models. This study is described in Chapter 5.

To minimise uncertainties in fibre strength distribution, analysis of a large data set of experimental results generated for a wide range of fibre gauge lengths is discussed in Chapter 6, so as to highlight the limitations of the standard Weibull analysis for representing fibre strength behaviour. The role of fibre dimensions on the fibre strength distribution is also discussed in this chapter.

In Chapter 7, the standard Weibull analysis has been adapted based on the Bayesian approach of using prior knowledge of how fibres break during the testing process. Fibre strength data is then analysed using this method to predict a more accurate statistical representation of the tensile strength behaviour of fibres used in composites.

The overall conclusions, perspectives, and scope for future work is described in Chapter 8. In the end, a new method for characterising the microscale properties of the matrix is introduced in Appendix B.

Graphical Outline



Chapter summary in French

Introduction

Les matériaux composites renforcés de fibres ont de très fortes capacités structurelles, en particulier lorsque des performances mécaniques associées à un poids léger sont recherchés. Ils sont donc largement utilisés dans les structures porteuses critiques pour l'industrie aérospatiale, aéronautique, automobile et de l'énergie éolienne. La sécurité en service et les évaluations fiables de la durée de vie sont des défis clés pour les applications structurelles hautes performances et nécessitent un grand soin lors de leur conception. La conception de structures en matériaux composites peut être assistée par des modèles pour prédire leurs propriétés mécaniques au niveau des composants et de la structure. De nombreux modèles proposent des solutions pour prédire au mieux la résistance des structures composites en se basant généralement sur les mécanismes d'endommagement intervenant au cœur du matériau.

Afin d'évaluer les prévisions faites par ces modèles, des exercices d'analyses comparatives de leurs performances ont été menés dans le monde. Il a été constaté que les prévisions faites par les différents modèles s'évaluaient sur une large gamme de valeurs, entraînant un manque de confiance de l'industrie dans ces modèles. Il existe de nombreuses études visant à obtenir une meilleure compréhension des mécanismes de défaillance dans les composites renforcés de fibres et ceci afin d'améliorer les modèles existants. Un autre problème provient de l'obtention des propriétés des constituants, variables d'entrée de ces modèles. Il existe d'importants défis expérimentaux et théoriques pour obtenir des données d'entrée fiables. Il existe également des variabilités inhérentes aux propriétés des constituants qui conduisent à une variabilité de la résistance des matériaux composites. Il est nécessaire que les modèles tiennent également compte de cette variabilité pour améliorer la fiabilité du comportement mécanique prédit.

En analysant les propriétés de résistance des fibres disponibles dans la littérature, il a été observé qu'il existe des différences dans les résultats rapportés par différents auteurs, même pour le même type de fibres. Les paramètres de la distribution de Weibull pour les fibres de carbone T700, qui sont très populaires dans les composites pour les applications structurelles, sont discutés dans ce chapitre et une grande dispersion a été observée.

Dans le but d'améliorer la compréhension des propriétés constitutives des composites renforcés de fibres, les recherches suivantes seront décrites dans cette thèse:

- Etude de la variation de la résistance à la traction et de la morphologie des fibres structurales*
- Identification et évaluation des paramètres critiques qui contribuent aux erreurs de mesure de la résistance des fibres*
- Quantification statistique de l'incertitude des paramètres de distribution de la résistance des fibres*
- Simulation de la conséquence de l'incertitude des propriétés d'entrée sur la variabilité des prédictions du modèle à l'échelle du composite*
- Formulation d'une technique améliorée de réduction des données pour modéliser la*

variation statistique de la résistance des fibres fragiles

La plupart des recherches décrites dans cette thèse portent sur les fibres afin de comprendre et d'améliorer leur processus de caractérisation. Les fibres sont les principaux constituants supportant la charge dans les composites unidirectionnels chargés en traction longitudinale. Une nouvelle méthode pour caractériser les propriétés microscopiques de la matrice est également introduite dans cette thèse.

Chapter 2

Fibre strength and Weibull distribution: state-of-the-art

Contents

2.1	Introduction	29
2.1.1	Fibres used in composite materials	30
2.2	Fibre strength	31
2.2.1	Weakest link model for fibre strength	31
2.2.2	Representation of fibre strength with Weibull distribution	32
2.2.3	Physical interpretation of Weibull distribution parameters	33
2.3	Fibre strength characterisation	33
2.3.1	Fibre bundle test	35
2.3.2	Fragmentation test	36
2.3.3	Loop test	37
2.3.4	Single fibre test	38
2.3.5	Estimation of Weibull parameters from fibre strength data set	40
2.4	Issues in determining fibre strength	41
2.5	Issues with the standard Weibull distribution	42
2.5.1	Extrapolation of distribution parameters	42
2.5.2	Discrepancy between experimental results and Weibull model	42
2.5.3	Uncertainty in results	43
2.6	Conclusions	44
	Chapter summary in French	46

2.1 Introduction

Fibres are known to be an essential constituent of many living things. They are present in nanostructures such as twisted strands of DNA and also in large and complex structures such as the muscles and tissues of both mammals and trees. Humankind has taken

inspiration from such structures to use fibres for the development of textile materials and fibre-reinforced composites. Fibres are widely used in composite materials to make light-weight and high-strength products. The reinforcement of polymeric matrices by fibres is found to bring about significant advancements in the mechanical behaviour of polymers. This provides added advantages such as high strength to weight ratio, excellent weathering stabilities and enhanced dimensional stabilities. This combination can generate some of the strongest and versatile materials that have ever been known or developed.

Most outstanding characteristics of composite materials are imparted by the fibres which are used to reinforce the matrix, as these fibres are the principal load bearing constituents of unidirectional composite materials. Failure of composite materials typically occurs due to the accumulation of fibre breaks. Knowledge of fibre strength is therefore crucial for understanding the failure behaviour of fibre reinforced composite materials and structures. Using computational strength models, which uses the fibre properties as input, a simulation of the effective properties of the composite materials can be made, enabling an estimation of failure onset [11, 12, 13, 15, 36].

Matter in the form of fibres is capable of possessing extraordinary properties of strength and stiffness. Fibres do not share the properties with the same material in bulk form, whilst some fibres do not even exist in bulk form. For e.g. Glass fibres can be hundreds of times stronger than glass in bulk form. This is because there are far fewer defects in fine fibres as compared to the bulk state. Therefore, an assembly of fibres making up the same volume as that in bulk form would be much stronger. This is also true for other materials. It is however important to note that this is true when the strength is considered in a direction parallel to the fibres in the fibre assembly. The fibre assembly is anisotropic unlike the case for the bulk material which has the same characteristics in all directions and is therefore isotropic.

2.1.1 Fibres used in composite materials

Different fibres are used as reinforcements in composite materials. The desired characteristics of most reinforcing fibres are high strength, high stiffness, and low density. Some commonly used fibres in composite materials are made of: Carbon, Glass, Aramid, Boron, etc. **Carbon** fibres are most widely used for advanced composites. They are available in many forms with a range of stiffness and strengths. **Glass** fibres are commonly used in low to medium performance composites, due to their high tensile strength and low cost. They are usually not used for very high performance applications because of their relatively low stiffness, and they are also prone to degradation in properties with exposure to hygrothermal conditions. **Aramid** (or Kevlar) fibres have relatively higher stiffness than glass fibres. Moreover, they have low density, high tensile strength, and good impact resistance and toughness. However, Kevlar composites have very low transverse tensile and longitudinal compressive strengths. They are also very sensitive to moisture absorption. **Boron** and other ceramic fibres typically have high stiffness and strength, and high use temperatures. They are usually used in high temperature applications with metal or ceramic matrices. Figure 2.1 shows rovings of some fibre types used in composite materials.

Carbon fibres, by far, are the most widely used fibres in high-performance structural



Figure 2.1: Rovings of some fibre types used in composite materials [37]. (a) Carbon (b) Glass (c) Aramid.

applications, for example in pressure vessels and aircraft components. For the rest of the thesis, most of the reviews, analysis, and concepts developed will be demonstrated using carbon fibres and their composites. Nevertheless, these concepts and theories are also applicable to other brittle fibres as well.

2.2 Fibre strength

The “strength” of a structure is defined as its ability to withstand an applied load without breaking. For a given single fibre, to assess its strength, a monotonic longitudinal load is applied to the fibre until its failure. This failure load is then normalized by the cross-section, possibly at the breaking point, to obtain the tensile strength of the fibre.

As mentioned by Timoshenko, Leonardo da Vinci was the first to study the strength of materials as a function of their size, when he demonstrated in the 1500s, that longer iron wires are weaker than shorter ones [38]. A major advancement was made by Mariotte in 1686, when he experimented with ropes and concluded that, “a long rope and a short one always support the same weight unless that in a long rope there may happen to be some faulty place in which it will break sooner than in a shorter”. Griffiths later explained this size dependency of strength based on the presence of flaws. Since a shorter fibre has a lower probability of having a flaw, it is more likely to have a higher strength. This reasoning also represented a physical basis of Da Vinci’s and Mariotte’s qualitative observations. Further investigations on size effects were made by Tipett (1925), Peirce (1926) and Frechet (1927). This progress culminated with the work of Weibull in 1939 [39, 40].

2.2.1 Weakest link model for fibre strength

Strength is not an intrinsic material property and structures or materials break from their weakest point, mainly due to the presence of flaws in the material. Therefore, analysis of tensile failure data provides insight into the distribution of flaws within fibre. Due to their inherently high aspect ratio (length over width), fibres can be compared to chains, as shown in Figure 2.2. As a chain, which is only as strong as its weakest link, fibre tensile strength depends on the tested length, also called the “gauge length”. The longer the fibre, the lower the applied load needed to break it and thus the lower the strength. Even for a given gauge length, there is obviously a variation in the strength of individual fibres due

to the distribution of defects in the volume or on the surface of fibres. The theoretical description of the weakest link model for representing fibre strength, as also demonstrated by Weibull, is described in Appendix A.

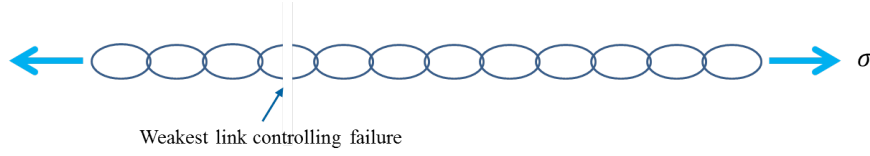


Figure 2.2: Schematic representation of a chain consisting of N links. The chain breaks at the weakest link.

2.2.2 Representation of fibre strength with Weibull distribution

Technical fibres used as reinforcements in organic matrix composite materials are usually brittle in nature. Strengths of brittle fibres such as carbon and glass are controlled by the stochastic distribution of defects inside them, due to which there are variations in the strength of individual fibres. Fibre strength, therefore, cannot be described by a single value and is typically represented by using a statistical function which characterizes the inherent variation in its strength. The most popularly used statistical function for representing strength of brittle fibres is the Weibull distribution [23]. The weakest link model outlined above, and detailed in Appendix A, was used as a basis by Weibull to represent the behaviour of a brittle solid for which failure of the material is induced due to the presence of a crack, developed from the most critical defect. The parameters of the Weibull distribution characterises the strength variation of fibres and are determined by appropriately fitting experimentally generated fibre strength data with the statistical function. The failure probability of a fibre, following the Weibull law, can be expressed as in Equation 2.1, which is popularly known as the 3-parameter Weibull distribution. For fibres of uniform cross-sections, the term V/V_0 can be replaced by L/L_0 , as shown in Equation 2.2.

$$P_R(\sigma) = 1 - \exp \left[- \left(\frac{V}{V_0} \right) \left(\frac{\sigma - \sigma_u}{\sigma_0} \right)^m \right], \text{ for } \sigma \geq \sigma_u \quad (2.1)$$

$$P_R(\sigma) = 1 - \exp \left[- \left(\frac{L}{L_0} \right) \left(\frac{\sigma - \sigma_u}{\sigma_0} \right)^m \right], \text{ for } \sigma \geq \sigma_u \quad (2.2)$$

with $P_R(\sigma) = 0$ for $\sigma < \sigma_u$.

Here, $P_R(\sigma)$ is the probability of fibre failure, L the characteristic gauge length, (V being the characteristic gauge volume), L_0 the reference gauge length, (V_0 being the reference gauge volume), σ the applied stress, σ_u the location parameter, σ_0 the scale parameter, m the shape parameter or Weibull modulus. The shape parameter (m) describes the range of variation in fibre strength data, i.e. the scatter around an average value, the scale parameter (σ_0) is the 63.2 percentile strength value of the distribution and the location parameter (σ_u) determines the starting point or the origin of the distribution. The term (L/L_0) is commonly used for comparing the fibre tensile strength generated for

different gauge lengths to a common reference length (L_0), and for extrapolating the scale parameter to other lengths, to account for the length effect [41].

When an experimentally determined fibre strength data set is analysed with this distribution, the best fitted distribution originates around the point of the smallest strength value in the data set. This determines the location parameter which represents the origin. It has also been called as the threshold parameter by some authors. Most studies have chosen to fix this location parameter σ_u to be zero. This results in a 2-parameter distribution which originates at zero strength value, and is given by Equation 2.3 or Equation 2.4, for the cases of non-uniform and uniform cross-sections, respectively. Equation 2.4 is also the most popularly used function for representing the strength behaviour of brittle fibres [26]. The limitations of using either of the 2 or 3-parameter Weibull distribution for representing the fibre strength behaviour would be discussed in another chapter.

$$P_R(\sigma) = 1 - \exp \left[- \left(\frac{V}{V_0} \right) \left(\frac{\sigma}{\sigma_0} \right)^m \right] \quad (2.3)$$

$$P_R(\sigma) = 1 - \exp \left[- \left(\frac{L}{L_0} \right) \left(\frac{\sigma}{\sigma_0} \right)^m \right] \quad (2.4)$$

2.2.3 Physical interpretation of Weibull distribution parameters

The effects of varying the shape (m), scale (σ_0) and location (σ_u) parameters on the resulting Weibull distribution is shown in Figure 2.3. These distributions have been obtained by varying one of the three parameters of the Weibull distribution, while fixing the other two. Figure 2.3(a) shows the effect of varying the shape parameter, Figure 2.3(b) shows the effect of varying the scale parameter, while Figure 2.3(c) shows the effect of varying the location parameter, on the resulting distributions. It should however be noted that these parameters of the Weibull distribution are not independent of each other and variations in the value of one parameter leads to variations in the values of the other parameters as well.

2.3 Fibre strength characterisation

Characterizing fibres is challenging, as the fibre diameter can be just a few microns especially for brittle technical fibres such as carbon. The very small cross-section of fibres makes them very delicate to handle leading to a very cumbersome process of fibre specimen preparation and testing [42]. These challenges significantly affect the accuracy of the prepared specimen and may lead to inaccurate fibre strength measurements [26, 35, 43]. Despite considerable progress in characterisation techniques, many obstacles still remain to obtain accurate fibre strength data.

There are different methods to obtain fibre strength and its distributions such as the fibre bundle tests, fibre fragmentation tests, single fibre tensile tests, loop tests, etc. However, each method has its own limitations. In the fibre bundle method, a bundle of fibre is tested by applying a load and observing the behaviour of the bundle as a whole. The single fibre fragmentation test embeds a fibre inside matrix and the composite is tested to

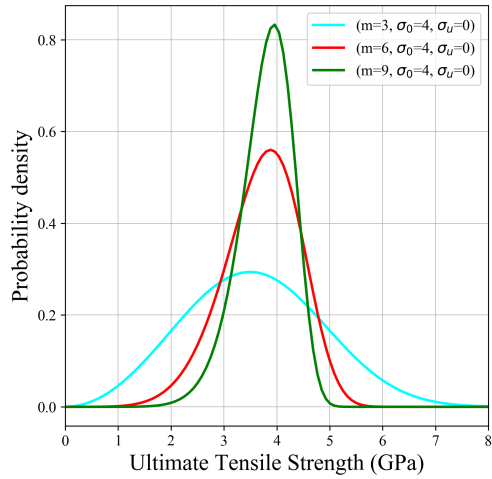
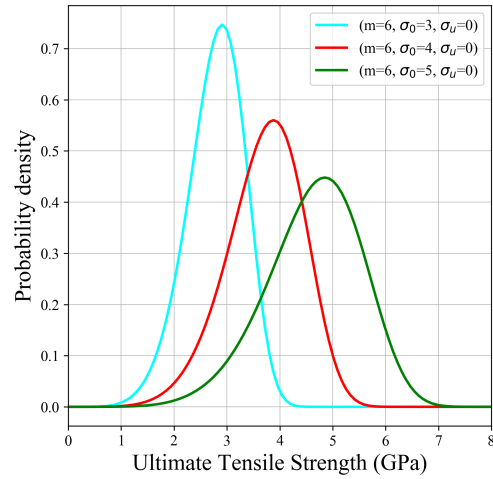
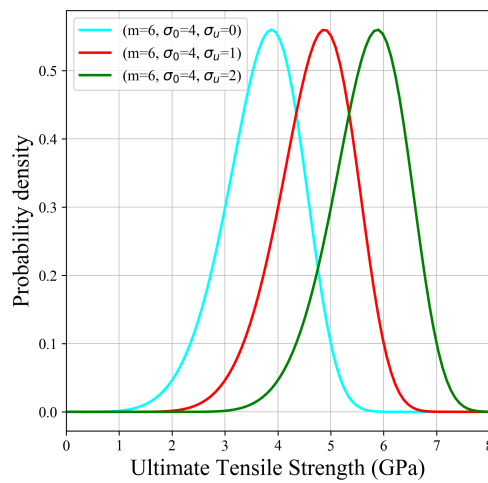
(a) Effect of shape parameter (m)(b) Effect of scale parameter (σ_0)(c) Effect of location parameter (σ_u)

Figure 2.3: Effects of the shape (m), scale (σ_0) and location parameters (σ_u) on Weibull distribution. For each case, the mentioned parameter has been varied while the other two parameters have been fixed. While σ_0 and σ_u are in GPa, m is unitless.

determine the parameters for the fibre strength distribution. The single fibre test is one of the most straightforward techniques however; it is a very laborious and time consuming process. The next subsections discuss these available techniques for the determination of fibre strength distribution, along with the challenges that are associated with each methodology.

2.3.1 Fibre bundle test

In fibre bundle tests, a bundle containing a large number of fibres is subjected to tensile loading and the load-strain curve is recorded. The load F and applied strain ε are then represented using an appropriate form of a Weibull distribution given by Equation 2.5, as discussed previously by a number of authors [44, 45, 46]. It is assumed that all fibres in the bundle are nominally identical, that they are perfectly aligned and are linear elastic in nature.

$$F = E_b \varepsilon \exp \left[-\frac{l}{l_0} \left(\frac{\varepsilon}{\beta_\varepsilon} \right)^\alpha \right] \quad (2.5)$$

where $E_b = AEN_0$, A is the single fibre cross-sectional area, E the modulus, N_0 the number of fibres in the bundle, l the bundle gauge length, l_0 the bundle gauge length, α the shape parameter, and β_ε is related to the scale parameter β as $\beta_\varepsilon = \beta/E$.

Limitations:

- The analysis is based on the assumption of equal load sharing amongst the surviving fibres of identical length. However, the spread of the individual fibre gauge length inside the bundle is unavoidable which may lead to unequal distribution of stress on the fibres. It has been shown that there may be a difference in the bundle length and fibre length. This difference, called slack, φ , introduces a non-linearity in the load-strain curve [47, 48] as shown in Figure 2.4.

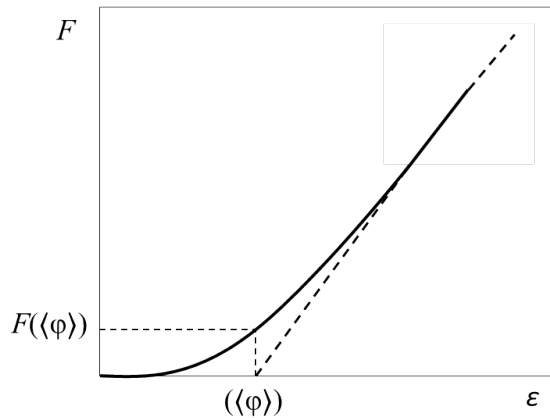


Figure 2.4: Schematic view of the initial part of the load-strain curve for a bundle test. Regenerated from [44].

- The fibres inside a bundle interact laterally with each other. This causes local shearing and contributes to the fibres adjacent to breaks [49, 50].
- When considering load transfer interactions, most strength models for fibre-reinforced composites use the idea that the entire surface area of each fibre is surrounded by the matrix material. Load transfer within the composite is then achieved through each individual fibre-matrix interaction, instead of through the interaction between a group of fibres and the matrix, as in fibre bundle test results.
- Depending upon the type of material and manufacturing process used for making the fibres, there can be significant variations in diameter of different fibres and in some cases, along the length as well. Due to this non-uniformity in fibre dimensions, the bundle test may not be a very appropriate method to determine fibre strength distribution.

2.3.2 Fragmentation test

In this method, a single fibre is embedded in a matrix and the composite is subjected to a longitudinal incremental displacement. The fibre inside the matrix breaks repeatedly at different locations along the length of the fibre, as demonstrated in the schematic in Figure 2.5. Polarized light is used to identify the sites of fibre breaks. Ultimately, a saturation point is reached when there are no further fibre breaks and there are a very large number of very short fibre segments. The number of fibre breaks is inspected continuously and is deduced to be a function of the applied load, until the onset of saturation. At each break, the corresponding stress is recorded, and the average fragment length is calculated. The Weibull shape and scale parameters are obtained from Equation 2.6. This methodology has been described by different authors [51, 52, 53, 54].

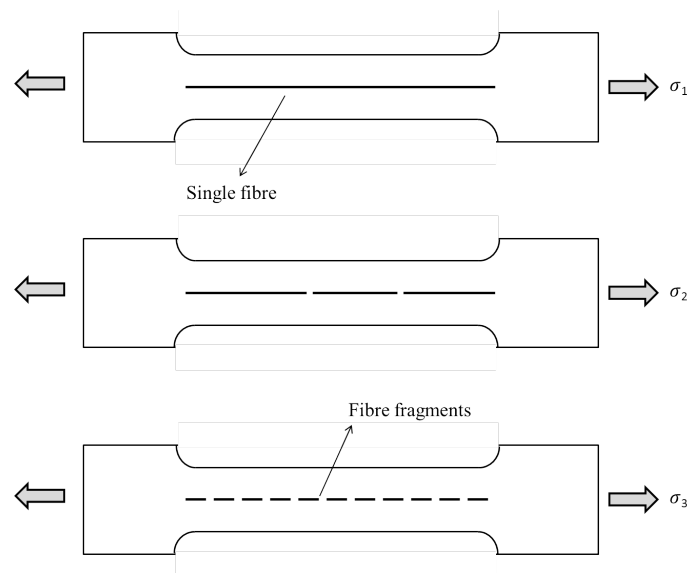


Figure 2.5: Schematic of a specimen for a single fibre fragmentation test. The fibre inside the matrix breaks repeatedly at different locations along the length of the fibre.

$$\sigma_f = \alpha L^{(-\frac{1}{\beta})} \Gamma\left(1 + \frac{1}{\beta}\right) \quad (2.6)$$

where L is the average fibre length, σ_f is applied stress, α and β are Weibull scale and shape parameters, respectively and Γ is the Gamma function.

Limitations:

- If the bonding at the interface of fibre and matrix is too strong, the fibre cracks may propagate into the matrix and cause the matrix to deform around the crack. On the other hand, if the bonding at the interface is weak, debonding between the matrix and fibre may occur which may result in the fibre slipping out of the matrix. This may change the gap between broken fibres and hamper load transfer to the remaining parts of the fibre [55].
- The theory of fragmentation requires that the fragmentation data is strictly log-normally distributed. It has also been found in different studies that the fibre fragment length distribution indeed follows a log-normal distribution, but only in the early fragmentation stages [51, 56].
- The calculation of fibre stress can be affected by residual stresses developed due to different rates of thermal expansions in fibres and matrix. It has been shown that the Weibull parameters can be very sensitive to residual stresses [54, 57]. For calibrating the fibre stresses, residual stresses need to be determined by comparing the fibre stress calculated using fragmentation tests to the stresses calculated from single fibre tests. Alternatively, it can be estimated using a method proposed by Tsai [58].
- It is assumed that fibre breaks are non-interacting in nature. This assumption is only valid if the fibre break density is very low. Several models have been developed to capture the effect of fibre break interactions [52, 59, 60, 61], some of which add a parameter called exclusion zone length [62]. However, such models are very sensitive to the stress transfer between matrix and fibres requiring very accurate information about the exclusion zone length; determining which is complex and it may also vary with fibre stress.

2.3.3 Loop test

Sinclair, in 1950, developed the loop test for measuring the strength and modulus of fibres. In this method, a loop is made from a single fibre as shown in Figure 2.6. This loop is confined in a plane by using glass plates on each side. The ends of the loop are pulled apart, which reduces the radius of curvature of the loop, which is then measured with the help of microscopy. Mechanics equations developed by other researchers are used to calculate the radius of curvature [63]. Using this information, along with the fibre diameter and elastic modulus, the stress of the fibre is estimated. The radius of curvature prior to the final failure of the fibre can be used to determine the strength of the fibre.

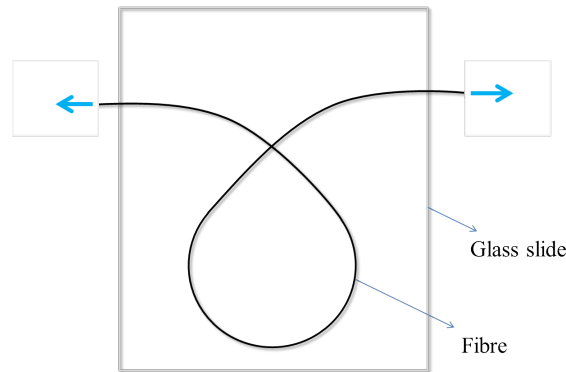


Figure 2.6: Schematic of a single fibre loop test. The ends of the fibre are pulled apart to increase the stress at the loop tip.

Limitations:

- The stress is maximum at the loop tip. However, there is a low probability of finding a flaw at this point. The weakest flaw, therefore, may not have a strong contribution to the failure of the fibre.
- The mechanics equations were derived assuming linear elasticity. This may introduce errors as many fibres, including carbon, are not linear elastic [64].
- Since the stress varies along the the length of the fibre, the measured fibre strength cannot be assigned to a specific gauge length [65].
- Slow and tedious sample preparation process.

2.3.4 Single fibre test

For determining the strength of fibres, individual fibres are tested one by one. In its simplest form, a single fibre is subjected to an increasing tensile load until failure. The measured failure load and fibre cross-sectional area are used to calculate the fibre strength. The test is repeated with a sufficient number of fibres to generate a set of fibre strength data. The data set is then fitted to the standard Weibull distribution equation given by Equation 2.4.

Before subjecting the fibres to a tensile load, fibre specimens need to be carefully prepared. As described in [37], several techniques for the preparation and mounting of fibres exist. These include processes of sticking, pinching or even knotting the fibre to prepare the specimen. Many standards are available that describe the methodology for preparing and testing single filament materials such as BS ISO 11566 [66], ASTM C1557 [67], ASTM D3379-75 [68], etc. The common steps followed in the single fibre testing process for determining fibre strength are as follows:

- A single fibre is removed from the fibre bundle and mounted on a card or cardboard frame with a central cut-out region [43], as shown in Figure 2.7.
- The ends of the fibre are then glued to the card or paper frame using epoxy, wax, or some other suitable adhesive at locations depending upon the required gauge length.

- The diameter of the fibre is usually measured at this moment using an appropriate measuring technique.
- The frame is gripped in the jaws of a tensile testing machine at the two ends.
- The sides of the card frame are cut which allows any applied load to be transferred directly to the fibres.
- The jaws of the testing machine are then pulled until the fibre breaks and the failure load of the fibre is recorded.
- The set of fibre strength values are used to find a representative Weibull distribution.

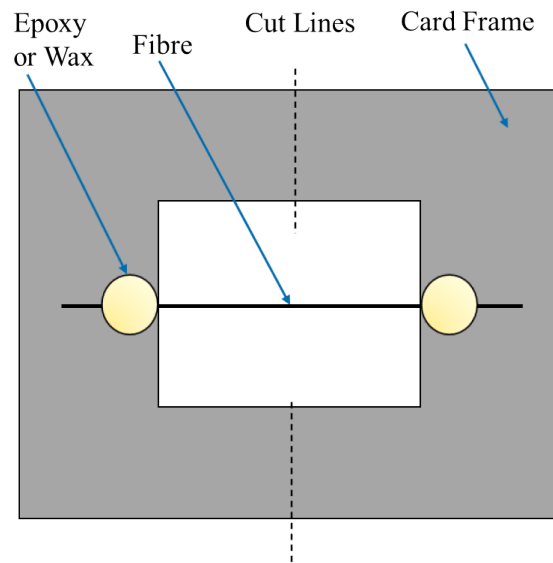


Figure 2.7: Schematic of a single fibre mounted on a card frame

The entire process of specimen preparation and testing is very cumbersome and time consuming. One major source of error with this method of specimen preparation is improper fibre alignment. If the glue on one end is not perfectly aligned with the other, it can result in misalignment of the fibre. This may also result in inaccurate measurement of gauge length. The quality of the data generated can be improved by addressing the sources of error which would minimise their impact on measured fibre strength and improve the accuracy. A sufficient number of single fibre strength data points are required to ascertain the parameters of the best fit statistical distribution which represents the fibre strength variation of the whole population. The time taken to generate a large experimental data set using this manual testing method is very long. Conversely, if a small data set is used then the representativeness of the fibre strength data set would be questionable due to sampling randomness. To generate a large data set, an improved and automated testing setup is required.

Limitations:

- Single fibre testing is a labour intensive and time consuming process.

- Accuracy of results depend strongly on the sample size used, which requires testing a large number of fibres.
- For proper execution of the test, it is important that the fibres are well aligned in the direction of applied load which depends upon the accuracy of the size and shape of paper tabs and proper mounting of fibres on top of these tabs. Since these steps are usually carried out manually, accuracy of the tests depends strongly on operator skills.
- It is possible that weak fibres may break during the extraction process. Hence, extreme care is required to protect the fibres from any unwanted forces which may break the fibres.

Another method of estimating fibre strength is by back-calculation from the results of impregnated fibre bundle tests (IFBT) [69]. The IFBT is well known test method for carbon and glass fibres and some companies also refer to it in their technical data sheets. The advantages of this method are similar to dry fibre bundle tests where a large number of fibres can be tested simultaneously and it is a less complicated method as compared to the single fibre tests. However, a drawback of this method is that the validity of results depends primarily on the accuracy of the micro-mechanical equations used for back-calculation.

Several issues concerning mostly the single fibre testing process that require special attention are discussed in Section 2.4.

2.3.5 Estimation of Weibull parameters from fibre strength data set

Once the fibre tensile strength data set is generated, the next step is to represent the strength values using Weibull analysis. The statistical analysis of a series of tensile tests on single fibres can be carried out in the following way: The results of n fibres are arranged in order of increasing failure stresses, i.e. $\sigma_1 < \dots < \sigma_i < \dots < \sigma_n$ and an experimental cumulative failure probability (or unreliability) $P_R(\sigma_i)$, should be provided for each fibre of rank i having failed at a stress σ_i . Unless an infinite number of fibres are tested, which is clearly impossible, the most general expression must take into account the possibility of fibres breaking at lower stresses than that of the weakest specimen as well as breaking at higher stresses than the strongest fibre tested. Rank methods determine the way an estimated unreliability is associated with each failure level. Various expressions of this probability have been proposed, depending mainly on the sample size. For sample sizes greater than 100, the problem of small sample bias become insignificant and the mean rank method could be used to estimate the unreliability using Equation 2.7.

$$P_R(\sigma_i) = \frac{i}{n+1} \quad (2.7)$$

For smaller sample sizes, the median rank method is preferred over other methods since it provides positions at a specific confidence level (i.e. 50%) and is thus best suited to some further work on confidence limits. The median rank method, estimates unreliability values based on the failure order number and the cumulative binomial distribution. If the sample

size is sufficient, i.e. more than 50 fibres, Benard's approximation can be used [70, 71], as given by Equation 2.8.

$$P_R(\sigma_i) = \frac{i - 0.3}{n + 0.4} \quad (2.8)$$

However, it is better to use median rank tables, or to directly calculate the median ranks from the cumulative binomial distribution. The median rank is, at a 50% confidence level, the value that the true probability of failure has for the i^{th} failure out of a sample of n fibres. It is calculated by solving Equation 2.9 for p .

$$0.5 = \sum_{k=i}^n \binom{n}{k} p^k (1-p)^{(n-k)} \quad \text{where} \quad \binom{n}{k} = \frac{n!}{k!(n-k)!} \quad (2.9)$$

2.4 Issues in determining fibre strength

Some important issues that influence the process of single fibre testing or affect the determination of the fibre strength distribution are listed as follows:

Proper alignment. It is important to ensure that the applied load is properly transferred to the fibre during a test. A small degree of fibre misalignment may lead to an incomplete load transfer. This may result in improper measurement of the failure load [72] and incorrect calculation of fibre strength. Bending stresses may also develop at the ends of fibres which may lead to failure of fibres at the clamping/bonded location [73, 74, 75].

Number of tests. Thomason [76] and Berger et al. [25] have studied the effect of sample size on the estimated fibre strength distribution. It has been shown that using a small number of fibre strength results for the analysis may cause wrong conclusions about the behaviour of strength distribution and related fibre properties. However, there is no general agreement amongst the different studies on the number of tests required to fully describe the strength behaviour of a fibre population [77, 78, 79]. Therefore, to avoid misinterpretation, a sufficient number of fibre strength data points are required. The number of experimental repeats should be decided accordingly depending on the testing method chosen. The accuracy of a statistical function that is used to represent the fibre strength distribution could be improved substantially if a large number of fibre strength data points are available for analysis. This would increase the reliability of the calculated parameter values for the representative statistical distribution.

Fibre extraction. Since the diameters of fibres are very small, the break load is very low. Many weak fibres therefore may break during the process of fibre extraction from a bundle and specimen preparation [41, 80]. As a result, the weaker portion of the fibre strength distribution may not be represented in the experimentally generated fibre strength data set. The elimination of weak fibre strengths would result in an incomplete data set which does not represent the entire fibre population correctly [44, 81].

Accurate measurement of cross-sectional area. For accurate calculation of fibre strength, it is vital that the applied load is calculated properly and the exact cross-sectional area of the fibre is accurately determined [82, 83, 84, 85]. Any error measured in cross-sectional area will affect the accuracy of the calculated fibre strength [86, 87].

Optimum gauge length. Computational composite material strength models require input fibre strength information for very small gauge lengths, sometimes in the range of a few micrometres [88]. Testing fibres at such small gauge lengths is practically impossible. Testing at either very short or very long gauge lengths is associated with respective complications. It is therefore important to determine an appropriate gauge length that is optimum for experimental testing [74, 75].

Representativeness. Last but not least is the representativeness of the distribution obtained. We can indeed wonder if the distribution on isolated fibres is representative of the strength distribution “in-situ”. This is an important issue that has been addressed by some authors. In particular, as already mentioned for fragmentation tests, “in situ” residual stresses [57] can affect the strength distribution. Other effects can be combined such as “in situ” multi-axial loading or changes in surface defects [89]. This is particularly true for glass fibres which are very sensitive to surface defects. This question of representativeness remains open.

2.5 Issues with the standard Weibull distribution

2.5.1 Extrapolation of distribution parameters

As already mentioned, a requirement for composite strength models is that the input fibre properties should be defined at specific gauge lengths. Most models require fibre properties for gauge lengths in the range of a few hundred micrometres to a few millimetres [12, 15, 20]. These lengths are usually smaller as compared to the gauge lengths commonly used for experimentation, mainly because practical limitations make it difficult to conduct experiments at very short gauge lengths. Therefore, almost all experimental data available is for fibre gauge lengths in the range of a few tens of millimetres [26]. The usual practice is to use results generated using longer fibre gauge lengths and then to extrapolate them to shorter gauge lengths using the Weibull scaling equation (Equation 1.2), as described in Section 1.3.1.

Several studies have mentioned that this extrapolation is not always accurate, especially when fibre strengths are extrapolated to very short gauge lengths [15]. There is thus a need to generate fibre strengths directly at short gauge lengths, in order to avoid the need to extrapolate the results. This requires addressing the issues in characterising short fibres, which will be discussed in the upcoming chapters of this thesis.

2.5.2 Discrepancy between experimental results and Weibull model

Several studies have shown that the experimental fibre strength data does not always fit the standard 2-parameter Weibull distribution given by Equation 2.4, i.e. there is a deviation from linearity on the Weibull plot [76]. While some authors have chosen

to ignore this deviation, several other authors have proposed to apply the 3-parameter Weibull distribution given by Equation 2.2 to represent the fibre strength behaviour in such cases.

To tackle this issue, many authors have developed several modified versions of the Weibull distribution, by contemplating the limitations of the standard Weibull distributions to represent the strength of fibres. An interpretation of this situation is that more than one failure mode may be possible in the material under test, for which case, modifications in the Weibull distribution equations have been proposed. The standard Weibull distribution function described in Section 2.2.2 assumes that there is only one type of flaw present in fibres, which determines its fracture behaviour. It has however been suggested by certain authors that multiple types of strength-determining flaws may also exist. To address that, multimodal Weibull distributions have been developed, such as the bimodal Weibull distribution given by Equation 2.10 [42]. Here $\sigma_{0,1}$ and $\sigma_{0,2}$ are scale parameters while m_1 and m_2 are Weibull moduli for the first and second flaw population, respectively.

$$P_R(\sigma) = 1 - \exp \left[- \left(\frac{L}{L_0} \right) \left(\frac{\sigma_f}{\sigma_{0,1}} \right)^{m_1} - \left(\frac{L}{L_0} \right) \left(\frac{\sigma_f}{\sigma_{0,2}} \right)^{m_2} \right] \quad (2.10)$$

Another type of distribution suggests adding an exponent α in the standard Weibull function to represent the dependency of fibre strength on gauge lengths, as given by Equation 2.11 [90].

$$P_R(\sigma) = 1 - \exp \left[- \left(\frac{L}{L_0} \right)^\alpha \left(\frac{\sigma_f}{\sigma_0} \right)^m \right] \quad (2.11)$$

Other similar distributions have also been proposed by Curtin et al. [84], Padgett et al. [24], Gurvich et al. [91], Phani [92] and Ibnabdeljalil [93]. The common problems with most of the developed distributions is that although they fit the fibre strength experimental data well, they are mainly based on curve fitting and do not have a solid physical background. Based on the goodness of fit, conclusions on the physical nature of the fibre strength behaviour have been made. This may have serious consequences as correlation may not necessarily mean causation. The fact that there can be limitations in the available experimental data has received less attention. More discussions on making such modifications on Weibull distribution has been provided in Section 8.2.

The discrepancy between experimental fibre strength data and the Weibull model would be addressed in detail in the later chapters of this thesis.

2.5.3 Uncertainty in results

It can be seen from Table 1.1 that different studies on T700 carbon fibres have carried out different number of tests for their analysis to determine the parameters of the Weibull distribution. The sample sizes used for most previous studies have been between 10-30. However, Danzer et al. [94] has shown that on the basis of results for a small sample size of 30 or less, it is not possible to differentiate between similar statistical functions.

Based on the size of the fibre strength data set used for analysis, the reliability of the different results can vary. Historically, assessments of significance in computed values of the strength distribution parameters have been made on the basis of visual examinations of graphical data or an appropriate data reduction technique using limited experimental data. There do not appear to be circumstances in which these assessments have been made on the basis of statistical analyses that account comprehensively for biases arising due to non-representativeness of the experimental data or measurement errors. Yet the values of the shape and scale parameters of the Weibull distribution are routinely reported with many significant figures (sometimes three or even more), and confidence intervals are rarely cited, an exception being Naito et al. (only standard deviations though) [95]. Assigning a level of confidence to fibre strengths and distributions using appropriate statistical techniques can be a way to add meaningful inferences about the population behaviour [43]. This knowledge can also potentially explain the observed differences in reported results by understanding the uncertainties in them.

Furthermore, it has been shown by Ilankeeran and Mohite [35], that each individual fibre strength measurement is prone to many experimental and statistical errors. However, very few studies have accounted for measurement errors when evaluating fibre strengths. The different causes which can contribute to errors in the fibre strength characterisation process will be identified, and their effect on the fibre strength and its distribution parameters will be statistically quantified in the upcoming chapters of the thesis.

2.6 Conclusions

The fibre strength distribution is the most important input parameter for composite strength models. Despite detailed investigations by many researchers, obtaining a representative Weibull distribution is still difficult. Contemplating the different limitations that each process contains, it seems that the classical single fibre testing process is still one of the most reliable and unambiguous means of characterising fibres or exploring their morphologies. The different individual steps in single fibre testing, however, leave scope for improvement, as discussed in Section 2.4. If the existing problems can be solved, the efficiency of the process can be significantly improved. The rest of the chapters in this thesis will aim at understanding and improving the single fibre testing process and the data reduction techniques, to assess the fibre strength distribution more accurately.

This thesis considers that the standard Weibull distributions are appropriate for representing the strength of fibres. However, how the fibre strength should be accurately modelled using the Weibull analysis will be discussed. The objective is not to obtain the best statistical representation of the experimentally generated fibre strength data by fitting it to existing models, but to find an accurate description of the fibre strength behaviour by appropriately analysing the fibre strength data and the data-reduction techniques used. The thesis focusses on improving the characterisation process for obtaining accurate and representative fibre strength distributions.

For improving the accuracy of the fibre strength distributions, it is crucial to improve the measured strength of individual fibres since any error in fibre strength would lead to errors in the corresponding fibre strength distribution. Prevention of measurement errors

requires a thorough understanding of the different parameters which might induce errors in measured fibre strength. However, it is true that despite best preventive measures, some errors are unavoidable in experimental measurements due to various reasons. Nevertheless, knowledge of these errors or uncertainty in experimentally determined fibre strength data can provide useful insights about the reliability that can be associated with model predictions, when uncertain fibre properties are fed as input to the models. Furthermore, different statistical techniques if applied to experimental fibre strength data can also provide useful information about the overall fibre strength behaviour. It can also help in obtaining a more accurate representation of the statistical variation in the strength of fibres inside an actual composite application.

The upcoming chapters will try to tackle the issues mentioned in this chapter.

Chapter summary in French

Résistance des fibres et distribution de Weibull: état de l'art

La défaillance des matériaux composites se produit généralement en raison de l'accumulation (localisée) des ruptures de fibres. La connaissance de la résistance des fibres est donc cruciale pour comprendre le comportement à rupture des matériaux et structures composites renforcés de fibres.

Les fibres techniques utilisées comme renforts dans les matériaux composites à matrice organique sont généralement de nature fragile. Les résistances des fibres fragiles telles que le carbone et le verre sont contrôlées par la distribution stochastique des défauts à l'intérieur de celles-ci, conduisant à des variations de la résistance des fibres individuelles. La résistance des fibres, par conséquent, ne peut pas être décrite par une seule valeur et est généralement représentée en utilisant une fonction statistique qui caractérise la distribution de la résistance. La fonction statistique la plus utilisée pour représenter la résistance des fibres fragiles est la distribution de Weibull. La caractérisation des fibres est difficile, car le diamètre de celles-ci ne dépasse pas quelques microns, en particulier pour les fibres de carbone. La très petite section transversale des fibres les rend très délicates à manipuler, ce qui conduit à un processus très fastidieux de préparation et de test des échantillons. Plusieurs méthodes sont disponibles pour accéder à la distribution de la résistance à rupture. Dans la méthode du faisceau de fibres, l'ensemble du faisceau est testé et les fibres sont supposées supporter une charge equi-répartie. Dans le test de fragmentation la distribution de la résistance à rupture peut être générée à partir d'une seule fibre noyée dans de la matrice, se pose la question de la représentativité. Enfin, le test sur fibre unitaire est l'une des techniques les plus simples et fiable mais c'est un processus long et laborieux.

Plusieurs difficultés influencent les résultats des tests sur fibre unitaire ou affectent la détermination de la distribution de la résistance des fibres. Il s'agit de l'alignement correct, du nombre de tests, de l'extraction des fibres, de la mesure précise de la section transversale, de la longueur optimale de jauge, etc. Dans ce chapitre, on considère que la distribution de Weibull standard à deux paramètres est appropriée pour représenter la résistance des fibres. Cependant, la façon dont la résistance de ces fibres doit être modélisée à l'aide de l'analyse de Weibull est discutée. L'objectif n'est pas d'obtenir la meilleure représentation statistique des données expérimentales en les ajustant aux modèles existants, mais de trouver une description juste de la résistance des fibres en analysant de manière appropriée l'ensemble des données disponibles. Afin d'améliorer les données sur la distribution de la résistance, il est crucial d'améliorer la mesure de la résistance sur les fibres pris individuellement, car toute erreur se répercute bien entendu sur la distribution. Minimiser les erreurs de mesure nécessite une compréhension approfondie des différents paramètres susceptibles de les induire. Quantifier ces erreurs ou incertitudes dans les données expérimentale fournit des informations permettant de quantifier la fiabilité des résultats obtenus via le modèle.

Chapter 3

Critical parameters in fibre strength measurement: identification and evaluation

***Abstract :** In this chapter, different possible sources of errors due to experimental limitations in the single fibre testing process have been identified. Their effect on fibre tensile strength has been analytically modelled. This model has been used to evaluate the uncertainty in experimentally determined fibre strength. A sensitivity analysis has been conducted to rank the relative significance of input quantities on the calculated fibre strength. Since composite models require fibre properties determined at very small gauge lengths, the results of the sensitivity analysis have been extrapolated to determine critical parameters for tests done at smaller gauge lengths of a few millimetres. It has been shown that for sufficiently long fibres, the strength depends mainly on the fibre diameter and failure forces, however for shorter gauge lengths, the effects of misalignment become very significant. This knowledge about the influence of different parameters on fibre strength can also help in designing improved single fibre testing systems capable of determining fibre strength more accurately.*

Contents

3.1	Introduction	49
3.2	Critical parameters in fibre strength measurement	50
3.2.1	Sources of uncertainty	50
3.2.2	Fibre tensile strength : Theoretical formulation	50
3.2.3	Measurement uncertainty	54
3.2.4	Experimentation	55
3.2.5	Evaluation of measurement uncertainty in input quantities	56
3.2.6	Propagation of uncertainty to fibre tensile strength	58
3.3	Sensitivity analysis	61
3.3.1	Sensitivity analysis for fibre tensile strength	62
3.3.2	Estimation of sensitivity for tensile strength at other gauge lengths	63
3.4	Conclusions	64
	Chapter summary in French	67

This chapter has been adapted from the following article:

F. Islam, S. Joannès, L. Laiarinandrasana, “Evaluation of critical parameters in tensile strength measurement of single fibres”, *Journal of Composites Science*. 2019, 3, 69.

3.1 Introduction

As described in Chapter 1, accurate fibre properties are crucial for composite strength models, however, various challenges in the characterisation process discussed in Chapter 2 introduces many uncertainties in the results. The first objective of this chapter is to identify the sources of uncertainties in experimentally determining the strength of a single fibre, which has not been considered by most previous studies. The effect of these sources of uncertainties on the measured fibre strength will also be quantified.

As already mentioned, a requirement for composite strength models is that the input fibre properties should be defined at specific gauge lengths. Almost all experimental data available is for fibre gauge lengths in the range of a few tens of millimetres [26]. The usual practice is to use results generated using longer fibre gauge lengths and then to extrapolate the properties to shorter gauge lengths using the Weibull scaling equation, as already discussed. This extrapolation can introduce more uncertainty in results as the standard Weibull scaling law may not be valid for all gauge lengths. If fibre properties are generated at shorter gauge lengths, it may be more appropriate and useful for the models as then the properties can directly be used as input without the need for extrapolation. However, tests done at shorter gauge lengths of a few millimetres are even more challenging, and more susceptible to experimental errors and uncertainties. In order to minimise these uncertainties, the effect of factors which contribute to these uncertainties should be minimised. The second objective of this chapter is thus to determine the most critical factors which lead to uncertainties in measurements of fibre tensile tests conducted at different gauge lengths.

In Section 3.2, different possible sources of errors due to experimental limitations in the fibre testing process have been identified and their effect on fibre tensile strength has been analytically modelled. This model has been used to statistically evaluate the uncertainties in experimentally determined fibre strength following the recommendations established by the “Guide to the expression of uncertainty in measurement” [96]. To determine the effect of the measurement uncertainty of input parameters on the calculated fibre strength, single fibre tensile tests using T700 carbon fibres have been conducted. T700 fibres are very commonly used as reinforcements in composites for structural applications. This section of the chapter addresses the following questions:

- *What are the different factors which affect fibre strength measurement?*
- *What uncertainties do these parameters introduce in the measured fibre strength?*

In Section 3.3, a sensitivity analysis has been conducted to understand the relative influence of different input parameters on the calculated fibre strength for different gauge lengths. This would help in identifying the most critical parameters which introduce errors and affect the accuracy of the calculated fibre strength. Minimising the effect of these critical parameters would help in improving the accuracy of the measured fibre tensile strength. The results from the sensitivity analysis will also be extrapolated to other gauge lengths in order to address the following question:

- *What are the critical parameters in fibre strength measurement at different gauge lengths?*

3.2 Critical parameters in fibre strength measurement

3.2.1 Sources of uncertainty

To determine fibre strength using the single fibre testing process, a single filament is subjected to a tensile test and different input quantities are measured which are used for calculating the strength. Improperly prepared fibre specimens can result in errors in measured fibre strength. Moreover, no measurement is perfectly accurate and there is some degree of uncertainty associated with every measurement. To illustrate these points, the standard card frame method of single fibre tensile testing has been used. The schematic diagram of a prepared fibre specimen is shown in Figure 3.1(a). For ensuring a good accuracy of the test, the following measures are important:

- To align the fibre with the loading direction as perfectly as possible,
- To control the gauge length as accurately as possible, since fibre strength is length dependent.

However, it is very difficult to align the fibres perfectly to the centreline and also to fix the gauge length accurately [43]; which can lead to errors, such as the one shown in Figure 3.1(b). These lead to angular misalignment of the fibre specimen and inaccurate measurement of gauge length, respectively (Figure 3.1(c)). The tensile machine itself may have a slight offset of the jaws. This is a common error and should be avoided by the tester as much as possible. This could also lead to alignment inaccuracy between the fibre and the loading direction. For the continuation of this work, no distinction will be made between these different sources of misalignment and the concerned quantities will be treated in such a way as to encompass all possible sources. The misalignment parameter is therefore treated as a whole. In particular, no mention will be made of the different fixing techniques and the results would be independent of the machines used for conducting single fibre tensile tests.

3.2.2 Fibre tensile strength : Theoretical formulation

Fibre strengths are not measured directly but are calculated using measured quantities, precisely by dividing the measured force to failure F_R by the cross-sectional area A of the fibre. Depending on the nature of the fibre, the section area can be constant (as for most synthetic fibres) or it may vary along the length as is the case for natural fibres and for which case the A -section should correspond to the section at the break point [87, 97]. Unless this breaking section measurement can be done in-situ or post-mortem, this data is often inaccessible and most of the time, a “mean” cross-section is used (average along the length), which is also the case for the present study. Given the high slenderness or aspect-ratio of the tested fibres and the very small sections considered, the notion of average over the length is still questionable. Assumptions which will be discussed later in this work must always be considered. Nevertheless, the basic functional relationship for calculating

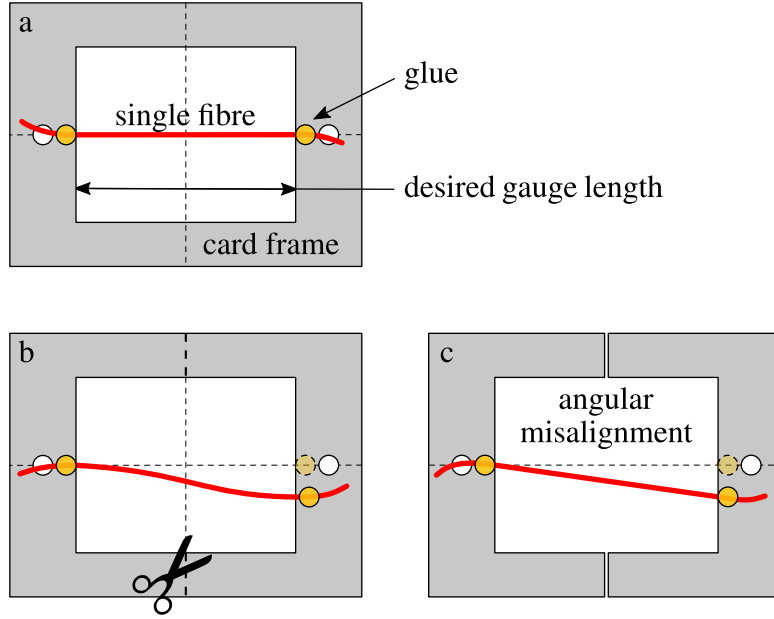


Figure 3.1: (a) Schematic diagram of a single fibre mounted on a card frame, (b) Major issues with sample preparation leading to inaccurate measurement of gauge length, (c) Angular misalignment in the fibre specimen

fibre strength¹ σ_R is given by Equation 3.1.

$$\sigma_R = \frac{F_R}{A} \quad (3.1)$$

As already explained, there can be misalignment between the fibre axis and the loading direction. Due to this misalignment, the entire load applied during the test may not be successfully transferred to the fibre. The effective load applied on the fibre depends on the conic angle of misalignment α . Figure 3.2 (top) shows the influence of misalignment on the effective force transferred to the fibre. Only a component $F_{\mathcal{R}}$ of the applied force F_R is successfully subjected onto the fibre, which varies depending on the misalignment angle. For a given angle of misalignment α , the effective force transferred to the fibre is $F_{\mathcal{R}} = F_R \cos \alpha$ and the corresponding fibre strength is obtained by Equation 3.2. If an assumption of perfect circularity can be made for the fibre cross-section, A value can be derived from the measurement of the diameter² D , which results in Equation 3.3.

¹or any stress at time t , i.e. $\sigma = \sigma(t)$ corresponding to the load $F = F(t)$; in that case Equation 3.1 will become $\sigma = F/A$

²Very often, only the “apparent” diameter is accessible to measurement and non-convex cross-sections lead to more challenges to determine A .

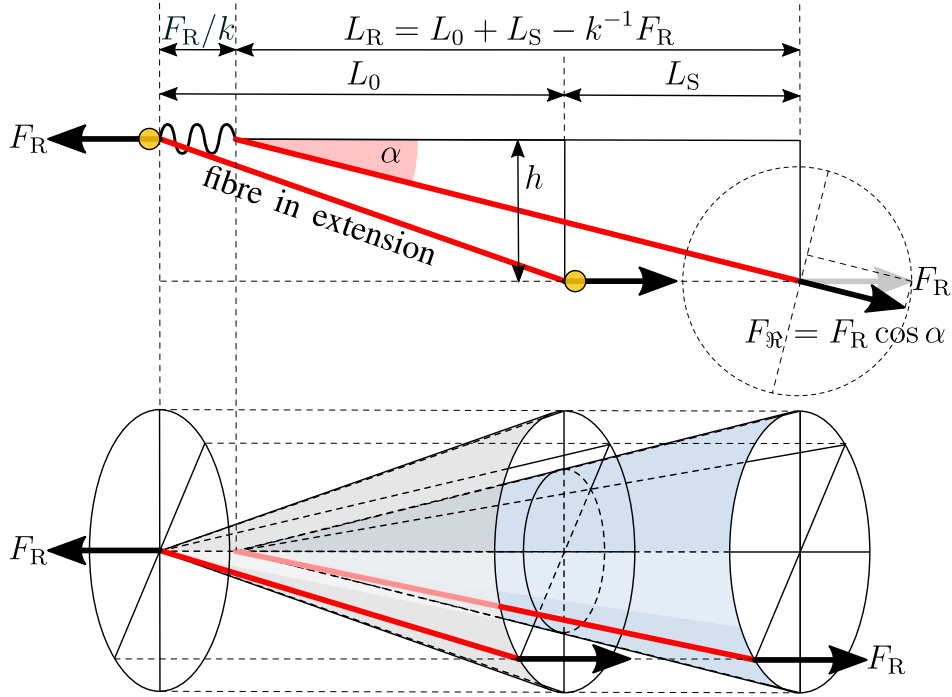


Figure 3.2: Schematic diagram showing the effect of fibre misalignment on the effective load transferred to the fibre. Figure on top also shows the effect of fibre elongation and system compliance on the instantaneous gauge length of the fibre, as measured by the displacement transducer. Figure on bottom shows that fibre misalignment can occur in any direction in 3-dimensions, i.e. the fibre can be positioned anywhere inside a cone of angle α .

$$\sigma_R = \frac{F_R \cos \alpha}{A} \quad (3.2)$$

$$= \frac{F_R \cos \alpha}{\pi D^2/4} \quad (3.3)$$

The misalignment angle α can further be resolved in terms of the misaligned distance h and L_R using the laws of trigonometry and is given by Equations 3.4 and 3.5. L_R is the recorded length of the fibre specimen and depends on the instantaneous separation of the cross-heads. The misalignment can be in any direction, depending upon the conical angle α , as shown in Figure 3.2. From Equations 3.5 and 3.3, the expression for fibre strength in terms of the measured quantities can be obtained, and is given by Equation 3.6.

$$\cos \alpha = \frac{L_R}{(L_R^2 + h^2)^{\frac{1}{2}}} \quad (3.4)$$

$$= \left(1 + \frac{h^2}{L_R^2}\right)^{-\frac{1}{2}} \quad (3.5)$$

$$\sigma_R = \frac{4F_R}{\pi D^2} \left[1 + \left(\frac{h}{L_R}\right)^2\right]^{-\frac{1}{2}} \quad (3.6)$$

L_R can be replaced by $L = L(t)$ if instantaneous values F and σ are used, since the alignment of the fibre would change with time as the jaws are separated from each other. It is dependent on the initial gauge length of the fibre L_0 , on fibre elongation due to application of tensile stress L_S , and on the stiffness of the testing system k (or compliance $c = 1/k$) and is given by Equation 3.7. This is also shown in Figure 3.2. From Equations 3.6 and 3.7 the expression for fibre strength can be obtained, and is given by Equation 3.8.

$$L_R = L_0 + L_S - k^{-1}F_R \quad (3.7)$$

$$\sigma_R = \frac{4F_R}{\pi D^2} \left[1 + \left(\frac{h}{L_0 + L_S - k^{-1}F_R}\right)^2\right]^{-\frac{1}{2}} \quad (3.8)$$

The stiffness k of the experimental setup is determined by taking the inverse of the system compliance, which was measured as per the guidelines mentioned in the standard [66]. The stiffness for the experimental setup used, including the fibre fixing system, was calculated to be around 6×10^3 N/m. Such a high stiffness has a negligible influence on the recorded failure length L_R of the fibre, especially for tests done using fibres of 30 mm initial gauge length, as in the present case. For such long gauge lengths and the T700 fibres that will be considered as an example, the contributions of the different quantities to L_R were calculated to be as follows: L_0 almost 98%, L_S about 2% and $k^{-1}F_R$ less than 0.01%. These contributions strongly depend on the gauge length and if a shorter gauge length of 5 mm was considered, the system compliance contribution to L_R would have been larger, although still only around 0.5%, as a first approximation. For this reason, the term $k^{-1}F_R$ was ignored from the fibre strength expression for the present case when compared with L_0 . This is also justified because its contribution to the output is about an order of magnitude smaller than the next significant quantity. However, these considerations would be completely different if a measure of the failure strain ε_R was desired. Indeed, in that case, failure strain $\varepsilon_R = (L_S - k^{-1}F_R)/L_0$, and the system stiffness/compliance contributes greatly³ to the extension measurement.

³About 25% contribution to the total extension in the case of a gauge length of 5 mm.

The final expression for fibres strength after ignoring the system stiffness/compliance contribution is given by Equation 3.9.

$$\sigma_R = \frac{4F_R}{\pi D^2} \left[1 + \left(\frac{h}{L_0 + L_S} \right)^2 \right]^{-\frac{1}{2}} \quad (3.9)$$

It can be seen from Equation 3.9 that the fibre strength depends on a number of measured input quantities. These quantities, already introduced, are force measurement from the load cell F_R , estimated misalignment distance h , initial gauge length of the fibre L_0 , extension in fibre measured from the displacement sensor L_S , and the measured value of the diameter D coming from an appropriate technique. Each input quantity has some level of measurement uncertainty, as no measuring instrument is perfectly accurate. As a result the calculated tensile strength of the fibre will also have an uncertainty associated with it. This uncertainty will be evaluated in the next subsections.

Another source of uncertainty could be the way in which the fibres are bonded to form a test specimen. Bonding inconsistencies can include slipping between the bond and the fibre during testing. However, this will mostly affect the measured strain and load jumps will also be present. These slipping effects are not considered (not occurring) in this work. To some extent the bonding uncertainty is also built into the compliance of the system.

When fibre misalignment exists, a curvature occurs near the ends of the fibre where it is bonded, since the fibre acts like a beam. Multi-axial stresses can develop in the fibre as a result of this. This effect will be larger for short fibres as compared to longer ones, but has not been considered in this study.

3.2.3 Measurement uncertainty

The word ‘‘uncertainty’’ stands for doubt, and thus in a generic sense ‘‘measurement uncertainty’’ means doubt about the validity of a result of a measurement [96]. It reflects the lack of knowledge on the value of the measured quantity. This uncertainty in measurement of any quantity would also influence other parameters which are calculated using these measured quantities. The measurement uncertainty for any given parameter can be calculated statistically if the variations are known for all quantities on which this parameter depends. This is evaluated by using a mathematical model for the parameter of interest (Y), which is a function of all input quantities on which it depends (X_1, X_2, \dots, X_n), as also represented by Equation 3.10.

$$Y = f(X_1, X_2, \dots, X_n) \quad (3.10)$$

Each measured input quantity by itself has some uncertainty associated with it. The uncertainty is determined from a distribution of the possible values for a given quantity, using one of the two commonly used methods. The first is a frequency based estimation method, using which the uncertainty is estimated from a series of observations for a given quantity. This method of evaluation of uncertainty based on frequency distributions is termed as Type A evaluation in statistics. The second method of evaluating uncertainty

is from a priori distribution which is based on some prior knowledge about the quantity. Evaluation of uncertainty based on priori distributions are termed as Type B evaluation. It is recommended to use quantitative data wherever possible for the evaluation of uncertainty, i.e. following the Type A evaluation method. However, either type of uncertainty is treated in the same way while evaluating their combined effect on the output.

3.2.4 Experimentation

Single fibre tensile tests were conducted following the procedure described in ASTM C1557-14 [66] to determine the strength of T700 carbon fibres. The equations proposed in this paper remain of course valid for other types of fibres, as long as the few assumptions which have been made are applicable. The universal tensile tester has been used for conducting the experiments. It was developed by Bunsell [98] and has been improved over the years with the introduction of more advanced transducers and sensors and a change from the vertical position to the horizontal position of the system. These changes have, for example, made it possible to study the effect of temperature on fibre strength and this improved setup has also been used very extensively to study many kinds of technical, natural and textile fibres [99, 100, 101, 102, 103]. Single fibres were extracted from the fibre bundles and mounted on paper frames containing cut-out slots of 30 mm in the middle, as shown in Figure 3.3, to fix the fibre gauge length L_0 to 30 mm, or as close as possible to this desired value.

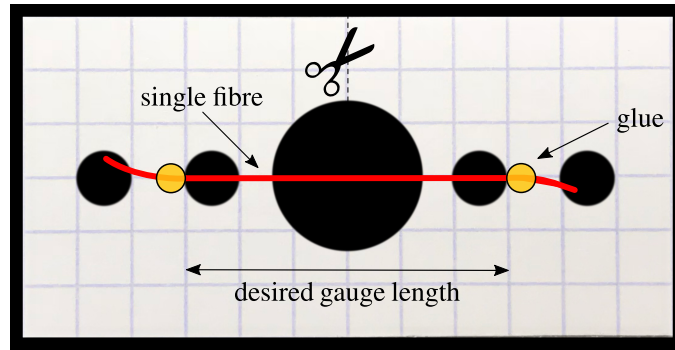


Figure 3.3: The actual card frame used for preparing the fibre specimens.

The diameter of each individual fibre specimen was measured at different locations along the fibre length before the fibre was subjected to the tensile test. A Mitutoyo laser scanning micrometre (LSM500) system was used for the measurements. This system allows rapid, non-contact, and accurate fibre dimensional measurements. The fibre is fixed between two grips and a perpendicular laser beam scans across the fibre. The time of obstruction of the light is recorded and the diameter is calculated. A total of 30 fibres were measured following the laser scanning scanning microscopy system and tested as per the given standard. A constant displacement rate of 1 mm/min was applied to stretch the fibres until failure. The failure load F_R was recorded using a 150 g Sensotec Model 31 load-cell and the fibre extension was measured using an LVDT displacement transducer ACT1000A from RDP Electronics Ltd. The test results were also compliance corrected as per the standard ASTM C1557-14.

The failure load was taken to be the load at which the fibre fracture occurs. Table 3.1 shows the measured values of all input quantities for one fibre tensile test example. Using these quantities and Equation 3.9, the best estimate value⁴ of fibre strength σ_R^{best} for the given example is calculated and is given as:

$$\sigma_R^{\text{best}} = 4.36 \text{ GPa} \quad (3.11)$$

Table 3.1: Best estimate values of all quantities for one single fibre tensile test

S.N.	Quantity	Value	Unit
1	F_R	0.16	N
2	h	1	mm
3	L_0	30	mm
4	L_S	0.69	mm
5	D	6.7×10^{-3}	mm

3.2.5 Evaluation of measurement uncertainty in input quantities

All quantities necessary for calculating fibre strength were determined through experimental measurements following the method described in the previous section. Each measurement has some amount of uncertainty associated with them. Measured quantities thus are sometimes reported as given by Equation 3.12 where x is the quantity being measured, x^{best} is the best estimate or the measured value and $u(x)$ is the corresponding measurement uncertainty.

$$x = x^{\text{best}} \pm u(x) \quad (3.12)$$

For each tensile test, the best estimate and the corresponding uncertainty for each input quantity was determined. For fibre diameter, the best estimate was determined by taking the average of all the multiple measurements taken at different locations along the fibre length. For the other quantities, i.e. applied force F_R , misalignment distance h , initial gauge length L_0 and elongation in fibre L_S , the best estimate was determined from the only measurement coming from the fibre tensile test.

Measurement uncertainty in fibre diameter $u(D)$ was determined using the Type A method. The standard deviation was calculated from the different diameter values measured along the length of a fibre, for each specimen. When multiple trials are performed to obtain the best estimate of a quantity, the standard deviation of the mean is an appropriate choice for representing the uncertainty in the measurement [96]. For example, from the multiple measurements D_i of the fibre diameter, the best estimate is determined by taking the average of all measurements, \bar{D} , and the uncertainty, $u(D)$, is provided by the corrected

⁴the value determined experimentally or calculated analytically, i.e. without considering any uncertainties.

standard deviation divided by the square root of the number of measures n_D as given by Equations 3.13 to 3.15.

$$D = \bar{D} \pm u(D) \quad (3.13)$$

$$\bar{D} = \frac{1}{n_D} \sum_{i=1}^{n_D} D_i \quad (3.14)$$

$$u(D) = \frac{1}{\sqrt{n_D}} \left[\frac{1}{n_D - 1} \sum_{i=1}^{n_D} (D_i - \bar{D})^2 \right]^{\frac{1}{2}} \quad (3.15)$$

For the given example, \bar{D} was evaluated at 6.725×10^{-3} mm from four recorded values $\{6.6, 6.8, 6.7, 6.8\} \times 10^{-3}$ mm and uncertainty in diameter measurement was calculated to be $u(D) = 0.055 \times 10^{-3}$ mm.

On the other hand, since for the other quantities, i.e. F_R , h , L_0 and L_S , the best estimate is taken from the only measurement coming from the instruments, their corresponding uncertainty was estimated using the Type B method. For this, the limiting precision, or the estimation error, or the tolerances of the measurement tool was used. The uncertainty for these quantities was estimated on the assumption of the rectangular probability distribution of the measurement tolerances or estimation errors, and can be given by Equation 3.16.

$$u^2(X) = \left(\frac{\Delta X}{\sqrt{3}} \right)^2 \quad (3.16)$$

where $u(X)$ can be replaced with $u(F_R)$, $u(h)$, $u(L_0)$ and $u(L_S)$, which are the measurement uncertainties for force, misalignment distance, initial gauge length, fibre extension, respectively while ΔX can be replaced with ΔF_R , Δh , ΔL_0 and ΔL_S , which are the measurement tolerances or estimation errors for the corresponding quantities.

The measurement uncertainty for all the quantities for the given fibre tensile test example is given in Table 3.2. For many commercial and industrial applications it is suggested to also calculate an expanded uncertainty $U(x)$ which is a measure of the required quality for the given quantity of interest x . The expanded uncertainty is determined for a required level of confidence using the expression given by Equation 3.17.

$$U_{95}(x) = t_{95} \times u(x) \quad (3.17)$$

where, t_{95} is a coverage factor for a 95% level of confidence. For many applications, the recommended level of confidence is 95% [96]. The value of t_{95} is 1.96 if the calculation is based on a very large number of measured quantities, i.e. $n \rightarrow \infty$. It should be noted that if the number n of measurements is small, the coverage factor should be taken from the T-distribution table for $n - 1$ degrees of freedom. This leads, for example to a coverage factor of about 3.18 for $n = 4$, which is the case for diameters measurements ($n_D = 4$). Table 3.2 also includes these expanded uncertainty values for the given input quantities.

For more critical applications, an even higher level of confidence may be required, and a confidence level of 99% is also commonly used. The coverage factor depends on the confidence level used and can be determined from the T-distribution table, as explained before. For a 99% confidence level, the coverage factor t_{99} is 2.58 for $n \rightarrow \infty$ and is 5.84 for $n = 4$. The expanded uncertainty values of all input quantities for the given fibre tensile test example, for a confidence level of 99% are also given in Table 3.2.

Table 3.2: Measurement uncertainty values of all input quantities for the given fibre tensile test example, along with expanded uncertainty for a confidence level of 95% and 99%.

S.N.	Quantity (X)	Measurement Uncertainty $u(X)$	Expanded Uncertainty $U_{95}(X)$	Expanded Uncertainty $U_{99}(X)$	Unit
1	F_R	1.27×10^{-3}	2.48×10^{-3}	3.28×10^{-3}	N
2	h	0.28	0.55	0.72	mm
3	L_0	0.34	0.66	0.88	mm
4	L_S	0.71	1.38	1.86	mm
5	D	5.5×10^{-5}	1.8×10^{-4}	3.2×10^{-4}	mm

Measurement uncertainties in these input quantities will also be propagated into the calculated fibre strength. The uncertainty propagated into fibre strength can be evaluated by combining the measurement uncertainties for each input quantity. The evaluation of this combined standard uncertainty for measured fibre strength is described in Section 3.2.6.

3.2.6 Propagation of uncertainty to fibre tensile strength

The standard uncertainty for a given parameter which is obtained from the determined uncertainties of a number of other quantities is known as combined standard uncertainty. It is estimated by appropriately combining the uncertainties of the input quantities using the law of propagation of uncertainty, as described in [96]. It is an estimated standard deviation of the parameter and characterizes the dispersion in its values. It is obtained by taking the positive square root of the combined variance of the fibre strength. The combined standard uncertainty for fibre strength $u_c(\sigma)$ as obtained from the combined variance $u_c^2(\sigma)$ is given by Equation 3.18.

$$u_c^2(\sigma) = \sum_{i=1}^N \left(\frac{\partial \sigma}{\partial x_i} \right)^2 u^2(x_i) \quad (3.18)$$

Each $(\partial \sigma / \partial x_i)$ is a partial derivative or sensitivity coefficient of fibre strength for each of the input quantities on which it depends. It describes how the output estimate, i.e. fibre strength, varies with changes in each input quantity. Each $u(x_i)$ is a standard uncertainty for an input quantity x_i as already described in Section 3.2.5. Variation in fibre strength arising due to uncertainty in an input quantity x_i is given by $(\partial \sigma / \partial x_i) u(x_i)$. The combined variance on fibre strength $u_c^2(\sigma)$ can be given by the sum of all variances generated due to uncertainties in each individual quantity x_i as given by Equation 3.18. This expression is valid when there is no correlation between the quantities on which

the parameter depends, as in the present case. The expression for the combined standard uncertainty of fibre strength given by Equation 3.18 can be expanded in terms of individual quantities and is given by Equation 3.19.

$$u_c^2(\sigma) = \left(\frac{\partial\sigma}{\partial F_R}\right)^2 u^2(F_R) + \left(\frac{\partial\sigma}{\partial h}\right)^2 u^2(h) + \left(\frac{\partial\sigma}{\partial L_0}\right)^2 u^2(L_0) + \left(\frac{\partial\sigma}{\partial L_S}\right)^2 u^2(L_S) + \left(\frac{\partial\sigma}{\partial D}\right)^2 u^2(D) \quad (3.19)$$

where, $u_c(\sigma)$ is combined standard uncertainty for fibre strength, $(\partial\sigma/\partial F_R)$ is sensitivity coefficient of fibre strength for applied force, $(\partial\sigma/\partial h)$ is sensitivity coefficient of fibre strength for misaligned distance, $(\partial\sigma/\partial L_0)$ is sensitivity coefficient of fibre strength for initial gauge length, $(\partial\sigma/\partial L_S)$ is sensitivity coefficient of fibre strength for fibre extension, $(\partial\sigma/\partial D)$ is sensitivity coefficient of fibre strength for measured fibre diameter, $u(F_R)$ is measurement uncertainty in applied force, $u(h)$ is measurement uncertainty in misaligned distance, $u(L_0)$ is measurement uncertainty in gauge length, $u(L_S)$ is measurement uncertainty in fibre extension and $u(D)$ is measurement uncertainty in fibre diameter.

The different sensitivity coefficients are determined as partial derivatives of fibre strength with respect to each input quantity and are given by Equations 3.20 to 3.24.

$$\frac{\partial\sigma}{\partial F_R} = \frac{4}{\pi D^2} \left[1 + \left(\frac{h}{L_0 + L_S}\right)^2\right]^{-\frac{1}{2}} \quad (3.20)$$

$$\frac{\partial\sigma}{\partial h} = -\frac{4F_R}{\pi D^2} \left[1 + \left(\frac{h}{L_0 + L_S}\right)^2\right]^{-\frac{3}{2}} \left(\frac{h}{L_0 + L_S}\right) \quad (3.21)$$

$$\frac{\partial\sigma}{\partial L_0} = \frac{4F_R}{\pi D^2} \left[1 + \left(\frac{h}{L_0 + L_S}\right)^2\right]^{-\frac{3}{2}} \left[\frac{h^2}{(L_0 + L_S)^3}\right] \quad (3.22)$$

$$\frac{\partial\sigma}{\partial L_S} = \frac{4F_R}{\pi D^2} \left[1 + \left(\frac{h}{L_0 + L_S}\right)^2\right]^{-\frac{3}{2}} \left[\frac{h^2}{(L_0 + L_S)^3}\right] \quad (3.23)$$

$$\frac{\partial\sigma}{\partial D} = -8\frac{F_R}{\pi D^3} \left[1 + \left(\frac{h}{L_0 + L_S}\right)^2\right]^{-\frac{1}{2}} \quad (3.24)$$

For the considered fibre tensile test example given earlier in Table 3.1, the sensitivity coefficient for each quantity is determined using Equations 3.20-3.24 and input data from Table 3.1, and the results are given in Table 3.3. The combined standard uncertainty for the calculated fibre strength can then be evaluated from Equation 3.19, using measurement

Table 3.3: Sensitivity coefficient values of all quantities

S.N.	Quantity	Value	Unit
1	$\partial\sigma/\partial F_R$	2.81×10^{10}	m^{-2}
2	$\partial\sigma/\partial h$	4.63×10^9	$N \cdot m^{-3}$
3	$\partial\sigma/\partial L_0$	1.51×10^8	$N \cdot m^{-3}$
4	$\partial\sigma/\partial L_S$	1.51×10^8	$N \cdot m^{-3}$
5	$\partial\sigma/\partial D$	-1.30×10^{15}	$N \cdot m^{-3}$

uncertainty from individual quantities from Table 3.2 and sensitivity coefficient values from Table 3.3.

The standard uncertainty for fibre strength for the considered example was calculated to be:

$$u_c(\sigma) = 0.08 \text{ GPa}$$

Fibre strength for the given tensile test example can now be represented as a combination of the best estimate σ_{best} and the calculated uncertainty u_c , shown as follows:

$$\sigma = 4.36 \text{ GPa with } u_c(\sigma) = 0.08 \text{ GPa}$$

Following the determination of combined standard uncertainty $u_c(\sigma)$ using Equation 3.19, the expanded uncertainty $U(\sigma)$ was also calculated. It was determined by using Equation 3.17, as explained earlier. The value of the coverage factors t_{95} and t_{99} as determined from the T-distribution table for 95% and 99% level of confidence are 1.96 and 2.58, respectively. Using $t_{95} = 1.96$ and $t_{99} = 2.58$, the expanded uncertainties were calculated from Equation 3.17 as $U_{95}(\sigma) = 0.16 \text{ GPa}$ and $U_{99}(\sigma) = 0.21 \text{ GPa}$. It is necessary to mention the values of coverage factor and level of confidence that has been used when results are reported in the form of expanded uncertainties. The fibre strength can then be reported as the best estimate σ_{best} along with its expanded uncertainties $U_{95}(\sigma)$ and $U_{99}(\sigma)$ as follows:

$$\sigma = (4.36 \pm 0.16) \text{ GPa, for a confidence level of 95\%}$$

$$\sigma = (4.36 \pm 0.21) \text{ GPa, for a confidence level of 99\%}$$

For all the 30 fibre tensile tests conducted, the best estimate for fibre strength σ and the corresponding measurement uncertainty $u_c(\sigma)$, are given in Table 3.4, in increasing order of strength values. The scatter in failure stress (fibre strength) vs failure strain is shown in Figure 3.4. As expected, the strength of fibres vary significantly with each other and hence cannot be represented using a single average value, because not all fibres possess a similar strength. These results will be represented by using a Weibull distribution [23] in the next chapter.

Table 3.4: Best estimates and measurement uncertainty of fibre strength for 30 tensile tests

S.N.	σ (GPa)	$u_c(\sigma)$ (GPa)	S.N.	σ (GPa)	$u_c(\sigma)$ (GPa)	S.N.	σ (GPa)	$u_c(\sigma)$ (GPa)
1	1.69	0.07	11	3.23	0.10	21	4.36	0.08
2	1.78	0.07	12	3.28	0.11	22	4.45	0.12
3	1.97	0.06	13	3.48	0.08	23	4.49	0.05
4	2.23	0.03	14	3.50	0.18	24	4.72	0.09
5	2.56	0.06	15	3.52	0.17	25	4.73	0.12
6	2.72	0.03	16	3.68	0.14	26	4.85	0.06
7	2.73	0.05	17	3.75	0.09	27	5.44	0.31
8	2.82	0.05	18	3.82	0.07	28	5.68	0.08
9	2.93	0.06	19	4.04	0.06	29	5.99	0.17
10	3.03	0.09	20	4.15	0.12	30	6.92	0.10

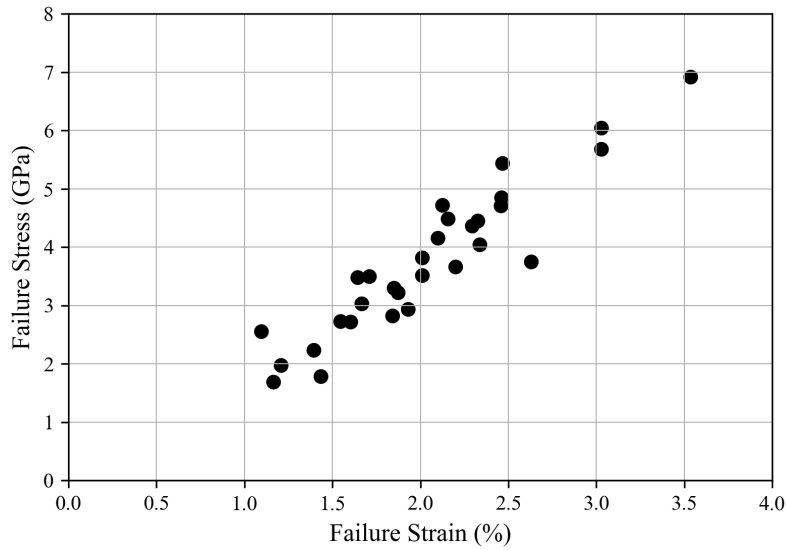


Figure 3.4: Failure stress vs failure strain scatterplot for all fibre tensile tests

3.3 Sensitivity analysis

It has been shown how uncertainty analysis focuses on quantifying the uncertainty in a model output, which is fibre tensile strength in the present study. An uncertainty analysis is ideally followed by what is known as a sensitivity analysis. While uncertainty analysis assesses the uncertainty in a model output that derives from uncertainty in inputs, a sensitivity analysis assesses the individual contributions of the inputs to the total uncertainty in outcomes of the analysis. An input can be classified as anything which causes a variation in the output of the model. Sensitivity analysis highlights the relative importance

of inputs in determining the outputs. A sensitivity analysis was conducted for single fibre tensile strength tests to determine the relative influence of the different input quantities on fibre strength and is described in Section 3.3.1.

3.3.1 Sensitivity analysis for fibre tensile strength

For the fibre strength model given by Equation 3.9, the input consists of the different quantities which determine the strength. Of the different known methods for sensitivity analysis, the method of derivatives is the most widely used [104]. According to this method, sensitivity of a given output Y for an input X , is a function of the derivative $\partial Y/\partial X$. In order to normalize the sensitivity for all quantities, this sensitivity is multiplied and divided by the standard deviations of the output and input, respectively, as given by Equation 3.25.

$$S_X^\sigma = \frac{\sigma_X \partial Y}{\sigma_Y \partial X} \quad (3.25)$$

where S_X^σ is the sensitivity of the output for an input quantity X and normalized by the standard deviations; σ_X is the standard deviation of the input; σ_Y is the standard deviation of the output and $\partial Y/\partial X$ is the partial derivative of the output for the given input quantity. It is also recommended to report the square of the sensitivity measure since the sum of squares of the sensitivity neatly normalizes to 1 for r different quantities, as given by Equation 3.26 [104].

$$\sum_{r=1}^n (S_{X_i}^\sigma)^2 = 1 \quad (3.26)$$

For the given fibre tensile test example discussed in Section 3.2, the sensitivity values for all 5 input quantities were calculated using Equation 3.25. The calculated sensitivity values for each input quantity along with its relative rank of influence is given in Table 3.5.

Table 3.5: Sensitivity measures of each input quantity for the given single fibre tensile test example

Rank	Input	Sensitivity	Sensitivity ²
1	D	0.89	0.79
2	F_R	0.45	0.20
3	h	1.63×10^{-2}	2.67×10^{-4}
4	L_S	1.33×10^{-3}	1.76×10^{-6}
5	L_0	6.35×10^{-4}	4.03×10^{-7}

Sensitivity measures of input quantities were also calculated for all the 30 tensile tests shown earlier in Table 3.4. From the obtained results, the average sensitivity value for each quantity was calculated and is given in Table 3.6.

From the sensitivity analysis it can be seen that the measured fibre diameter D is the most sensitive or critical parameter for the determination of fibre strength from the single

Table 3.6: Average sensitivity measures for each input quantity for the set of 30 single fibre tensile test

Rank	Input	Sensitivity	Sensitivity ²
1	D	0.81	0.66
2	F_R	0.48	0.23
3	h	0.02	2.33×10^{-4}
4	L_S	1.26×10^{-3}	1.58×10^{-6}
5	L_0	6.03×10^{-4}	3.64×10^{-7}

fibre tensile testing process. This is followed by the measured force of fibre failure F_R . The other parameters are relatively much less significant and do not contribute much to the accuracy of the calculated fibre strength. It is however very important to note that, for the present study, the sensitivity indices have been calculated for single fibre tensile strength tests conducted at a gauge length of 30 mm. However, since different studies use different gauge lengths varying from 1-50 mm for determining fibre tensile strength, it would be useful to estimate the relative sensitivities of the input quantities for tensile tests conducted at other gauge lengths as well. For a different gauge length, the relative sensitivities of all the input quantities may change. Estimation of sensitivity measures of the input quantities for fibre tensile tests at other gauge lengths have been discussed in Section 3.3.2.

3.3.2 Estimation of sensitivity for tensile strength at other gauge lengths

As mentioned previously, fibre properties determined at smaller gauge lengths may be more appropriate to be used as input for composite strength and damage models. However, tests done at small gauge lengths are more susceptible to experimental errors and uncertainties. In order to minimise these uncertainties, the effect of critical quantities which contribute to these uncertainties have to be minimised. These critical quantities may be different for tests done at different gauge lengths. An estimation of these critical quantities different gauge lengths will be discussed in this subsection.

To determine the sensitivity indices for input quantities at different gauge lengths, the fibre strength data for a gauge length of 30 mm, from Table 3.4 was used. Since the tensile strengths of brittle fibres are assumed to follow the Weibull distribution, the fibre failure forces for all 30 tensile tests were extrapolated to different shorter gauge lengths using a modified form of the Weibull scaling function, given earlier by Equation 1.2. This extrapolation has been made under the assumption that the fibre cross-sectional area remains constant during the test, which permits the extrapolation of failure loads to fibres of shorter gauge lengths. The other assumption was that the failure strain of the fibres does not vary significantly for different gauge lengths. Both of these assumptions are realistic and already well established in the literature. Using the extrapolated data, fibre strength and the corresponding uncertainty was calculated for all the fibres using Equation 3.9 and the method described in Section 3.2.6, respectively. This was followed by the calculation of sensitivity measures for all quantities as already described. The sensitivity indices for

all input quantities and for different gauge lengths are given in Table 3.7 and depicted graphically in Figure 3.5. It can be seen that as the gauge length is decreased from 30 mm to 20 mm, the sensitivity measures for all quantities remain fairly consistent. However, fibre misalignment h which was relatively insignificant for tests at 30 mm gauge length increases in significance and can no longer be ignored. For a shorter gauge length of 10 mm, fibre misalignment becomes even more significant. The other quantities, i.e. measured fibre extension L_S and measured fibre gauge length L_0 are also observed to slightly increase in significance. On further reducing the gauge length to 5 mm, the sensitivity of fibre misalignment increases further and it becomes one of the most critical parameters. The significance of fibre extension and fibre gauge length can also be observed to increase. Since the sensitivity measure is a relative quantity, this increase comes at a cost of a decrease in sensitivity for the other major quantities, i.e. fibre diameter and failure force, which are both observed to decrease in relative significance. If the gauge length is reduced to 2.5 mm, the significance of the following input quantities: fibre misalignment, fibre extension and fibre gauge length further continue to increase substantially due to which the significance of the other quantities, i.e. failure forces and fibre diameter continue to decrease drastically.

Table 3.7: Sensitivity indices of different input quantities in tensile strength measurement of fibres at different gauge lengths

	30 mm	20 mm	10 mm	5 mm	2.5 mm
Input ↓	S	S	S	S	S
D	0.81	0.83	0.85	0.74	0.33
F_R	0.48	0.45	0.38	0.25	0.08
h	0.02	0.04	0.15	0.47	0.62
L_S	1.26×10^{-3}	4.36×10^{-3}	0.04	0.23	0.61
L_0	6.03×10^{-4}	2.09×10^{-3}	0.02	0.11	0.29

Taking into consideration the results from the sensitivity analysis, it would be recommended to be very careful when conducting experimental studies with the single fibre testing methodology using fibres of very short gauge lengths. This is to avoid unwanted errors in measured fibre tensile strength due to fibre misalignment, improper measurement of fibre gauge length and fibre extension since it becomes very difficult to accurately control these quantities when fibres of a very small gauge length are used. The sensitivity of fibre tensile strength to these quantities is very high and even small measurement errors in these input quantities may lead to large inaccuracies in estimated strength.

3.4 Conclusions

In this chapter, different possible sources of errors due to experimental limitations in the fibre testing process have been identified. Their effect on fibre tensile strength has been analytically modelled. This model was then used to statistically evaluate the uncertainties in experimentally determined fibre strength. Additionally, a sensitivity analysis has been conducted using a differential method, to rank the relative significance of input quantities

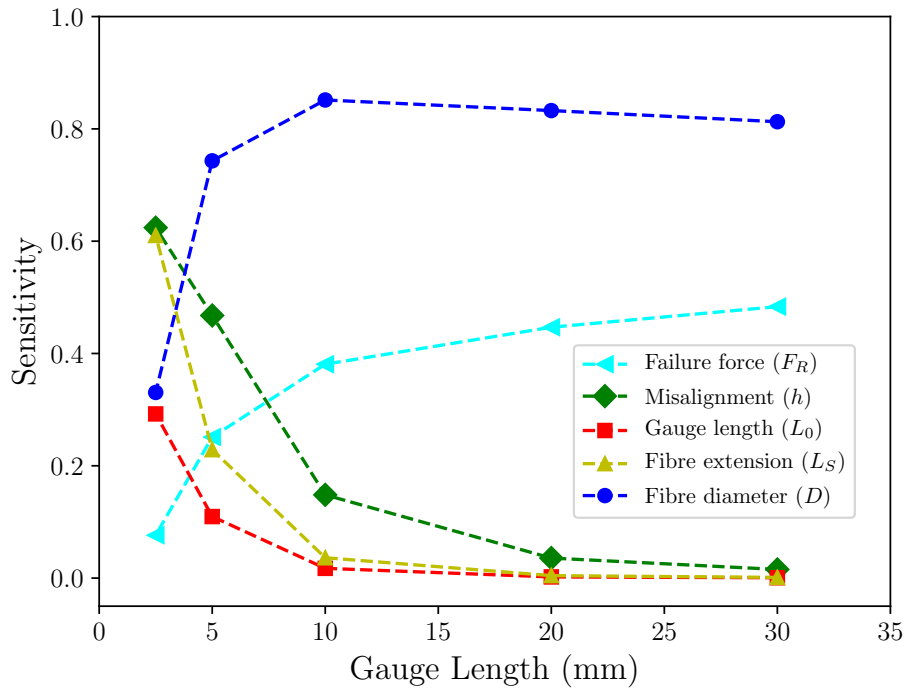


Figure 3.5: Sensitivity indices of different input quantities in tensile strength measurement of fibres at different gauge lengths

on the calculated fibre strength. It has been shown that for fibres of a sufficiently large gauge length, the measured fibre diameter is the most sensitive or critical parameter for accurate estimation of fibre tensile strength. Different fibre geometry measurement techniques include the laser scanning microscopy, laser diffraction measurement, optical microscopy, scanning electron microscopy, transmission electron microscopy, etc. Each measurement system offers different levels of uncertainty and not all measurement systems may be feasible for a given type of fibre. Based on the level of accuracy required and the feasibility of use for specific materials, an appropriate choice of fibre dimensional measurement method can be used. Further discussion on fibre dimensional measurement is given in Chapter 6.

Measured fibre diameter is followed by the measured force of fibre failure, in terms of relative importance. The other parameters are found to be relatively much less critical. However, composite strength and damage models require fibre properties for small length scales. The sensitivity analysis has shown that for tests done at shorter gauge lengths, the effect of other quantities, especially the fibre misalignment become very significant. This makes the fibre strength measurement susceptible to unwanted errors as it becomes very difficult to accurately control these quantities when fibres of very small gauge length are used for tensile testing, and hence great care is required when analysing results generated at very small gauge lengths. This knowledge about the influence of different parameters on measured fibre strength can help in designing improved single fibre testing systems

capable of determining fibre strength more accurately.

As mentioned earlier, fibre strength is typically represented by a statistical distribution, which is commonly determined using a set of fibre strength data points. The uncertainties in individual fibre strength values, will therefore, also propagate into the resulting distribution, and add uncertainty in the parameters of the statistical distribution function. In the next chapter, a Monte-Carlo statistical study will be conducted to quantify this uncertainty in the parameters of the fibre strength Weibull distribution. If uncertainty in the input fibre strength distribution is large, the predictions made by composite strength models would also be uncertain, since the fibre strength distribution is used as input in these models for predicting the material and structural behaviour. The knowledge of uncertainty in fibre strength used as model input can then also help in estimating the reliability of the predictions made by these composite strength models.

Chapter summary in French

Paramètres critiques dans la mesure de la résistance des fibres: identification et évaluation

Dans ce chapitre, différentes sources possibles d'erreurs dues aux limites expérimentales des tests sur fibres unitaires ont été identifiées. Leur effet sur la résistance à la traction des fibres a été modélisé analytiquement. Ce modèle a ensuite été utilisé pour évaluer statistiquement les incertitudes sur la résistance des fibres déterminée expérimentalement. Une analyse de sensibilité a été réalisée pour classer l'importance relative des paramètres expérimentaux sur la résistance calculée des fibres. Il a été démontré que pour des fibres d'une longueur de jauge suffisamment grande, le diamètre de fibre mesuré est le paramètre le plus sensible ou critique pour une estimation précise de la résistance à la traction des fibres. Elle est suivie par la force mesurée en importance relative. Les autres paramètres s'avèrent relativement moins critiques. Cependant, les modèles exploitant ces résistances à rupture nécessitent d'extrapoler les propriétés pour de très petites longueurs de jauge. L'analyse de sensibilité a montré que pour les tests effectués à des longueurs de jauge plus courtes, l'effet d'autres quantités, en particulier le désalignement des fibres, devient très important. Cela rend la mesure de la résistance des fibres très dépendant du système utilisé pour préparer et conduire les essais. Cette meilleure connaissance de l'influence des différents paramètres expérimentaux sur la résistance en traction des fibres peut aider à concevoir des systèmes de test améliorés et capables de fournir des données plus précises.

Comme mentionné précédemment, la résistance des fibres est généralement représentée par une distribution statistique. Les incertitudes dans les valeurs de résistance des fibres individuelles se propagent également dans la distribution résultante

Chapter 4

Uncertainty in fibre strength distribution

***Abstract :** The work described in this chapter aims at understanding the influence of measurement uncertainty (determined in the previous chapter), and of sampling randomness, on the parameters of the fibre strength Weibull distribution. Tensile strength data for T700 carbon fibres obtained in the previous chapter using the single fibre testing process has been analysed for this uncertainty assessment and a parametric bootstrap method has been used for the statistical evaluation of confidence limits. It has been shown that although both these causes of uncertainty are critical, the sampling randomness has a larger influence on the uncertainty of fibre strength, as compared to the measurement uncertainty. Choosing an insufficient sample size for analysis can thus result in uncertain or even inaccurate fibre strength properties, which would limit the reliability of composite strength model predictions. The knowledge of the causes and effects of these uncertainties can help in taking appropriate measures for improving the accuracy of results.*

Contents

4.1 Introduction	71
4.1.1 Causes of uncertainty in Weibull parameters	71
4.2 Uncertainty due to measurement	72
4.2.1 Fibre strength distribution	73
4.2.2 Estimation of measurement uncertainty on Weibull parameters	74
4.3 Uncertainty due to sampling randomness	76
4.3.1 Confidence Interval	77
4.3.2 Calculation of confidence interval for Weibull parameters	77
4.3.3 Confidence Region	81
4.3.4 Effect of sample size	82
4.4 Conclusions	83
Chapter summary in French	85

This chapter has been adapted from the following article:

S. Joannès, F. Islam, L. Laiarinandrasana, “Uncertainty in fibre strength characterisation due to uncertainty in measurement and sampling randomness”, *Applied Composite Materials*, 2020, 27, 165-184.

4.1 Introduction

The previous chapter describes that there can be uncertainties in measured single fibre tensile strengths. When a set of fibre strength data is represented by a statistical distribution, these uncertainties can also be carried into the parameters of the distribution. It is possible that the distribution does not accurately capture the actual strength variation of the fibre population [105, 106]. When such uncertain fibre properties are used as input for composite models, the predictions made by the models on strength and damage behaviour of composite structures will also be unreliable [107, 108, 109]. Mentioning the associated uncertainties has not been a usual practice in most previous studies when fibre strength properties have been reported, the knowledge of which can help in understanding the causes of discrepancies in the results available in literature.

This chapter aims at quantifying the uncertainty in the parameters of the fibre strength Weibull distribution, determined using single fibre test results. Apart from the limited precision of measurement tools used (as discussed in the previous chapter), uncertainties can also arise from many other sources such as the inconsistency of the individual performing the measurement, choice of sample size used, sampling error, etc. The representativity of the fibre strength data set which is used for analysing the variations in fibre strength, can be a major source of uncertainty in the resulting distribution parameters [36, 105]. The accuracy of determined fibre strength distribution can be improved by minimising the effect of these factors. This will also enhance the capability of composite strength models to estimate the behaviour of composite structures more accurately.

These aims would be achieved by addressing the following questions:

- *What are the possible causes of uncertainty in the fibre strength distribution?*
- *How uncertainty in individual fibre strengths affects the statistical distribution?*
- *How representative are sample sizes commonly used for determining fibre strength distributions?*

4.1.1 Causes of uncertainty in Weibull parameters

Some possible causes for uncertainties in parameters of Weibull distribution are described as follows:

- **Testing methodology:** Different authors have used different experimental techniques for the determination of Weibull parameters. These mainly include the single fibre testing process [78], fragmentation process [51] and the fibre bundle testing process [110]. Some other less commonly used methodologies have also been used [26]. The effect of experimental techniques on the determined Weibull parameters have already been discussed by Andersons et al. [44].
- **Analysis methodology:** To determine Weibull parameters from experimental results by fitting the data to a model, different data reduction techniques can be used such as the least squares method, maximum likelihood method, etc. Different rank determining methods also exist [111, 112]. The chosen method to analyse the data may have some influence on the obtained results.

- **Measurement uncertainty:** Another factor that can affect the results are measurement errors [35]. Fibre strength is calculated using measured quantities and in general, every measurement has imperfections which can give rise to errors in the result, as shown in the previous chapter. This may also contribute to the uncertainty in the final fibre strength distribution [96].
- **Sampling randomness:** To determine perfectly accurate Weibull parameters, an infinite number of fibres will have to be tested. Since doing that is impracticable, there will always be some doubts on the representativeness of the chosen sample used for analysis. This may be a major source of uncertainty.
- **Inconsistency in the material itself:** Fibre strength is controlled mainly by the distribution of defects inside them. Slight variations in manufacturing conditions can lead to differences in the microstructure of the material, and thus differences in the distribution of internal defects. This may also impact the properties of the fibres produced. Moreover, fibres are most often tested from bobbins – as is the case in the present work – but it can also be tested after a few transformation steps such as spreading during textile manufacturing. The step in the textile manufacturing process, at which the fibres are tested can also lead to differences in results. More discussions on this topic has been provided elsewhere [113].

Most of the times, very limited or no information about the above factors is provided in the available literature on fibre strength distributions, which makes the quantitative comparisons complicated. The focus of the present study is on the effect of two causes mentioned in the above list: measurement uncertainty and sampling randomness. They have been discussed in Sections 3.2.3 and 4.3, respectively.

4.2 Uncertainty due to measurement

Uncertainty, in theory, represents the state of unpredictability or unreliability. Uncertainty of the Weibull distribution parameters mean the lack of knowledge or confidence on the values of the calculated quantities. As described in the previous chapter, fibre strengths are calculated using measured quantities coming from instruments. Each measured quantity has some amount of measurement uncertainty or error, which results in an uncertainty or error in the calculated fibre strength as well [36]. Since the distribution parameters are calculated using experimentally measured fibre strength data, the uncertainties or errors in measured fibre strengths can also be transferred into the resulting Weibull distribution.

For determining the fibre strength Weibull distribution and for estimating the uncertainty in its distribution parameters, fibre strength data for T700 fibres given in Chapter 3 was used. The calculated fibre strengths σ and the corresponding measurement uncertainty $u_c(\sigma)$ for the 30 fibres are given in Table 3.4. Using this fibre strength data set, a representative Weibull distribution can be estimated. The standard procedure for estimating the parameters of the Weibull distribution is described in Section 4.2.1. Following this, the estimation of uncertainty on Weibull distribution parameters due to uncertainty in individual fibre strengths is described in Section 4.2.2.

4.2.1 Fibre strength distribution

The calculated fibre strength data from Table 3.4 was represented with the standard 2-parameter Weibull distribution following the method described in Section 2.3.5 and the corresponding Weibull plot is shown in Figure 4.1. The shape and scale parameters of the Weibull distribution were determined using the maximum likelihood estimation method; which were calculated to be $m = 3.23$ and $\sigma_0 = 4.19$ GPa, respectively. They are also given in Table 4.1. The points on Figure 4.1 represent the experimental fibre strength values and the straight line is the best fitted 2-parameter Weibull distribution model obtained from the cumulative density function of Equation 2.4.

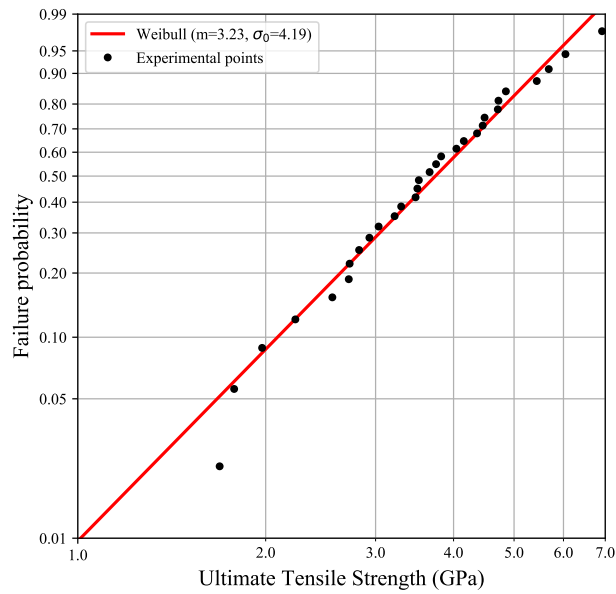


Figure 4.1: Estimated Weibull plot for experimentally determined fibre strength

Table 4.1: Weibull parameters for experimentally determined fibre strengths

Shape parameter m	Scale parameter σ_0 (GPa)
3.23	4.19

Each of the calculated fibre strengths has some level of uncertainty associated with it due to the uncertainty of measurement. Having a measurement uncertainty practically means that if it was somehow possible to go back in time and conduct a tensile test using the same fibre again to determine the strength, the result obtained may have been different. It would deviate from the best estimate due to uncertainty in measurement of the quantities on which it depends. Consequently, the corresponding Weibull distribution for fibre strength would also be different, and would have different values of shape and

scale parameters. This means that there would also be uncertainties associated with the calculated Weibull shape and scale parameters. The estimation of uncertainty in Weibull parameters has been discussed in the following section.

4.2.2 Estimation of measurement uncertainty on Weibull parameters

Since it is practically impossible to physically test fibres that have already been tested, uncertainty in Weibull parameters arising from measurement cannot be obtained from experimental results. Simulated values for fibre strength have thus been used to determine their Weibull distributions.

A large number of fibre strength data sets similar to the one determined experimentally were simulated, under the assumption that uncertainty in fibre strength follows a normal distribution. It is common to assume that the measurement uncertainty follows a normal distribution [96]. Taking the experimentally calculated fibre strength results as reference, virtual fibre strength values were randomly generated from the assumed normal distribution with the experimental fibre strength value as the mean, and the calculated uncertainty as the standard deviation of the distribution, respectively. One hundred virtual fibre strength points were simulated around each experimental point, as also depicted in Figure 4.2. The solid points represent the experimental fibre strength data points (same as in Figure 4.1) while the hollow points represent the simulated data points. Only about 10 simulated points for each experimental point are shown in the figure for clarity. Virtual fibre strength data sets were generated by randomly extracting one point from each of these clusters to form a data set of 30 virtual fibre strength data points. A total of 100 similar data sets were generated with each set comprising of 30 fibre strength values, same size as that of the reference data set. Each simulated data set was fitted to a Weibull distribution, all 100 of such simulated Weibull plots are shown in Figure 4.2.

The shape and scale parameters for each simulated distribution are determined and the results are summarized in Table 4.2. The shape parameter m was found to vary between 3.09 and 3.38 with an average value of 3.22 and having a standard deviation of 0.06. The best estimate for m and the uncertainty Δm can be represented by the average value and the standard deviation, respectively. The scale parameter σ_0 was found to vary between 4.12 GPa and 4.25 GPa with an average value of 4.18 GPa and having a standard deviation of 0.03 GPa. The shape and scale parameters in terms of best estimates and associated uncertainties are given as follows:

$$m = 3.22 \text{ with } u(m) = 0.06$$

$$\sigma_0 = 4.18 \text{ GPa with } u(\sigma_0) = 0.03 \text{ GPa}$$

As already mentioned in the previous chapter, the guide to uncertainty measurement recommends calculation of an expanded uncertainty $U(x)$ for a quantity of interest x , for commercial and industrial applications. The expanded uncertainties for a 95% level of confidence can be calculated following Equation 3.17 which gives $U_{95}(m) = 0.12$ and $U_{95}(\sigma_0) = 0.06$. The shape and scale parameters in terms of their expanded uncertainties are given as follows:

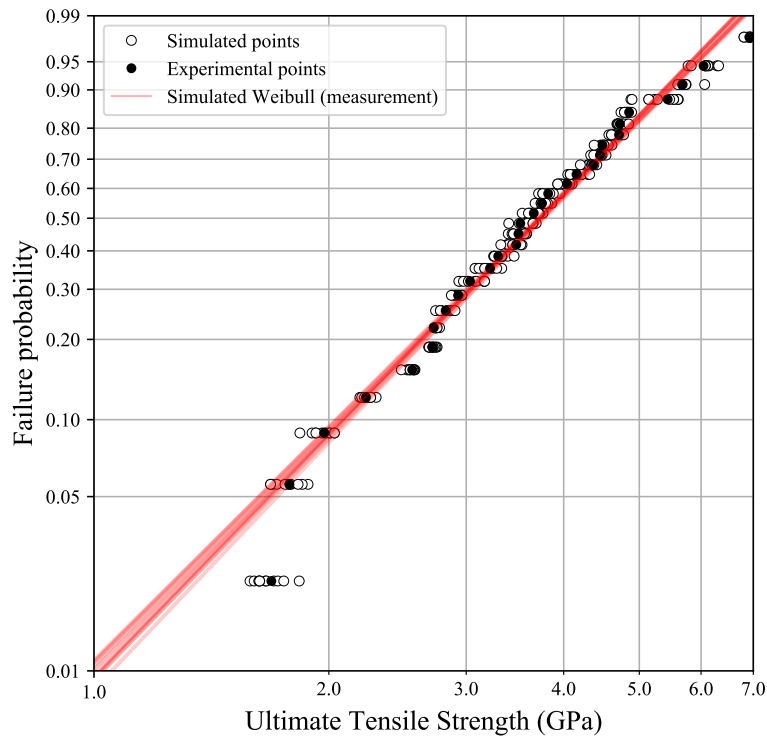


Figure 4.2: Weibull distributions simulated by varying fibre strength data points within the uncertainty region

Table 4.2: Weibull parameters for virtual fibre strength data sets

	Shape parameter m	Scale parameter σ_0 (GPa)
Mean	3.22	4.18
Standard deviation	0.06	0.03
Expanded uncertainty	0.12	0.06

$$m = 3.22 \pm 0.12, \text{ for a confidence level of } 95\%$$

$$\sigma_0 = 4.18 \pm 0.06 \text{ GPa, for a confidence level of } 95\%$$

The variation in shape parameter values is about 4% from the best estimate value on each side whilst the scale parameter is shown to vary by about 1.5% on each side from its best estimate. The variation in parameter values by itself is small. However, as also mentioned earlier, for modelling the strength of composite materials Weibull parameters for very short

gauge lengths are required. These can sometimes be even in the range of a few micrometres for some models [15]. The Weibull parameters determined at experimental gauge lengths are extrapolated to shorter gauge lengths using Equation 1.2. Table 4.3 shows how the uncertainties are amplified when the Weibull scale parameter is extrapolated to shorter gauge lengths up to 0.1 mm. If extrapolation is done up to the range of a few micrometres, as required by certain models, the uncertainties will be even larger. This will also result in uncertain model predictions.

Table 4.3: Amplification of measurement uncertainties of the Weibull Scale parameter (σ_0) upon extrapolation to shorter gauge lengths.

Gauge length (mm)	Scale parameter, σ_0 (with expanded uncertainty at 95% confidence level) (GPa)
30	4.18 ± 0.06
10	5.77 ± 0.16
4	7.56 ± 0.25
1	11.41 ± 0.51
0.1	22.54 ± 1.45

From this analysis, it can be seen that the uncertainty resulting due to the uncertain measurement of individual fibre strength is not very substantial. However, this is true only if the fibre strength data is generated using a sufficiently long gauge length, as in the present case. This is because the effect of measurement limitations is small for tests conducted at large gauge lengths and the measured tensile strength is more accurate. However, for shorter gauge lengths of a few micrometres and below, measurement uncertainty of the instruments and experimental constraints limit the accuracy of the fibre strength data generated. Their effect on the uncertainty of the distribution parameters in this case will also be expected to be significant [36]. For minimizing the uncertainty due to measurement inaccuracies, it is recommended that a sufficiently large gauge length is used for generating the fibre strength data.

4.3 Uncertainty due to sampling randomness

The determination of uncertainty in fibre strength and its Weibull distribution parameters described in Section 3.2.3 considers only the effect of measurement. Individual measurement uncertainties for each input quantity are considered for obtaining the overall uncertainty on end results. However, as mentioned in Section 4.1.1, uncertainties in Weibull distribution parameters can also arise due to many other factors. The representativity of the chosen sample to determine the distribution is another major factor, especially in the case when single fibre test results are used, as in the present study. Many challenges are associated with fibre strength characterisation, as already described in Chapters 2 and 3. Due to the time consuming and cumbersome nature of the single fibre testing process, only a limited number of fibres can be tested to determine the Weibull distribution. This limits the sample size of the data set generated. This data set is assumed to represent

the fibre strengths for the whole fibre population in consideration. Conducting Weibull analysis using a fibre strength data set of an insufficient sample size may lead to sampling errors. To comprehend the effect of sampling randomness on the uncertainty of the Weibull distribution, a confidence interval can be calculated, as described in the following section.

4.3.1 Confidence Interval

In statistics, a random sample is selected from a larger population and results are estimated based on this sample. However, it is uncertain how well the selected sample represents the underlying population. This uncertainty can be comprehended by computing a confidence interval which provides a range of values which are likely to contain the results of the investigated parameter. Confidence intervals are calculated at a given confidence level, since the interval does not necessarily include the true value of the parameter. For example, a confidence interval calculated at a 95% confidence level, also known as a 95% confidence interval, has the following meaning: When a parameter is estimated many times from samples similar to the original one, then the real and unknown value of the parameter for the whole population will lie within the confidence interval, 95% of the times [114]. The term “confidence interval” refers to the interval estimate along with its confidence coefficient.

A confidence interval is sometimes considered identical to a credible interval; the two are however different from each other. The first corresponds to a frequentist approach while the second to a Bayesian approach. A 95% credible interval has the following meaning: Given an observed data, there is a 95% probability that the true value of an unknown parameter lies within a credible interval. The calculated numerical values for the two intervals may often be similar, but they have different meanings and should not be confused with each other. For the present study, a 95% confidence interval was calculated for the parameters of the Weibull distribution. The steps involved in the calculation are described in Section 4.3.2.

4.3.2 Calculation of confidence interval for Weibull parameters

There are different methods of calculating a confidence interval for Weibull statistics, such as Fisher’s matrix bounds, Beta-Binomial bounds, likelihood ratio bounds, Monte Carlo bounds, etc. [111, 115, 116]. They are briefly described as follows:

Fisher’s matrix bounds The Fisher’s matrix bounds are parametric in nature, i.e. they follow an underlying distribution. It has been found that they tend to be more optimistic than rank based non-parametric bounds, specially for small sample sizes. Thus, many statisticians prefer to use non-parametric bounds.

Beta Binomial bound The Beta Binomial bound follows the non-parametric approach, i.e. no underlying distribution is assumed, for calculating the confidence interval and is less mathematically intensive. The procedure is similar to the method of calculating median ranks.

Likelihood ratio bound The likelihood ratio bound also follows a simple methodology and are usually preferred over the Fisher's matrix bounds, specially when smaller sample sizes are analysed. They are based on a given likelihood equation and the results can be represented graphically as a contour plot. The extreme values of the contour plots are used for determining the required bounds.

Monte Carlo bound These could be parametric or non-parametric and is sometimes called the bootstrap method (parametric or non-parametric). For the parametric case, a model is fitted to the data, often by maximum likelihood, and samples of random numbers are drawn from this fitted model. A more rigorous method of calculating pivotal confidence bounds also exist.

For the present study, Monte Carlo parametric confidence intervals were chosen as they are relatively straightforward to determine and provide good approximations of the confidence interval estimate. The steps followed for calculating the confidence intervals for parameters of the Weibull distribution using the parametric bootstrap method, are listed as follows:

- Calculation of the parameters for the 100 Weibull distributions simulated earlier by considering the effect of measurement uncertainty. These simulated Weibull distributions have been already shown in Figure 4.2.
- Generation of 100 virtual fibre strength data sets for each synthetic Weibull distribution generated in Step 1. This was done by randomly extracting 30 data points from a given distribution, to form another set. This was repeated 100 times to generate the 100 virtual fibre strength data sets required. This results in a total of 100×100 (=10,000) virtual data sets and simulates the effect of sampling randomness.
- Estimation of the best fit Weibull distribution parameters for all the 10,000 synthetic sample sets.
- Calculation of 2.5th and 97.5th percentile values of these distribution parameters. These values represent the lower and upper bounds of the 95% confidence interval.

A total of 10,000 different synthetic fibre strength data sets were randomly extracted following the steps mentioned above. Each data set comprised 30 fibre strength values covering the entire possible range of fibre strengths, within limits. Each synthetic data set was fitted to a 2-parameter Weibull distribution. The parameters for each distribution were determined using the maximum likelihood method. All simulated distributions are shown in Figure 4.3, with the ones based on measurement uncertainty being in the central region and are surrounded by the ones based on sampling randomness. The shape and scale parameters for all simulated distributions are tabulated together. To determine the 95% confidence intervals, the 2.5th and 97.5th percentile values were extracted for the shape and scale parameters. The associated confidence interval estimated from the simulated results is given in Table 4.4. The width of estimated 95% confidence interval for shape parameter m is 1.99 which is more than half of the best estimate value while the interval estimated for the scale parameter σ_0 is 0.97 GPa which is about a quarter of the best estimate value. The Weibull parameters of the simulated distributions are

also represented with the help of histograms of the shape and scale parameters, as shown in Figure 4.4. Scatter between the shape and scale parameters of the simulated Weibull distributions is shown in in Figure 4.5.

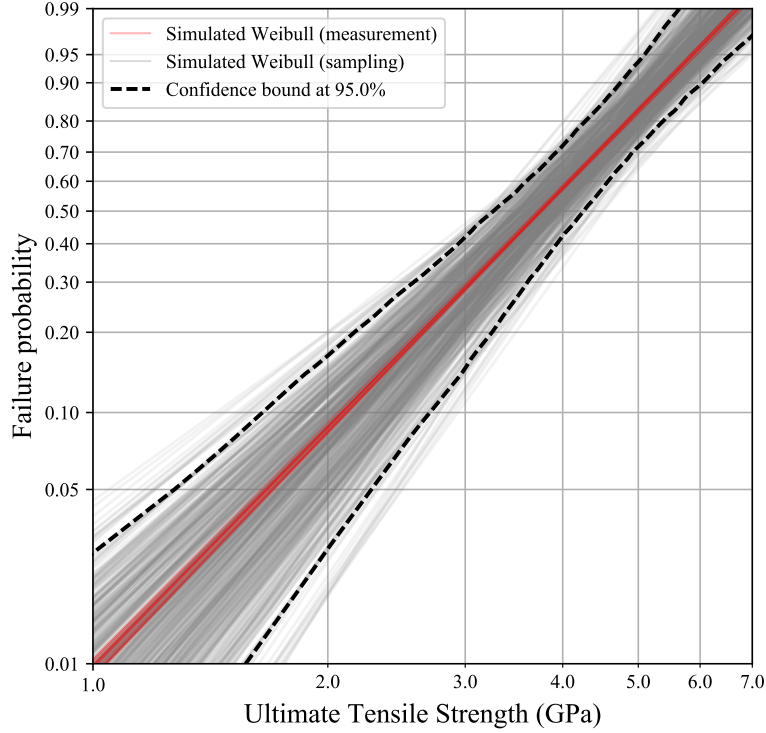


Figure 4.3: Simulated Weibull distributions based on sampling and measurement uncertainty.

Table 4.4: Weibull parameters and associated 95% confidence interval for overall uncertainty due to measurement and sampling.

	Shape parameter m	Scale parameter $\sigma_0(GPa)$
Mean	3.38	4.17
95% Confidence Interval	2.54 – 4.53	3.69 – 4.66
Confidence width	1.99	0.97
Standard deviation	0.51	0.25
Expanded uncertainty at 95%	1.00	0.49

The Weibull parameters can be reported in the form of best estimates of the parameter along with the corresponding uncertainty. The best estimate is represented by the mean of the data sets. The uncertainty in Weibull parameters is represented by the standard

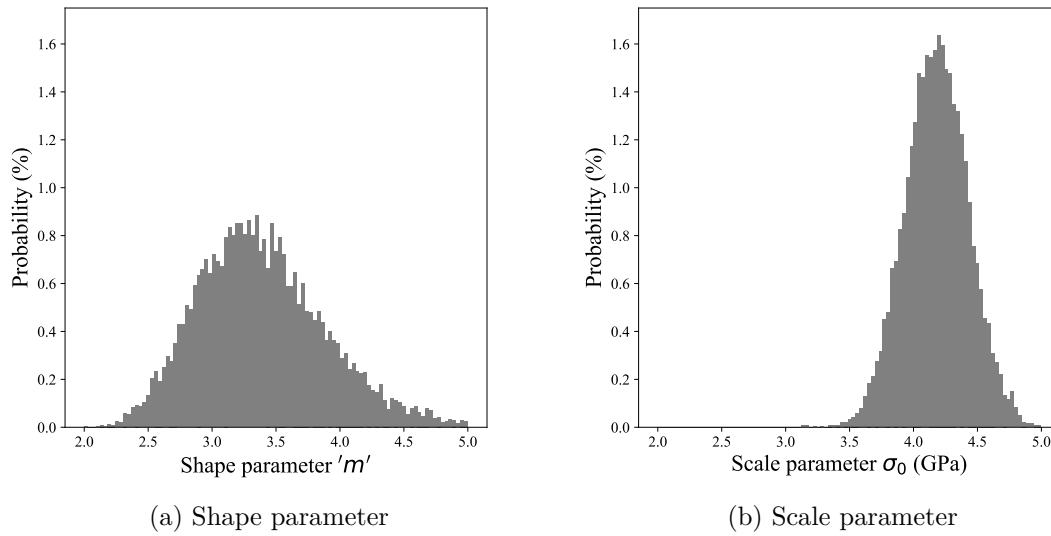


Figure 4.4: Histograms of the Weibull parameter values of the simulated distributions, for: (a) Shape parameter (b) Scale parameter.

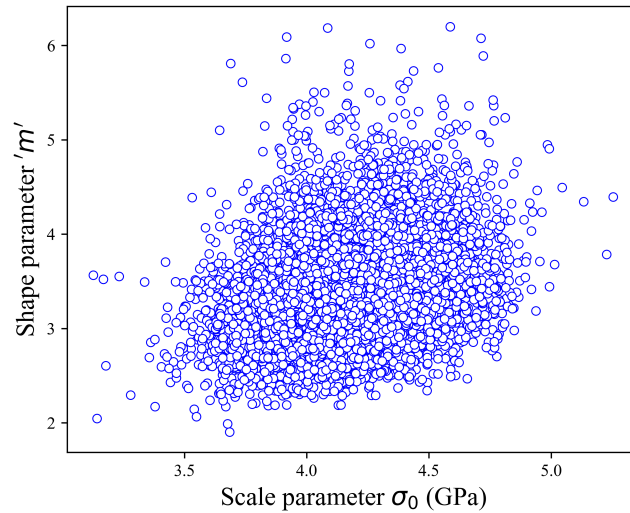


Figure 4.5: Scatter between the shape and scale parameters of the simulated Weibull distributions.

deviation of the data sets, given in Table 4.4 and is also shown as follows:

$$m = 3.38 \text{ with } u(m) = 0.51$$

$$\sigma_0 = 4.17 \text{ GPa with } u(\sigma_0) = 0.25 \text{ GPa}$$

The expanded uncertainties can be calculated using Equation 3.17 for a 95% level of confidence which gives $U_{95}(m) = 1.00$ and $U_{95}(\sigma_0) = 0.49$. The shape and scale parameters in terms of their expanded uncertainties are given as follows:

$$m = 3.38 \pm 1.00, \text{ for a confidence level of 95\%}$$

$$\sigma_0 = 4.17 \pm 0.49 \text{ GPa, for a confidence level of 95\%}$$

It is observed that the uncertainty in Weibull parameters arising due to the effect of sampling is very large. Upon extrapolation to shorter gauge length, the uncertainty associated with the Weibull scale parameter may become even more significant. Table 4.5 shows how the uncertainties are amplified when the Weibull scale parameter is extrapolated to shorter gauge lengths upto 0.1 mm. If extrapolation is done up to the range of a few micrometres, as required by certain models, the uncertainties would be even larger. If these values are used as input to model the properties of any product or structure which uses such fibres, there would be a significant uncertainty in those properties as well. Hence, it is very important that such uncertainties in fibre strength distribution parameters are clearly reported and also appropriately incorporated during computer strength modelling of any structure which uses such fibres.

Table 4.5: Amplification of uncertainties (due to sampling randomness) of the Weibull Scale parameter (σ_0) upon extrapolation to shorter gauge lengths.

Gauge length (mm)	Scale parameter, σ_0 (with expanded uncertainty at 95% confidence level) (GPa)
30	4.17 ± 0.49
10	5.77 ± 0.88
4	7.56 ± 1.59
1	11.41 ± 3.60
0.1	22.54 ± 11.35

These simulations were done using sample sizes of 30 fibres. In order to reduce the uncertainty due to the effect of sampling randomness, choosing a fibre strength data set of a large sample size is therefore recommended for determining Weibull distribution parameters from single fibre test results. None of the works reported in Table 1.1 related to single fibre tests (SFT) however, had used more than 30 fibre strength results.

4.3.3 Confidence Region

From the simulated Weibull distributions, a confidence region can also be determined. For this, it is useful to calculate a quantity called B-Strength, which is defined here.

B-Strength: It may be of interest to determine the value at which a given percentage of the specimen population will fail. This quantity is similar to the one named B-life but since the quantity of interest is strength in the present case, it has been called B-strength. Considering B50 strength for example, 50% of the fibre population is expected

to have strength of less than this value. The scale parameter σ_0 then by definition is the B63.2 strength, i.e. 63.2% of the fibre population is expected to have a strength of less than this value. The B50 strength can be determined by substituting the value for 50% failure probability, i.e. 0.50 in the Weibull failure distribution equation given by Equation 2.4. A direct way to determine the B50 strength is by drawing a horizontal line at failure probability of 0.50 in the Weibull plot given in Figure 4.1, finding its intersection with the best estimated Weibull line, and reading the corresponding strength value from the horizontal axis. The B50 strength is calculated to be 3.74 GPa for the present case, which means that 50% of the fibres in the population are expected to have a strength of less than 3.74 GPa. Hence, B50 strength can also be called as median failure strength.

The steps for the calculation of a confidence region are as follows:

- From a simulated distribution, B-strength is calculated for all failure probabilities from 0.01 to 1.00, at intervals of 0.01 (i.e. B01, B02, . . . , B99, B100).
- Similarly, for all other simulated distributions, B-strength values are calculated for all failure probabilities.
- For a given failure probability, all calculated B-strength values coming from different simulated distributions are tabulated together. This is repeated for each failure probability.
- If a 95% confidence level is sought, the 2.5th and 97.5th percentile values for each B-strength are then connected, to form the upper and lower bounds of the confidence region, respectively, as shown in Figure 4.3.
- The region between these two confidence bounds gives the 95% confidence region.

For selective B-strengths, the best estimated values along with the 95% confidence intervals for uncertainty due to the combined effect of measurement uncertainty and sampling are shown in Table 4.6. For the B50 strength, for example, the best estimate is 3.74 GPa. All best estimate values are the results coming from the Weibull distribution obtained from the experimental results. Considering the uncertainty, the 95% confidence interval in which the B50 strength is expected to lie is 3.25 - 4.24 GPa, i.e. within a bound width of 0.99 GPa. Similarly, other B-strength values can also be determined. It can be seen from Table 4.6 that width of the 95% confidence interval is fairly consistent for all B-strengths.

4.3.4 Effect of sample size

Different authors have chosen different sample sizes for single fibre testing, as shown in Table 1.1. The sample size usually varies between 10-30 [117]. The choice of the number of test results introduces uncertainty on the estimated Weibull parameters due to sampling randomness. It is evident that Weibull parameters determined from large sample sizes are more reliable than those obtained using a small sample size [76], as also indicated by the discussions presented in this chapter.

To obtain an indication of the effect of varying the fibre strength sample sizes, on the esti-

Table 4.6: Best estimated values for selective B-strengths along with the 95% confidence intervals for overall uncertainty due to measurement and sampling

B-strength	Best Estimate (GPa)	95% Confidence Interval (GPa)	Width (GPa)
B20	2.64	2.19 - 3.16	0.97
B40	3.40	2.96 - 3.91	0.95
B50	3.74	3.25 - 4.24	0.99
B60	4.08	3.58 - 4.55	0.97
B80	4.85	4.30 - 5.30	1.00

mated confidence interval, more fibre strength experiments were conducted following the same single fibre testing methodology described in Chapter 3. Three sets of experimental results having different sample sizes were extracted to determine their scale parameters σ_0 (i.e. B63.2 strength), and also to estimate the corresponding 95% confidence interval for uncertainty due to sampling, by simulating Weibull distributions using the method described in Section 4.3.2. The estimated confidence intervals for different fibre strength sample sizes are given in Table 4.7. It can be seen that as the sample size increases, the confidence interval on the scale parameter becomes narrower. The narrower the confidence interval, the less the uncertainty. Narrow confidence intervals thus represent more accurately estimated results. It is therefore recommended that a sufficiently large set of experimentally generated fibre strength data is used for determining the representative Weibull distributions. This can minimize the uncertainty due to sampling randomness, and maximize the accuracy of the estimated distribution parameters. To obtain more realistic effects of large sample sizes on the improvements in statistical confidence of Weibull distributions, a large set of experimental fibre strength data will be analysed in Chapter 6.

Table 4.7: Effect of sample size on estimated 95% confidence interval of Weibull scale parameter σ_0 (B63.2 strength)

Sample size N	Best Estimate (GPa)	95% Confidence Interval (GPa)	Width (GPa)
15	4.22	3.55- 5.24	1.49
30	4.25	3.77 - 4.78	1.01
45	4.18	3.81 - 4.57	0.76

4.4 Conclusions

The influence of practical limitations on the accuracy of fibre strength distribution parameters has been studied in this chapter. Limitations such as unavoidable measurement uncertainties and the randomness introduced due to the sampling effect have been statistically analysed with the help of Monte Carlo bootstrap methods. The uncertainties arising

due to these two reasons have been quantified in terms of a confidence interval, which provides a range of possible values which the distribution parameters are expected to take. It has been shown that although both the causes of uncertainty are critical, the sampling randomness has a larger influence on the uncertainty of the estimated fibre strength results while the uncertainty resulting due to the uncertain measurement of individual fibre strength was not very substantial, for fibres of gauge length 30 mm. However, this will be true only for fibre strength data generated using a sufficiently long gauge length of a few tens of millimetres. This is because uncertainties due to measurement limitations are small for tests conducted at larger gauge lengths, and thus the measured tensile strength is more accurate. However, for shorter gauge lengths of a few millimetres, measurement uncertainty of the instruments and experimental constraints restricts the accuracy of the fibre strength data generated. Their effect on the uncertainty of the distribution parameters in this case is also expected to be significant [36].

It is obvious that if such uncertain fibre strength distributions are used as input to model the properties of any product or structure which uses such fibres, there will be significant uncertainty in those properties as well. Hence, it is very important that such uncertainties in fibre strength distribution parameters are clearly reported and also appropriately incorporated during computer strength modelling of any structure which uses such fibres. The understanding gained in this chapter about the uncertainty in fibre strength distribution parameters also empower users to estimate the confidence that can be placed on the predictions made by composite strength models on the damage and failure behaviour of composite structures. This can be done by using the obtained fibre strength properties (along with uncertainty) as input for the predictive models to determine the variability in the model predictions. This study will be demonstrated in the next chapter.

Chapter summary in French

Incertitude dans la répartition de la résistance des fibres

Ce chapitre porte sur le caractère aléatoire introduit en raison de l'échantillonnage. Des méthodes de type Monte Carlo permettent de quantifier les incertitudes associées. La représentativité de la taille de l'échantillon choisie pour l'analyse est cruciale. Dans la plupart des études de la littérature, un nombre insuffisant de données est utilisé pour quantifier la distribution à rupture des fibres. Cela se traduit par une grande incertitude sur les paramètres de la distribution mais également à d'éventuelles méprises sur le comportement à rupture des fibres.

Dans ces travaux, Il est montré que, bien que les deux causes d'incertitude soient critiques (fibre unitaire et échantillonnage), le caractère aléatoire de l'échantillonnage a une plus grande influence sur l'incertitude des résultats, notamment pour les fibres de longueur de jauge d'une trentaine de millimètres. Cela reste vrai que pour des longueurs de jauges suffisantes. Pour des longueurs de jauge plus courtes, de quelques millimètres, l'incertitude de mesure des instruments et les contraintes expérimentales limitent la précision des données sur la résistance des fibres unitaires. Leur effet sur l'incertitude des paramètres de distribution devient également très significatif.

Il est évident que si de telles distributions, incertaines, sont utilisées comme données d'entrée pour modéliser les propriétés de résistance de tout produit ou structure composites, les incertitudes sur les prédictions s'en trouvent impactées.

Chapter 5

Variability in predictions of composite strength models due to uncertain input properties

***Abstract :** The understanding of uncertainty in fibre strength distribution gained from the previous chapters has been used for estimating the variations in structural predictions of composite strength models, and for determining the sensitivity of the model predictions to errors/uncertainties in input parameters. To evaluate this, a composite strength model developed at Mines Paris-Tech was used for predicting the strength and lifetime of composite structures based on uncertain input data. The structural behaviour predicted by the model is found to be highly sensitive to the expected uncertainties in the parameters of the fibre strength distribution used as input. Uncertainties in the input fibre strength distribution are, for this reason, a big hindrance to the reliability of the predictions made by composite strength models.*

Contents

5.1	Introduction	89
5.2	Mines ParisTech model	89
5.2.1	Mechanism of longitudinal tensile failure of unidirectional composites	90
5.2.2	Microscopic scale: Fibre failure model and the RVE	90
5.2.3	Macroscopic analysis: Simplified FE^2 model	91
5.3	Methods	91
5.3.1	Steps in simulation	91
5.3.2	Simulation framework	93
5.3.3	Input fibre strength: Hypothetical properties with uncertainties	94
5.3.4	Loading conditions	95
5.4	Results and discussions	97
5.4.1	Monotonic loading	97
5.4.2	Sustained loading	100
5.5	Conclusions	102
	Chapter summary in French	104

5.1 Introduction

It has been discussed in the previous chapter that there can be uncertainties in the parameters of the fibre strength Weibull distribution that are used as input in composite strength and damage models, for predicting the mechanical behaviour of composite structures. These uncertainties in input data also means that the mechanical behaviour predicted by the models can also be uncertain or variable. The understanding of uncertainties gained from the previous chapters can further be used for estimating the variations in model predictions, and for determining the sensitivity of the model predictions to errors/uncertainties in input parameters.

The aim of this chapter is to determine the expected variability in the mechanical response of composites, as predicted by composite strength models, based on uncertainties in the input fibre strength distribution. The influence of uncertainties evaluated in the previous chapters, on the failure stress and time-to-failure of unidirectional (UD) carbon/epoxy composites will be quantified. This chapter essentially answers the following question:

How does uncertain input fibre strength data affect the structural behaviour predictions of composite strength models?

To evaluate the influence of uncertainty in input fibre strength on model predictions, a composite strength model developed at Mines ParisTech was used [12]. This model considers physical processes such as the kinetics of fibre failure and its interactions with the surrounding matrix. It was first developed in 2005 and has been improved over the years to simulate different loading conditions during service of composite structures such as pressure vessels. For the present study, the strength and lifetime of a composite structure is simulated under two different practical loading conditions to elucidate the sensitivity of different structural responses to the parameters of the input fibre strength distribution. The model is described in Section 5.2.

5.2 Mines ParisTech model: Simulating composite failure induced by fibre breaks

In fibre reinforced composite structures such as pressure vessels, failure occurs in the unidirectional composite layers due to fibre failure. Failure processes in unidirectional composites at the scale of individual fibres are difficult to observe experimentally. The strength and lifetime of composite structures are often studied through computational models, such as the multiscale finite element model developed at Mines ParisTech by Blassiau, Bunsell and Thionnet [88]. This model addresses the stochastic kinetics of fibre failure to simulate the strength and lifetime of composite materials. It follows a multiscale approach where the analysis of the damage process in composites at the micro and macroscale are combined. The mechanics of load transfer around fibre breaks at the microscale is analysed to predict the structural response of the material. The motivation behind using such an approach is the desire to capture, as far as possible, the physical mechanisms at the origin of composite failure. A good agreement has been observed between the predictions of the model and experimental results obtained from acoustic emission [118] and micro-computed tomography [119]. A brief description of the model is

presented here. For a more detailed description of the model, the reader can refer to other works [2, 13, 16, 88, 120, 121].

5.2.1 Mechanism of longitudinal tensile failure of unidirectional composites

Failure in unidirectional fibre reinforced composites under monotonically increasing tensile loading is understood to occur in the following steps:

- Damage begins by the occurrence of isolated random fibre breaks.
- Clusters of fibre breaks start developing and further damage is no longer random but is increasingly controlled by previous fibre breaks.
- Fibre break clusters multiply quickly leading to an unstable state, at which point the composite fails in a sudden-death manner.

5.2.2 Microscopic scale: Description of the fibre failure model and the Representative Volume Element

At the microscale, the heterogeneous nature of the composite material is simulated by considering the fibre and matrix material behaviour separately. A Representative Volume Element (RVE) is defined and is shown in Figure 5.1. It is a parallelepiped having a square cross-section consisting of 32 fibres, each of 4 mm length, and distributed in a regular square array. An RVE represents a small volume of the material which is sufficient to predict the macroscopic property of interest, which for the present case is the longitudinal tensile strength of the composite. The length of the RVE L is 4 mm, while the width and height are 0.05 mm each, as shown in Figure 5.1. The RVE is assumed to have 32 intact fibres initially. Upon the application of a longitudinal tensile load, fibre breaks are assumed to develop, and the RVE changes its state of damage sequentially. From the undamaged state, the RVE is considered to undergo 6 different stages of damage before reaching the failed state. The different stages of damage of the RVE are shown in Figure 5.2. The different damage stages correspond to 1, 2, 4, 8, 16, 32 broken fibres, respectively. The RVEs corresponding to each of these damage states have been referred to as C-32 for 1 in 32 fibres broken, C-16 for 1 in 16 fibres broken, and analogously C-8, C-4, C-2 and C-1, as shown in Figure 5.2. The damaged cells can also be described in terms of i -plets ($i = 1, 2, 4, 8, 16, 32$), where i is the number of broken fibres in the cell, as also shown in Figure 5.2. For each of the damaged RVEs, stresses in the remaining fibres are pre-calculated using finite element analysis. This overstress is represented in terms of load transfer coefficients, and is stored in a database for future use. A simplified multiscale process is then used to carry out the simulations for composite structure failure at the macroscale, as described in Section 5.2.3. At the microscale, the input data needed are the fibre and matrix properties.

Other than the number of broken fibres in the RVE, the model is also capable of taking into account the following other effects: stochastic nature of fibre strength, shear deformation and viscoelastic nature of the matrix, debonding at the fibre/matrix interface, local variations in fibre volume fraction. However, not all of these factors were considered for the present study [88].

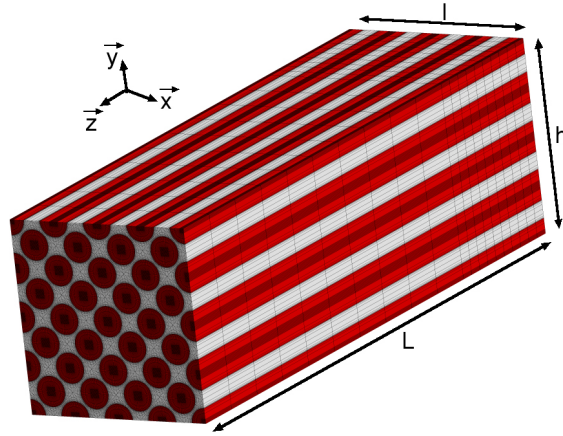


Figure 5.1: Representative Volume Element at the microscopic scale with the fibres distributed in a regular square array. Here, $L = 4$ mm, $l = h = 0.05$ mm, and fibre volume fraction $V_f = 64\%$ [120].

5.2.3 Macroscopic analysis: Simplified FE^2 model for composite structure failure calculation

At the macroscale, failure of the composite structure was simulated using a multiscale FE^2 approach, which was developed for computational efficiency. At this scale, the fibres and matrix are homogenised into a single orthotropic material. The finite element problem is solved only at the macroscale. However, the analysis makes use of the microscopic load transfer coefficients (k_r), calculated in the previous step.

The flowchart shown in Figure 5.3 explains the multiscale simulation process. The simulation starts at the macroscale, where the composite is modelled using a linear elastic transversely isotropic material behaviour. The stiffness matrices at different Gauss points are assigned based on the respective damage state. The applied loads are updated and the macroscopic stress tensor at each Gauss point (RVE) is calculated. Following this, a transition is made to the micromechanical framework at each Gauss point. The material is now treated as heterogeneous and the stresses in different fibres are updated based on the precomputed load transfer coefficients stored in the database. If the updated stresses in the fibres exceed a randomly assigned fibre strength based on the input Weibull distribution, the damage state is updated to the next RVE (see Figure 5.2 for RVEs of all damaged states). The microscopic damage state is then used to update the elastic properties of the homogenised material at the macroscale, by appropriately modifying the stiffness matrix of the material. Following this, the simulation moves to the next time step and the process is repeated.

5.3 Methods

5.3.1 Steps in simulation

To begin the calculations, at each Gauss point (RVE), 5 values of fibre strength are assigned. These values come from the input fibre strength Weibull distribution. These fibre strength

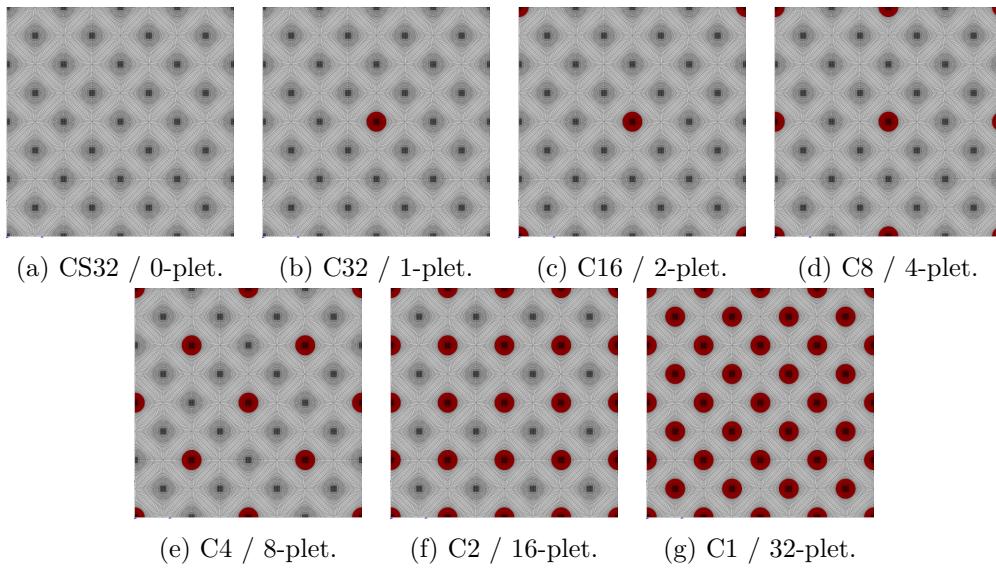


Figure 5.2: RVEs of the material damage state resulting from sequential fibre breaks and corresponding i-plets. Broken fibres are shown in red [88].

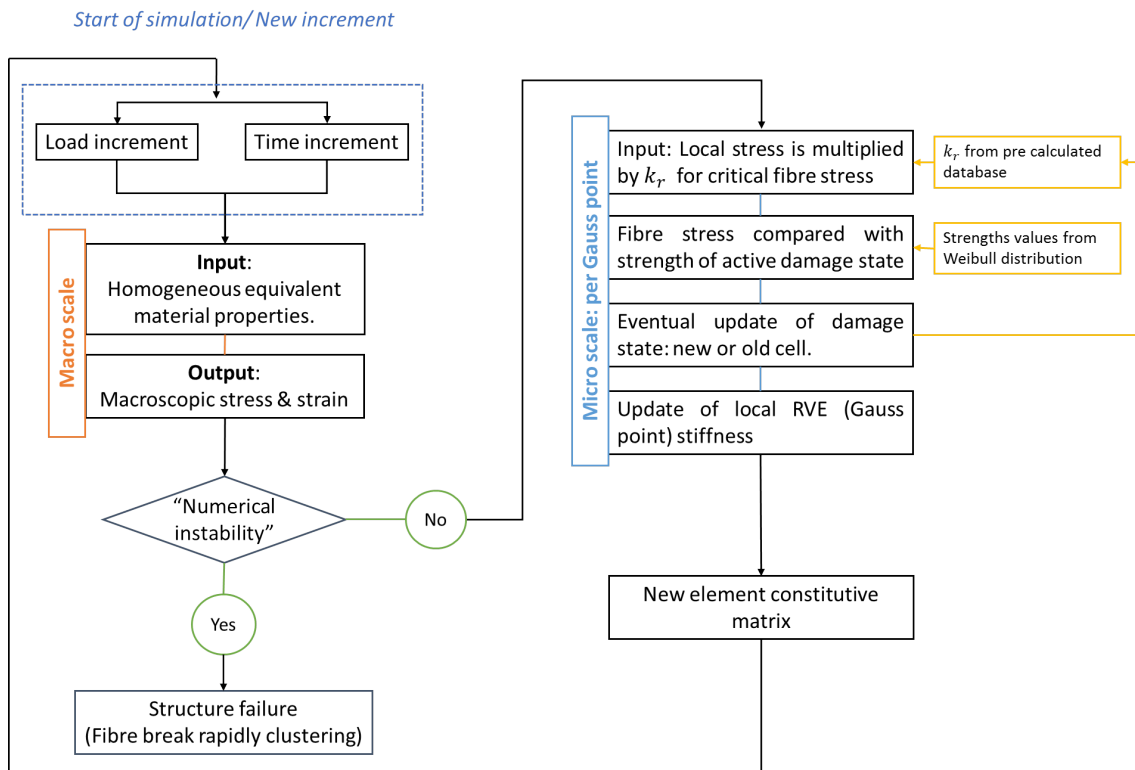


Figure 5.3: Flowchart of the simplified FE^2 multiscale fibre break model. Adapted from [13].

values correspond to the different damaged cells shown in Figure 5.2, and allow the damage

to evolve from CS32 state to that of C1 state in 5 steps (skipping the C32 cell, as it was found to have a negligible influence on simulation results [121]). The multiscale simulation process is iterative and proceeds as follows:

- If the monotonic loading condition is analysed, the external load on the structure is incremented at fixed intervals of time. If the sustained loading condition is analysed, the increment of time is made without any load increment.
- The macroscopic stress field on the structure is calculated using finite element analysis.
- The analysis moves into the microscale. Using the knowledge of the macroscopic stress, the microscopic stresses in the intact fibres are calculated. The calculated fibre stress is then compared to the input fibre strength values, to determine the number of broken fibres in the RVE.
- The macroscopic behaviour of the new homogenous material is calculated as a function of the new damage state.
- The entire process is repeated.

5.3.2 Simulation framework

The objective of the study described in this chapter is to determine the influence of the input fibre strength Weibull distribution on the structural predictions of the model. For this, the mechanical behaviour of carbon/epoxy unidirectional (UD) composites under tensile loading has been simulated. Such unidirectional composites are used for many structural applications such as filament wound composite pressure vessels and pipes.

A uniform density of force was applied to the cross-sectional surface at the ends, parallel to the longitudinal direction of the specimen. Two main types of loadings were simulated: monotonically increased loading up to failure, and monotonically increased loading until a certain point followed by a constant load thereafter. The loading conditions have been explained later in Section 5.3.4.

Finite element mesh

The structure studied was a parallelepiped specimen of dimensions $64 \text{ mm} \times 4 \text{ mm} \times 1 \text{ mm}$, as shown in Figure 5.4(a). Similar structures have also been studied previously with the model [122, 123]. To build the finite element mesh, three dimensional linear brick elements C3D8 were used. Each finite element was formed of 8 RVEs, and therefore had 8 Gauss points, each one corresponding to a single RVE as shown in Figures 5.4(b) and (c). The finite element had dimensions of $8 \text{ mm} \times 0.1 \text{ mm} \times 0.1 \text{ mm}$. This whole structure was represented by a mesh of 3200 elements. Although the size of the structure is small compared to structural applications, it contains about 13000 fibres in the cross-section. The elastic coefficients of the unidirectional ply are summarized in Table 5.1 [124].

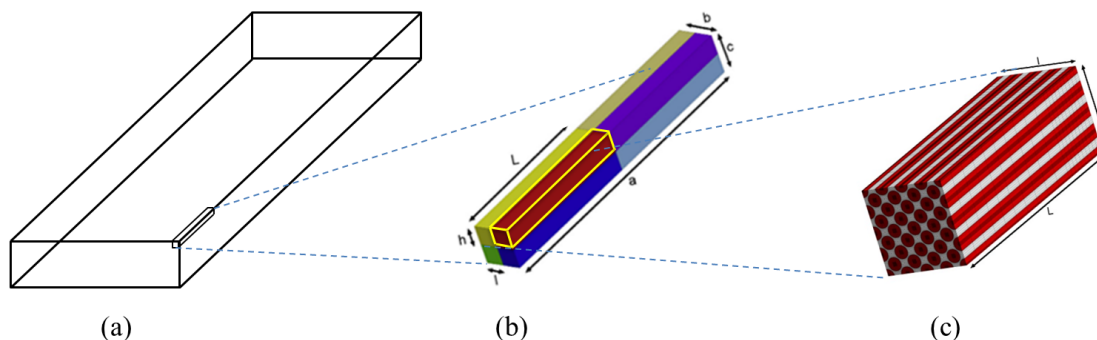


Figure 5.4: (a) Specimen of dimensions 64 mm \times 4 mm \times 1 mm. (b) A C3D8 linear 3-D brick element consisting of 8 RVEs. (c) An RVE with 32 fibres [12].

Table 5.1: Elastic properties of an undamaged UD ply for 64% fibre volume fraction.

E_{11}	$E_{22}=E_{33}$	$\nu_{12} = \nu_{13}$	ν_{23}	$G_{12} = G_{13}$	G_{23}
145.0 GPa	12.5 GPa	0.29	0.40	5.5 GPa	7.0 GPa

5.3.3 Input fibre strength distribution: Hypothetical properties based on uncertainties

The fibre strength distributions to be fed as input to the models were generated based on experimentally determined fibre strength results and statistically determined uncertainties, as calculated in Chapter 4. Based on the selected distributions, a Monte-Carlo process was used to assign a set of 5 fibre strength values to each individual fibre inside the simulated composites, one for each of the 5 sequential damage states.

The objective of the study described in this chapter is to understand the variability in the predictions of composite strength models, induced as a result of uncertain input fibre strength properties. A parametric investigation was carried out using the model described before. This investigation concerns the parameters of the fibre strength Weibull distribution. Consequently, the analysis is based on hypothetical fibre properties. However, the fibre strength properties were chosen to closely mimic the fibre strength behaviour determined experimentally, as described in the previous chapter. It is important to clearly mention that the goal of the study was not to make a comparison between simulations and actual experimental results, but to obtain a range of variability in the simulation results coming from the predictive composite strength models.

To understand how these hypothetical fibre properties are linked to real T700 carbon fibres, the following explanation must be understood. As described in Chapter 4, the shape and scale parameters of the fibre strength Weibull distribution of T700 carbon fibres of 30 mm gauge length, as calculated for a sample of 30 fibre strength data points, in terms of their expanded uncertainties are as follows:

$$m = 3.38 \pm 1.00, \text{ for a confidence level of 95\%}$$

$$\sigma_0 = 4.17 \pm 0.49 \text{ GPa (4170} \pm 490 \text{ MPa), for a confidence level of 95\%}$$

Considering these uncertainties, the estimated Weibull parameters can lie anywhere between the given confidence intervals [22]. To determine the influence of this uncertainty, the input fibre strength Weibull parameters were varied between the given uncertainty limits, and its influence on the model predictions will be observed. The shape and scale parameter values were varied at 3 different levels, as shown in Table 5.2.

Table 5.2: Different levels of the shape and scale parameters of the input fibre strength distribution

Level	Shape parameter, m	Scale parameter, σ_0 (MPa)
1	3.0	4000
2	4.0	4500
3	5.0	5000

For the first study, the shape parameter was fixed at 4.0 and the scale parameter was varied between 4000, 4500, and 5000 MPa. For the second study, the scale parameter was fixed at 5000 MPa and the shape parameter was varied between 3.0, 4.0, and 5.0.

5.3.4 Loading conditions

Two types of loading conditions were considered: monotonic and sustained loading.

Monotonic loading: For this case, the applied tensile loading on the specimen was monotonically increased at 1 MPa/s. The load was increased until a numerical instability was reached, indicating specimen failure.

Figure 5.5(a) shows a characteristic stress-strain curve depicting the behaviour of the specimen under monotonic loading condition. The whole curve can be defined by three stages. During Stage 1, the strain increases at a quasi-linear rate with the applied tensile stress. During Stage 2, which appears as a plateau, the predicted strain increases rapidly with a small increment in the applied tensile stress. This represents the region of numerical instability. Following this, Stage 3 takes place, where a linear increase of strain is observed for an increasing applied tensile load. This represents the condition when all the fibres in the composite are broken. The failure stress of the specimen is given by the first knee point, as also highlighted in Figure 5.5(a). It is estimated by considering the hypothetical intersection point of the lines in Stages 1 and 2 [12]. It should be understood that the Stages 2 and 3 are never observed experimentally but are only accessible through simulations, and are useful in determining the failure point of the simulated composite specimens. Figure 5.5(b) shows the corresponding evolution of the fibre break density with increase in stress. Fibre break density is the average number of broken fibres in the RVEs of 32 fibres.

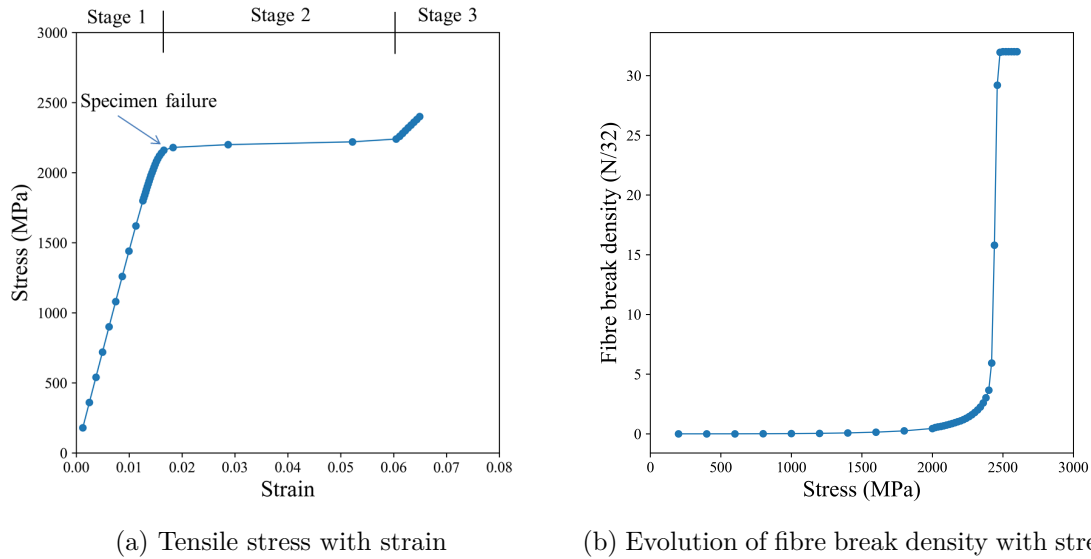


Figure 5.5: Characteristic curves for the monotonic loading condition

Sustained loading: For structural applications such as composite pressure vessels, the time dependent behaviour of the matrix can result in progressive damage as such structures are often under load for a very long time. Such structures can be assessed using slow burst tests [2, 125]. To simulate a similar situation, the tensile load on the specimen was monotonically increased at 1 MPa/s until a given load F_{SL} . Following this, the tensile load was maintained constant at this peak level. This allows the viscoelastic effect of the matrix to operate. The specimen was maintained at this constant peak load until numerical instability was reached. The peak load was chosen as: $F_{SL} = 0.96 \times F_{ML}$, where F_{ML} was the failure stress obtained for the monotonic loading condition for the same input properties. $0.96 \times F_{ML}$ was chosen as it corresponds to the stress value at which the instability was observed to originate in the monotonic loading condition.

Figure 5.6(a) shows a characteristic curve of the the strain-time behaviour for the sustained loading condition. The whole curve for the simulated strain-time behaviour can be defined by three stages. During Stage 1, the strain increases at a quasi-linear rate with the applied tensile stress (which is a function of time). During Stage 2, which appears as a plateau, the predicted strain increases very slowly with time. The end of this region represents the region of numerical instability. Following this, Stage 3 takes place, where a linear increase of strain is observed for increasing time. This represents the condition when all the fibres in the composite are broken. The time to failure of the specimen is given by the second knee point, as also indicated in Figure 5.6(a). It is estimated by considering the hypothetical intersection point of the lines in Stages 2 and 3 [12]. Figure 5.6(b) shows the corresponding evolution of the fibre break density.

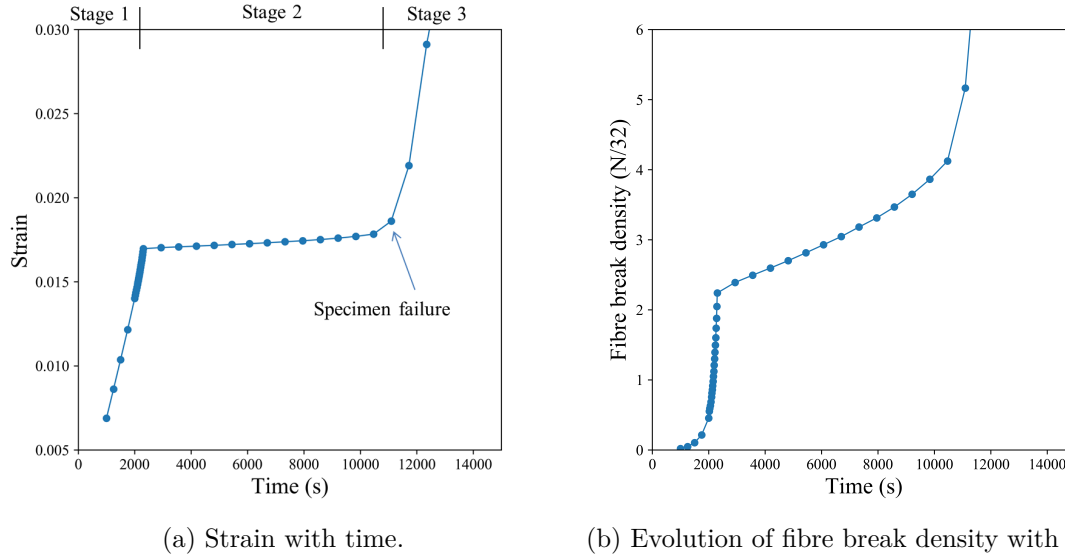


Figure 5.6: Characteristic curves for the sustained loading condition

5.4 Results and discussions

The effects of variations in the Weibull parameters of the input fibre strength distributions, for both loading conditions are shown here. A total of 10 simulations were carried out for both loading conditions analysed, and the median case is reported.

5.4.1 Monotonic loading

Effect of variation in the scale parameter

Figure 5.7(a) shows different curves for the simulated stress-strain behaviour of the composite when the scale parameter of the input fibre strength distribution was varied, while keeping the shape parameter fixed. The corresponding evolution of the fibre break density with applied stress for the different cases are shown in Figure 5.7(b). The calculated failure stress values for the different cases are given in Table 5.3. The standard deviation of the failure stresses for the repeated numerical tests was about 0.2%, as also observed in previous similar studies [22]. The failure stress can be seen to increase with an increase in scale parameter of the input fibre strength distribution. This is an expected behaviour because a large scale parameter value practically means that the average strength of fibres is high, and accordingly the simulated failure stress of such composites is also high. What is more interesting to note is that the observed variation in the predicted failure stress is about 10% from the mean case, on both sides. The failure stress is seen to be significantly dependent on the scale parameter. The model predictions are thus highly sensitive to the expected uncertainties in the scale parameter of the fibre strength distribution used as input. A similar variability in the evolution of fibre break density was also observed, as can be seen in Figure 5.7(b). Uncertainties in input fibre strength distribution are, for this reason, a big hindrance to the reliability of the predictions made by composite strength models.

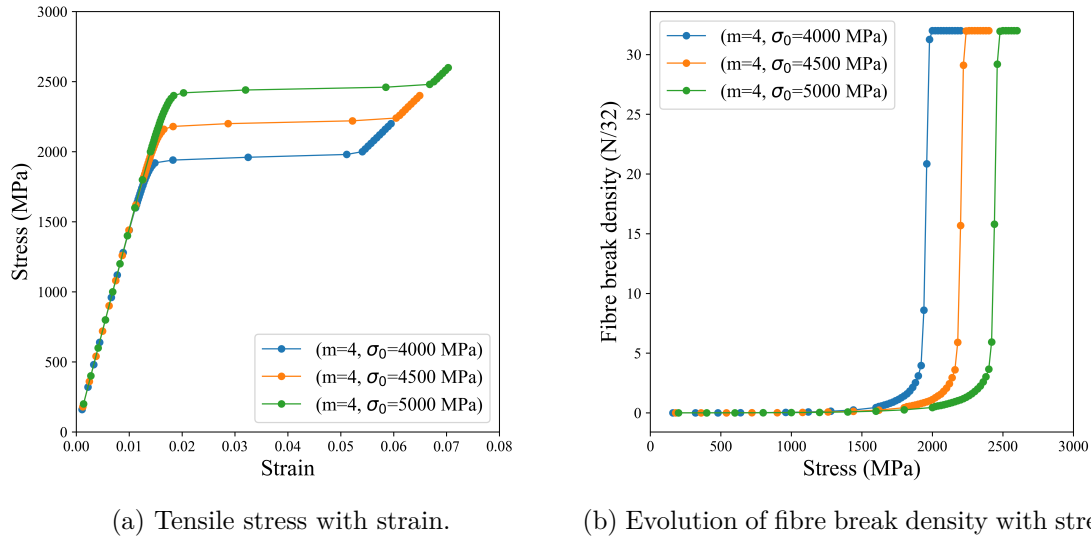


Figure 5.7: Simulated composite behaviour for different input fibre strength distributions with varying scale parameters.

Table 5.3: Simulated failure stress values of the composite for input fibre strength distributions having different scale parameters and same shape parameter

Shape parameter, m	Scale parameter, σ_0 (MPa)	Failure stress (MPa)
4.0	4000	1960
	4500	2130
	5000	2380

Effect of variation in the shape parameter

Figure 5.8(a) shows different curves for the simulated stress-strain behaviour of the composite when the shape parameter of the input fibre strength distribution was varied. The corresponding evolution of the fibre break density with applied stress for the different cases is shown in Figure 5.8(b).

The calculated failure stress values for the different cases are given in Table 5.4. Again, the standard deviation of the failure stresses for the repeated numerical tests was about 0.2%. The failure stress increases, very slightly, with increasing shape parameter of the input fibre strength distribution. This variation can be attributed to the following reason: A small shape parameter value typically means that the scatter in the strength of fibres in a population is large. This means that the probability of having very weak fibres in the distribution is also higher. It has been postulated by some previous studies that presence of weak fibres in the population control the failure behaviour of unidirectional composites [11]. This means that the failure stress of composites with fibres having a low shape pa-

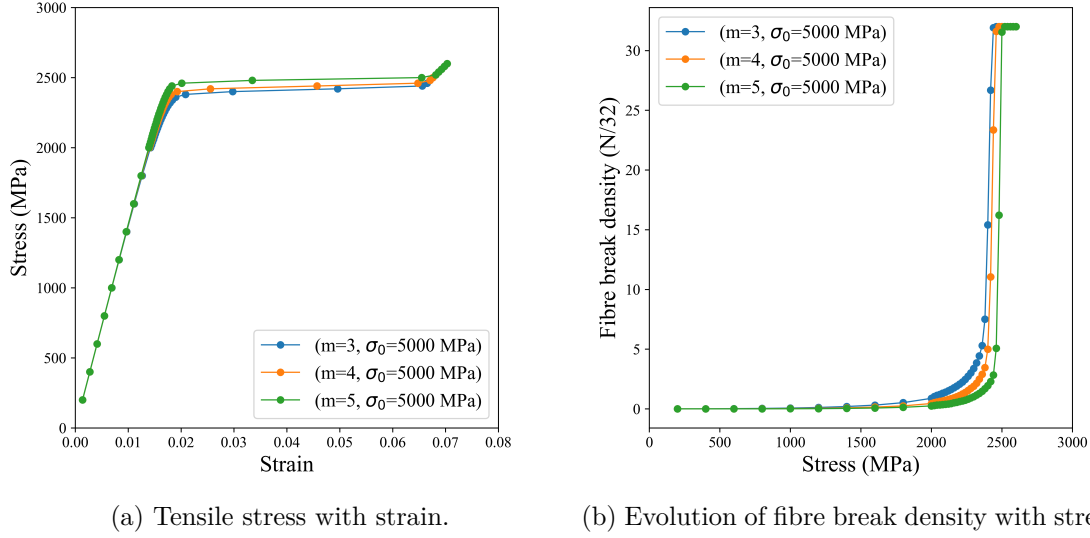


Figure 5.8: Simulated composite behaviour for different input fibre strength distributions with varying shape parameters.

parameter (and thus larger scatter in fibre strength and therefore a larger proportion of weak fibres) is comparatively lower than those with fibres having a larger shape parameter (and thus a smaller scatter in fibre strength and therefore a smaller proportion of weak fibres). However, the observed variability in the predicted failure stress values is very small and is close to the range of the standard deviation. This variability is much smaller than the one observed for changes in input scale parameters for which case a very large variation in predicted failure stress was observed. Similarly, a very small variability in the evolution of fibre break density was also observed, as can be seen in Figure 5.7(b).

Table 5.4: Simulated failure stress values of the composite for input fibre strength distributions having different shape parameters and same scale parameter

Shape parameter, m	Scale parameter, σ_0 (MPa)	Failure stress (MPa)
3.0	5000	2340
4.0		2380
5.0		2440

Even though the uncertainty considered in the input hypothetical material properties was numerically higher for the Weibull shape parameter (m) as compared to that in the scale parameter (σ_0), the variability in model predictions was found to be significantly larger when changes in the scale parameter were made.

5.4.2 Sustained loading

Under the sustained loading condition, the fibre breakage process is influenced by the relaxation of the matrix. Consequently, new fibre breaks develop continuously when the specimen is subjected to stress over a period of time. The observed effects of variations in the scale and shape parameter of the input fibre strength distributions, on the model predictions for sustained loading are described here. To recall, the tensile load on the specimen was monotonically increased until a peak stress of $F_{SL} = 0.96 \times F_{ML}$, where F_{ML} was the failure stress obtained for the monotonic loading condition for the same input properties. Following this, the specimen was maintained at the constant peak load until numerical instability was reached.

Effect of variation in the scale parameter

Figure 5.9(a) shows different curves for the simulated strain vs time behaviour of the composite specimen when the scale parameter of the input fibre strength distribution was varied, while keeping the shape parameter fixed. The corresponding evolution of the fibre break density with time for the different cases is shown in Figure 5.9(b). The calculated lifetime of the structure (time to failure or numerical instability) for the different cases are given in Table 5.5. The standard deviation of the time to failure for the repeated numerical tests was about 1.5%, as also observed in previous similar studies [22].

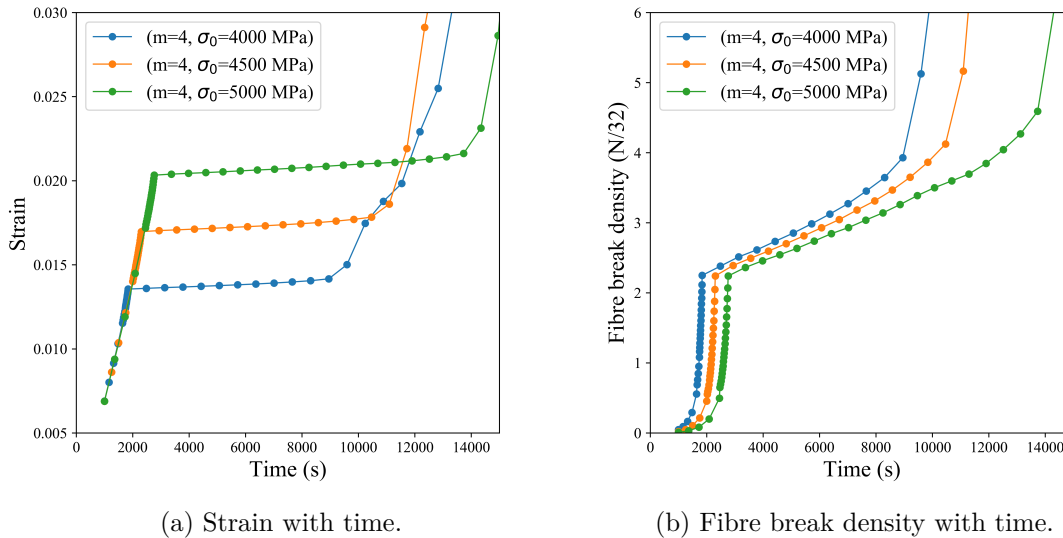


Figure 5.9: Simulated composite behaviour for different input fibre strength distributions with varying scale parameters, under the sustained loading condition.

The time to failure of the structure can be seen to increase with an increase in scale parameter of the input fibre strength distribution. As already explained for the monotonic loading case, this is an expected behaviour because a large scale parameter value means that the average strength of fibres is large, and accordingly the composite structure survives for a longer period of time. More interesting to note is the observed variation in the

Table 5.5: Simulated lifetime of the composite structure for input fibre strength distributions having different scale parameters and same shape parameter

Shape parameter, m	Scale parameter, σ_0 (MPa)	Lifetime (s)
4.0	4000	9422 (2.62 h)
	4500	10935 (3.04 h)
	5000	14129 (3.92 h)

predicted time to failure of the composite structure. A variation of 500 MPa (about 10%) in the input scale parameter of the fibre strength distribution, due to uncertainty, resulted in a variation in the predicted lifetime of about 15-30% from the mean case. The time to failure of the composite specimen was thus also found to be strongly affected by uncertainties in the scale parameter of the input fibre strength distribution. Relatively smaller difference in the evolution of fibre break density was observed, which was seen to follow a similar trend, as shown in Figure 5.9(b).

Effect of variation in the shape parameter

Figure 5.10(a) shows different curves for the simulated strain vs time behaviour of the composite structure when the shape parameter of the input fibre strength distribution was varied, while keeping the scale parameter fixed. The corresponding evolution of the fibre break density with time for the different cases are shown in Figure 5.10(b). The calculated lifetime of the structure for the different cases is given in Table 5.6. Again, the standard deviation of the time to failure for the repeated numerical tests was about 10%.

Table 5.6: Simulated lifetime of the composite structure for input fibre strength distributions having different shape parameters and same scale parameter

Shape parameter, m	Scale parameter, σ_0 (MPa)	Lifetime (s)
3.0	4500	10419 (2.90 h)
4.0		12096 (3.36 h)
5.0		14064 (3.91 h)

Unlike the results of the monotonic loading case, variations in the shape parameter was observed to affect significantly the time to failure of the composite specimen. An error of 1.0 (about 25%) in the shape parameter (for e.g., from $m = 4.0$ to $m = 5.0$) resulted in a variation of about 16% in the predicted lifetime of the specimen. (from 3.36 h to 3.91 h). Uncertainty in the shape parameter, thus, affects the time to failure of the structure significantly. This behaviour is different from that of the monotonically increasing loading case, where the failure stress of the structure increased only very minutely, with increasing shape parameter of the input fibre strength distribution. The physical explanation for the observed variation in the lifetime of the composite structure with changes in the shape

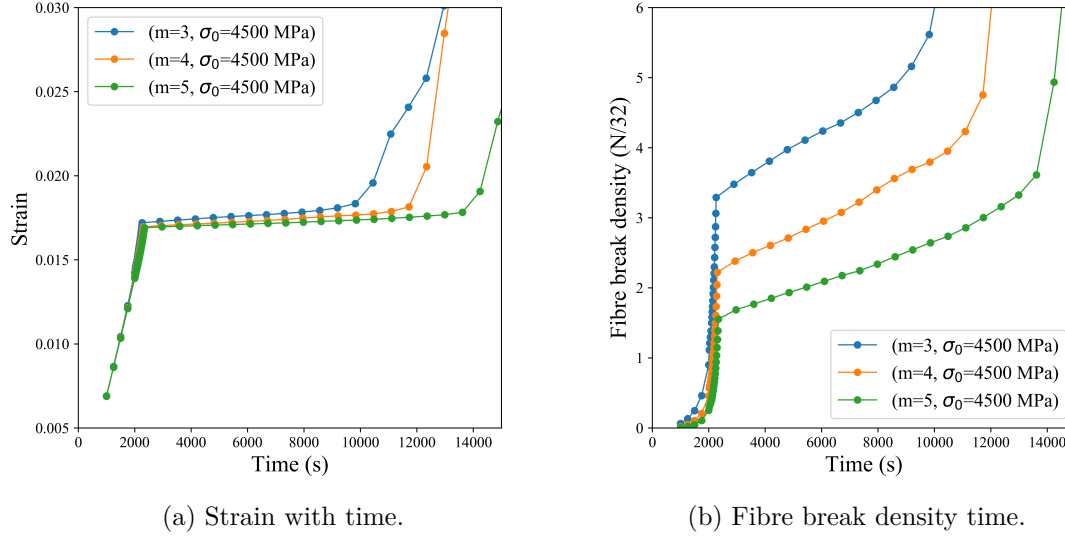


Figure 5.10: Simulated composite behaviour for different input fibre strength distributions with varying shape parameters, under the sustained loading condition.

parameter of the input fibre strength distribution, is that, the greater the scatter in fibre strength (attributed to a lower shape parameter value), the earlier the structure fails when subjected to sustained loading. This also reinforces the hypothesis that the lifetime of composite structures is dominated by the strength of weak fibres in the population [11].

It can also be seen in Figure 5.10, that although the strain to failure values of the composite structures are almost the same, the evolution of the fibre break density is very different for the different input fibre strength distributions. The fibre break density, when the structure is loaded at 96% of the failure stress is higher when the structure has a larger number of weak fibres. This variation in fibre break density is much larger than that observed when the scale parameter was varied, given in Figure 5.9(b). One possible explanation for this observed behaviour could be that, when the shape parameter of the input fibre strength distribution is low, there is comparatively a larger number of very weak fibres present in the structure. It is the failure of these weak fibres which results in a higher fibre break density.

5.5 Conclusions

The structural behaviour predicted by the composite strength model is found to be highly sensitive to the expected uncertainties in the parameters of the fibre strength distribution used as input. The Mines ParisTech model used for the study extrapolates fibre strength results to a gauge length of 4 mm for the simulations. This also adds uncertainty in the model predictions. For the present study, simulations were made for a very small structure. Much larger variations in the model predictions can be expected when actual composite structures are simulated, as also confirmed by Widjaja et al. [126]. Uncertainties in the input fibre strength distribution are, for this reason, a big hindrance to the reliability of

the predictions made by composite strength models.

The knowledge of variability in model predictions can also be useful for estimating the confidence interval which can be assigned to the predictions made by computational models, if these models are used as replacements for actual mechanical tests. Although using high design safety factors on the influential parameters make it possible to secure composite structures in a deterministic manner, it conceals the extent of the risk that is being taken in doing so, and also results in overdesign. Therefore, structural reliability analysis based on omnipresent uncertainties can provide the required risk information to engineers, if it can be appropriately conducted [35, 127].

In order to minimise such uncertainties in fibre strength results, the knowledge about the contributions of different factors which lead to uncertainty can empower researchers to take appropriate measures. Since it has been shown in Chapter 4 that the sampling randomness is a major cause of uncertainty, it would be recommended to use a sufficiently large set of experimentally generated fibre strength data, in order to minimize the sampling effect and maximize the accuracy of the estimated distribution parameters. The next chapter will try to address this need of a large fibre strength data set for analysis, by using an improved and semi-automated experimental process. In order to avoid the need for extrapolating fibre strength results so as to minimise potential uncertainties, characterisation of fibre strength at a gauge length of 4 mm will also be discussed. The mechanical properties of fibres will be analysed and appropriate statistical techniques will be applied to the generated data to re-evaluate uncertainties. This can help in adding meaningful inferences about the fibre population behaviour.

Chapter summary in French

Variabilité des prévisions des modèles de résistance composite en raison de propriétés d'entrée incertaines

Afin d'évaluer l'influence de l'incertitude de la résistance sur les prévisions à l'échelle du composite, un modèle développé à Mines ParisTech a été utilisé. Ce modèle prend en compte les processus physiques tels que la rupture des fibres et ses interactions avec la matrice environnante. Le développement de ce modèle a commencé en 2005 et a été amélioré au fil des ans pour simuler différentes conditions de chargement en service sur des structures composites telles que des réservoirs sous pression interne.

À l'aide de ce modèle, la résistance et la durée de vie d'une structure composite (ici une éprouvette) sont simulées dans deux conditions de chargement différentes (chargement monotone et chargement en fluage) pour élucider la sensibilité des différentes réponses structurelles aux paramètres de la distribution de la résistance des fibres unitaires.

Les résultats observés sur les incertitudes des paramètres de forme (m) et d'échelle (σ_0) de la distribution de Weibull, ont été répertoriés comme suit:

Chargement monotone:

- La contrainte de rupture dépend de manière significative du paramètre d'échelle. La variation observée de la contrainte à rupture est d'environ 10% (plus élevé ou plus bas) par rapport au cas moyen.*
- La sensibilité des prédictions du modèle au paramètre de forme est négligeable.*

Chargement en fluage:

- Le délai de rupture de l'échantillon composite s'est également révélé fortement affecté par les incertitudes du paramètre d'échelle. Une incertitude attendue de 500 MPa (environ 10%) dans le paramètre d'échelle entraîne une variation de la durée de vie d'environ 15 à 30% (plus élevée ou plus basse).*
- Une incertitude attendue de 1,0 (environ 25%) dans le paramètre de forme a entraîné une variation d'environ 16% de la durée de vie prévue de l'échantillon. L'incertitude dans le paramètre de forme affecte donc de manière significative le temps de défaillance de la structure.*

Le comportement structurel prédit par le modèle se révèle être très sensible aux incertitudes sur les paramètres de la distribution de résistance des fibres unitaires. Le modèle de Mines ParisTech utilisé pour l'étude extrapole les résultats de résistance des fibres à une longueur de jauge de 4 mm pour les simulations. Cela ajoute également de l'incertitude dans les prévisions du modèle. Pour la présente étude, des simulations ont été faites pour une très petite structure. Des variations beaucoup plus importantes des prévisions du modèle peuvent être attendues lorsque des structures composites réelles sont simulées. Les incertitudes dans la distribution de résistance des fibres sont, pour cette raison, un gros obstacle à la fiabilité des prévisions faites par les modèles de résistance des composites.

Minimiser ces incertitudes passe par une meilleure connaissance des contributions des différents facteurs à l'origine de ces incertitudes. Le caractère aléatoire de l'échantillonnage

est une cause majeure d'incertitude, il est recommandé d'utiliser un ensemble suffisamment grand de données afin de minimiser l'effet d'échantillonnage. Afin d'éviter la nécessité d'extrapoler les résultats de résistance à des longueurs de jauges plus faibles, il convient de proposer des méthodes expérimentales plus appropriées.

Chapter 6

Experimental and statistical investigation of fibre properties

***Abstract :** Fibre tensile strength and dimensional data for T700 carbon fibres has been generated at three different gauge lengths of 4, 20 and 30 mm, using an improved and semi-automated experimental methodology. The variability in strength and modulus of short fibres was found to be much larger than that of longer fibres. Statistical analysis of this large data set has helped in estimating the effect of sample size on reducing the uncertainties in results. Analysis of fibre dimensional data has helped in developing a better understanding of the surface morphology of T700 carbon fibres. The results also highlight the limitations of the standard Weibull analysis for representing fibre strength behaviour. The need for better analysis of the fibre strength data in order to provide a more accurate description of the fibre strength behaviour has been emphasized.*

Contents

6.1	Introduction	109
6.2	Material and methods	110
6.2.1	Material	110
6.2.2	Methods	110
6.2.3	Advantages of using the semi-automated testing method	114
6.3	Experimentation	116
6.3.1	Fibre dimensional measurement	116
6.3.2	Fibre tensile strength measurement	118
6.4	Results and discussions	118
6.4.1	Fibre dimensional analysis	118
6.4.2	Measurement of Poisson's ratio	121
6.4.3	Tensile strength	124
6.4.4	Strength distribution	127
6.4.5	Effect of sample size on the confidence interval	131
6.5	Conclusions	132
6.5.1	Scope for improvement in the fibre testing system	135
	Chapter summary in French	136

This chapter has been adapted from the following article:

F. Islam, S. Joannès, S. Bucknell, Y. Leray, A. Bunsell, L. Lailarinandrasana, "Investigation of tensile strength and dimensional variation of T700 carbon fibres using an improved experimental setup", *Journal of Reinforced Plastics and Composites*, 2020, 39 (3-4), 144-162.

6.1 Introduction

As discussed in Chapter 4, for an accurate and reliable statistical representation of the fibre strength behaviour, a large sample set of fibre strength data is required. This need for a large fibre strength data set for reliable analysis has also been highlighted by a number of previous studies [76, 25, 37, 26]. Obtaining a large sample set of fibre strength data can be problematic since the standard fibre testing process is usually very challenging and time consuming, as already mentioned in the previous chapters. Most previous studies on fibre strength characterisation have therefore been limited to a small sample size for analysis. The sample sizes used for most previous studies on T700 carbon fibres have been between 10-30, as also shown in Table 1.1. Based on the results of such an analysis, conclusions are drawn on the strength behaviour of the whole fibre population. However, it has been demonstrated in Chapter 4, that even a sample size of 30, results in a large statistical uncertainty in obtained results. To reduce this uncertainty, a large and accurate data set of fibre strength is required. It is comprehensible that analysis conducted on a large sample size can provide more reliable results than those obtained from a smaller sample size [128]. The need for a large set of fibre strength data for analysis will be addressed in this chapter by using a semi-automated testing methodology.

It has also been mentioned in Chapter 2 that composite strength models require fibre properties at small gauge lengths. For e.g., the composite strength model used for the study in Chapter 5 requires fibre strength information for a gauge length of 4 mm, which it obtains by extrapolation. However, it has also been demonstrated in Chapter 4, that the extrapolation of the Weibull parameters introduces more uncertainties in results. To avoid the need for extrapolation, characterisation of fibre strength at a gauge length of 4 mm will also be described in this chapter. As discussed in Chapter 3, there are many issues with the experimental determination of fibre strength at such small gauge lengths when using the standard testing methodologies. A testing methodology which minimises these issues would be used for generating data.

It was also shown statistically in Chapter 3 that for fibres of long gauge lengths, the fibre diameter measurement is the most critical parameter for an accurate determination of fibre strength. A detailed dimensional analysis of T700 carbon fibres will also be conducted to provide further insights into the surface morphology of the fibres through statistical analysis.

The present chapter tackles the above mentioned issues by addressing the following questions:

- *Can the uncertainty in the fibre strength distribution be reduced by using a large data set for analysis?*
- *Can fibre strength be characterised at short gauge lengths?*
- *What is the role of fibre dimensions in providing the best statistical representation of the fibre strength behaviour?*

Based on the questions raised above, the objectives of this chapter are, firstly, to generate a large set of fibre strength and dimensional data, at both short and long fibre gauge lengths. An improved and semi-automated experimental system, developed by Dia-Stron

Ltd. will be used, so as to overcome the typical challenges faced by the standard testing methodology discussed in the previous chapters. The second objective is to statistically analyse the experimental results generated for the different fibre gauge lengths. The fibre strength results will be analysed in order to evaluate the potential reduction of statistical uncertainties in the fibre strength distribution, and the dimensional data will be analysed to better understand the surface morphology of carbon fibres. Additionally, an attempt to measure the Poisson's ratio of fibres will be made. The learnings from this chapter will also be used for highlighting major issues in the statistical representation of the fibre strength behaviour.

6.2 Material and methods

6.2.1 Material

Bobbins of T700SC carbon fibres manufactured by Toray were used for the study, as also used for the study demonstrated in Chapter 3. The properties provided by the manufacturers data sheet are given in Table 6.1. Fibre dimensional analysis and single fibre tests for tensile strength measurement were conducted on the fibres extracted from these procured bobbins.

Table 6.1: Fibre properties supplied by the manufacturer

Characteristics	Unit	min	max
Tensile Strength	MPa	4510	-
Young's Modulus	GPa	221	240
Elongation at break	%	1.9	-

6.2.2 Methods

In the following subsections, the semi-automated system used for the study will be described. This system helps in addressing the need of a large data set for analysis by overcoming the problems faced by the standard single fibre testing methods.

Fibre dimensional measurement method

The sensitivity analysis demonstrated in Chapter 3 has highlighted the importance of dimensional measurement of fibres for accurate estimation of fibre strength [43]. It has been statistically established that for fibre gauge lengths commonly used for testing, the fibre diameter is the most critical parameter for accurate determination of fibre strength. To determine the variations in fibre diameter and cross-sectional area, an automated and non-contact measurement system, the Fibre Dimensional Analysis System (FDAS770), developed by Dia-Stron Ltd. was used. The FDAS770 is based on the principles of laser scanning microscopy and installs a Mitutoyo laser scanning micrometre (LSM500). The system allows non-contact, rapid and accurate fibre dimensional measurements and has also previously been used for studies involving dimensional analysis of different types of

fibres [129, 130]. An isometric view of the setup is shown in Figure 6.1(a), its working in Figure 6.1(b) and a zoomed-in image of the translation stage is shown in Figure 6.1(c).

To ensure that the fibres do not fail during the process of handling and transfer to the measurement setup, the specimens were handled using a fixture specifically designed to lift and manoeuvre the fibres. This fixture also ensured that the fibre gauge length is fixed and that there is no tension on the fibre specimens. After placing the fibre specimen on the setup, the rotating sample arms allow a complete 360-degree inspection of the fibre. The linear translation stage allows different fibre segments to be measured in the axial direction, i.e. along the length. The combined rotation and translation movements provide a complete 3-dimensional analysis of the fibre. The system facilitates a measuring range of 5-2000 micrometres with an accuracy of 0.3 micrometres.

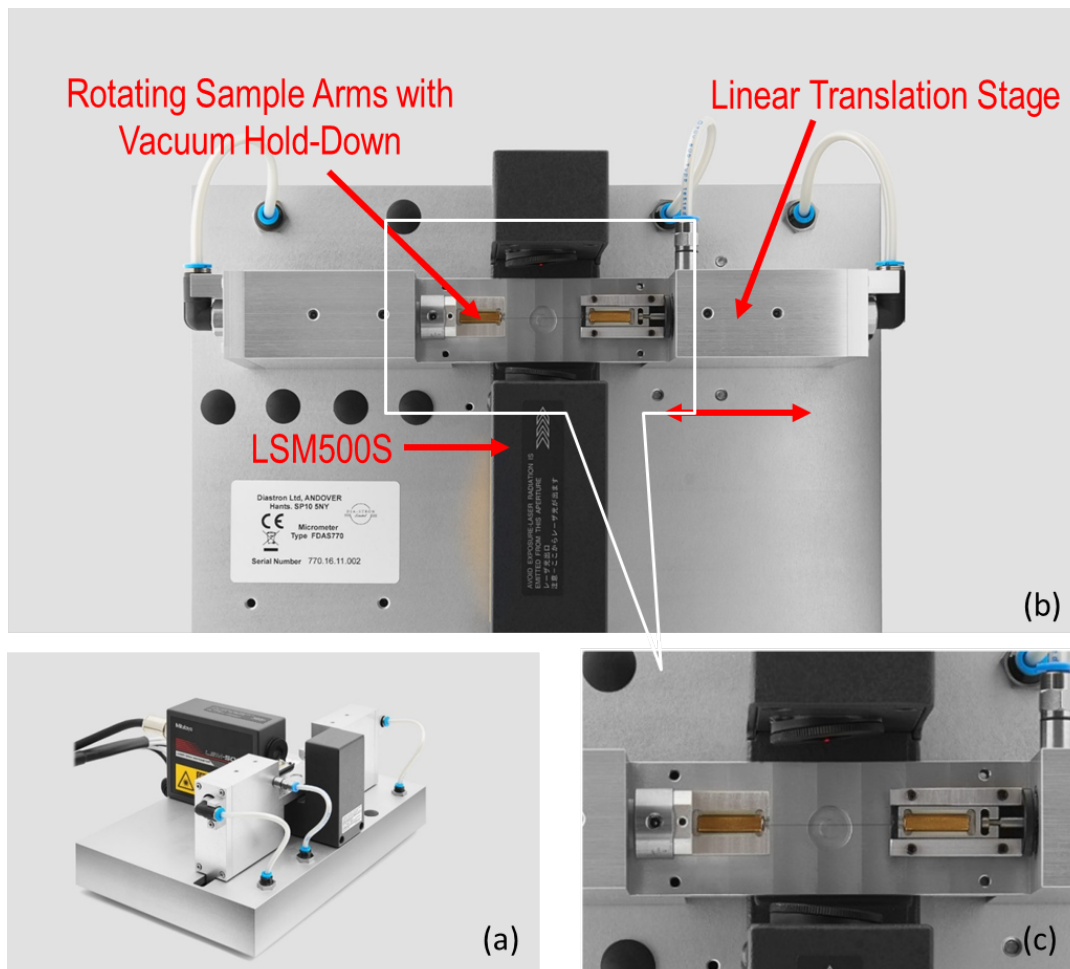


Figure 6.1: (a) Dia-Stron Fibre Dimensional Analysis System (FDAS770, Isometric view). (b) Working of the FDAS770 (top view). (c) Zoomed-in image of the translation stage.

Single fibre testing method

To overcome the challenges faced by the standard method of testing single fibres, an improved single fibre testing setup was developed by Dia-Stron Ltd. The entire testing process for determining the strength of a single fibre has been divided into 3 steps. Improvements introduced in each step to address the existing challenges will be discussed in the following subsections. The steps include:

- Specimen preparation
- Specimen loading
- Specimen testing

Specimen preparation. This system replaces the paper frames (demonstrated earlier in Chapters 2 and 3) with plastic tabs, as shown in Figure 6.2(a). These tabs impart rigidity to the prepared specimen. Single carbon fibres are randomly selected from the fibre yarn, and each end of the fibre is mounted on a plastic tab. The tabs are separated by a distance equal to the required gauge length, which is defined by exclusive cassettes which also act as a platform for holding all prepared specimens. A fibre selection and vacuum pick-up pen assists with filament separation from the yarn. The plastic tabs have fine grooves at the ends which prevents any lateral movement of fibres on the tab. For this, each end of a fibre is supported on 2 grooves of a tab (the other 2 grooves are disregarded). The wells at the fibre ends (one at each end) are then filled with an adhesive which then locks the fibre in its position. This ensures excellent alignment and also fixes the gauge length of the fibre specimen very accurately, as also shown in Figure 6.2(b). Using the standard method of sample preparation using a paper tab results in a few millimetres of misalignment, which is quite large. Using the plastic tab can thus bring significant improvements in specimen preparation and in minimising misalignment. EMI Optocast 3553 UV curing adhesive is used to bond the fibres to the tabs. The adhesive on each tab was cured by exposing it to UV light at a wavelength of 365 nm for about 15 seconds. Figure 6.3 shows a cassette loaded with 20 fibre specimens. Each specimen comprises of two tabs holding a single fibre in its grooves.

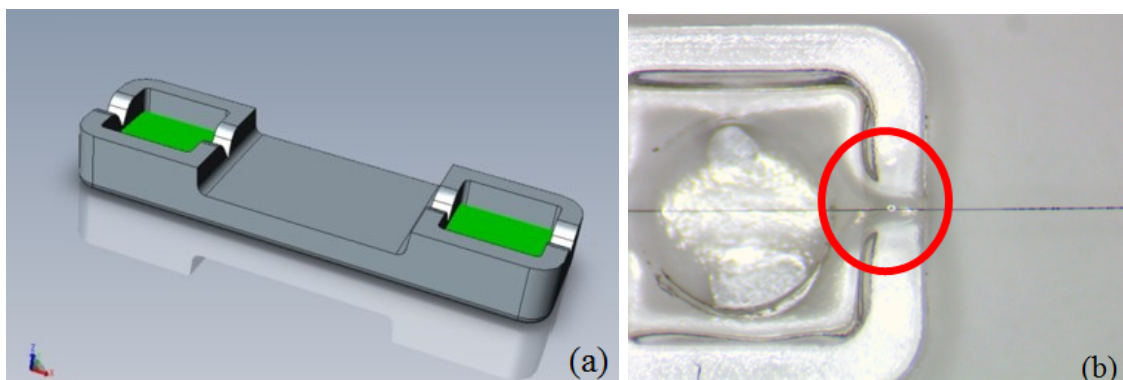


Figure 6.2: (a) Plastic tabs used for mounting one end of a fibre. (b) Well defined gauge length with proper alignment.

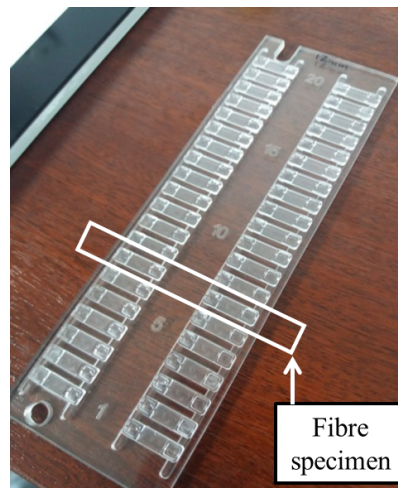


Figure 6.3: A 20 sample cassette loaded with fibre specimens ready to be tested.

Specimen loading. Once the cassette is ready with a set of fibre specimens, each specimen is transferred from the cassette to the testing site via an Automated Loading System (ALS1500), as shown in Figure 6.4. The system operates automatically using vacuum suction which allows efficient and safe transport of the fragile specimens from the storage cassette to the measurement modules. The main benefits of using the automated loading system are: (1) increase in the testing productivity, due to a continuous and unsupervised process, (2) reduction in the number of specimens that fail during transport, due to the elimination of most manual handling errors during specimen transfer and mounting, and (3) improvement in data quality, due to the avoidance of unwanted and inconsistent handling loads.

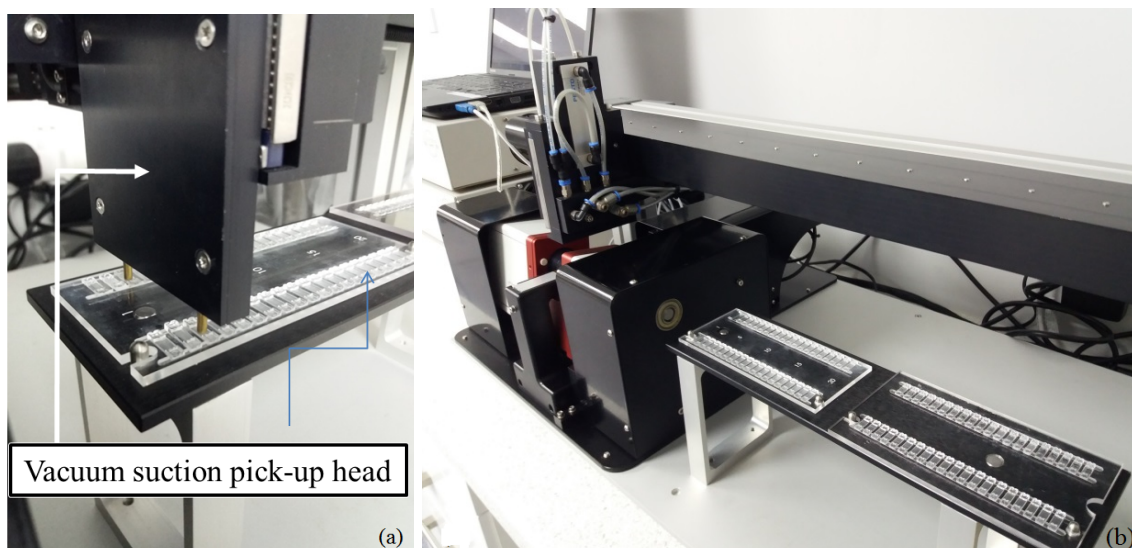


Figure 6.4: (a) ALS Vacuum suction for specimen pick up (b) transfer of specimen to testing site.

Specimen testing. After collecting and loading a sample, the mechanical testing is conducted by an automated system called LEX/LDS. This system integrates a Linear Extensometer (LEX820) with a Laser Diffraction System (LDS0200) into one module, and is shown in Figure 6.5(a). The whole setup around the testing site is shown in Figure 6.5(b). The LEX820 is a high resolution extensometer developed specifically for fine fibre applications. A DC micrometer drive offers exceptionally smooth travel combined with high positional repeatability. The module is useful for fibres which fail at low strain values and provides highly detailed stress/strain data. This makes it very suitable to test brittle technical fibres such as carbon. The LEX820 ensures fibre straightness and orthogonality with the laser beam for high precision diameter measurements. It also offers a high range of extension up to 53 mm, and a high range of extension speed up to 2.6 mm/s. The LEX820 was equipped with a high-precision load cell which provided a resolution of 0.05 mN, which is an order of magnitude lower than that used previously in Chapter 3 of the thesis. This further helps in minimising the uncertainty in measurements.

The LDS0200 provides direct, non-contact diameter measurements of the fibres before tensile tests. The measurement principle is based on laser diffraction which enables diameter measurements down to a few microns. For the calculation of tensile strength, fibre cross-sectional area is calculated using the measured diameter. The technical specifications and compliance correction for conducting the tests are in conformance with the standard ASTM C1557-14.

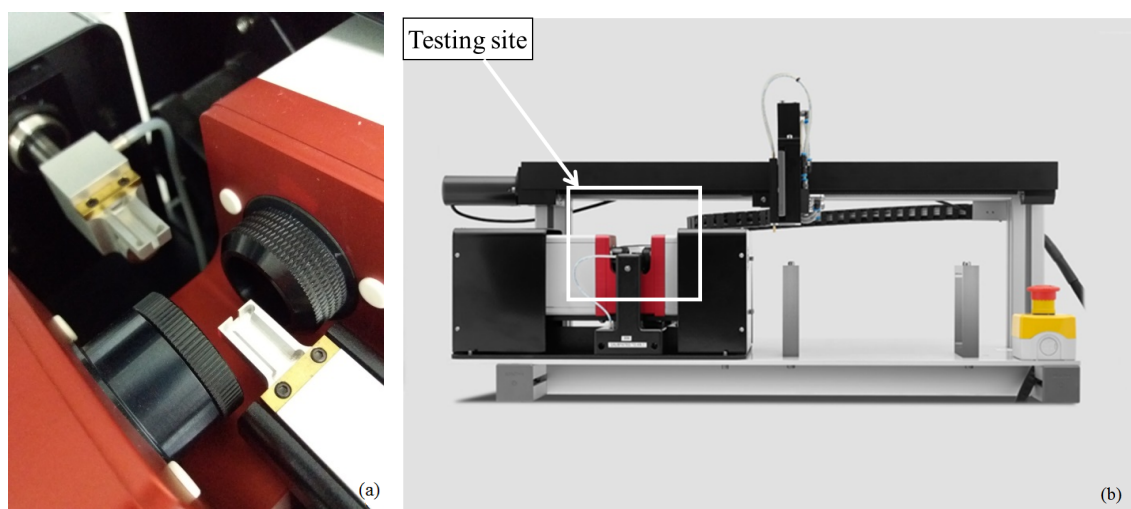


Figure 6.5: (a) Testing site: Combination of the LEX/LDS system. (b) Testing setup installed with the LEX/LDS system [131].

6.2.3 Advantages of using the semi-automated testing method

Following are some of the advantages of using the semi-automated testing system, over the standard single fibre testing methodology:

- **Alignment :** ASTM C1557 recommends that the axis of the fibre should be coaxial with the line of action of the testing machine within d , to prevent spurious bending

strains and stress concentrations [66].

$$d \leq L_0/50$$

where; d is the tolerance (in m), and L_0 is the fibre gauge length (in m).

Specimen preparation using paper tabs requires utmost precision and depends strongly on user skill to align the fibres properly on the paper tab. The paper tab then has to be aligned to the loading direction to achieve proper alignment between fibre and loading direction. This makes it very difficult to achieve a proper degree of alignment while using this method, especially for smaller gauge lengths. By comparison, plastic tabs in the used method locked any lateral movement of fibres and aligned the fibres properly in the direction along the length of the tab.

- **Gauge length correction :** The fibres are pre-tensioned before testing to remove any slack in the fibre specimen. This may change the original separation between plastic tabs and hence the effective gauge length. The new system measured the exact extension applied for tensioning and corrected the effective gauge length accordingly before proceeding with the test. This was not possible when using the manual method of paper tabs.
- **Specimen preparation time :** Using the manual method, the total time required to prepare a set of 20 fibre specimens is around 3.5 hours. This includes preparation of paper tabs of precise dimensions, mounting single fibres on each tab and the application of adhesive to fix the gauge length as required. The specimens are then left to cure for more than 12 hours. The individual specimens are then transferred to the test setup one at a time for experimentation. The testing process for a set of 20 specimens takes about 1.5 hours in total. Using the semi-automated system cuts down the specimen preparation time to around 1 hour including the time required for curing. The prepared specimens can then be mounted onto a cassette following which the entire testing process is automated. This process reduced the total preparation and testing time to around 2.5 hours, with an effective involvement time of only about 1 hour compared to more than 5 hours for the manual process. This allowed testing a large number of fibres in a comparatively much smaller time.
- **Reduced specimen failure during preparation and transport :** While using the manual testing process, the specimen is subjected to many external and unwanted forces at different stages of preparation and transport. This often leads to specimen failure before the actual test. Using the semi-automated system eliminates most unwanted and accidental forces which helped in preserving the majority of specimens for the final test.
- **Ability to test at shorter gauge lengths :** Using a cassette-based specimen set simplified the preparation process for single fibre specimens and the added grooves on plastic tabs ensured proper alignment of fibres. This allowed specimens to be prepared and tested at a reduced gauge length. The present system thus allowed fibre specimens to be prepared and tested at small gauge lengths of 4mm.

The points of similarities and differences between the semi-automated and standard manual single fibre testing process have been highlighted in Table 6.2.

Table 6.2: Comparison of semi-automated and standard manual single fibre testing methods

	Standard testing	Automated testing
Specimen preparation	Fibre mounted on flat paper tabs	Fibre mounted on plastic tabs with grooves
Fibre extraction	Hand held	Using vacuum/suction pen
Fibre mounting process	Manual	Using vacuum/suction pen
Fibre alignment	Depends upon user skill	Near perfect alignment with the help of grooves on plastic tabs
Gauge length	Depends on size of paper tab and locations of glue (which depends on the accuracy of paper tab length)	Fixed due to locking of plastic tabs in cassettes
Specimen preparation time (set of 20 fibres)	~3.5 hours (excluding adhesive curing time) ~12 hours (including adhesive curing time)	~0.75 hours (excluding adhesive curing time) ~1 hour (including adhesive curing time)
Specimen mounting process	Manually lifted and placed on test setup	Automated transfer of specimens from cassettes to test setup using Dia-Stron ALS
Gauge length correction	No	Gauge length corrected after pre-tensioning the fibres
Intermediate Step	Paper tabs slit manually to allow load transfer	No intermediate step
Load application	Automatic	Automatic
Specimen test time (set of 20 fibres)	~1.5 hours (Manual)	~1.5 hours (Automated, can be left to run on its own)
Total time	5 hours	2.5 hours
Total person hours (set of 20 fibres)	5 hours	1 hour

6.3 Experimentation

6.3.1 Fibre dimensional measurement

A detailed dimensional study on T700 carbon fibres was conducted to capture any dimensional irregularities in such fibres. This was in addition to the fibre diameter measured for calculating the tensile strength of fibres. A total of 10 fibres were used for this study, the length of each fibre being 25 mm. Fibre specimens were measured using the FDAS770 system to measure the apparent diameter of the fibres. For conducting this part of the study,

the movement of the fibre dimensional measurement system was numerically controlled in order to allow dimensional measurement along the axial as well as radial directions of the fibre. Fibre dimensional measurements were taken by first fixing T700 carbon fibres centrally onto the stage and measuring the apparent fibre diameter. Variation in fibre diameter along the length was captured by shifting the stage linearly, i.e. along the axial direction of fibre. The measurement was taken along the total length of 25 mm at intervals of 1 mm. To measure the fibre diameter variation in the angular direction of the fibre (or due to angular orientation), the fibre specimen was rotated by 10 degrees about its axis. The fibre diameter was again measured similarly along the entire length, for this new angular position. This was repeated for 19 different angular positions from 0 up to 180 degrees, at equal intervals of 10 degrees. The combined rotation and translation of the fibre together provided dimension measurements at a total of 475, i.e. 25×19 , different locations on the fibre surface. This has been schematically represented in Figure 6.6 by unwrapping the fibre surface on a 2-D plane. The different central points at which fibre dimensions were recorded are shown by the intersection of the horizontal and vertical lines in Figure 6.6(c). The results are discussed in Section 6.4.1. A limitation of using such a system for measuring fibre dimensions in the angular direction (for estimating the fibre cross-sectional area of the fibre) is that any concavity in the fibre surface would remain unnoticed. Although T700 carbon fibres are not known to have concave surfaces, these limitations must be considered when using using such a measurement system with other carbon fibres such as T300, and natural fibres [87, 97].

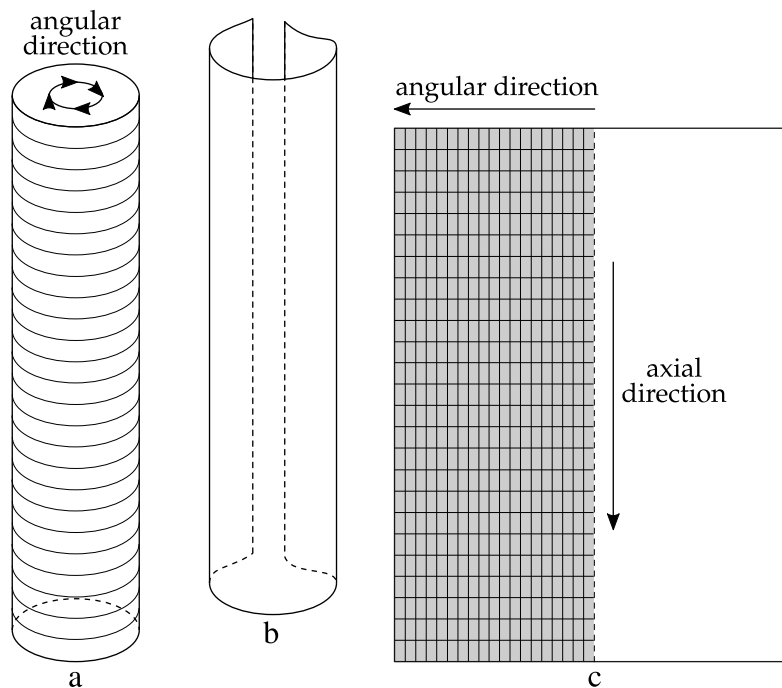


Figure 6.6: Schematic diagram of unwrapping a fibre surface on a 2-D plane to show the different locations at which dimensional measurements were recorded.

6.3.2 Fibre tensile strength measurement

T700 carbon fibres were tested for tensile strength using the automated testing system described in Section 6.2.2. Using this system overcomes many of the issues with the standard testing methodology discussed in Chapters 2 and 3, and reduces the experimental errors or uncertainties significantly. Fibres were tested at three different gauge lengths of 4 mm, 20 mm and 30 mm. As mentioned in Chapter 2, a requirement for composite strength models is that the input fibre properties should be defined at specific gauge lengths. These required lengths are usually smaller when compared to the gauge length usually used for experimentation. The usual practice is thus to use results generated using long gauge lengths and then to extrapolate the properties to shorter gauge lengths using the Weibull scaling function given by Equation 1.2. This has inspired the idea behind choosing the gauge lengths of the tests in the present study. 30 mm and 20 mm are the most commonly used lengths while the Mines ParisTech composite strength model described in Chapter 5 requires input properties for fibres of 4 mm gauge length.

Testing fibres at three different gauge lengths also allowed the compliance of the system to be calculated, which was then used to calibrate all the measurements, as discussed in later sections. The semi-automated system allowed testing a large sample set of fibres in a relatively short time period. The total number of fibre strength results determined for each gauge length are given in Table 6.3. This number is much larger than any of the previously reported studies.

Table 6.3: Total number of fibre strength results determined for each gauge length

S.N.	Gauge Length (mm)	N
1	4	120
2	20	135
3	30	350

6.4 Results and discussions

6.4.1 Fibre dimensional analysis

The variations in measured fibre diameters are represented with histograms for each gauge length, as shown in Figure 6.7. The range and frequencies of the fibre diameters were found to be very similar for all the three gauge lengths, as given in Table 6.4. It can be seen that all three measures of central tendencies, i.e. the mean, median and mode are similar for the three cases. There is, however, a slight scatter in the measured fibre diameter values, which was found to vary mostly between 6.5 to 7.5 μm .

Variation of fibre diameter along the length.

Figure 6.8(a) shows the variation in measured fibre diameter along the length (i.e. in the axial direction) for one of the fibres investigated (say Fibre 1). Different plots represent

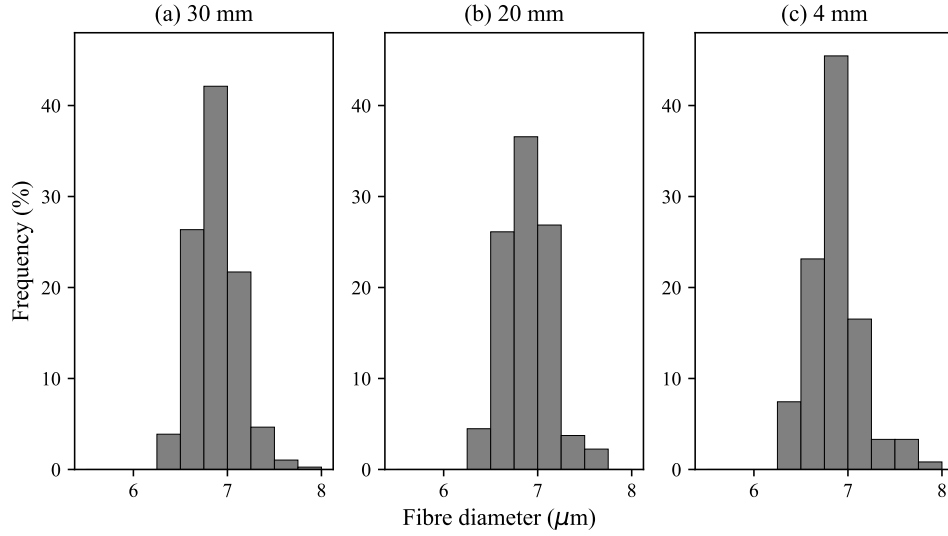


Figure 6.7: Histograms showing the variations in measured fibre diameters for all fibres of the different gauge lengths: (a) $L_0=30$ mm, (b) $L_0=20$ mm, (c) $L_0=4$ mm

Table 6.4: Mean, median and mode values of fibre diameters for the different gauge lengths

Gauge Length \rightarrow	30 mm	20 mm	4 mm
Mean (μm)	6.87	6.88	6.86
Median (μm)	6.86	6.89	6.83
Mode (μm)	6.75-7.00	6.75-7.00	6.75-7.00

measurements at different angular orientations. Only results at intervals of 20° are shown for clarity. The apparent diameter measured was found to be very consistent and varied between $7.4 - 7.6 \mu\text{m}$ along the length, which is less than 2% from the mean value. When the measurement was repeated using the same fibre, similar results were obtained with the same locations of maxima and minima, which confirms the reliability of the measurements. Although fibre diameter on average was found to vary in the range $6.8 - 7.8 \mu\text{m}$ between different fibre specimens, the variation for individual fibres was found to be within 2-3% along the length for most fibres.

However, for two of the ten fibres investigated, a much larger variation in apparent fibre diameter was observed along the length, as can be seen in Figure 6.8(b) (say Fibre 2). The apparent fibre diameter in this case is seen to vary in the range $7.2 - 8.0 \mu\text{m}$ along the length which is about 10% of the mean fibre diameter and is a significantly large variation. The measured fibre strength can then vary by almost 20% of the mean fibre strength. This will also affect the accuracy of the corresponding estimated Weibull strength distribution. If such a fibre were used for measuring fibre strength, the exact location where fibre diameter was measured would strongly influence the measured fibre strength value. The true sectional-area that should be used however, is the section where the tensile fibre

fracture actually occurs, access to which is not straightforward.

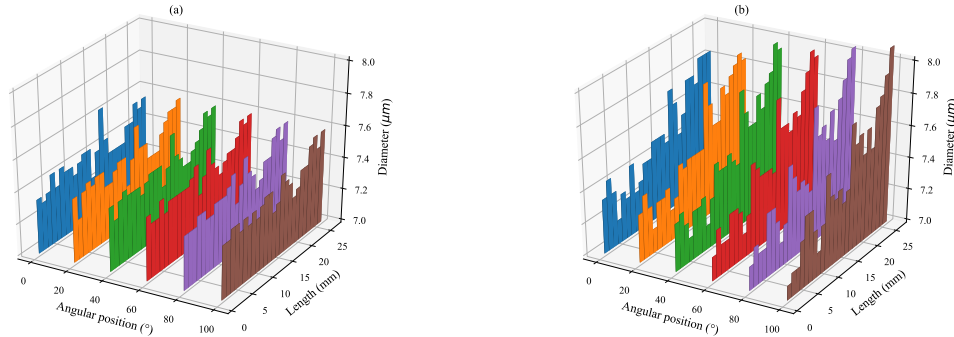


Figure 6.8: Variation in apparent fibre diameter along the axial length for different angular positions: (a) for Fibre 1. (b) for Fibre 2

Variation of fibre diameter in angular direction (orientation).

It can also be noticed from Figure 6.8(b) that for a fixed position along the length of fibre, the diameters measured for different angular positions were not constant. This suggests a possibility of non-circularity in fibre cross-section. To examine this, measured fibre diameters at specific locations on the axial axis, and for different angular positions were plotted on a polar scale. Polar plots for Fibre 1 and Fibre 2 at one particular position are shown in Figure 6.9. It can be seen from Figure 6.9(b) that fibre 2 shows variations in diameter in the angular direction, i.e. the apparent cross-section is not circular but more of an elliptical shape. Fibre 1 on the other hand, can be seen to have a very circular cross-section, as shown in Figure 6.9(a).

The level of non-circularity may vary from fibre to fibre, but it was observed that the fibres which showed variations in diameter along the length also showed non-circularity in cross-sections. Due to these variations in fibre dimensions, the classical assumption of assuming a circular and constant cross-section along the length may not always be appropriate. Measuring the fibre diameter at only one location and orientation in order to determine the fibre stress can result in inaccurate fibre strength calculation. A hypothesis can be made that it might be a better practice to first measure the fibre diameters at different angular positions to determine the cross-sectional area and then additionally measuring cross-sectional areas at different axial positions along the length to cover the entire gauge length. The minimum calculated cross-sectional area can then be used for calculating the fibre stress. This may increase the accuracy of the calculated fibre strength. This is because the probability of fibre fracture at the narrowest region may be higher due to increased stress concentration in that region. However, it is also likely that the fibre fracture occurs at the location of a critical defect, and not necessarily at the narrowest section. This hypothesis would be analysed in the next subsections.

If the non-circularity of fibres is considered, using the standard Weibull functions given by Equations 2.2 and 2.4 would no longer be appropriate; due to the variation in fibre

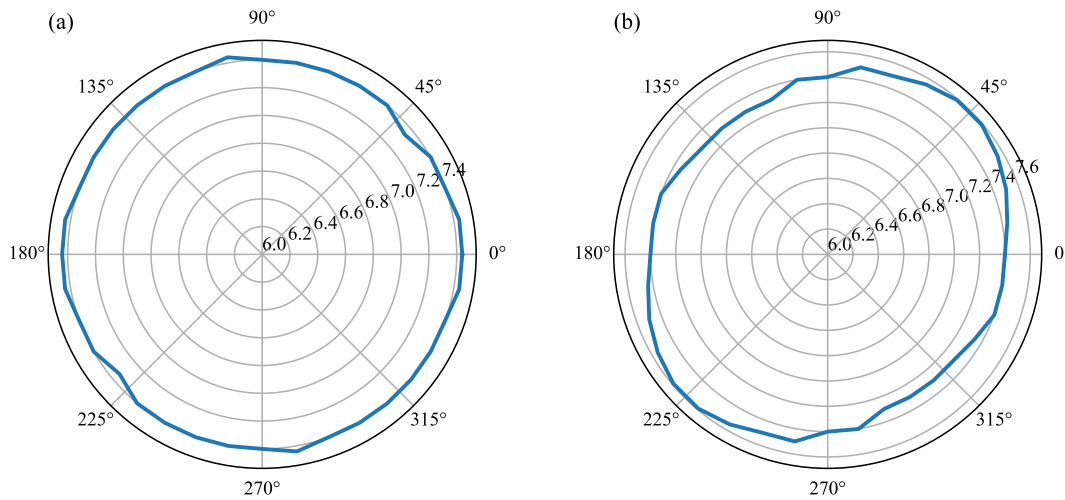


Figure 6.9: Variation in measured fibre diameter along the angular direction, for a fixed plane (apparent cross-section), for: (a) fibre 1 (b) fibre 2. Unit: micrometres.

cross-sections along the length. A simple error analysis reveals that based on whether the smallest or largest apparent fibre diameter is measured, and whether the narrowest or the widest fibre section is considered, the calculated fibre strength can vary significantly. For e.g., the minimum and maximum calculated fibre strength for the case of fibre 2 in Figure 6.9(b) can vary by about 11.2 %. Similarly, the minimum and maximum calculated fibre strength for the case of fibre 1 in Figure 6.8(b) can vary by about 16.6 %. The more generalized Weibull functions based on the volume relationship, as given by Equations 2.1 and 2.3, may be more useful in such cases. The term L/L_0 in the Weibull distribution functions should therefore be replaced by V/V_0 , where V is a characteristic gauge volume and V_0 is a reference gauge volume.

External defects in carbon fibres which can be introduced during the fabrication process can also be picked up by the laser diffraction measurement system, especially the surface flaws. However, measurement irregularities can also occur due to the presence of dust particles on the fibre surface. A detailed microscopy analysis can distinguish the differences between the two.

6.4.2 Measurement of Poisson's ratio

Carbon fibres are commonly assumed to have transversely isotropic properties due to their internal structure and cylindrical geometry. The stiffness tensor for this is characterised by 5 independent coefficients. However, the anisotropic properties of fibres are not easily measurable [132, 133], and most composite strength models therefore consider fibres to have isotropic properties. Knowledge of the anisotropic properties of the fibre can help in improving such models. Poisson's ratio is an important quantity to characterise the anisotropic property of any material. However, measuring the Poisson's ratio for carbon fibres is challenging, mainly due to the small size of the fibres. Very few studies have

previously attempted to measure the Poisson's ratio of carbon fibres, and the results from [134], back from 1991, is very widely used. Some other studies have also tried to reverse engineer the anisotropic properties of carbon fibres [135, 136].

An attempt to measure the axial Poisson's ratio of the T700 carbon fibres was made. Strain in the lateral direction was measured by monitoring the variation in fibre diameter upon the application of tensile load, using the laser diffraction system, as also used earlier. Strain in the longitudinal direction was measured by the elongation applied to the fibre, as recorded by the linear extensometer. Considering a fibre with circular cross-section, the Poisson's ratio (ν) is given by Equation 6.1, while the measured longitudinal (ε_L) and lateral (ε_T) strains are given by Equations 6.2 and 6.3, respectively. Figure 6.10 shows a schematic of the change in axial and lateral dimensions of the fibre on elongation.

$$\nu_{LT} = -\frac{\varepsilon_T}{\varepsilon_L} \quad (6.1)$$

$$\varepsilon_L = \frac{l' - l}{l} \quad (6.2)$$

$$\varepsilon_T = \frac{d' - d}{d} \quad (6.3)$$

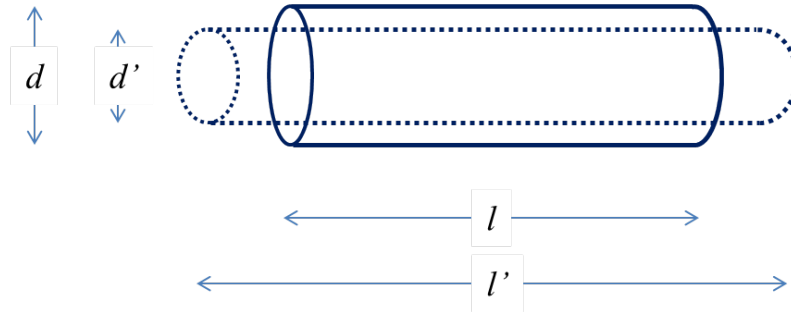


Figure 6.10: Schematic of the change in axial and lateral dimensions of the fibre on elongation.

To measure these dimensions, the fibre was loaded on the tensile testing system in the same way as explained in Section 6.2. A linear extension of 1 mm/min was applied on the fibre, as a result of which the fibre elongated in the longitudinal direction while the dimensions in the lateral dimensions were reduced. This phenomenon of subsequent elongation and compressions is also demonstrated schematically in Figure 6.10.

Figure 6.11 shows the actual reduction in measured fibre diameter with elongation. A clear trend of reduction in the measured fibre diameter can be observed. However, the reduction in measured fibre diameter is comparable to the resolution of the measuring instrument. Nevertheless, if the time series data is normalised over time, an approximation of the reduction in fibre diameter can be made. The measured diameters were as follows: $l = 30$ mm, $l' = 30.57$ mm, $d = 6.88$ μm , $d' = 6.83$ μm . Based on this data and

Equations 6.1, 6.2, and 6.3, the approximate Poisson's ratio was calculated to be 0.38. In another study, Mounier et al. [135] applied an ultrasound spectroscopy technique and evaluated the Poisson's ratio of T700 carbon fibres to be 0.31.

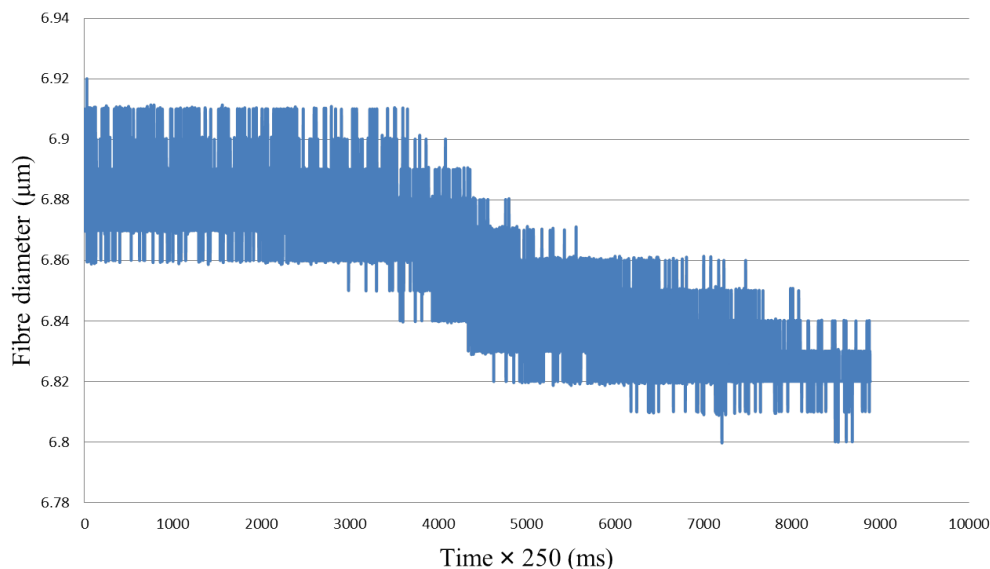


Figure 6.11: Reduction in measured fibre diameter with elongation.

Limitations of the study

The Poisson's ratio, calculated using Equations 6.1, 6.2, and 6.3 depends strongly on the measured diameters before and after the elongation. However, the reduction in fibre diameter was comparable to the resolution offered by the laser diffraction system, as can also be seen from Figure 6.11. This raises doubts over the accuracy of the measurements made, and hence on the calculated Poisson's ratio. The Poisson's ratio given by Equations 6.1 is very sensitive to the diameter measurements and even an error of $0.01 \mu\text{m}$ in the measured diameter would result in a very significant error (of about 20%) in the calculated Poisson's ratio. A measurement technique which can offer a better resolution is required to determine the Poisson's ratio of carbon fibres confidently and accurately. Additionally, if an estimation of uncertainty in the previously reported Poisson's ratio can be made, it would be useful in understanding the confidence that can be placed when using these results, very few of which exists.

Fluctuations in the measurements as observed in Figure 6.11 can also occur due to vibrations from the mechanical instruments, or any wind in the vicinity of the testing region. Although care was taken to minimise the effects of vibrations by conducting the tests on damping beds, conducting the tests in vacuum can potentially overcome the effect of winds, if any.

6.4.3 Tensile strength

The manufacturer's data sheet provides one estimated value for the strength and failure strain of fibres, as shown in Table 6.1. However, it is known that usually a variation is observed in strengths of different fibres, as also in the present study. The tensile strength for all gauge lengths was found to vary from 2 to 8 GPa with most fibres having a strength between 3-6 GPa as can be seen from the boxplot in Figure 6.12. Fibres with higher strength values (say, above 6 GPa) were mostly observed for the specimens with a 4 mm gauge length, and lower strength values were associated for the fibres with longer gauge lengths of 20 mm and 30 mm. The solid horizontal line represents the median strength value while the dashed horizontal line represents the mean strength value, for each gauge length. Fibre strength on average was found to decrease with increasing gauge length. This strength behaviour is also in agreement with the weakest link theory, according to which, fibres of short gauge length are comparatively stronger than fibres of longer gauge lengths, as also described in Section 2.2.1. The failure of brittle fibres is controlled by the distribution of defects. For longer gauge lengths (or for larger volumes), the probability to meet a critical defect increases; this increases the probability of failure for longer fibres, which thus have lower strengths on average.

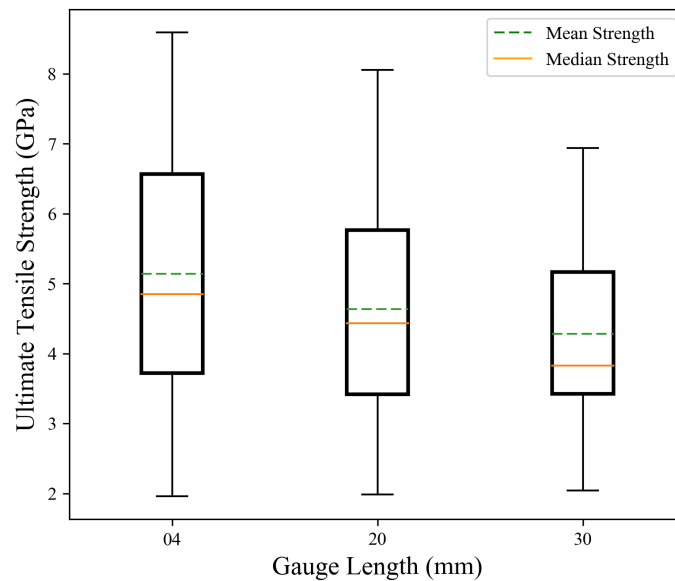


Figure 6.12: Boxplots for fibre strengths for the three gauge lengths with mean and median values

Strengths of all the fibres were plotted against the corresponding failure strain for all gauge lengths, and are shown in Figures 6.13, 6.14 and 6.15. The histograms for fibre strength and failure strain can be seen to be very similar for all the three cases. The straight line on the plots represents the average Young's modulus of the fibres. The average Young's modulus of the 30 mm, 20 mm, and 4 mm fibres was found to be 232.6 GPa, 231.0 GPa and 234.3 GPa, respectively, as also given in Table 6.5. This is well within the range

prescribed by the manufacturer, which is 221-240 GPa. However, there was an increase in the coefficient of variation in the Young's modulus of fibres with decreasing the gauge length. This is also apparent from the increased scatter in fibre strength data points, especially for tests at gauge length of 4 mm (Figure 6.15). This is because of the many experimental issues in conducting tensile tests with fibres of very short gauge lengths, as described in Chapter 2. It was also demonstrated in Chapter 2 that the tensile test measurements at short gauge lengths are prone to measurement errors due to an increased effect of fibre misalignment, which may contribute to uncertainty [43].

It should also be emphasized that the Young's modulus given was determined by averaging any variation with strain. Since fibres are known to stiffen at higher values of applied strain [137], the fibres which break at high strain values have slightly higher Young's modulus than the average value, i.e. points at the ends of the strain distribution lie slightly above the straight line of average Young's modulus, as seen in the strength vs strain scatter plots.

Table 6.5: Mean, standard deviation and coefficient of variation (CoV) of the average Young's modulus for tests done at the three gauge lengths

Gauge Length →	30 mm	20 mm	4 mm
Mean (GPa)	232.6	231.0	234.3
Standard deviation (GPa)	10.4	12.1	24.6
CoV (%)	4.46	5.25	10.5

Strengths of fibres were also plotted against their diameters, as shown in Figure 6.16. The mean diameter value of all the fibres was $6.9 \mu\text{m}$. No specific correlation can be observed between fibre strength and their mean diameters. This suggests that fibre strength is not controlled by its size or cross-sectional area but more likely by the distribution of defects inside them. Since critical defects are randomly distributed inside the fibres, irrespective of their visible cross-section, the fibre strength is also randomly scattered. The hypothesis made earlier that considering the non-circularity of fibre cross-section might result in more accurate fibre strength measurements could therefore not be verified. Although it has also been shown in Chapter 3 that fibre diameter measurement is the most critical parameter for accurate fibre strength measurement, if fibre strength is controlled by the distribution of defects in the fibre, minor non-circularity may not affect the fibre strength distribution significantly. However, a strong correlation between fibre strength and diameter is usually observed for natural fibres [87, 138]. This is mainly because of a much larger variability in the diameter of natural fibres.

It can be observed that the average fibre tensile strength is within the range reported in the literature. However, due to variations in strength of individual fibres, they are represented in terms of their best fit Weibull distribution parameters. Representation of the obtained fibre strength data with Weibull distribution is discussed in the next section.

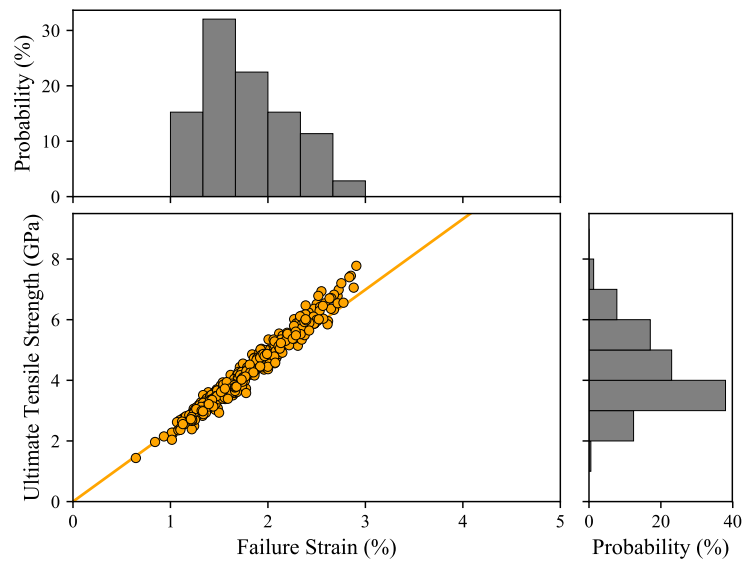


Figure 6.13: Fibre strength plotted against failure stress for all fibres, along with corresponding histograms, for tensile tests done at gauge lengths of 30 mm. The straight line represents the mean Young's modulus.

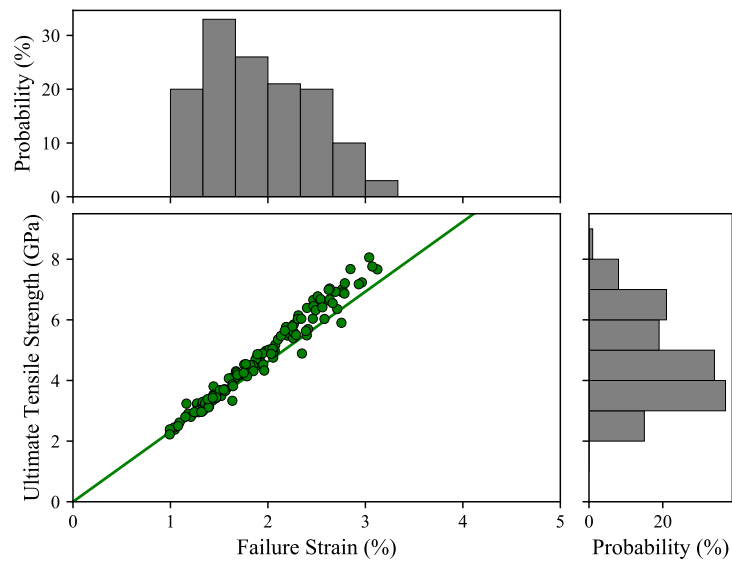


Figure 6.14: Fibre strength plotted against failure stress for all fibres, along with corresponding histograms, for tensile tests done at gauge lengths of 20 mm. The straight line represents the mean Young's modulus

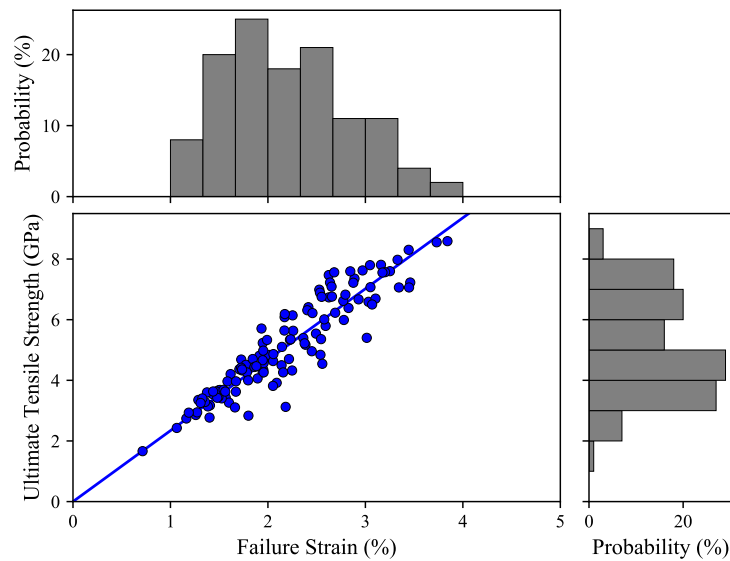


Figure 6.15: Fibre strength plotted against failure stress for all fibres, along with corresponding histograms, for tensile tests done at gauge lengths of 4 mm. The straight line represents the mean Young's modulus

6.4.4 Strength distribution

As mentioned earlier, Weibull distribution is the most popular statistical function used to represent strength of brittle fibres. The experimentally generated fibre strength data sets were analysed using the standard 2-parameter Weibull distribution given by Equation 2.4. The best-fit Weibull distribution parameters were determined using the maximum likelihood method and are listed in Table 6.6. An advantage of using a logarithmic statistical function such as the Weibull distribution is that it offers a very informative 2-D graphical plot that helps to convey the analysis results visually, on a logarithmic scale, as shown in Figure 6.17. The experimental fibre strength data points generated for all three gauge lengths are shown against their respective cumulative failure probabilities; and the straight lines represent the corresponding best fit 2-parameter Weibull distributions. The vertical axis represents the failure probability which is the percentage of fibre population that is expected to fail for a given applied stress value; while the horizontal axis represents corresponding tensile strength (or failure stress).

Although the 2-parameter Weibull distribution is popularly used among researchers for representing the fibre strength variation, it can be clearly observed from the given Weibull plots in Figure 6.17 that the experimental fibre strength data points do not fit the standard 2-parameter Weibull model very well and deviates from it at the lower regions on the strength axis. The experimental points follow a non-linear curvature while the Weibull model represents a straight line. This behaviour has also been highlighted by a few previous studies. The popularly used 2-parameter standard Weibull distribution may therefore not be the most appropriate statistical representation for the fibre strength data generated.

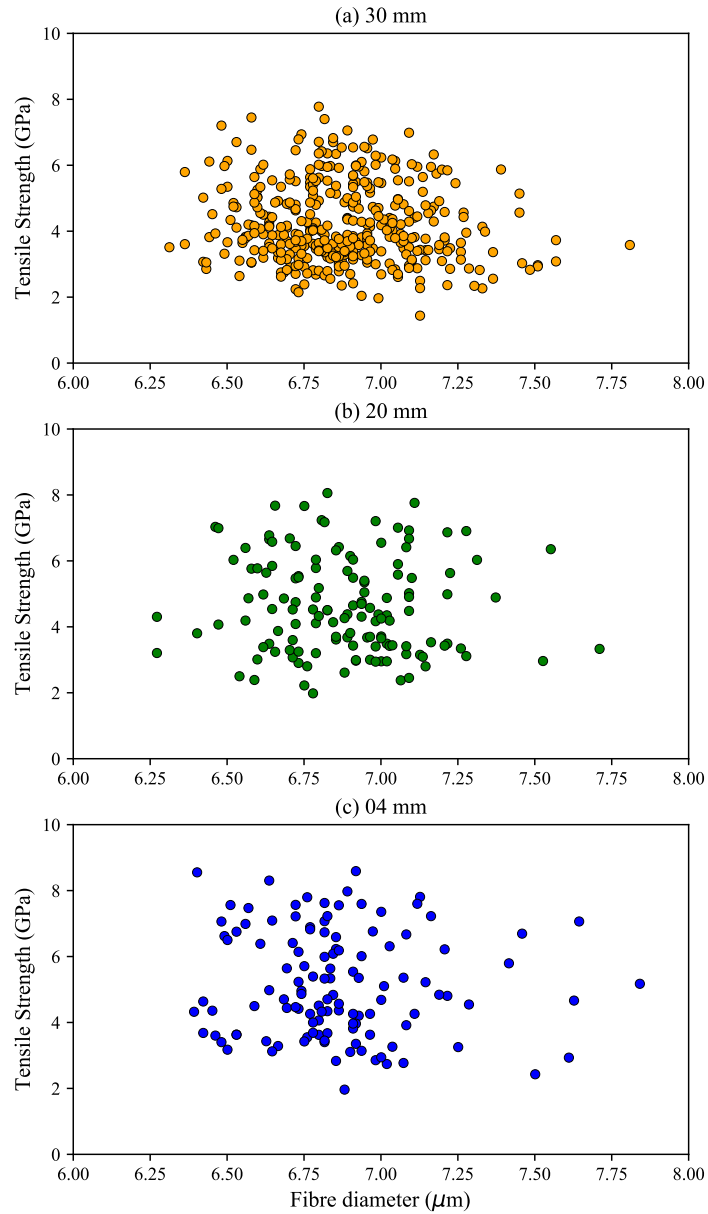


Figure 6.16: Fibre strength plotted against fibre diameter for all fibres, for tensile tests done at all the different gauge lengths

For cases where a smaller data set is used for analysis, this behaviour is usually not very prominent and may go unnoticed. Since most previous studies have used between 10-

Table 6.6: Maximum likelihood parameters for the 2-parameter Weibull distribution

2-parameter Weibull distribution			
Gauge Length	Shape parameter	Scale parameter	Location parameter
(mm)	m	σ_0 (GPa)	σ_u (GPa)
4	3.55	5.72	0
20	3.50	5.16	0
30	3.48	4.63	0

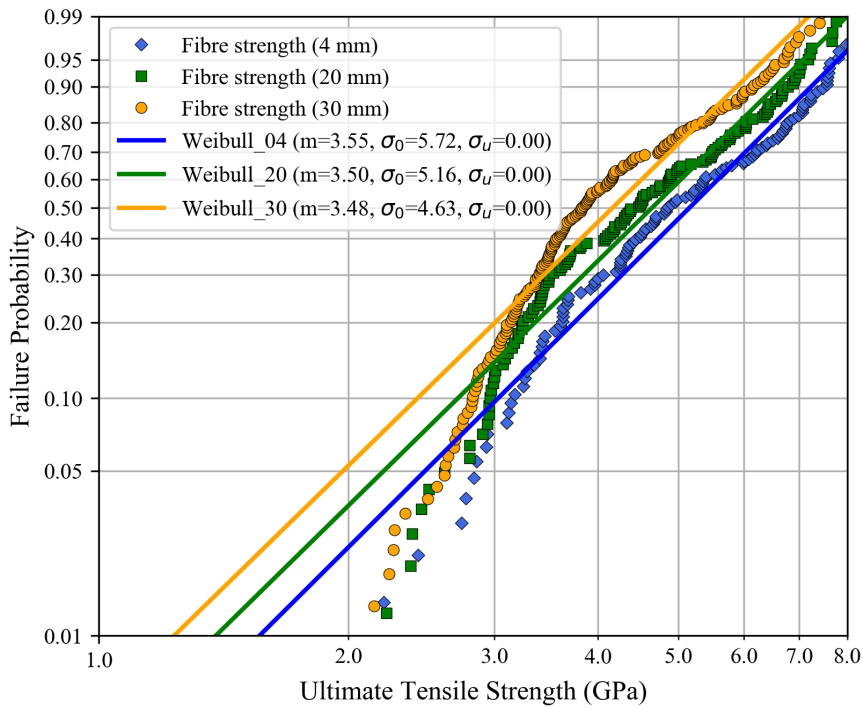


Figure 6.17: Best fit Weibull plots for the 2-parameter distribution for all three gauge lengths, along with experimental data points

30 fibre strength data points for the statistical analysis, it is very likely that any such non-linear behaviour could have been overlooked.

To understand the reasons for this deviation, it is important to understand the definition of the Weibull distribution. The 2-parameter Weibull distribution given by Equation 2.4 is obtained by starting with the generalized version given by Equation 2.2 and fixing the location parameter $\sigma_u = 0$, thus making the assumption that the minimum possible fibre

strength value is 0. However, the experimentally determined data set in the present study was found to have a minimum strength value of around 2 GPa, for all gauge lengths. These data sets do not contain many values in the range 0-2 GPa. When these data sets are fitted to a 2-parameter Weibull distribution, as in Figure 6.17, deviation from linearity in the lower regions of strength is observed.

The absence of weaker strength data points in the set may be due to the fibre preselection effect. Since the diameter of carbon fibres is very small, they have very low breaking forces. Many weak fibres are therefore not able to survive the applied external loads during specimen preparation and break during the process of fibre extraction and preparation. Fibre preselection effect will also depend on the way fibre specimens are prepared. For e.g., using an external solvent such as ethanol for removing the sizing on the fibres. This will weaken the bonding between neighbouring fibres to some extent, and would enable fibre removal from the tow relatively easier, and will reduce the threshold strength of the fibres which break. It is important to mention here that for the tests discussed earlier in Chapter 3, sample preparation was done using ethanol for separating the fibres in the tow, whereas for the tests conducted on the automated machine discussed in this Chapter no external solvent was used for sample preparation, which might have resulted in breakage of more fibres during sample preparation. This elimination of these weak fibre strengths from the data set causes a deviation in linearity when represented on a logarithmic scale.

However, if a 3-parameter Weibull distribution (Equation 2.3) is used for representing the fibre strength data, it is capable of capturing this non-linear behaviour of fibre strength, as shown in Figure 6.18. The corresponding distribution parameters are given in Table 6.7. It may be tempting to conclude that the 3-parameter Weibull distribution is the best representative statistical function for fibre strengths as it fits the experimental data points in a better way. However, the problem does not lie necessarily with the statistical function. For brittle fibres such as carbon, the experimental data itself may not be a correct representative of the actual fibre population, due to the fibre preselection effect explained earlier. Hence, using the 3-parameter Weibull distribution to represent the fibre strength behaviour may not be very appropriate either. There is a need to analyse the fibre strength data set statistically, to find an appropriate methodology that can be used to analyse this incomplete data set for estimating a function that can represent the actual fibre strength behaviour more accurately [105]. This issue will be tackled in the next chapter.

Table 6.7: Maximum likelihood parameters for the 3-parameter Weibull distribution

3-parameter Weibull distribution			
Gauge Length (mm)	Shape parameter m	Scale parameter σ_0 (GPa)	Location parameter σ_u (GPa)
4	2.32	3.93	1.67
20	2.02	3.15	1.85
30	1.88	2.55	1.91

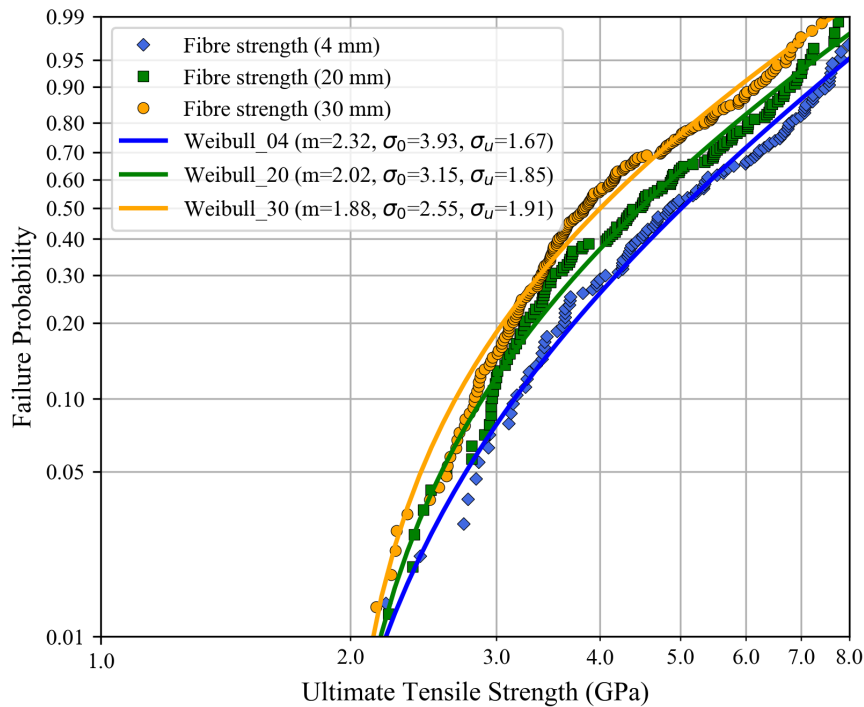


Figure 6.18: Best fit Weibull plots for the 3-parameter distribution for all three gauge lengths

6.4.5 Effect of sample size on the confidence interval of the strength distribution

It can be said that use of a large data set for analysis reduces the uncertainty in the obtained fibre strength distribution. To comprehend this reduction in uncertainty a confidence interval on the parameters of interest can be computed. However, the fibre strength data in the present case does not seem to fit the standard Weibull distributions. Therefore, using a ‘parametric’ method of computing the confidence interval, similar to the one demonstrated in Chapter 4, is not appropriate. A ‘non-parametric’ method of computing the confidence interval, which does not rely on a specific statistical function, has been used.

Non-parametric bootstrap method of computing the confidence interval

The method can be used to analyse an available sample of fibre strength data which represents a given population. As also for the case of the parametric method, and for the purpose of this study alone, the available sample is considered to be a good estimate of the population of interest, since the objective is only to comprehend the possible reduction in uncertainties. However, instead of fitting the fibre strength data to the Weibull distribution and analysing the parameters of the distribution, the data is analysed directly in this case. This method is hence a non-parametric method [139]. So, instead of simulating

Weibull distributions using the Monte-Carlo method, synthetic fibre strength data sets are simulated. This is done by randomly drawing fibre strength values from the available data set, one by one, and with replacement. Repeating this process with a Monte-Carlo method results in many bootstrap sample sets. From each bootstrap sample, the statistic of interest is computed. For the present case, the median strength (B50 strength) of the fibre strength distribution is analysed.

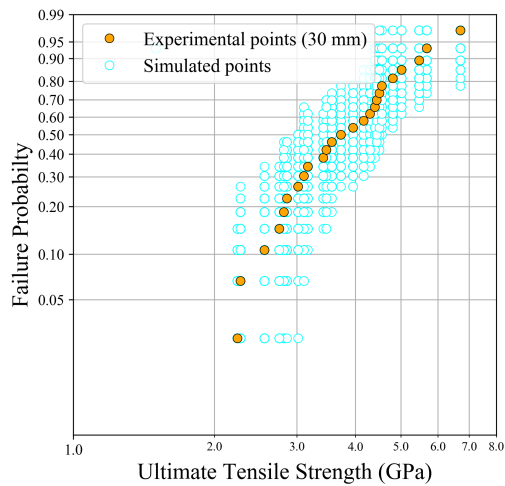
To determine the effect of sample size on the confidence interval of the results, fibre strength data generated at 30 mm gauge length was analysed. The steps followed for computing a confidence interval for median strength of the distribution, via the non-parametric bootstrap method are described as follows:

- From the experimental fibre strength data set, a given number X of fibre strength data points were extracted.
- This sample set of X points were assumed to be a representative sample for the strength of the fibre population.
- A synthetic fibre strength data set of size X was generated by randomly drawing fibre strength values from the available data set, one by one, and with replacement.
- A total of 500 synthetic sample sets of fibre strength data were generated.
- The median strength value (B50 strength) from each data set was extracted, to form a set of median strengths of all simulated data sets.
- The 2.5th and 97.5th percentile values of these median strengths were calculated. These values represent the lower and upper bounds of the 95% confidence interval of the median strength.

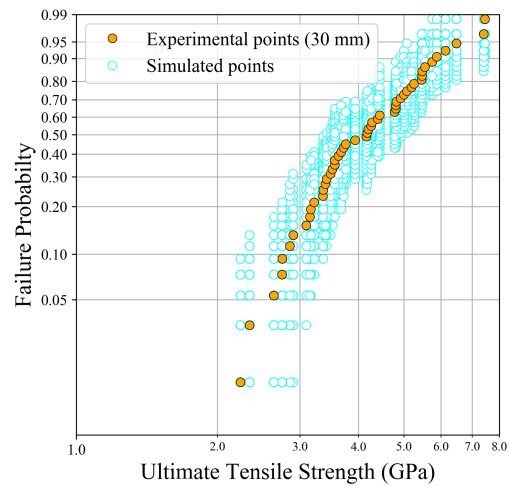
The 95% confidence interval using the steps described above were calculated for four different sample sizes of $X = 25, 50, 100$ and 200 fibre strength data points, to evaluate their influence on the obtained results. The simulated fibre strength data sets along with the experimental results, for the cases of different sample sizes are shown in Figure 6.19. The calculated confidence intervals for the corresponding cases are given in Table 6.8. It can be seen that the confidence interval of the median (B50) strength of the fibre strength data set becomes narrower on increasing the sample size of the data set used for analysis, as expected. The decrease in the width of confidence interval is not monotonous and the confidence width seems to converge towards an asymptotic value when a sample size of around 200 is reached. Depending upon the nature of the application and the safety factors required for modelling predictions, an appropriate sample size can be chosen for generating input fibre strength data. Or in other words, a ratio of an optimal confidence level to testing effort can be defined.

6.5 Conclusions

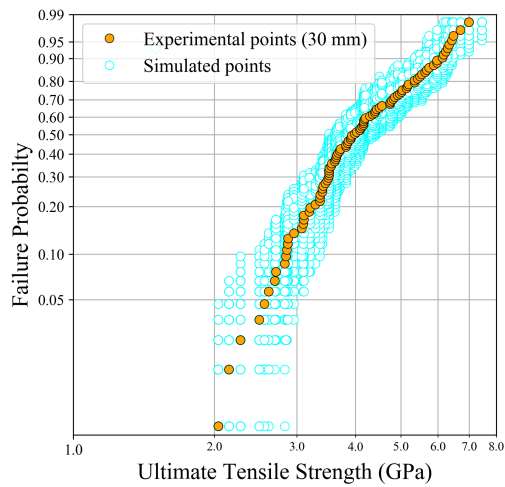
Tensile strength and dimensional variation of T700 carbon fibres have been investigated using an improved and semi-automated experimental methodology and statistical analysis. The experimental system used has improved the single fibre testing process by overcoming the usual experimental limitations discussed in the previous chapters. Using



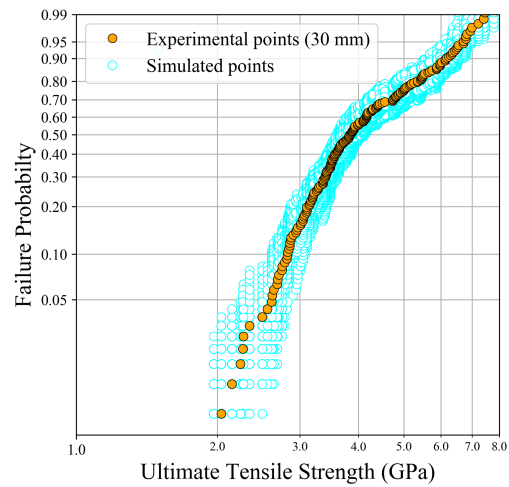
(a) Sample size $X = 25$



(b) Sample size $X = 50$



(c) Sample size $X = 100$



(d) Sample size $X = 200$

Figure 6.19: Simulated fibre strength data sets along with the experimental results, for the cases of different sample sizes of (a) $X = 25$, (b) $X = 50$, (c) $X = 100$, (d) $X = 200$. It can be observed that the scatter or uncertainty in simulated fibre strength data points reduces on increasing the sample size used for analysis.

Table 6.8: Effect of sample size on the confidence interval of the median strength of the simulated fibre strength data sets.

S.N.	Sample size (X)	Confidence Interval (C.I.) of B50 strength. (GPa)	Width of C.I. (GPa)
1	25	3.21 - 4.40	1.19
2	50	3.67 - 4.41	0.74
3	100	3.70 - 4.18	0.48
4	200	3.64 - 3.99	0.35

the semi-automated system also facilitated the generation of a large set of experimental data required for a detailed statistical analysis.

Fibre strength data for T700 carbon fibres has been generated for three different fibre gauge lengths: 4, 20 and 30 mm. This data set used for analysis is much larger than the ones used for any previous studies reported in literature. Fibre strength has been shown to be scattered in a range of 2-8 GPa with shorter fibres having larger strengths on average, which is in agreement with the weakest link theory. Although the tests at different gauge lengths yielded very similar Young's moduli, it was found that the coefficient of variation was large for tests conducted at shorter gauge lengths, as required by composite strength models. This is because the testing of short fibres is associated with many experimental issues which restrict the accuracy of the measurements made. Although using the present testing system has reduced these issues by a significant extent, some uncertainties still exist, and there is scope for improving the testing systems further. Use of a large sample size for analysis has also shown to improve the statistical confidence in obtained results. Based on the nature of application, fibre strength data set of an appropriate sample size should be used for analysis.

A detailed dimensional analysis of the surface morphology of T700 carbon fibres was also conducted. It was found that not all fibres have a circular cross-section, which is contrary to the popular assumption. Existence of a non-circular fibre cross-section limits the use of the existing methods of fibre strength determination and statistical analysis. An attempt to measure the Poisson's ratio of T700 carbon fibres was found to be very challenging due to the very high measurement precision required. If an even more precise dimensional measurement system can be incorporated in the fibre tensile testing system, the Poisson's ratio can be measured with a better accuracy.

Preliminary statistical analysis of the large fibre strength data has further reinforced the hypothesis that the standard Weibull analysis may not be appropriate to accurately capture the inherent fibre strength variations; and a discrepancy between the experimental fibre strength and the Weibull model is observed. This behaviour has commonly been overlooked by many previous studies as the sample sizes used for most cases are insufficient to highlight this behaviour. There is a need for a better description of the fibre strength behaviour. To tackle this issue, in the next chapter, a generalized Weibull analysis based on Bayesian approach of using prior knowledge will be described. This methodology considers the practical limitations of mechanical testing, and the fibre preselection to understand

the deficiencies in the data, which are then incorporated in the analysis. It can be used to determine the true fibre strength behaviour, using deficient experimental data.

Additionally, some suggestions to potentially improve the fibre testing system further are listed here.

6.5.1 Scope for improvement in the fibre testing system

- **Gauge length** : Practical problems are encountered when testing fibres at either very small or very large gauge lengths. The effect of clamping and misalignment will be significantly greater in the case of fibre specimens with a very small gauge length. Conversely, testing fibres at very large gauge lengths may eliminate weaker fibres which may break prematurely during handling, and the effect of preselection will be greater. From a practical point of view, there may therefore be an optimal gauge length that would minimize the combined effect of clamping and fibre preselection. It would be useful to determine this gauge length and use it as a standard.
- **Clamping effects/Determination of failure location** : A valid test result is considered to be one in which fibre failure does not occur in the gripping region. However, using either the manual or automated methods it is difficult to locate the exact region of break after failure occurs. Determining the exact region of failure can help in eliminating improper test results. Acoustic emission techniques can also be used for estimating the failure location. A sensor can be installed at each end of the fibre being tested, and comparing the signals from the two can give an estimate of the fibre failure location. A system which is sensitive enough to pick up the signals appropriately would be required.
- **Diameter variation** : To determine the fibre strength, the measured failure load is divided by the fibre cross-sectional area. Due to the very small fibre size, measuring the fibre cross-section can be very difficult. The usual practice is to measure the fibre diameter at one particular location along the gauge length of the fibre and then calculate the area based on the assumption of circularity in fibre section. Depending upon the type and manufacturing process used, this may not always be an accurate assumption and there may be variations in diameter along the axial or angular direction, as already shown in Section 6.4.1. For determining the accurate fibre strength value, the cross-sectional area at the exact location of failure would be required. This point further highlights the need to determine the exact failure location of the fibre.
- **Fibre alignment** : Although the grooves in the plastic tabs used to fix the fibres provide a good alignment of the fibre with the specimen prepared. The laser diffraction system already used for diameter measurement can also be used for improving the relative alignment between the fibre and the testing system. The laser diffraction system is capable of rotating about the fibre axis to find a position which maximises the signals. It can further be used for ensuring that the fibre specimen is placed at the most suitable position to minimise misalignment.

Chapter summary in French

Investigation expérimentale et statistique des propriétés des fibres

Dans ce chapitre, la résistance à la traction et la variation dimensionnelle des fibres de carbone T700 ont été étudiées en utilisant une méthodologie expérimentale semi-automatisée et une analyse statistique. Le système expérimental utilisé a permis d'améliorer le processus de test des fibres unitaires en surmontant les limites expérimentales habituelles discutées dans les chapitres précédents. L'utilisation du système semi-automatisé a également facilité la génération d'un large ensemble de données expérimentales nécessaires à une analyse statistique détaillée. Les données sur la résistance des fibres de carbone T700 ont été générées pour trois longueurs de jauge différentes: 4, 20 et 30 mm. Cet ensemble de données utilisé pour l'analyse est beaucoup plus grand que ceux utilisés pour toutes les études antérieures rapportées dans la littérature.

Dans ce chapitre, il est montré que la résistance des fibres est dispersée dans une plage de 2-8 GPa avec les fibres plus courtes ayant des résistances plus grandes en moyenne, ce qui est en accord avec la théorie du maillon le plus faible. Bien que les tests à différentes longueurs de jauge aient donné des modules de Young très similaires, il a été constaté que le coefficient de variation était beaucoup plus important pour les tests effectués à des longueurs de jauge plus courtes. En effet, le test à 4mm de longueur de jauge est associé à de nombreux problèmes expérimentaux qui limitent la précision des mesures effectuées. Bien que l'utilisation du système de test actuel ait considérablement réduit ces problèmes, certaines incertitudes subsistent. Une analyse dimensionnelle détaillée de la morphologie des fibres de carbone T700 a également été réalisée. Il a été constaté que toutes les fibres n'ont pas une section transversale circulaire, ce qui complique les analyses et augmente les incertitudes.. Une tentative pour mesurer le coefficient de Poisson des fibres de carbone T700 s'est avérée très difficile en raison de la très haute précision de mesure requise. Cependant, la tendance observée est malgré tout intéressante à discuter.

L'analyse statistique des données obtenue fait apparaître une différence entre la résistance expérimentale des fibres et le modèle de Weibull. Cette différence n'apparaît que pour un nombre suffisant de données et n'a donc pas donné lieu à beaucoup de travaux. Il convient de faire la différence entre ce qui est mesurée et ce qui provient réellement des fibres.

Chapter 7

Weibull analysis based on Bayesian approach

***Abstract:** The standard Weibull analysis has been adapted based on the Bayesian approach of using prior information about fibres which break during testing to predict a more accurate statistical representation of the tensile strength behaviour of fibres used in composites. The analysis contemplates the preselection effect in modelling the fibre strength behaviour. This has been demonstrated using experimental fibre tensile strength data for T700 carbon fibres. The presented methodology can enhance the accuracy of fibre strength distribution whilst using the limited resources available.*

Contents

7.1	Introduction	139
7.2	Cause of misfit: Fibre preselection effect	140
7.2.1	Fibre preselection effect	140
7.2.2	Simulated experiment for demonstrating fibre preselection effect	140
7.2.3	Need for improvements in analysis	143
7.3	Truncated Weibull analysis based on Bayesian approach	143
7.3.1	Existence of truncation in fibre strength data	143
7.3.2	Theoretical formulation	144
7.4	Experiments, Results and Discussions	147
7.4.1	Experimentation	147
7.4.2	Fibre strength results	147
7.4.3	Standard Weibull analysis	147
7.4.4	Truncated Weibull analysis	150
7.5	Conclusions	153
	Chapter summary in French	154

This chapter has been adapted from the following article:

F. Islam, S. Joannès, L. Laiarinandrasana, A. Bunsell, “Weibull analysis based on Bayesian approach to model the strength behaviour of brittle fibres”, (*Under Review*)

7.1 Introduction

It was found in the previous chapter, that when a large set of experimental fibre strength data was used so as to minimise the uncertainty in Weibull parameters due to sampling, the fibre strength data did not comply with the standard 2-parameter Weibull function, i.e. there was discrepancy on the graphical plot between the experimental data points and the Weibull model. Similar behaviour has also been observed by some other studies [76, 90].

Since it has been shown in Chapter 3 that uncertainties in individual fibre strength values are very small (typically less than 0.1 GPa [36]), they cannot explain the observed non-linear behaviour. If the objective is to determine a statistical function which can represent the experimentally generated fibre strength data sets, the 3-parameter Weibull distribution (Equation 2.2) can be used, as demonstrated in the previous chapter. However, this distribution assumes that the minimum strength value in the data set also represents the strength of the weakest fibre in the population. This assumption may not be correct, as weaker fibres may also be present in the population; the strength of which are difficult to determine due to the fibre preselection effect [76], as also explained later. The aim is not to find the best statistical representation of the available data, but to determine the best representative strength distribution. Thus, although the 3-parameter distribution may represent the available data set very well, it may still be inappropriate for representing the actual fibre strength behaviour of the population.

To address the misfit between experimental points and the Weibull model, many authors have developed several modified versions of the Weibull distribution, some of which have been described in Chapter 2. The common problems with most of the developed distributions is that although they fit the fibre strength experimental data well, they are mainly based on curve fitting and do not have a solid physical background. With the objective of overcoming these issues, the present chapter addresses the following question:

How to analyse the experimental fibre strength data to model the accurate fibre strength behaviour?

To overcome the limitations of the standard Weibull analysis to represent the strength of fibres, a generalized Weibull analysis based on the Bayesian approach of utilising prior knowledge will be presented in this chapter. This analysis takes into consideration the fibre preselection effect, the existence of which has been mentioned by some previous studies [25, 76, 140]. In these previous studies, existence of the fibre preselection effect was highlighted, and arbitrarily chosen values were used to represent the experimental limitations. However, in the present study, this factor will be derived from experimental results and will be based on the knowledge of how fibres break during the different stages of the testing process, and the number of fibres that break in each stage. The analysis will thus more accurately contemplate the practical limitations of mechanical testing, which is the novelty of this study. Moreover, this preselection effect will be analytically represented in the standard Weibull distributions by incorporating a truncation factor in the analysis, which can hold different values depending upon the fibre material and testing conditions. Analysing experimentally generated fibre strength data using the presented methodology can enhance the accuracy of the results obtained and will help in extracting

more useful information from the limited experimental resources available. This will therefore also improve the reliability of the predictions made by composite strength models on the behaviour of composite materials and structures.

7.2 Cause of misfit: Fibre preselection effect

7.2.1 Fibre preselection effect

The accountability for misfit between fibre strength experimental data and the 2-parameter Weibull model does not lie entirely with the statistical distribution but mainly with the data used for determining the distribution. Data sets generated experimentally by conducting single fibre tensile tests are usually devoid of the strength of weak fibres and does not accurately represent the strength of all the fibres present in composite materials and structures. This is due to the effect of fibre preselection during which many fibres break before their strength can be determined. The test does not start only once the fibre is loaded, but it actually begins from the point the fibre is extracted from the bundle/roving. The entire testing process is divided into several stages which includes, extracting a single fibre from the bundle, mounting the fibres on fixtures or tabs, transfer of the prepared specimen to the test setup and the application of a tensile load for strength measurement. Most technical fibres used as reinforcements for composite materials have diameters in the range of a few micrometres [43, 105]. The breaking force for such small fibres is also very low. For high strength carbon fibres used as reinforcements in composite materials such as T700, the breaking loads are in the range of a few grams. Owing to such small breaking loads, fibres that are very weak and have strength values below certain limit may not be strong enough to survive the sample preparation and testing process. As a result, strengths of such fibres are usually not determined and they are thus not represented in the data set. Moreover, when a single fibre is extracted from a bundle, it is subjected to frictional force from surrounding fibres; while some fibres can even be twisted around each other. This can result in breakage of some fibres being extracted. This elimination of the fibre strength values from the data set, especially from the weak region, causes a deviation in linearity on the Weibull plot, as the available strength data does not follow the same inherent variations as those of the standard 2-parameter Weibull distribution. The prior knowledge that the fibre testing process is subjected to the preselection effect needs to be incorporated in the analysis when determining the representative fibre strength distribution.

7.2.2 Simulated experiment for demonstrating the effects of fibre preselection effect

To demonstrate the fibre preselection effect on the resulting Weibull distribution, numerical experiments were conducted using simulated fibre strength data. This was done in two steps:

Step 1: 100 fibre strength data points were randomly extracted from a standard 2-parameter Weibull distribution having shape and scale parameters of 4.0 and 4.5 GPa, respectively, and are shown in Figure 7.2 as solid points. The shape and scale parameters

were chosen based on the average of different Weibull distribution parameter values reported in literature [141]. It can be seen that the points can be approximately represented by a straight line. The fit depends on the number of simulated points and a data set of infinite points will result in all points falling in a perfect straight line.

Step 2: To simulate the effect of fibre preselection, each simulated fibre strength data point from the previous step was compared to a specific break limit. All data points having strength values below a certain break limit were removed from the data set obtained in the previous step. This is equivalent to censoring the strength of all those fibres which are very weak to survive the entire process of fibre specimen preparation, mounting and testing. The break limit may be different for different fibres. Due to twisting between fibres and the presence of friction, certain fibres may be more difficult to extract than others, and have a higher break limit. For each simulated fibre strength value from the previous step, the break limit was randomly chosen from a folded normal distribution (or half-normal distribution) with a mean of 2 GPa and a standard deviation of 0.5 GPa. This distribution is also shown in Figure 7.1 and was chosen so that the break limit varies mainly between 2-3 GPa, similar to what is observed experimentally for T700 carbon fibres [105, 128, 142]. Only those fibre strength values which exceeded the respective break limit were considered to survive the testing process, and the rest were rejected. This selection and rejection process of individual fibre strength data points has also been demonstrated in Table 7.1 for the first 10 out of the 100 simulated points. The rest of the simulated points survived the process since they all had strength values higher than the simulated break limit. They have not been shown in Table 7.1, but can be seen in Figure 7.2. The surviving fibre strength data points determined by this method to account for the fibre preselection effect have also been represented on the Weibull plot, together with the originally simulated data set, as shown in Figure 7.2. It can be seen that the smallest fibre strength value amongst the surviving fibres now acquires the smallest failure probability. The number of points in the surviving set is smaller due to elimination of some points, as demonstrated in Table 7.1. For this reason, the assigned failure probability values are slightly different for individual points in the two sets, as also apparent in Figure 7.2.

Table 7.1: Truth table demonstrating the survival and failure of fibres to simulate the preselection effect. X represents a rejected point while O represents a selected point.

S.N.	Simulated strength (GPa)	Break limit (GPa)	Decision
1	1.28	2.15	X
2	1.51	2.53	X
3	1.68	2.28	X
4	1.80	2.13	X
5	1.92	2.67	X
6	2.18	2.06	O
7	2.25	2.43	X
8	2.34	2.32	O
9	2.38	2.24	O
10	2.52	2.21	O

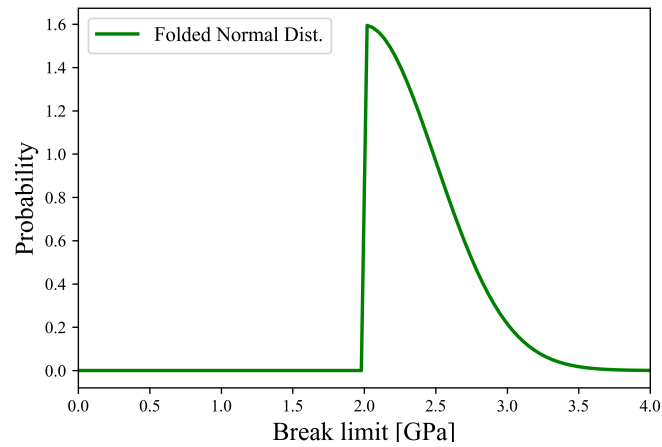


Figure 7.1: Distribution used for determining the break limit for individual fibre strength values. It is a folded normal distribution with a mean of 2 GPa and a standard deviation of 0.5 GPa.

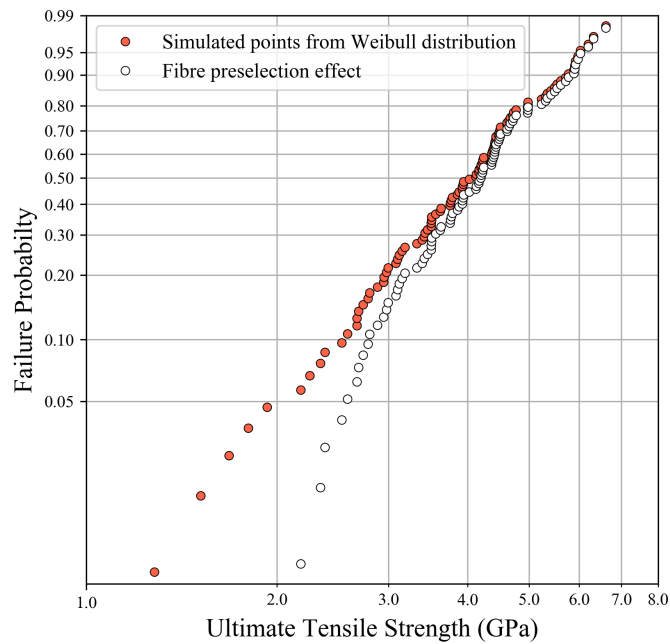


Figure 7.2: Weibull plot showing simulated fibre strength data for a Weibull distribution with $\sigma_0=4.5$ GPa and $m = 4.0$, along with the fibre strength data set after simulating the fibre preselection effect.

7.2.3 Need for improvements in analysis

It has been shown that fibres having strengths that lie between zero and the smallest measurable value may also be present in the actual fibre bundle but are not represented in the data set. There is a need to analyse the experimental data set statistically to find an appropriate technique that can investigate this incomplete data set and determine the actual fibre strength distribution of the population. To analyse such a data set, appropriate measures need to be followed to address the existence of this truncation (as described in the next section), or incompleteness of the data set. Berger and Jeulin [25] also suggested using a truncation parameter to represent experimentally generated single fibre strength data set. This truncation parameter can account for the fibre preselection effect which introduces limitations in experimentation and as a result of which many fibres break during the specimen preparation, mounting and testing process. The fibre testing process has been carefully analysed to observe the truncation limit in the experimental process and to determine the number of fibres which are affected by it. Contemplating this knowledge, a generalised Weibull analysis based on Bayesian approach of using prior information has been formulated for analysing experimentally generated single fibre strength data, and is explained in Section 7.3.

7.3 Truncated Weibull analysis based on Bayesian approach

7.3.1 Existence of truncation in fibre strength data

For the process of strength and dimensional measurement, fibres need to have a minimum strength so that they can sustain the unavoidable external forces during specimen preparation and handling. Weaker fibres usually break during the process and are not able to survive until final testing. Therefore, in most experimentally generated fibre strength data set obtained from single fibre tests; there is a small range of fibre strength that is not represented. In statistical terms, such a data set which does not include observations in the analysis that are beyond a boundary value is known as a truncated data set. Since it is always the weaker portion of fibre strength spectrum that is inaccessible, the fibre strength data set is said to be left truncated. The limit below which data is not available is known as the point of truncation or truncation limit. This limit can be different for different fibres, as described in the simulated experiments in Section 7.2.2. However, for simplicity of the analysis and to explain the methodology, this limit will be considered to be constant. For fibre strength, the truncation limit can be represented as σ_r . Only those fibres which have strength greater than σ_r value will be able to survive the testing process for the strength to be measured. If the location parameter σ_u is zero (implying that fibre strength can hold any positive value), an experimentally determined data set will not contain any points with strength between zero and σ_r as fibres with those strength, if present, would have broken before they could be tested. This is schematically represented in Figure 7.3(a) and the range of inaccessible fibre strength values is highlighted. However, fibres need to have a finite strength to exist, and hence, the threshold limit (or location parameter) may not necessarily be zero but hold a finite positive value as shown in Figure 7.3(b). For certain materials this threshold value may be close to the truncation limit and for this case the entire range of possible fibre strength values are experimentally accessible, shown in Figure 7.3(c). This also includes those cases for

which the threshold limit (or the location parameter) is greater than the truncation limit, since for these cases the entire range of possible fibre strengths would be experimentally accessible. Although there may not be a direct relationship between the two quantities, an empirical relationship between the truncation and threshold limit can be determined and is given by Equation 7.1. This is valid for all possible combinations of the location parameter and the truncation limit. Varying the value of ω between 0 and 1 will result in one of the three cases as also given in Table 7.2. Cases 1 and 3 are extreme end cases while Case 2 is a generic case which can have infinite possibilities depending upon the value of ω .

$$\sigma_u = (1 - \omega)\sigma_r \quad (7.1)$$

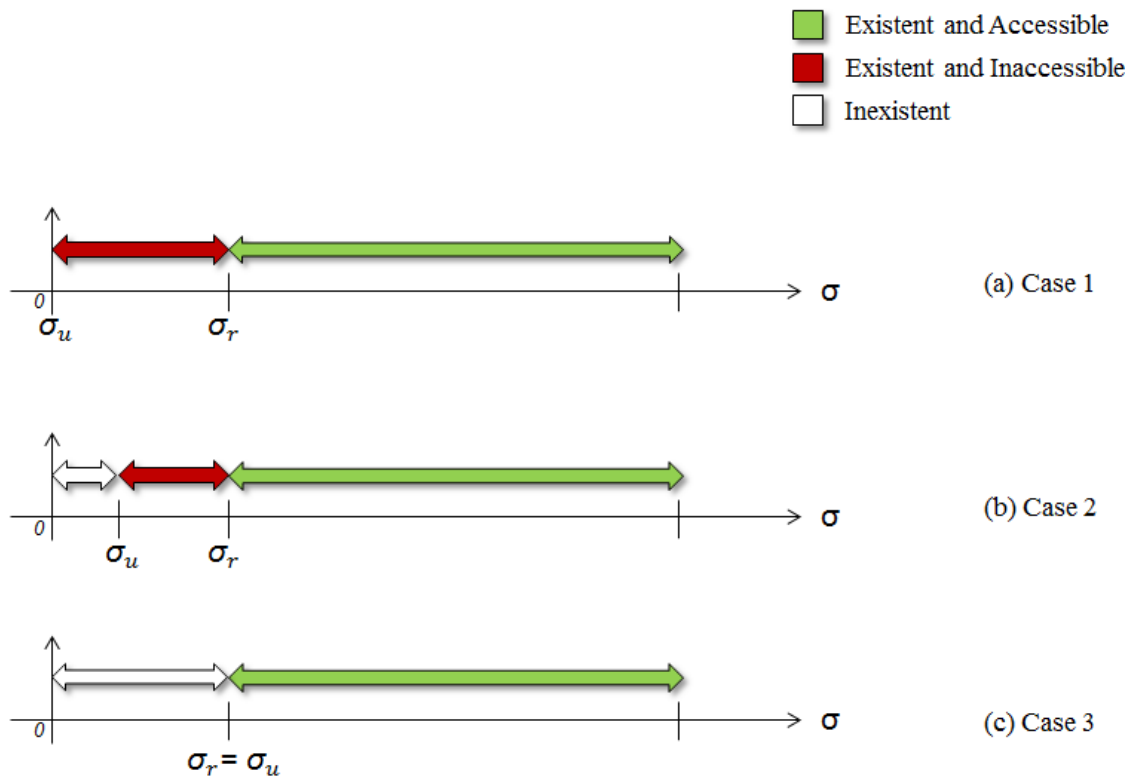


Figure 7.3: Relationship between location parameter (σ_u) and truncation limit (σ_r) for different cases. (a) Case 1: $\sigma_u = 0$ (b) Case 2: $0 < \sigma_u < \sigma_r$ (c) Case 3: $\sigma_u = \sigma_r$

7.3.2 Theoretical formulation

In order to model the effect of truncation on the fibre strength distribution, concepts from the Bayes theorem of conditional probability can be applied. Using this, it is possible to determine the probability of an event based on prior knowledge of conditions that affect the results. This can be done by considering different conditions of fibre strength as different events, as described further. Fibres which have strength value lower than σ_r , i.e. when $\sigma_f < \sigma_r$ (where σ_f is the strength of a fibre) would break during the fibre extraction

Table 7.2: Relationship between location parameter (σ_u) and truncation limit (σ_r) for different values of ω .

Case	ω	Truncation limit, σ_r	Location parameter, σ_u
1	1	σ_r	0
2	$0 < \omega < 1$	σ_r	$0 < \sigma_u < \sigma_r$
3	0	σ_r	σ_r

process from the bundle or during sample preparation. Only fibres having strength above σ_r would survive, i.e. when $\sigma_f > \sigma_r$, let this be event A . A random fibre subjected to a monotonically increasing tensile load would survive until the fibre strength stays greater than the applied stress σ , i.e. when $\sigma_f > \sigma$, let this be event B . According to the theory of conditional probability, the survival probability of a fibre considering the preselection process can be written as $P(B | A)$, and is given by Equation 7.2, where $P(B | A)$ is the probability that both events A and B occur. Theoretically, $P(A)$ is called a prior, and it represents the prior knowledge or the initial degree of belief in event A . $P(B | A)$ is called a posterior, and it represents the degree of belief in the event B having accounted for A . Since A and B are independent events, $P(B \cap A)$ can be replaced by $P(B)$ as shown in Equation 7.3. Substituting the actual terminologies for events A and B , Equation 7.4 represents the survival probability of a fibre of strength σ_f for an applied stress σ , under the condition that the fibre strength value lies above the truncation limit σ_r .

$$P(B | A) = \frac{P(B \cap A)}{P(A)} \quad (7.2)$$

$$= \frac{P(B)}{P(A)} \quad (7.3)$$

$$P_S(\sigma_f \geq \sigma | \sigma_f \geq \sigma_r) = \frac{P_S(\sigma_f \geq \sigma)}{P_S(\sigma_f \geq \sigma_r)} \quad (7.4)$$

$$= \frac{\exp \left[- \left(\frac{L}{L_0} \right) \left(\frac{\sigma - \sigma_u}{\sigma_0} \right)^m \right]}{\exp \left[- \left(\frac{L}{L_0} \right) \left(\frac{\sigma_r - \sigma_u}{\sigma_0} \right)^m \right]} \quad (7.5)$$

$$= \exp \left[- \left(\frac{L}{L_0} \right) \left(\frac{(\sigma - \sigma_u)^m - (\sigma_r - \sigma_u)^m}{\sigma_0^m} \right) \right] \quad (7.6)$$

$$P_R(\sigma) = 1 - \exp \left[- \left(\frac{L}{L_0} \right) \left(\frac{(\sigma - \sigma_u)^m - (\sigma_r - \sigma_u)^m}{\sigma_0^m} \right) \right] \quad (7.7)$$

Equation 7.6 represents the survival probability following a truncated 3-parameter Weibull distribution. The general equation for the failure probability of a fibre can be obtained from the relation, $P_R(\sigma) = 1 - P_S(\sigma)$, and is given by Equation 7.7.

For very brittle fibres the truncation limit may be significantly large, as they are more fragile and are prone to fail during handling and testing. For example, single fibre tensile tests have shown that for T700 carbon fibres the truncation limit σ_r may lie around 2 GPa. The location parameter σ_u would lie somewhere in between 0-2 GPa. The exact location is inaccessible as it lies in the “blind spot” region of the fibre strength spectrum. However, it follows the empirical relationship given by Equation 7.1. The location parameter can be varied by varying the value of ω between 0 and 1, which would result in one of the three possible cases already discussed. The value of ω can be estimated by a user depending upon material behaviour, previous experimental experiences, and the number of fibres which break during the testing process. Incorporating this empirical relationship in the failure probability equation gives Equation 7.8.

$$P_R(\sigma) = 1 - \exp \left[- \left(\frac{L}{L_0} \right) \left(\frac{(\sigma - (1 - \omega)\sigma_r)^m - (\sigma_r - (1 - \omega)\sigma_r)^m}{\sigma_0^m} \right) \right] \quad (7.8)$$

The generalized truncated Weibull distribution Equation 7.8 can be simplified for the three different cases by varying the value of ω between 0 and 1, as shown:

Case 1: For this case, $\omega = 1$, which according to Equation 7.1 makes the location parameter $\sigma_u = 0$. The simplified failure probability is given by Equation 7.9. This is equivalent to a 2-parameter Weibull distribution (since $\sigma_u = 0$), with truncation.

$$P_R(\sigma) = 1 - \exp \left[- \left(\frac{L}{L_0} \right) \left(\frac{\sigma^m - \sigma_r^m}{\sigma_0^m} \right) \right] \quad (7.9)$$

Case 2: This case is governed by the generalized truncated Weibull distribution given by Equation 7.8. It can have infinite possible expressions depending upon the chosen value of ω .

Case 3: For this case, $\omega = 0$, which makes $\sigma_u = \sigma_r$, i.e. the location parameter takes the same value as the truncation limit. Substituting it in the failure probability Equation 7.8 will result in a very similar equation as that of a standard 3-parameter Weibull distribution and is given in Equation 7.10. It is however not exactly the same as it contains the truncation limit σ_r , unlike the 3-parameter Weibull distribution which has the location parameter σ_u , at the same position.

$$P_R(\sigma) = 1 - \exp \left[- \left(\frac{L}{L_0} \right) \left(\frac{\sigma - \sigma_r}{\sigma_0} \right)^m \right] \quad (7.10)$$

It is important to note that the truncation limit σ_r is different from the location parameter σ_u . Truncation limit is the minimum strength required for the fibre to be tested while the location parameter represents the actual minimum strength of the weakest fibre present in the fibre population. The location parameter (threshold limit) σ_u is a characteristic of the fibre material, whereas truncation limit σ_r arises due to experimental limitations to test weaker filaments. Although different, the existence of either a truncation or a threshold limit can result in a deviation between the data and the standard 2-parameter Weibull

distribution on a Weibull plot, and should be addressed using the corresponding method. For example, the misfit between experimental fibre strength data and the standard Weibull model can be addressed by using a truncation limit, as described here.

7.4 Experiments, Results and Discussions

7.4.1 Experimentation

To apply the method discussed in Section 7.3 to actual experimental results, fibre strength data for T700 carbon fibres was used. From the data generated in Chapter 6, a set of 100 fibre tensile strength values determined at a gauge length of 30 mm, were randomly extracted.

7.4.2 Fibre strength results

The extracted fibre strength data set is shown in Table 7.3. A histogram was generated to visualize the variability in the data, and is shown in Figure 7.4. The fibre strength is observed to vary between 2-7 GPa. There are no data points below 2 GPa, which means that the data set is left truncated. This generated data is in agreement with many other previous experimental studies on single fibre tensile strengths, as also described earlier. It is interesting to note however, that many fibres break during the intermediate steps of the testing process, i.e. during fibre extraction, fibre mounting, specimen preparation, and specimen transfer to the testing site. As a result of this, a total of about 450 fibres had to be tested to obtain the total of 350 tensile test results generated. A more detailed discussion on the number of fibres which are unable to survive the fibre testing process has been provided elsewhere [113]. The number of fibres that break during these intermediate steps also gives an estimate of the truncation limit associated with the given fibre and testing process.

Table 7.3: Single fibre tensile strength data set for a gauge length of 30 mm.

2.14	2.81	3.10	3.37	3.61	3.91	4.18	4.74	5.02	5.97
2.27	2.82	3.14	3.42	3.63	3.91	4.26	4.74	5.04	5.97
2.34	2.83	3.15	3.43	3.66	3.99	4.27	4.77	5.13	6.01
2.49	2.86	3.20	3.48	3.67	3.99	4.28	4.80	5.19	6.13
2.56	2.90	3.26	3.50	3.71	4.02	4.29	4.81	5.25	6.13
2.62	2.94	3.27	3.52	3.75	4.03	4.37	4.85	5.34	6.23
2.64	3.05	3.29	3.55	3.77	4.13	4.41	4.87	5.43	6.35
2.70	3.06	3.32	3.55	3.79	4.16	4.43	4.91	5.68	6.51
2.75	3.07	3.36	3.56	3.82	4.17	4.55	4.92	5.74	6.52
2.78	3.10	3.36	3.59	3.84	4.17	4.56	5.01	5.88	6.71

7.4.3 Standard Weibull analysis

The fibre strength data set was first analysed using the standard versions of the Weibull distribution, i.e. the standard 2 and 3-parameter Weibull distribution models, given by

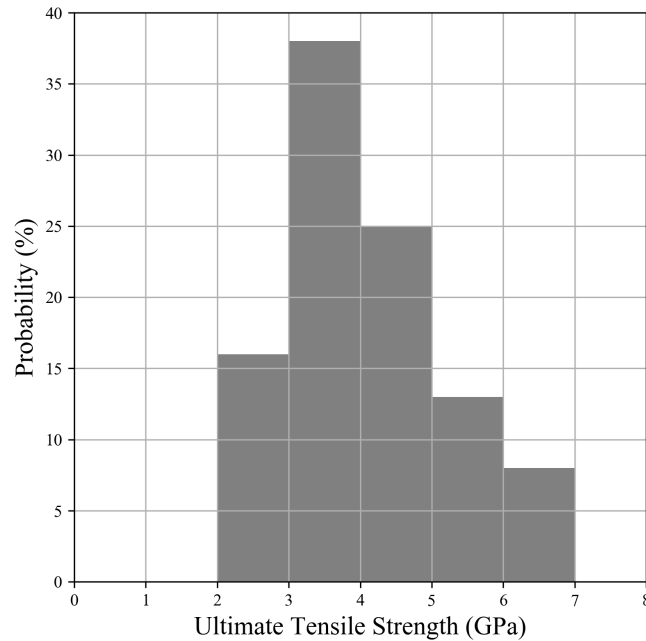


Figure 7.4: Histogram of the experimentally generated fibre strength data.

Equation 2.4 and Equation 2.2, respectively. The estimated maximum likelihood parameters for both the distributions are given in Table 7.4. The corresponding logarithmic Weibull plots for both are plotted together along with the experimental data points, as shown in Figure 7.5. It can be seen from Table 7.4 that the parameters for the two distributions are different from each other. However, it will be incorrect to make any comparisons between these results as the parameters from these two types of distributions do not represent the same quantities, physically. The same values of shape parameter have different interpretations for the 2 and 3-parameter Weibull distributions. For example, a shape parameter value of $m = 4$ for the 2-parameter Weibull distribution will represent a different scatter in its data as compared to the same shape parameter value for a 3-parameter Weibull distribution.

Table 7.4: Parameters for standard Weibull distributions.

Distribution ↓	Shape, m	Scale, σ_0 (GPa)	Location, σ_u (GPa)
Standard 2-parameter Weibull	3.94	4.51	0
Standard 3-parameter Weibull	1.93	2.31	2.03

It can be seen from Figure 7.5 that the standard 2-parameter Weibull distribution model is unable to accurately represent the experimentally generated fibre strength data set. There is an apparent deviation, mainly at the left end of the distribution where the

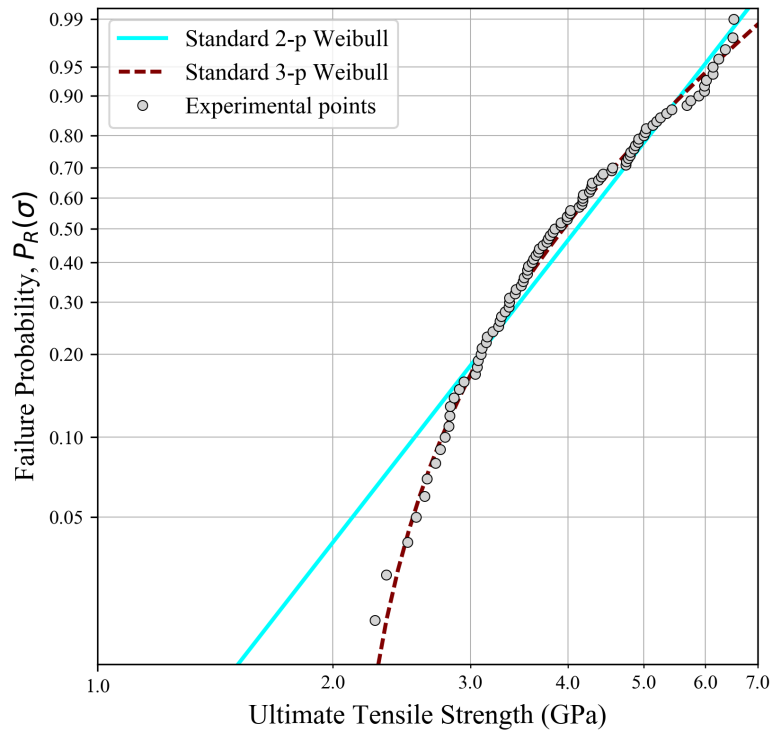


Figure 7.5: Best representative standard 2 and 3-parameter Weibull distributions along with experimental fibre strength data.

experimental points and the Weibull model are seen to deviate from each other. This deviation is not surprising and is observed because the data set is left-truncated, i.e. there is a region towards the left tail of the fibre strength distribution for which the fibre strength information is unavailable. This behaviour is also very similar to the one observed in the fibre preselection simulation study shown in Figure 7.2, which further confirms the hypothesis of the existence of a fibre preselection effect. This effect was also apparent in the histogram shown in Figure 7.4, with no data points with strength value between of 0-2 GPa. As mentioned earlier, if the objective is to determine a good-fit between a statistical function and the experimental data, using the 3-parameter Weibull distribution (Equation 2.2) will address the requirement by fitting the experimental points very well, as can be seen from Figure 7.5. However, this distribution may not be an appropriate representation of fibre strengths in the actual fibre population. This analysis assumes the sample data to be a correct representative of the fibre strength of the population. The “blind spot” in the fibre strength spectrum will not be considered and the fibre preselection effect will remain ignored. There is a need to conduct appropriate statistical analyses on this biased data set by considering the truncation in order to determine the actual fibre strength behaviour. The truncated Weibull analysis introduced in the previous section is capable of addressing the incompleteness of the fibre strength data set, as described in the

next section.

7.4.4 Truncated Weibull analysis

On examining the fibre strength data set given in Table 7.3, it is observed that the minimum fibre strength value measured is 2.19 GPa. For simplicity, the truncation limit is fixed at $\sigma_r = 2$ GPa for conducting the truncated Weibull analysis. Varying the value of ω between 1 and 0 results in one of the three cases described in Table 7.2. The estimated maximum likelihood parameter values for three different cases are given in Table 7.5 and the corresponding Weibull plots for the distributions are shown in Figure 7.6 with dashed lines. Since there are infinite possibilities for case 2, depending upon the chosen value of ω ($0 < \omega < 1$), results are shown only for a randomly chosen value of $\omega = 0.5$, for this case.

Table 7.5: Parameters for truncated Weibull distributions for different cases.

Case	ω	Truncation limit, σ_r (GPa)	Shape, m	Scale, σ_0 (GPa)	Location, σ_u (GPa)
1	1	2	3.44	4.35	0
2	0.5	2	2.78	3.37	1
3	0	2	1.98	2.35	2

Following this preliminary analysis, the obtained parameters of the generalized truncated Weibull distribution can further be used to obtain a more accurate representation of the fibre strength behaviour. As mentioned earlier, a truncated Weibull distribution model contemplates the incompleteness of the data set during analysis. It is obtained by the addition of a fixed truncation limit (σ_r) to the standard Weibull distribution. This provides additional information that the data set is incomplete and that strength data values lying in between σ_u and σ_r are unavailable. This does not alter the characteristics of the other parameters, which still hold the same physical meanings. Consequently, if the truncation limit is disregarded after calculation, the remaining quantities; i.e. the shape, scale and location parameters will represent the Weibull distribution which would ideally have been obtained if the entire fibre strength data set was accessible. These quantities can be used to predict the actual fibre strength behaviour. On excluding the truncation limit, the parameters for the predicted Weibull distributions for the three cases are obtained and are given in Table 7.6. The corresponding plots for the predicted distributions for the three cases are shown in Figure 7.6 with solid lines. Since for the first case the location parameter $\sigma_u = 0$, it belongs to the family of the 2-parameter Weibull distribution whereas cases 2 and 3 belong to the 3-parameter Weibull distribution family, since σ_u values for them are non-zero.

The difference between the predicted and standard Weibull distributions depends on the level of fibre preselection for that case. Considering case 1 for example, for which the fibre preselection effect is the most significant (maximum spread of inaccessible region for fibre strength, as shown in Figure 7.3(a)), the difference between the predicted and standard Weibull distribution is very large, as is apparent from Figure 7.6(a). As a

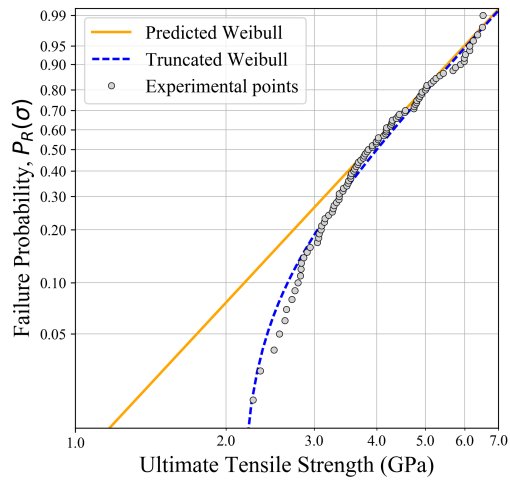
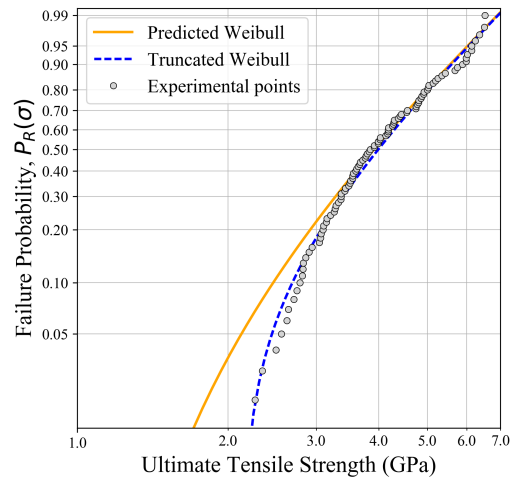
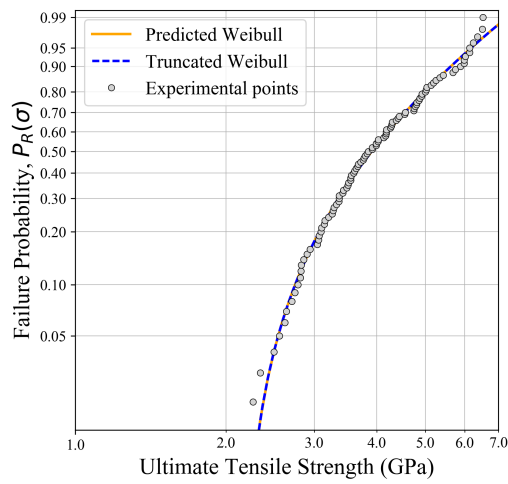
(a) Case 1: $\omega = 1$ (b) Case 2: $\omega = 0.5$ (c) Case 3: $\omega = 0$

Figure 7.6: Truncated and predicted Weibull distributions for the three cases.

Table 7.6: Parameters for predicted Weibull distributions for the 3 cases.

Case	Shape, m	Scale, σ_0 (GPa)	Location, σ_u (GPa)	Type
1	3.44	4.35	0	} 2-parameter Weibull
2	2.78	3.37	1	
3	1.98	2.35	2	} 3-parameter Weibull

result, the available experimental data spreads over a slightly narrower range than it would have if the entire fibre strength range was available. Due to this reason, when the standard 2-parameter Weibull distribution is used for representing this experimental data, the resulting distribution is shifted to the right and is also slightly narrower as compared to what it would have been if the entire fibre strength data set was available, i.e. including the weaker strength points. There is no effect of fibre preselection for case 3, i.e. there is no truncation and the entire fibre strength region is experimentally accessible. For this case, the predicted Weibull distribution is same as the standard Weibull distribution.

These differences between the predicted and standard Weibull distributions can also be observed by comparing the shape and scale parameter values for each distribution from Table 7.4 and Table 7.6, respectively. The shape parameter value for the standard distribution is $m = 3.94$. This is comparatively larger than the shape parameter value for the predicted Weibull distribution which is $m = 3.44$. The larger shape parameter signifies a narrower distribution. Similarly, a larger scale parameter value is observed for the standard distribution, $\sigma_0 = 4.51$ GPa. This shows that the standard distribution is shifted towards the right as compared to the predicted case ($\sigma_0 = 4.35$ GPa), which contemplates the possibility of having weaker fibre strength data points as well. This difference in the parameters of the fibre strength distribution will also result in differences in predicted behaviour of composite structures when these results are used as input in composite strength models, as described in Chapter 5. For example, if we compare the parameters of the fibre strength Weibull distribution obtained using the standard Weibull analysis with those obtained using the truncated Weibull analysis (Case 1), we find a variation of about 10% in the shape parameter and about 4% in the scale parameter. Based on the understanding gained from Chapter 5, it can be estimated that this would result in variations in predictions of up to 6% in strength and 12% in lifetime of the structures. Not using a truncated Weibull distribution for representing fibre strength can thus result in over predicting the strength and lifetime of composite structures.

The choice of the truncation limit has been shown to affect the obtained fibre strength distribution, as also seen clearly from the difference cases shown in Figure 7.6. An appropriate choice of this truncation limit helps in determining an accurate fibre strength distribution, by appropriately considering the presence of weaker fibres in the distribution. The weak fibres in the population have also been hypothesized to dominate the lifetime of composite structures [11]. Based on the choice of the truncation limit, the predictions of the composite strength model will also be affected. Prior knowledge about broken fibres should be considered in order to make an informed choice about this truncation limit.

The improvement in the understanding of the fibre strength distribution will thus help in estimating the mechanical behaviour and lifetime of composite structures more accurately.

7.5 Conclusions

Contemplating the discrepancy between the experimental data points and the Weibull model on a graphical plot, the limitations of the standard Weibull distributions for representing the tensile strength behaviour of brittle fibres has been discussed in this chapter. The utility of the standard Weibull analysis popularly used for representing fibre strength behaviour has been highlighted. It has been shown that the problems do not lie with the available statistical distributions but with the experimentally generated fibre strength data sets. Fibre tensile strength data sets generated experimentally are not always reliable representatives of the strength of the fibres inside a fibre bundle or composite material. Due to the effect of fibre preselection, weaker fibres are unable to be tested and are thus not represented in the experimentally determined data set. The test does not start only once the fibre is loaded, but it actually begins from the point the fibre is extracted from the bundle/roving. Due to very small breaking loads, fibres that are very weak and have strength values below certain limit may not be strong enough to survive the sample preparation and testing process. As a result, strengths of such fibres are usually not determined and they are thus not represented in the data set. This has been shown, with the help of simulations, to result in a truncation in the obtained fibre strength data and also in the resulting strength distribution. It has also been shown that analysing this incomplete data with the standard Weibull functions may result in incorrect conclusions about the physical nature of the strength behaviour of fibres. This error can also propagate into the predictions made by composite strength models which use the fibre strength information as input, and can lead to overestimated predictions for the mechanical properties and lifetime of composite structures.

Since the standard Weibull analysis by itself is inappropriate for representing the actual fibre strength behaviour, the effect of truncation in fibre strengths has been analytically modelled in the standard Weibull function. A generalized Weibull analysis based on Bayesian approach of using prior knowledge has been presented which considers the effect of fibre preselection in analysing fibre strength data. The analysis has been described with the help of experimentally generated fibre tensile strength results for T700 carbon fibres. Using the presented Weibull analysis, it is possible to predict the actual Weibull distribution which can represent the strength behaviour of the fibres which are present inside a composite material. Ideally, this distribution could also have been obtained if the entire fibre strength spectrum was experimentally accessible. However, since that is practically not possible, the truncated Weibull analysis can be used for representing the actual strength behaviour of fibres used in composite materials.

Chapter summary in French

Analyse de Weibull basée sur l'approche Bayésienne

L'écart entre les données expérimentales et le modèle de Weibull est discutée dans ce chapitre.. Il est montré que les problèmes ne résident pas dans les distributions statistiques disponibles mais dans les ensembles de données de résistance générés expérimentalement.

En raison de l'effet de la présélection/extraction des fibres, les fibres les plus faibles ne sont généralement pas représentées dans la distribution expérimentale. Le test sur fibre unitaire ne démarre pas une fois que la fibre est chargée, mais il commence en réalité dès l'extraction de la fibre. En raison de leur faibles charges à rupture, certaines fibres peuvent ne pas être suffisamment solides pour survivre au processus de préparation des échantillons. Il en résulte une troncature dans la distribution de résistance résultante.

Il a également été montré que l'analyse de ces données incomplètes peut entraîner des conclusions incorrectes sur le comportement à rupture des fibres. Cette erreur peut également se propager dans les prédictions faites par les modèles de résistance sur les structures composite et peut conduire à des prédictions surestimées.

Une analyse de Weibull généralisée basée sur l'approche bayésienne de l'utilisation des connaissances antérieures est présentée dans ce chapitre. Cette analyse prend en compte l'effet de la présélection des fibres dans l'analyse des données et est appliqué au cas des fibres de carbone T700.

En utilisant l'analyse statistique proposée, il est possible de prédire la distribution de Weibull qui serait la plus probable pour représenter le comportement à rupture des fibres. Idéalement, cette distribution présumée correspond à l'ensemble du spectre de résistance des fibres, expérimentalement inaccessible.

Chapter 8

Conclusions and perspectives

8.1 Conclusions

This thesis attempted to develop a better understanding of the constituent properties of fibre reinforced composites, to quantify the uncertainties associated with these properties, and to improve the characterisation processes.

The sensitivity analysis discussed in Chapter 3 has shown that the standard method of testing single fibres for strength measurement is susceptible to many errors, due to the different challenges faced in characterisation. Measured fibre strength is therefore associated with uncertainties. Magnitude of these errors or uncertainties depends on the gauge length of the fibres used for testing. For tests done at short gauge lengths (a few millimetres and below), the effect of input quantities, especially the fibre misalignment, becomes very significant. It becomes very difficult to accurately control the input quantities when fibres of such short gauge length are used for tensile testing. This results in significant uncertainty in measured fibre strength, and hence great care should be taken when characterising fibres at such short gauge lengths, in order to minimise errors. Expected uncertainties should also be quantified while reporting such results. Weibull distributions obtained for strength of such short fibre gauge lengths will also be statistically uncertain, as demonstrated in Chapter 4. The negative implications of using such uncertain input data with composite models for making structural predictions, as demonstrated in Chapter 5, further reinforces the need for accurate input data for predicting reliable structural behaviour. Certain aspects hypothesized for improving the accuracy of input data include usage of more accurate and larger fibre strength data sets for analysis. Although this was fulfilled to an extent by using the semi-automated fibre testing methodology, it has raised questions about the applicability of the standard Weibull analysis for determining the fibre tensile strength behaviour using experimental results directly, as demonstrated in Chapter 6. The generalised Weibull analysis based on the Bayesian approach of using prior information about prematurely failed fibres can be used for representing the fibre strength behaviour, as described in Chapter 7.

The knowledge about the uncertainties in individual constituent properties has shown to help in determining their influence on the variability in the predicted mechanical behaviour

and integrity of composite structures. The knowledge of this variability in model predictions can also be useful for structural reliability analysis, e.g., for estimating the confidence interval which can be assigned to the predictions made by computational models, if these models are used as replacements for actual mechanical tests. Although using high design safety factors on the influential parameters make it possible to secure composite structures in a deterministic manner, it conceals the extent of the risk that is being taken in doing so. Therefore, structural reliability analysis based on omnipresent uncertainties can provide information about the associated risks to engineers, enabling them to have a better control of the safety margin, if it can be appropriately conducted.

An in-depth investigation of the fibre strength characterisation following the single fibre testing methodology, using both the standard and improved semi-automated testing methods, and also the analysis of the data reduction processes commonly used, has helped in identification of possible sources of errors in measured fibre strength and in the parameters of the Weibull strength distribution. Understanding of the different aspects of characterising the constituent properties of composites, developed as a result of this thesis, also helps in differentiating between different causes of uncertainties in results, i.e. whether the uncertainties arise due to material variability, experimental errors, sampling randomness, or the method used to analyse the results. This knowledge can help in improving the characterisation process for estimating a more accurate statistical function which can represent the strength behaviour of the fibres in composite materials. The knowledge of the influence of different parameters on measured fibre strength can also help in designing improved fibre testing systems capable of determining fibre strength more accurately. Incorporating the different suggestions made in this thesis, for e.g., using a large fibre strength data set for analysis, ensuring minimum measurement errors during testing, and choosing an appropriate data-reduction technique will help in generating accurate and useful input for composite strength models. More accurate constituent properties used as input would allow these models to make reliable predictions about structural behaviour such as the strength and lifetime of composite structures.

The issue of discrepancy between experimental fibre strength data and the Weibull model is an ongoing topic of research in the composites community. While many studies consider this discrepancy to occur due to the incompetency of the standard Weibull distributions to represent the fibre strength behaviour, a few others have mentioned the possibility of the fibre preselection effect to be the major cause. Since the strength of fibres which might have been broken due to this effect is inaccessible, the fibre preselection effect has been demonstrated using simulated results. It would therefore be useful to keep track of the fibres which break during the different stages of sample preparation and testing, which has the potential to highlight the presence of such an effect. The present study also considers this effect for determining the truncation limit during Weibull analysis.

Weibull theory is a statistical theory, that is used for representing the fibre strength behaviour. It is not based on physical models of the fracture process. Interpretation of the Weibull parameters in terms of flaw density and severity is an ambitious approach and great care should be taken in using Weibull plots to draw conclusions on the mechanics or physics of the fibre fracture process.

Finally, even in the ideal scenario where the fibre, matrix and interfacial properties are

measured accurately, differences between model predictions and experimental results may still occur. This is because every predictive model requires a set of assumptions about the complex composite failure mechanisms, which limits the accuracy of the predictions. Nevertheless, lack of reliable input data is a major cause for the lack of reliable model predictions.

8.2 Fibre strength and Weibull distribution: A perspective

8.2.1 *Limitations of extrapolating fibre strength to shorter gauge lengths*

Fibre strength Weibull distributions determined for different gauge lengths are given by Table 8.1, as also already shown in Chapter 6. As already known, composite strength models require information for strength distributions at small gauge lengths, usually ranging between a few millimetres to a few micrometres. When the Weibull scale parameter σ_0 , obtained for 30 mm is extrapolated to shorter gauge lengths using the Weibull scaling Equation 1.2, the obtained scale parameter at different gauge lengths follow the line shown in Figure 8.1. The Weibull scale parameter obtained from experimental results are shown by points. While the extrapolated and experimental results show a good agreement when the extrapolation is done from 30 mm to 20 mm, the results are overestimated by about 30% when the extrapolation is done to a smaller length of 4 mm.

Table 8.1: Weibull distribution parameters for different gauge lengths

Gauge Length (mm)	Shape parameter m	Scale parameter σ_0 (GPa)
4	3.55	5.72
20	3.50	5.16
30	3.48	4.63

Such a behaviour has also previously been observed by Pickering et al. [143] and Watanabe et al [42]. Watanabe suggested using a bi-modal Weibull distribution to represent the results, in which case, the extrapolated and experimental results showed a better match with the Weibull plot. Bi-modal Weibull distribution represents an existence of two types of flaw populations in the fibre, which controls the fracture process. The hypothesis being that the fibre failure could occur due to flaws present on the surface or within the volume of the material. However, the discussion provided in the next section advocates against this hypothesis.

The differences between the extrapolated and experimental results could be due to some or all of the following hypothesized reasons:

- There are flaws of different sizes in the material. Failure due to smaller flaws has different characteristics than the failure due to comparatively larger flaws. Using a bi-modal Weibull distribution to represent the fibre strength behaviour will also be

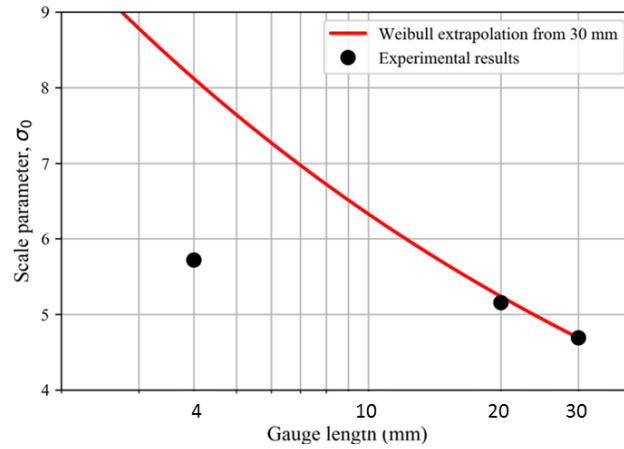


Figure 8.1: Comparison of the scale parameters obtained from extrapolation with that obtained from experimental results.

justified in which case, if the existence of different flaw sizes can be established.

- The Weibull parameters obtained experimentally for the short gauge length are inaccurate, due to larger measurement errors while testing short fibres.
- The shape parameter used for extrapolating the scale parameter to shorter gauge lengths is inaccurate. A larger value of the shape parameter would provide better results.
- Fibre strengths at short and large gauge lengths do not follow the same Weibull distribution.
- There is uncertainty in both the shape and scale parameters of the Weibull distribution obtained from experimental results. This uncertainty is significantly large for the 4 mm case. When these parameters are extrapolated, the uncertainties are also magnified.
- Fibre strength increases with decreasing gauge length, but only until a certain limit, below which fibre strength reaches a saturation state. This hypothesis also supports the observations made by Phoenix et al., who reported that fibres of gauge length 5 mm and 0.5 mm have similar strengths [144].
- Parameters of the Weibull distribution are not unique. The same physical distribution can be represented by different combinations of distribution parameters. Small variations in different parameter combinations are likely, but it is unlikely that such a large difference in the scale parameter could occur entirely due to this reason.

8.2.2 *Is it statistically appropriate to modify the Weibull distribution?*

To comprehend the pertinence of the Weibull distribution for representing the tensile strength behaviour of technical fibres, the analogy between the weakest link theory and

the Weibull distribution should be considered. It has been explained in Appendix A. Although the Weibull distribution has its roots in the weakest link theory, the two concepts are distinct. The popularly used form of the Weibull distribution, as given by Equation 8.1, is a combination of the Weakest link theory and Weibull's representation of the survival probability. The term (L/L_0) has its origin in the weakest link theory, while the term (σ/σ_0) is an empirical function suggested by Weibull and should ideally be obtained from experimental results.

$$P_R(\sigma) = 1 - \exp \left[- \left(\frac{L}{L_0} \right) \left(\frac{\sigma}{\sigma_0} \right)^m \right] \quad (8.1)$$

Many authors have developed modified versions of the Weibull distribution, to overcome the discrepancies between experimental results and the Weibull model. An interpretation of this situation is that more than one failure mode may be possible in the tested material, and the standard Weibull distribution function is inappropriate to capture the strength behaviour of such fibres. Survival probabilities in such a case can be multiplicative and a modified version of the Weibull distribution, such as the one given by Equation 8.2 can adequately describe the strength from two independent flaw populations. This is also within the scope of the weakest link theory. Nonetheless, the presence of multiple flaw populations has to be well justified. However, it has been shown by Naito et al. [95] that for carbon fibres tested at gauge lengths between 1 mm and 250 mm, very similar fracture surfaces are observed, indicating the presence of a unique type of flaw which controls the fracture behaviour. Alternatively, another similar distribution is sometimes used, where the two exponential terms in Equation 8.2 are multiplied by q and $(1 - q)$, resulting in addition of probabilities, where q is a mixing parameter, and depends on the proportion of the two types of flaws. Such a distribution is inconsistent with the weakest link theory, which is obtained by multiplication of individual failure probabilities.

$$P_R(\sigma) = 1 - \exp \left[- \left(\frac{L}{L_0} \right) \left(\frac{\sigma_f}{\sigma_{0,1}} \right)^{m_1} - \left(\frac{L}{L_0} \right) \left(\frac{\sigma_f}{\sigma_{0,2}} \right)^{m_2} \right] \quad (8.2)$$

Another modified version of the Weibull distribution suggests adding an exponent α in the standard Weibull function to represent the dependency of fibre strength on the gauge length, as given by Equation 8.3. Not only is α only an empirical parameter used to fit the experimental data, but the resulting distribution is also inconsistent with the weakest link theory.

$$P_R(\sigma) = 1 - \exp \left(- \left(\frac{L}{L_0} \right)^\alpha \left(\frac{\sigma_f}{\sigma_0} \right)^m \right) \quad (8.3)$$

8.3 Scope for future work

- The knowledge of the location where a fibre breaks during a tensile test can improve the accuracy of measured strength of fibres, especially those which have a non-uniform cross-section. It will provide information about the location of defects in the fibres. Even for fibres of a uniform section, the knowledge about the location of

fibre breaks can be used to ensure that the tests have been performed correctly. It will ensure that any incorrect test results are disregarded, such as the ones where the fibres break at the location of the clamp/glue. A system which is able to detect the exact location on the fibre where it breaks will therefore be very useful. Acoustic emission techniques can be used for estimating the failure location. A sensor can be installed at each end of the fibre being tested, and comparing the signals from the two can give an estimate of the fibre failure location. A system which is sensitive enough to pick up the signals appropriately would be required. The fibres which fail close to the clamping location can still be considered for analysis, unless the failure is caused due to external factors such as bending due to misalignment.

The knowledge of the location of fibre breaks can also be used to check if there is any correlation between the measured strength of fibres and the location where it breaks, which can highlight possible clamping effect, if any.

- A method of sequential testing of fibres can be developed to test fibres at even shorter gauge lengths. This can be done by subjecting only a very small portion of a single fibre to stress, and measuring the load at which failure occurs. However, the effect of any misalignment for such short gauge lengths would be very large, as statistically evaluated in Chapter 3, and will have to be minimised to ensure an accurate strength determination with minimum uncertainties.
- The laser diffraction system used for measuring fibre diameter, described in Chapter 6, can also be used for minimising fibre misalignment during testing. The system is capable of rotating around the fibre axis to find a position which maximises the signals for measurement. It can further be used for ensuring that the fibre is placed in the most suitable position to minimise misalignment.
- The analytical model for used in Chapter 3 for evaluating uncertainties in measured fibre strength can also be extended to evaluate uncertainties in the measurement of strain and the longitudinal Young's modulus of fibres. However, these models will be more complex due to the interacting nature of the different model parameters, and the uncertainty analysis, in which case, will have to consider the correlation between different input quantities. The method of uncertainty analysis for correlated input quantities will have to be used in this case for estimating uncertainties [96]. Better techniques for strain measurement, as suggested in the next point, will be useful in minimising such uncertainties.
- A strain measurement system which is capable of measuring the local strain at different regions along the length of the fibre can provide very useful information on how the local strain varies between the fibre break location and at farther distances from it. This can also possibly highlight the distribution of defects inside the fibres.
- Fibres are considered to be transversely isotropic in nature, and are described by 5 independent elastic constants. These include the Young's modulus and the Poisson's ratio in the symmetry plane, the Young's modulus and the Poisson's ratio in the axial direction, and the shear modulus. However, the datasheets of manufacturers typically only contain the stiffness and strength of the fibre in the axial direction. The anisotropic properties of fibres are sometimes reverse engineered from macro-

scale experimental results [136]. A more reliable methodology of estimating the anisotropic properties of fibres can also improve the accuracy of composite strength models.

- To be able to determine the axial Poisson's ratio of carbon fibres confidently and accurately, a fibre diameter measurement technique which offers an improved resolution is required. Additionally, an estimation of uncertainty in the Poisson's ratio can be made, which would be useful in understanding the confidence that can be placed in these results. More accurate and reliable measurements of input quantities will be required to minimise these uncertainties.
- In Chapter 6, a large set of fibre strength data generated at gauge lengths of 4 mm, 20 mm, and 30 mm was analysed. The strength data at other intermediate and shorter gauge lengths can be compared and analysed with respect to the material microstructure and failure behaviour. This can be useful in analysing the applicability of the Weibull distribution for different gauge lengths and also in highlighting any limitations in extrapolating fibre strength data.

Chapter summary in French

Conclusions et perspectives

Cette thèse a proposé une démarche visant à améliorer notre compréhension des propriétés liées aux fibres, renforts pour les composites, de quantifier les incertitudes associées à ces propriétés et d'améliorer les processus de caractérisation.

Une étude approfondie de la caractérisation de la résistance des fibres unitaires a été proposée. L'utilisation combinée de test semi-automatisés ainsi que l'analyse des processus de réduction des données, a aidé à identifier différentes pistes pour améliorer les données de résistance à rupture sur les fibres. Ce travail permet de différencier les différentes causes d'incertitudes dans les résultats, à savoir si les incertitudes surviennent en raison de la variabilité des matériaux, en raison d'erreurs expérimentales, en raison d'un échantillonnage aléatoire ou en raison de la méthode utilisée pour analyser les résultats. La meilleure connaissance de l'influence des différents paramètres sur la résistance mesurée des fibres peut également aider à concevoir des systèmes de test améliorés, comme cela est proposé dans ce travail.

Bibliography

- [1] X. Zhang, J. Zhao, and Z. Wang, “Burst pressure prediction and structure reliability analysis of composite overwrapped cylinder,” *Applied Composite Materials*, vol. 25, pp. 1269–1285, Dec 2018.
- [2] H. Chou, A. Bunsell, G. Mair, and A. Thionnet, “Effect of the loading rate on ultimate strength of composites. application: Pressure vessel slow burst test,” *Composite Structures*, vol. 104, pp. 144 – 153, 2013.
- [3] *Overview of the global composites market - at the crossroads*. JEC Group, 2017.
- [4] *BMW - USA Website*, accessed January 22, 2020.
- [5] *Airbus Website*, accessed January 22, 2020.
- [6] *Composites World Website*, accessed January 22, 2020.
- [7] *Eco-Globe Website*, accessed January 22, 2020.
- [8] *Wikipedia- List of jet airliners*, accessed January 22, 2020.
- [9] *BP Energy Outlook - 2019 Edition*. BP p.l.c., 2019.
- [10] L. Mishnaevsky, K. Branner, H. Petersen, J. Beauson, M. McGugan, and B. Sørensen, “Materials for wind turbine blades: An overview,” *Materials*, vol. 10, p. 1285, Nov 2017.
- [11] A. Bunsell and A. Thionnet, “Life prediction for carbon fibre filament wound composite structures,” *Philosophical Magazine*, vol. 90, no. 31-32, pp. 4129–4146, 2010.
- [12] A. Thionnet, H. Y. Chou, and A. Bunsell, “Fibre break failure processes in unidirectional composites. part 2: Failure and critical damage state induced by sustained tensile loading,” *Applied Composite Materials*, vol. 22, pp. 141–155, Apr 2015.
- [13] S. Blassiau, A. Thionnet, and A. Bunsell, “Micromechanisms of load transfer in a unidirectional carbon fibre–reinforced epoxy composite due to fibre failures. part 1: Micromechanisms and 3d analysis of load transfer: The elastic case,” *Composite Structures*, vol. 74, no. 3, pp. 303–318, 2006.
- [14] S. Pimenta, “8 - fibre failure modelling,” in *Numerical Modelling of Failure in Advanced Composite Materials* (P. P. Camanho and S. R. Hallett, eds.), Woodhead Publishing Series in Composites Science and Engineering, pp. 193 – 224, Woodhead Publishing, 2015.

- [15] Y. Swolfs, I. Verpoest, and L. Gorbatikh, “Issues in strength models for unidirectional fibre-reinforced composites related to weibull distributions, fibre packings and boundary effects,” *Composites Science and Technology*, vol. 114, pp. 42 – 49, 2015.
- [16] A. Bunsell, L. Gorbatikh, H. Morton, S. Pimenta, I. Sinclair, M. Spearing, Y. Swolfs, and A. Thionnet, “Benchmarking of strength models for unidirectional composites under longitudinal tension,” *Composites Part A: Applied Science and Manufacturing*, vol. 111, pp. 138 – 150, 2018.
- [17] S. L. PHOENIX and I. J. BEYERLEIN, “1.19 - statistical strength theory for fibrous composite materials,” in *Comprehensive Composite Materials* (A. Kelly and C. Zweben, eds.), pp. 559 – 639, Oxford: Pergamon, 2000.
- [18] A. Kaddour and M. Hinton, “Maturity of 3d failure criteria for fibre-reinforced composites: Comparison between theories and experiments: Part b of wwfe-ii,” *Journal of Composite Materials*, vol. 47, no. 6-7, pp. 925–966, 2013.
- [19] E. Sitnikova, D. Li, J. Wei, X. Yi, and S. Li, “On the representativeness of the cohesive zone model in the simulation of the delamination problem,” *Journal of Composites Science*, vol. 3, no. 1, 2019.
- [20] A. Thionnet, H.-Y. Chou, and A. Bunsell, “Fibre break failure processes in unidirectional composites. part 1: Failure and critical damage state induced by increasing tensile loading,” *Applied Composite Materials*, vol. 22, pp. 119–140, Apr 2015.
- [21] E. K. Gamstedt and S. Östlund, “Fatigue propagation of fibre-bridged cracks in unidirectional polymer-matrix composites,” *Applied Composite Materials*, vol. 8, pp. 385–410, Nov 2001.
- [22] H. Y. Chou, A. Thionnet, A. Mouritz, and A. R. Bunsell, “Stochastic factors controlling the failure of carbon/epoxy composites,” *Journal of Materials Science*, vol. 51, pp. 311–333, Jan 2016.
- [23] W. Weibull, “A statistical distribution function of wide applicability,” *Journal of Applied Mechanics*, pp. 293–297, 1951.
- [24] W. J. Padgett, S. D. Durham, and A. M. Mason, “Weibull analysis of the strength of carbon fibers using linear and power law models for the length effect,” *Journal of Composite Materials*, vol. 29, no. 14, pp. 1873–1884, 1995.
- [25] M.-H. Berger and D. Jeulin, “Statistical analysis of the failure stresses of ceramic fibres: Dependence of the Weibull parameters on the gauge length, diameter variation and fluctuation of defect density,” *Journal of Materials Science*, vol. 38, pp. 2913–2923, Jul 2003.
- [26] Y. Swolfs, I. Verpoest, and L. Gorbatikh, “A review of input data and modelling assumptions in longitudinal strength models for unidirectional fibre-reinforced composites,” *Composite Structures*, vol. 150, pp. 153 – 172, 2016.
- [27] S. Feih, K. Manatpon, Z. Mathys, A. G. Gibson, and A. P. Mouritz, “Strength degradation of glass fibers at high temperatures,” *Journal of Materials Science*, vol. 44, pp. 392–400, Jan 2009.

- [28] H. Xiao, Y. Lu, M. Wang, X. Qin, W. Zhao, and J. Luan, “Effect of gamma-irradiation on the mechanical properties of polyacrylonitrile-based carbon fiber,” *Carbon*, vol. 52, pp. 427 – 439, 2013.
- [29] S. Deng, L. Ye, Y.-W. Mai, and H.-Y. Liu, “Evaluation of fibre tensile strength and fibre/matrix adhesion using single fibre fragmentation tests,” *Composites Part A: Applied Science and Manufacturing*, vol. 29, no. 4, pp. 423 – 434, 1998.
- [30] V. Lutz, J. Duchet-Rumeau, N. Godin, F. Smail, F. Lortie, and J. Gérard, “Ex-pan carbon fibers vs carbon nanotubes fibers: From conventional epoxy based composites to multiscale composites,” *European Polymer Journal*, vol. 106, pp. 9 – 18, 2018.
- [31] W. Na, G. Lee, M. Sung, H. N. Han, and W.-R. Yu, “Prediction of the tensile strength of unidirectional carbon fiber composites considering the interfacial shear strength,” *Composite Structures*, vol. 168, pp. 92 – 103, 2017.
- [32] M. Matveev, A. Long, and I. Jones, “Modelling of textile composites with fibre strength variability,” *Composites Science and Technology*, vol. 105, pp. 44 – 50, 2014.
- [33] T. Zhang, L. Qi, S. Li, X. Chao, W. Tian, and J. Zhou, “Evaluation of the effect of pyc coating thickness on the mechanical properties of t700 carbon fiber tows,” *Applied Surface Science*, vol. 463, pp. 310 – 321, 2019.
- [34] Y. Zhou, Y. Wang, Y. Xia, and S. Jeelani, “Tensile behavior of carbon fiber bundles at different strain rates,” *Materials Letters*, vol. 64, no. 3, pp. 246 – 248, 2010.
- [35] P. Ilankeeran, P. Mohite, and S. Kamle, “Axial tensile testing of single fibres,” *Modern Mechanical Engineering*, vol. 2, no. 4, pp. 151–156, 2012.
- [36] F. Islam, S. Joannès, and L. Laiarinandrasana, “Evaluation of critical parameters in tensile strength measurement of single fibres,” *Journal of Composites Science*, vol. 3, no. 3, 2019.
- [37] A. R. Bunsell, S. Joannès, and A. Marcellan, *Handbook of Properties of Textile and Technical Fibres*. Woodhead Publishing, 2018.
- [38] S. Timoshenko, *History of the strength of materials*. McGraw-Hill, New York, 1953.
- [39] Z. P. Bazant and E.-P. Chen, “Scaling of Structural Failure,” *Applied Mechanics Reviews*, vol. 50, pp. 593–627, 10 1997.
- [40] W. Weibull, “A statistical theory of the strength of materials,” 1939.
- [41] I. J. Beyerlein and S. Phoenix, “Statistics for the strength and size effects of micro-composites with four carbon fibers in epoxy resin,” *Composites Science and Technology*, vol. 56, no. 1, pp. 75 – 92, 1996.
- [42] J. Watanabe, F. Tanaka, H. Okuda, and T. Okabe, “Tensile strength distribution of carbon fibers at short gauge lengths,” *Advanced Composite Materials*, vol. 23, no. 5-6, pp. 535–550, 2014.
- [43] F. Islam, S. Joannès, S. Bucknell, Y. Leray, A. Bunsell, and L. Laiarinandrasana, “Improvements in determination of carbon fibre strength distribution using automa-

- tion and statistical data analysis,” in *Proceedings of the Fiber Society’s Spring 2018 Conference*, 2018, June.
- [44] J. Andersons, R. Joffe, M. Hojo, and S. Ochiai, “Glass fibre strength distribution determined by common experimental methods,” *Composites Science and Technology*, vol. 62, no. 1, pp. 131 – 145, 2002.
- [45] F. Bensadoun, I. Verpoest, J. Baets, J. Müssig, N. Graupner, P. Davies, M. Gomina, A. Kervoelen, and C. Baley, “Impregnated fibre bundle test for natural fibres used in composites,” *Journal of Reinforced Plastics and Composites*, vol. 36, no. 13, pp. 942–957, 2017.
- [46] T. S. Creasy, “A method of extracting weibull survival model parameters from filament bundle load/strain data,” *Composites Science and Technology*, vol. 60, no. 6, pp. 825 – 832, 2000.
- [47] S. Phoenix, “Probabilistic strength analysis of fibre bundle structures,” *Fibre Science and Technology*, vol. 7, no. 1, pp. 15 – 31, 1974.
- [48] S. S. Abramchuk, A. F. Ermolenko, and P. V. D., “Estimating the characteristics of reinforcing fibers by testing fiber bundles,” *Mechanics of Composite Materials*, vol. 20, no. 1, pp. 1 – 5, 1984.
- [49] R. Hill and E. Okoroafor, “Weibull statistics of fibre bundle failure using mechanical and acoustic emission testing: the influence of interfibre friction,” *Composites*, vol. 26, no. 10, pp. 699 – 705, 1995.
- [50] A. F. Ermolenko, S. S. Abramchuk, and V. D. Protasov, “Evaluating parameters of the strength distribution of reinforcing fibers interacting on a lateral surface by testing their bundles,” *Mechanics of Composite Materials*, vol. 21, pp. 1–4, Jan 1985.
- [51] B. Yavin, H. E. Gallis, J. Scherf, A. Eitan, and H. D. Wagner, “Continuous monitoring of the fragmentation phenomenon in single fiber composite materials,” *Polymer Composites*, vol. 12, no. 6, pp. 436–446, 1991.
- [52] M. Shioya and A. Takaku, “Estimation of fibre and interfacial shear strength by using a single-fibre composite,” *Composites Science and Technology*, vol. 55, no. 1, pp. 33 – 39, 1995.
- [53] J. Andersons, R. Joffe, M. Hojo, and S. Ochiai, “Fibre fragment distribution in a single-fibre composite tension test,” *Composites Part B: Engineering*, vol. 32, no. 4, pp. 323 – 332, 2001.
- [54] C. Hui, D. Shia, and L. Berglund, “Estimation of interfacial shear strength: an application of a new statistical theory for single fiber composite test,” *Composites Science and Technology*, vol. 59, no. 13, pp. 2037 – 2046, 1999.
- [55] F. M. Zhao, T. Okabe, and N. Takeda, “The estimation of statistical fiber strength by fragmentation tests of single-fiber composites,” *Composites Science and Technology*, vol. 60, no. 10, pp. 1965–1974, 2000.

- [56] F. Thuvander, E. Gamstedt, and P. Ahlgren, "Distribution of strain to failure of single wood pulp fibres," *Nordic Pulp and Paper Research Journal*, vol. 16, no. 1, pp. 46–56, 2001.
- [57] M. Detassis, A. Pegoretti, C. Migliaresi, and H. D. Wagner, "Experimental evaluation of residual stresses in single fibre composites by means of the fragmentation test," *Journal of Materials Science*, vol. 31, pp. 2385–2392, May 1996.
- [58] S. Tsai and H. Hahn, *Introduction to composite materials*. Technomic, 1980.
- [59] W. Curtin, "Exact theory of fibre fragmentation in a single-filament composite," *Journal of Materials Science*, vol. 26, no. 19, pp. 5239–5253, 1991.
- [60] J. Andersons, R. Joffe, and R. Sandmark, "Constrained fragmentation of composites under uniaxial loading," *Mechanics of Composite Materials*, vol. 31, no. 1, pp. 26–33, 1995.
- [61] C.-Y. Hui, S. Phoenix, M. Ibnabdeljalil, and R. Smith, "An exact closed form solution for fragmentation of Weibull fibers in a single filament composite with applications to fiber-reinforced ceramics," *Journal of the Mechanics and Physics of Solids*, vol. 43, no. 10, pp. 1551–1585, 1995.
- [62] W. A. Curtin, "Fiber fragmentation in a single-filament composite," *Applied Physics Letters*, vol. 58, no. 11, pp. 1155–1157, 1991.
- [63] H. Fukuda, M. Yakushiji, and A. Wada, "A loop test to measure the strength of monofilaments used for advanced composites," *Advanced Composite Materials*, vol. 8, no. 3, pp. 281–291, 1999.
- [64] N. Toyama and J. Takatsubo, "An investigation of non-linear elastic behavior of cfrp laminates and strain measurement using lamb waves," *Composites Science and Technology*, vol. 64, no. 16, pp. 2509 – 2516, 2004.
- [65] W. Jones and J. Johnson, "Intrinsic strength and non-hookean behaviour of carbon fibres," *Carbon*, vol. 9, no. 5, pp. 645–650, IN15–IN18, 651–655, 1971.
- [66] *ASTM C1557 - 14: Standard Test Method for Tensile Strength and Young's Modulus of Fibers*. ASTM Standards, 2014.
- [67] International Organization for Standardization, *ISO 11566:1996 Carbon fibre – Determination of the tensile properties of single-filament specimens*.
- [68] ASTM Standards, *ASTM D3379-75 Standard Test Method for Tensile Strength and Young's Modulus for High-Modulus Single-Filament Materials*.
- [69] F. Bensadoun, I. Verpoest, J. Baets, J. MÃ¼ssig, N. Graupner, P. Davies, M. Gomina, A. Kervoelen, and C. Baley, "Impregnated fibre bundle test for natural fibres used in composites," *Journal of Reinforced Plastics and Composites*, vol. 36, no. 13, pp. 942–957, 2017.
- [70] A. Benard and E. C. Bos-Levenbach, "Translation of: "het uitzetten van waarnemingen op waarschijnlijkheids-papier" (the plotting of observations on probability paper)," *Statistica Neerlandica*, vol. 7, pp. 163 – 173, 1953.

- [71] J. M. van Zyl and R. Schall, "Parameter estimation through weighted least-squares rank regression with specific reference to the weibull and gumbel distributions," *Communications in Statistics - Simulation and Computation*, vol. 41, pp. 1654–1666, 2012.
- [72] A. Kelly and W. Tyson, "Tensile properties of fibre-reinforced metals - copper/tungsten and copper/molybdenum," *J. Mech. Phys. Sol.*, vol. 13, no. 329, 1965.
- [73] S. Phoenix and R. G. Sexsmith, "Clamp effects in fiber testing.," *Journal of Composite Materials*, vol. 6, pp. 322–337, 1972.
- [74] E. Stoner, D. Edie, and S. Durham, "An end-effect model for the single-filament tensile test," *Journal of Materials Science*, vol. 29, no. 24, pp. 6561–6574, 1994.
- [75] R. Gulino and S. Phoenix, "Weibull strength statistics for graphite fibres measured from the break progression in a model graphite/glass/epoxy microcomposite," *Journal of Materials Science*, vol. 26, no. 11, pp. 3107–3118, 1991.
- [76] J. Thomason, "On the application of Weibull analysis to experimentally determined single fibre strength distributions," *Composites Science and Technology*, vol. 77, pp. 74 – 80, 2013.
- [77] S. Phoenix, P. Schwartz, and H. Robinson, "Statistics for the strength and lifetime in creep-rupture of model carbon/epoxy composites," *Composites Science and Technology*, vol. 32, no. 2, pp. 81–120, 1988.
- [78] W. Yu and J. Yao, "Tensile strength and its variation of pan-based carbon fibers. I. statistical distribution and volume dependence," *Journal of Applied Polymer Science*, vol. 101, no. 5, pp. 3175–3182, 2006.
- [79] K. Goda and H. Fukunaga, "The evaluation of the strength distribution of silicon carbide and alumina fibres by a multi-modal weibull distribution," *Journal of Materials Science*, vol. 21, no. 12, pp. 4475–4480, 1986.
- [80] L. Yang and J. Thomason, "Effect of silane coupling agent on mechanical performance of glass fibre," *Journal of Materials Science*, vol. 48, no. 5, pp. 1947–1954, 2013.
- [81] J. Yao and W. Yu, "Tensile strength and its variation for PAN-based carbon fibers. II. Calibration of the variation from testing," *Journal of Applied Polymer Science*, vol. 104, no. 4, pp. 2625–2632, 2007.
- [82] A. Watson and R. Smith, "An examination of statistical theories for fibrous materials in the light of experimental data," *Journal of Materials Science*, vol. 20, no. 9, pp. 3260–3270, 1985.
- [83] T. Tanaka, H. Nakayama, A. Sakaida, and N. Horikawa, "Estimation of tensile strength distribution for carbon fiber with diameter variation along fiber," *Materials Science Research International*, vol. 5, no. 2, pp. 90–97, 1999.
- [84] W. Curtin, "Tensile strength of fiber-reinforced composites: III. Beyond the traditional weibull model for fiber strengths," *Journal of Composite Materials*, vol. 34, no. 15, pp. 1301–1332, 2000.

- [85] T. Parthasarathy, "Extraction of weibull parameters of fiber strength from means and standard deviations of failure loads and fiber diameters," *Journal of the American Ceramic Society*, vol. 84, no. 3, pp. 588–592, 2001.
- [86] J. Yao, W. Yu, and D. Pan, "Tensile strength and its variation of PAN-based carbon fibers. III. Weak-link analysis," *Journal of Applied Polymer Science*, vol. 110, no. 6, pp. 3778–3784, 2008.
- [87] C. Baley, M. Gomina, J. Breard, A. Bourmaud, and P. Davies, "Variability of mechanical properties of flax fibres for composite reinforcement. a review," *Industrial Crops and Products*, p. 111984, 2019.
- [88] A. Thionnet, H. Chou, and A. Bunsell, "Fibre break processes in unidirectional composites," *Composites Part A: Applied Science and Manufacturing*, vol. 65, pp. 148 – 160, 2014.
- [89] A. Dibenedetto, M. Gurvich, and S. Ranade, "On in-situ evaluation of fibre strength distribution," *Journal of Materials Science Letters*, vol. 16, pp. 1791 – 1792, 1997.
- [90] T. Okabe and N. Takeda, "Size effect on tensile strength of unidirectional cfrp composites— experiment and simulation," *Composites Science and Technology*, vol. 62, no. 15, pp. 2053 – 2064, 2002.
- [91] M. R. GURVICH, A. T. DiBENEDETTO, and S. V. RANADE, "A new statistical distribution for characterizing the random strength of brittle materials," *Journal of Materials Science*, vol. 32, pp. 2559–2564, May 1997.
- [92] K. K. Phani, "Strength distribution and gauge length extrapolations in glass fibre," *Journal of Materials Science*, vol. 23, pp. 1189–1194, Apr 1988.
- [93] M. Ibnabdeljalil and S. Phoenix, "Scalings in the statistical failure of brittle matrix composites with discontinuous fibers—i. analysis and monte carlo simulations," *Acta Metallurgica et Materialia*, vol. 43, no. 8, pp. 2975 – 2983, 1995.
- [94] R. Danzer, "Some notes on the correlation between fracture and defect statistics: Are weibull statistics valid for very small specimens?," *Journal of the European Ceramic Society*, vol. 26, no. 15, pp. 3043 – 3049, 2006.
- [95] K. Naito, J.-M. Yang, Y. Tanaka, and Y. Kagawa, "The effect of gauge length on tensile strength and weibull modulus of polyacrylonitrile (pan)- and pitch-based carbon fibers," *Journal of Materials Science*, vol. 47, pp. 632–642, Jan 2012.
- [96] *JCGM 100: Evaluation of measurement data - Guide to the expression of uncertainty in measurement*. 2010.
- [97] A. Del Mastro, F. Trivaudey, and V. Placet, "Modelling the influence of 3d plant fibres morphology on their tensile behaviour," in *5th International Conference on Innovative Natural Fibre Composites for Industrial Applications*, (Roma, Italy), p. 4 p, oct 2015.
- [98] A. R. Bunsell and J. W. S. Hearle, "A mechanism of fatigue failure in nylon fibres," *Journal of Materials Science*, vol. 6, pp. 1303–1311, Oct 1971.

- [99] A. Marcellan, A. Bunsell, L. Laiarinandrasana, and R. Piques, "A multi-scale analysis of the microstructure and the tensile mechanical behaviour of polyamide 66 fibre," *Polymer*, vol. 47, no. 1, pp. 367 – 378, 2006.
- [100] J. Wollbrett-Blitz, S. Joannès, R. Bruant, C. Le Clerc, M. Romero De La Osa, A. Bunsell, and A. Marcellan, "Multi-axial mechanical behavior of aramid fibers and identification of skin/core structure from single fiber transverse compression testing," *Journal of Polymer Science Part B: Polymer Physics*, vol. 54, no. 3, pp. 374–384, 2016.
- [101] V. Jauzein and A. Bunsell, "Bio-composite aspects of silk: the sericin sheath acting as a matrix," *Journal of Materials Science*, vol. 47, pp. 3082–3088, Apr 2012.
- [102] J. M. H. Ramirez, A. R. Bunsell, and P. Colomban, "Microstructural mechanisms governing the fatigue failure of polyamide 66 fibres," *Journal of Materials Science*, vol. 41, pp. 7261–7271, Nov 2006.
- [103] C. Le Clerc, B. Monasse, and A. R. Bunsell, "Influence of temperature on fracture initiation in pet and pa66 fibres under cyclic loading," *Journal of Materials Science*, vol. 42, pp. 9276–9283, Nov 2007.
- [104] A. Saltelli, M. Ratto, T. Andres, *et al.*, *Global Sensitivity Analysis. The Primer*. John Wiley and sons, Ltd., 2008.
- [105] F. Islam, S. Joannès, S. Bucknell, Y. Leray, A. Bunsell, and L. Laiarinandrasana, "Towards accurate and efficient single fibre characterization to better assess failure strength distribution," in *Proceedings of the 18th European Conference on Composite Materials (ECCM-2018)*, 2018, June.
- [106] F. Islam, L. Laiarinandrasana, and S. Joannès, "Effect of uncertainty in characterization on the variability of fibre strength distributions," in *ICRACM 2019 - 6th International Conference on Recent Advances in Composite Materials*, (Varanasi, India), Feb. 2019.
- [107] T.-K. Hwang, C.-S. Hong, and C.-G. Kim, "Size effect on the fiber strength of composite pressure vessels," *Composite Structures*, vol. 59, no. 4, pp. 489 – 498, 2003.
- [108] H. Chen and D. G. Baird, "Prediction of young's modulus for injection molded long fiber reinforced thermoplastics," *Journal of Composites Science*, vol. 2, no. 3, 2018.
- [109] S. Shah, S. Karuppanan, P. Megat-Yusoff, and Z. Sajid, "Impact resistance and damage tolerance of fiber reinforced composites: A review," *Composite Structures*, vol. 217, pp. 100 – 121, 2019.
- [110] Z. Chi, T. W. Chou, and G. Shen, "Determination of single fibre strength distribution from fibre bundle testings," *Journal of Materials Science*, vol. 19, pp. 3319–3324, Oct 1984.
- [111] R. B. Abernethy, *The New Weibull Handbook*. 2008.

- [112] I. Pobocikova and Z. Sedliackova, “Comparison of four methods for estimating the weibull distribution parameters,” *Applied Mathematical Sciences*, vol. 8, no. 83, pp. 4137–4149, 2014.
- [113] A. Rajpurohit, S. Joannès, F. Islam, V. Singery, S. Bucknell, and L. Laiarinandrasana, “Characterization and statistical analysis of single fiber strength of fibers at various processing stages,” in *ICCM 22 - 22nd International Conference on Composite Materials*, (Melbourne, Australia), Aug. 2019.
- [114] J. VanderPlas, “Frequentism and bayesianism: A python-driven primer,” *PROC. OF THE 13th PYTHON IN SCIENCE CONF. (SCIPY 2014)*, 2014.
- [115] J. Symynck and F. D. Bal, “Monte-carlo pivotal confidence bounds for weibull analysis, with implementations in r,” *The XVI-th International Scientific Conference “Tehnomus” “Stefan cel Mare” University of Suceava - ROMANIA*, 2011.
- [116] B. Wang, F. Islam, and G. W. Mair, “Evaluation methods for estimation of weibull parameters used in monte carlo simulations for safety analysis of pressure vessels,” *Materials Testing*, vol. 63, no. 4, pp. 379–385, 2021.
- [117] P. Zinck, E. Mäder, and J. F. Gerard, “Role of silane coupling agent and polymeric film former for tailoring glass fiber sizings from tensile strength measurements,” *Journal of Materials Science*, vol. 36, pp. 5245–5252, Nov 2001.
- [118] A. Thionnet, A. Bunsell, and H.-Y. Chou, “Intrinsic Mechanisms Limiting the Use of Carbon Fiber Composite Pressure Vessels,” *Journal of Pressure Vessel Technology*, vol. 138, 07 2016. 060910.
- [119] A. Scott, I. Sinclair, S. Spearing, A. Thionnet, and A. Bunsell, “Damage accumulation in a carbon/epoxy composite: Comparison between a multiscale model and computed tomography experimental results,” *Composites Part A: Applied Science and Manufacturing*, vol. 43, no. 9, pp. 1514 – 1522, 2012.
- [120] A. Thionnet, H.-Y. Chou, and A. Bunsell, “Fibre break failure processes in unidirectional composites. part 1: Failure and critical damage state induced by increasing tensile loading,” *Applied Composite Materials*, vol. 22, pp. 119–140, Apr 2015.
- [121] S. Blassiau, A. Thionnet, and A. Bunsell, “Micromechanisms of load transfer in a unidirectional carbon fibre–reinforced epoxy composite due to fibre failures. part 2: Influence of viscoelastic and plastic matrices on the mechanisms of load transfer,” *Composite Structures*, vol. 74, no. 3, pp. 319 – 331, 2006.
- [122] A. Thionnet, H. Y. Chou, and A. Bunsell, “Fibre break failure processes in unidirectional composites. part 3: Unidirectional plies included in laminates,” *Applied Composite Materials*, vol. 22, pp. 157–169, May 2015.
- [123] F. Islam, S. Joannès, and L. Laiarinandrasana, “Propagation of uncertainty from constituents to structural assessments in composite strength modelling,” in *ICCS 23 - 23th International Conference on Composites Structures*, (Porto, Portugal), Sept. 2020.

- [124] S. Blassiau, *Modélisation des phénomènes microstructuraux au sein d'un composite unidirectionnel carbone/epoxy et prédiction de durée de vie : contrôle et qualification de réservoirs bobinés*. Theses, École Nationale Supérieure des Mines de Paris, Mar. 2005.
- [125] G. Mair, M. Hoffmann, F. Scherer, A. Schoppa, and M. Szczepaniak, "Slow burst testing of samples as a method for quantification of composite cylinder degradation," *International Journal of Hydrogen Energy*, vol. 39, no. 35, pp. 20522 – 20530, 2014.
- [126] M. P. Widjaja, F. Islam, S. Joannès, A. Bunsell, G. Mair, and A. Thionnet, "Effect of input properties on the predicted failure of a composite pressure vessel using a multiscale model," in *FiBreMoD Conference*, (Leuven, Belgium), KU Leuven, Dec. 2019.
- [127] A. R. Bunsell, A. Thionnet, and H. Y. Chou, "Intrinsic safety factors for glass & carbon fibre composite filament wound structures," *Applied Composite Materials*, vol. 21, pp. 107–121, Feb 2014.
- [128] F. Islam, S. Joannès, S. Bucknell, Y. Leray, A. Bunsell, and L. Laiarinandrasana, "Investigation of tensile strength and dimensional variation of t700 carbon fibres using an improved experimental setup," *Journal of Reinforced Plastics and Composites*, vol. 39, no. 3-4, pp. 144–162, 2020.
- [129] W. Garat, S. Corn, N. L. Moigne, J. Beaugrand, and A. Bergeret, "Dimensional variations and mechanical behaviour of natural fibres from various plant species in controlled hygro/hydrothermal conditions," in *Proceedings of the 18th European Conference on Composite Materials (ECCM-2018)*, June, 2018.
- [130] R. J. Lunn, Y. Leray, S. Joannès, F. Islam, S. Bucknell, and D. M. Stringer, "Further Insights into the Fatigue of Hair Fibres through Statistical Analysis and Relevance to Hair Care Applications," in *HairS'19 , DWI*, (Schluchsee, Germany), Sept. 2019.
- [131] *Dia-Stron website*, accessed January 22, 2020.
- [132] V. Placet, M. Blot, T. Weemaes, H. Bernollin, G. Laurent, F. Amiot, C. Clemy, and J. Beaugrand, "Transverse compressive properties of natural fibres determined using micro mechatronics systems and 2D full -field measurements," in *4th International Conference on Natural Fibers*, (Porto, Portugal), July 2019.
- [133] C. Baley, Y. Perrot, F. Busnel, H. Guezenoc, and P. Davies, "Transverse tensile behaviour of unidirectional plies reinforced with flax fibres," *Materials Letters*, vol. 60, no. 24, pp. 2984–2987, 2006.
- [134] I. Krucinska and T. Stypka, "Direct measurement of the axial poisson's ratio of single carbon fibres," *Composites Science and Technology*, vol. 41, no. 1, pp. 1 – 12, 1991.
- [135] D. Mounier, C. Poilâne, C. Bûcher, and P. Picart, "Evaluation of transverse elastic properties of fibers used in composite materials by laser resonant ultrasound spectroscopy," in *Acoustics 2012* (S. F. d'Acoustique, ed.), (Nantes, France), Apr. 2012.

- [136] R. Sevenois, D. Garoz, E. Verboven, S. Spronk, F. Gilabert, M. Kersemans, L. Pyl, and W. V. Paepegem, “Multiscale approach for identification of transverse isotropic carbon fibre properties and prediction of woven elastic properties using ultrasonic identification,” *Composites Science and Technology*, vol. 168, pp. 160 – 169, 2018.
- [137] W. Curtis, J. Milne, and W. Reynolds, “Non-hookean behaviour of strong carbon fibres,” *Nature*, vol. 220, pp. 1024–1025, 1968.
- [138] A. D. Mastro, F. Trivaudey, V. Guicheret-Retel, V. Placet, and L. Boubakar, “Investigation of the possible origins of the differences in mechanical properties of hemp and flax fibres: A numerical study based on sensitivity analysis,” *Composites Part A: Applied Science and Manufacturing*, vol. 124, p. 105488, 2019.
- [139] D. Berrar, “Introduction to the non-parametric bootstrap,” in *Encyclopedia of Bioinformatics and Computational Biology* (S. Ranganathan, M. Gribskov, K. Nakai, and C. Schönbach, eds.), pp. 766 – 773, Oxford: Academic Press, 2019.
- [140] V. Lavaste, J. Besson, and A. R. Bunsell, “Statistical analysis of strength distribution of alumina based single fibres accounting for fibre diameter variations,” *Journal of Materials Science*, vol. 30, pp. 2042–2048, Jan 1995.
- [141] S. Joannès and F. Islam, “Uncertainty in estimation of fibre strength distribution due to measurement errors and choosen sample size,” *Applied Composite Materials*, vol. 27, pp. 165–184, 2020.
- [142] F. Islam, S. Joannès, A. Bunsell, and L. Laiarinandrasana, “Adaptation of Weibull analysis to represent strength behaviour of brittle fibres,” in *ICCM 22 - 22nd International Conference on Composite Materials*, (Melbourne, Australia), Aug. 2019.
- [143] K. Pickering and T. Murray, “Weak link scaling analysis of high-strength carbon fibre,” *Composites Part A: Applied Science and Manufacturing*, vol. 30, no. 8, pp. 1017 – 1021, 1999.
- [144] S. L. Phoenix and R. G. Sexsmith, “Clamp effects in fiber testing,” *Journal of Composite Materials*, vol. 6, no. 3, pp. 322–337, 1972.
- [145] S. Behzadi, P. T. Curtis, and F. R. Jones, “Improving the prediction of tensile failure in unidirectional fibre composites by introducing matrix shear yielding,” *Composites Science and Technology*, vol. 69, no. 14, pp. 2421 – 2427, 2009. The Sixteenth International Conference on Composite Materials with Regular Papers.
- [146] J. P. Foreman, S. Behzadi, D. Porter, and F. R. Jones, “Multi-scale modelling of the effect of a viscoelastic matrix on the strength of a carbon fibre composite,” *Philosophical Magazine*, vol. 90, no. 31-32, pp. 4227–4244, 2010.
- [147] E. M. Odom and D. F. Adams, “Specimen size effect during tensile testing of an unreinforced polymer,” *Journal of Materials Science*, vol. 27, pp. 1767–1771, Apr 1992.
- [148] T. Hobbiebrunken, B. Fiedler, M. Hojo, and M. Tanaka, “Experimental determination of the true epoxy resin strength using micro-scaled specimens,” *Composites Part A: Applied Science and Manufacturing*, vol. 38, no. 3, pp. 814 – 818, 2007.

- [149] J. Misumi, R. Ganesh, S. Sockalingam, and J. John W Gillespie, “Experimental characterization of tensile properties of epoxy resin by using micro-fiber specimens,” *Journal of Reinforced Plastics and Composites*, vol. 35, no. 24, pp. 1792–1801, 2016.
- [150] X. Sui, M. Tiwari, I. Greenfeld, R. L. Khalfin, H. Meeuw, B. Fiedler, and H. D. Wagner, “Extreme scale-dependent tensile properties of epoxy fibers,” pp. 993 – 1003, 2019.

Appendix A

Weakest link model and Weibull distribution

Weibull presented an analogy between the failure of brittle solids and the breaking of a chain in which failure is controlled by the strength of the weakest link in the chain [23, 40], as shown in Figure A.1.

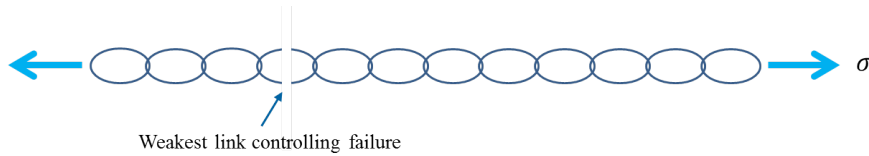


Figure A.1: Schematic representation of a chain consisting of N links. The chain breaks at the weakest link.

Given that a chain consists of N links connected to each other, the survival of the chain under an applied stress requires that each of its links survive this stress. For the survival of a link, it should have a failure stress σ_f greater than the applied stress σ , i.e. $\sigma_f > \sigma$. Let event \mathbf{X} be such that $\sigma_f > \sigma$. If $P_S(\mathbf{X})$ is the survival probability of the chain and $P_s(\mathbf{X})$ is the survival probability of an individual link, the survival probability of the chain under an applied stress σ is given by Equations A.1 and A.2; since survival of individual links are independent events. If $P_R(\sigma)$ is the probability of failure of the chain and $P_r(\sigma)$ is the probability of failure of an individual link, Equation A.3 is obtained¹. For a given applied stress σ , the failure probability of each link, $P_r(\sigma)$, is the probability that this applied stress is greater than or equal to the failure stress of the link. Equation A.4 is obtained by rearranging Equation A.3, and is, in its simplest form, a statement of the weakest link theory. It also serves as a foundation for tensile strength models of brittle solids.

$$P_S(X) = [P_s(X)]^N \quad (\text{A.1})$$

$$P_S(\sigma_f > \sigma) = [P_s(\sigma_f > \sigma)]^N \quad (\text{A.2})$$

¹Since failure and survival probability are related as, $P_R(\sigma) = 1 - P_S(\sigma)$ and $P_r(\sigma) = 1 - P_s(\sigma)$

$$1 - P_R(\sigma) = [1 - P_r(\sigma)]^N \quad (\text{A.3})$$

$$P_R(\sigma) = 1 - \exp [N \ln \{1 - P_r(\sigma)\}] \quad (\text{A.4})$$

In Equation A.4 the term $\ln[1 - P_r(\sigma)]$ can be replaced by a monotonic function. Weibull chose to replace this with $-[(\sigma - \sigma_u)/\sigma_0]^m$ for $\sigma \geq \sigma_u$ and zero for $\sigma < \sigma_u$, where σ is the applied stress, σ_u is the stress below which there is zero probability of failure, known as the threshold stress or location parameter and σ_0 and m are material parameters. σ_0 is known as scale parameter and m is known as Weibull shape parameter. To extend this equation to a brittle fibre of length L , the fibre can be considered to be composed of many small links L_0 each containing one defect, similarly as in the case of a chain. For this case, the cross sectional area of the volume can be considered to be constant, such that N can be replaced by L/L_0 . The failure probability of a specimen, following the Weibull law, can then be expressed as in Equation A.5. Equation A.5 is popularly known as the 3-parameter Weibull distribution.

$$P_R(\sigma) = 1 - \exp \left[- \left(\frac{L}{L_0} \right) \left(\frac{\sigma - \sigma_u}{\sigma_0} \right)^m \right] \quad (\text{A.5})$$

Appendix B

Microscale matrix properties

Contents

B.1 Introduction	177
B.2 Microscale matrix properties: state of the art	178
B.3 Materials and methods	180
B.3.1 Materials	180
B.3.2 Specimen preparation	180
B.3.3 Microscopy	180

B.1 Introduction

In carbon fibre reinforced polymer composite materials, the matrix usually has a higher strain to failure than the carbon fibres. When the first fibre breaks upon longitudinal loading, the role of the matrix is to transfer load to the adjacent fibers. Load transfer occurs through the interface and the matrix to the adjacent fibers through a shear dominated multi-axial mechanism. Additional fiber breaks are developed on further loading which leads to the ultimate failure of composites. In addition to the fiber strength distribution, the matrix resin properties also play an important role on load transfer and stress concentration.

Many studies have been conducted to understand the role of the matrix resin properties on the axial tensile strength of unidirectional fibre reinforced composites. Behzadi [145] and Foreman [146] have reported that yielding behavior of matrix resin strongly affects the tensile strength of unidirectional composites. Experimentally determined matrix properties are introduced into computational composite models to capture the effect of matrix properties on the failure of composite materials. Tests to establish the properties of the matrix, for example, material strength, are performed on laboratory scale specimens. However, width of the matrix resin region that exists between fibers in composites can vary from submicron to micrometer scales. For example, in carbon fibre composites, the average distance between fibers is in the range of a few micrometres. The experimentally determined properties are therefore at lengths scales of orders of magnitude higher than

that found inside composite materials. Similar to the size effect in strength of technical fibres, several studies have also reported the presence of size effect in the properties of thermoset resins, which are commonly used as matrix in composite materials [147]. This is because thermoset resins are brittle in nature, and like most brittle materials, they are sensitive to defects, which control their strength. These defects have a stochastic nature and are randomly located in the material. The probability of finding defects inside a specimen therefore depends upon the chosen size, which explains the variation of material strength with tested size.

To capture the microscale properties, a few studies have recently been conducted which generates and tests fibres for determining the mechanical properties of the matrix material. These studies are described in Section B.2. The shortcomings with those methods have been described, following which a novel method for microscale matrix characterisation has been proposed in Section B.3. A new method for the experimental determination of microscale matrix strength is introduced in this work. Neat epoxy resin fibres were produced and tensile tests were performed on these fibres. This work is in line with the overall objectives of the FiBreMoD project, of developing methods to accurately estimate properties of constituents to be used in composite strength and damage models as input for predicting structural behaviour.

B.2 Microscale matrix properties: state of the art

Despite the potential of higher mechanical properties of the inter-fibre layers of matrix in fibre reinforced composites, only very few studies have dealt with the size effects in epoxy resins. Odom and Adams [147] tested laboratory scale dog-bone shaped specimens and observed a large difference between the strength of large and small specimens. They reported that smaller samples had significantly higher strengths.

Even fewer studies have tried to determine the actual mechanical properties of the matrix material at the length scales observed in fibre reinforced composite materials. The following reported studies have tried to determine the microscale properties of the matrix by proposing methods to produce μm -sized epoxy fibers:

Hobbiebrunken et al. [148] explained a process of obtaining microscale epoxy fibres by manipulating curing of the epoxy during the vitrification process. Figure B.1(a) shows a schematic of the fibre preparation process. Thin fibres can be seen to be formed between the cup and the plate when the cup is pulled away from the plate. The diameters of the fibres were found to be in a range of 22.3–51.4 μm , with an average value of 36.7 μm . Fibres were tested at a gauge length of 6 mm to determine their tensile strength. Their analysis of the fracture surfaces of the resin fibres showed some differences to the fracture surfaces of the bulk resin specimens. They observed that the crack initiated by nucleation of voids or pre-existing flaws. The size of the voids were in the range of 2 μm and thus much smaller than the size measured from the fracture surface of the bulk resin specimens. The average strength of epoxy fibres was found to be very high and remarkably close (60%) to the theoretical strength of the epoxy material.

Misumi et al. [149] developed a syringe based preparation method of micro-scale epoxy fiber specimens, to evaluate epoxy resin mechanical properties at length scales represen-

tative of matrix resin in CFRP. Figure B.1(b) shows a schematic of the fibre preparation process. Five different types of epoxy resin systems were used for preparing the fibres, the diameters of which were in the range of 100–150 μm . These fibres were used for tensile testing. It was shown that epoxy microfibers showed ductile behavior with distinct yield point in all resin systems, unlike macroscopic specimens which exhibited brittle behavior without any yield point. It was also shown that the epoxy micro-fiber specimens had significantly higher failure strain and ultimate stress as compared to the macroscopic specimens. Their results thus showed that epoxy resin potentially has much higher ductility and strength at smaller length scales.

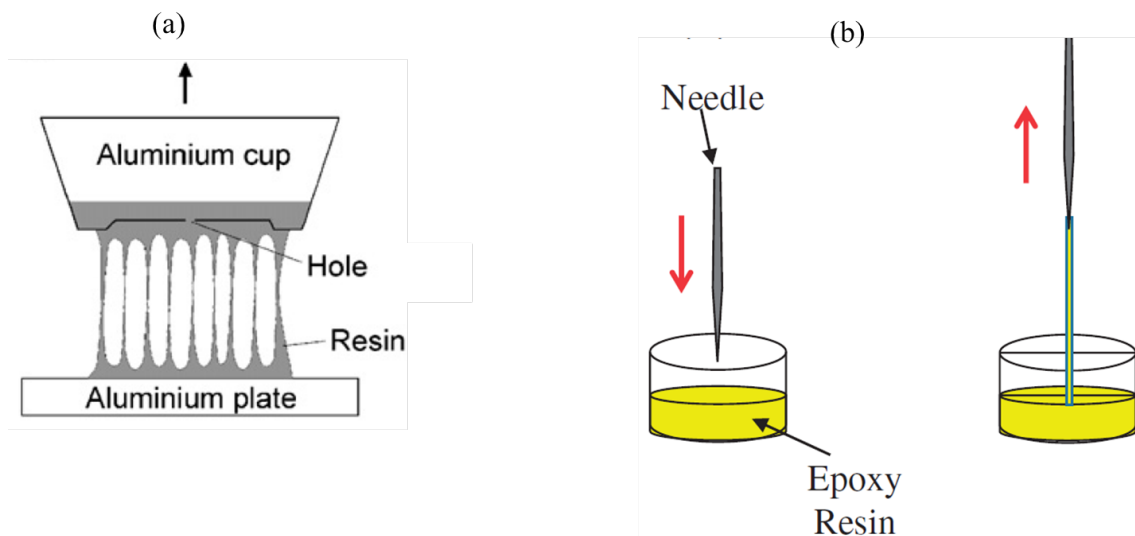


Figure B.1: (a) Fibre manufacturing process used by Hobbiebrunken et al. [148]. (b) Fibre manufacturing process used by Misumi et al. [149]

Sui et al. [150] prepared epoxy fibres by pouring epoxy from the tip of a spatula located at a certain height. The hanging fibres gradually formed thinner fibres under the effect of gravity, while cooling down to room temperature over time. Fibres of varying diameter were prepared by varying the amount and viscosity of epoxy used for the preparation, such that lower amount of epoxy resulted in thinner fibres, and vice versa. The prepared fibres had diameters ranging from 20–350 μm . Dogbone specimens were also prepared for comparing the microscale properties to that at laboratory scale. On testing the fibres, they observed significant size effects in the Young's modulus, strength, and toughness in the prepared specimens. Moreover, they observed highly ductile behaviour in the epoxy fibres, and as reported, the failure strain values reached upto 112% in certain cases. The reported failure strain was much larger than other similar studies.

In all the studies described above, the prepared matrix fibres were circular in cross-section. However, the matrix phase in fibre reinforced composites is never circular in cross-section. It is irregular in shape, as can be seen in Figure B.2. It can be understood to be formed of many irregular concave faces joined together. The best solution would have been to isolate the matrix region from the composites to perform mechanical tests, but that is not possible. Therefore, a novel method for microscale matrix characterisation, which tries to

replicate this matrix cross-section has been proposed in Section B.3.

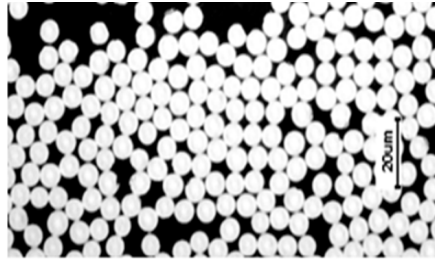


Figure B.2: Cross-section of a carbon fibre reinforced composite material. The epoxy phase can be seen to have non-regular shapes [22].

B.3 Materials and methods

B.3.1 Materials

To demonstrate the proposed method of fabricating non-circular matrix fibres, Epoxy Sicomin SR 8500 resin with KTA 313 hardener was used.

B.3.2 Specimen preparation

For the preparation of epoxy fibres, circular wires made of teflon, 0.8 mm in diameter were used. The surface of these wires were then coated with a thin layer of epoxy. A group of 2 or 3 wires were then brought together and consolidated, as shown in Figure B.3. A few rounds of twists were made on this group of wires so as to ensure that they do not separate from each other. The group of wires were then put in the oven to allow the resin to cure as per the standard procedure. Upon curing, the epoxy settled in the cavities near the point of contact of consecutive wires, as shown in Figure B.3. The teflon wires and the epoxy fibres were carefully removed from each other.

B.3.3 Microscopy

Figure B.4 shows a prepared epoxy fibre of length 4 mm (approximately) using the methodology explained in the previous section. The fibre is twisted along the length due to the twists given to the teflon wires for consolidation.

Figure B.5 shows microscopic images of the fibre preparation process. The cross-section of the wires can be seen with epoxy settled in the cavities between the wires. The size of the epoxy fibres can be regulated by varying the amount of epoxy used for coating the teflon wires. The two images are shown to produce epoxy fibres of different sizes based on the amount of epoxy used for coating.

Figure B.6 shows a microscopic image of the cross-section of a prepared epoxy fibre.

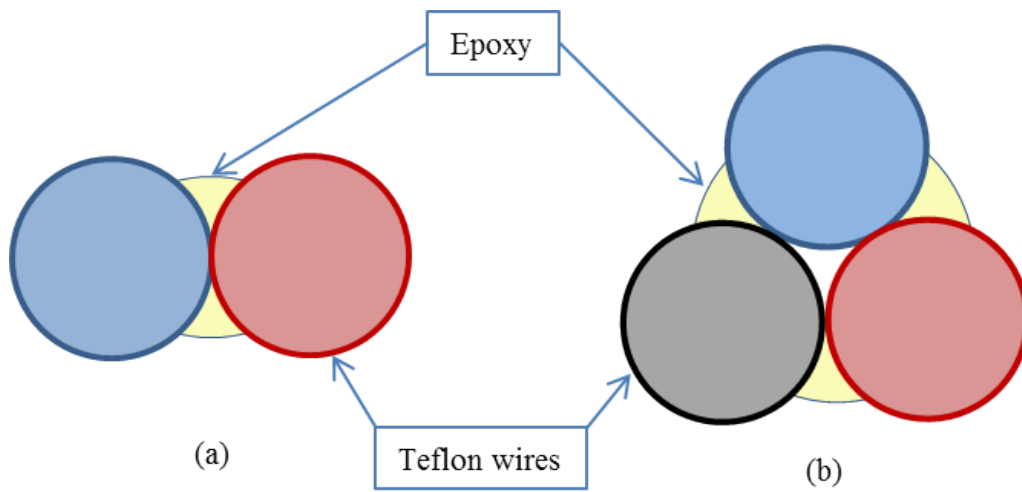


Figure B.3: Schematic of the cross section of the group of wires. The epoxy settled in the cavities near the point of contact of consecutive wires resulting in epoxy fibres.



Figure B.4: An epoxy fibre. The fibre is twisted along the length due to the twists given to the teflon wires for consolidation.

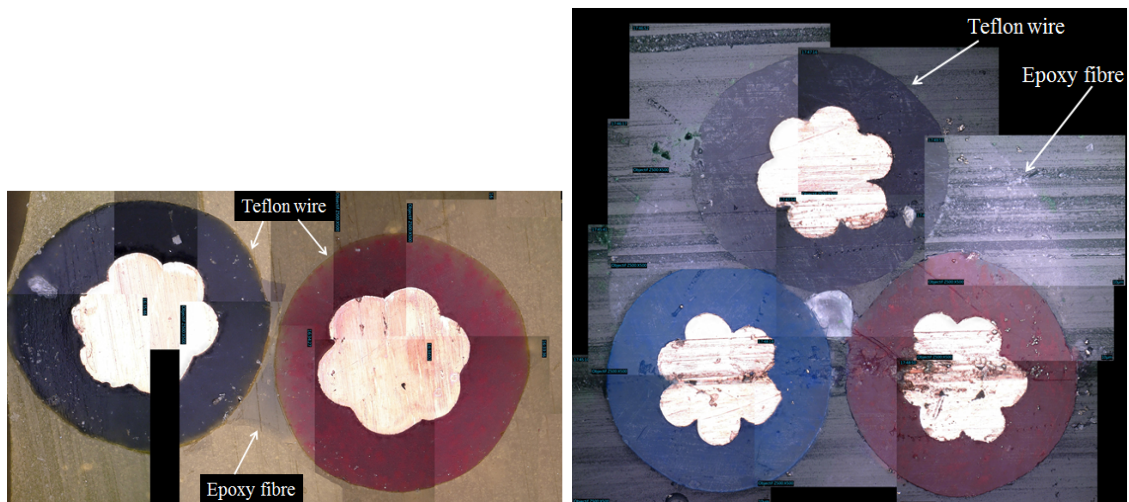


Figure B.5: Microscopic image of the cross-section of the wires with epoxy settled in the cavities between the wires.



Figure B.6: Microscopic image of the cross section of a prepared epoxy fibre.

RÉSUMÉ

Les matériaux composites renforcés de fibres sont largement utilisés pour les applications structurelles à hautes performances mécaniques. La prédiction de la tenue en service et de la durée de vie sont des paramètres clés pour ce type d'applications. Aussi, la conception des structures composites peut être assistée par des modèles à différentes échelles du matériau. Pour garantir la précision des simulations, ces modèles nécessitent des données d'entrée les plus fiables possibles, notamment en ce qui concerne les propriétés des constituants. Malgré leur très large utilisation, de très grandes différences sont rapportées dans la littérature pour les propriétés à rupture des fibres de carbone T700.

Dans cette thèse, une étude expérimentale et statistique approfondie a été menée pour identifier les origines des variations observées sur la résistance à la traction des fibres. Il s'agit de tenter de séparer ce qui provient de l'essai et ce qui provient de la fibre elle-même. Les résultats expérimentaux ont permis d'identifier les paramètres critiques qui contribuent à l'incertitude dans la détermination de la résistance des fibres et d'évaluer leur importance, notamment sur la fiabilité des prédictions menées à l'échelle du composite. Une technique de réduction des données basée sur l'approche bayésienne permet en outre de s'approcher davantage des propriétés à rupture probables des fibres et ainsi mieux appréhender leur comportement.

MOTS CLÉS

Distribution de Weibull, fibres de carbone T700, test des fibres, quantification de l'incertitude, modélisation

ABSTRACT

Fibre reinforced composite materials are widely used for high-performance and critical structural applications. The design of composite material structures can be assisted by computational models for predicting their mechanical properties at both component and structural level. These models require very accurate constituent properties as input to make reliable predictions about the strength and lifetime of composite structures. However, a good understanding of the constituent properties of fibre-reinforced polymer composites is still lacking. For e.g., despite their wide use, very large differences are observed in the literature for properties of T700 carbon fibers.

This thesis aims to advance the understanding of the constituent properties of fibre reinforced composites. To achieve this, an extensive experimental and statistical study has been conducted to understand the variations in the tensile strength of fibres and their morphology. These results have been analysed to identify and evaluate the critical parameters which contribute to errors or uncertainty in determining the parameters of the fibre strength Weibull distribution. This knowledge of uncertainties in constituent properties has also been used to highlight the variabilities they introduce on the output structural behaviour predicted by composite strength models. To further improve the fibre strength characterisation process, a data-reduction technique based on Bayesian approach of using prior knowledge of deficiencies in experimental data has been developed to model the tensile strength variation of brittle fibres. Additionally, new directions to accurately characterize the in-situ microscale properties of the matrix have been proposed.

KEYWORDS

Weibull distribution, T700 carbon fibres, strength, single fibre testing, uncertainty quantification, modelling